Multi-Agent System Based Special Protection and Emergency Control Scheme against Cascading Events in Power System

Liu, Zhou

Publication date:
2013

Multi-Agent System Based Special Protection and Emergency Control Scheme against Cascading Events in Power System

By

Zhou Liu

Department of Energy Technology

A Dissertation Submitted to

The Faculty of Engineering, Science and Medicine, Aalborg University

in Partial Fulfillment for the Degree of Doctor of Philosophy

October 2013

Aalborg, Denmark

AALBORG UNIVERSITY
Department of Energy Technology
Pontoppidanstraede 101
9220 Aalborg East
Denmark

ISBN: 978-87-92846-31-0

Printed in Denmark by Aalborg University

Mandatory Page

Thesis title

Multi-Agent System Based Special Protection and Emergency Control Scheme against Cascading Events in Power System

Name of PhD student

Zhou Liu

Name and title of supervisor and any other supervisors

Professor Zhe Chen

List of publication:

Published paper:

[1] Z. Liu, Z. Chen, Y. Hu, "Wide Area Protection Scheme Preventing Cascading Events based on Improved Impedance relay", *2013 China-Korea Relay Protection Forum*, Xinjiang, Sep. 2013.

[2] Z. Liu, Z. Chen, H. Sun, Y. Hu, "Wide Area Protection Scheme Preventing Cascading Events Caused by Load Flow Transferring", *Power & Energy Society General Meeting*, Vancouver, July, 2013.

[3] Z. Liu, Z. Chen, H. Sun, Y. Hu, "Multi Agent System Based Process Control in Wide Area Protection against Cascading Events", *POWERTECH 2013*, France, Grenoble, June, 2013.

[4] Z. Liu, Z. Chen, H. Sun, C. Liu, Y. Hu, "Multi Agent System Based Wide Area Protection against Cascading events", *The 10th International Power and Energy Conference (IPEC)*, Ho Chi Minh City , Dec. 2012.

[5] Z. Liu, Z. Chen, H. Sun, C. Liu, "Emergency Load Shedding Strategy Based on Sensitivity Analysis of Relay Operation Margin against Cascading Events", *IEEE PES International Conference on Power Systems Technology (POWERCON)*, Auckland, New Zealand, Oct. 2012.

[6] Z. Liu, Z. Chen, H. Sun, C. Liu, "Control and Protection Cooperation Strategy for Voltage Instability", *47th International Universities' Power Engineering Conference (UPEC)*, London, Sep. 2012.

Submitted papers:

[7] Z. Liu, Z. Chen, H. Sun, Y. Hu, "Multi Agent System Based Wide Area Protection and control Scheme against Cascading Events", *IEEE Transactions on Power Delivery.* Second reviewing.

[8] Z. Liu, Z. Chen, H. Sun, Y. Hu, "A Multi Agent System Based Wide Area Protection Scheme against Voltage Instability Induced Cascading Events", *IET Generation, Transmission & Distribution*, Submitted.

This present report combined with the above listed scientific papers has been submitted for assessment in partial fulfillment of the PhD degree. The scientific papers are not included in this version due to copyright issues. Detailed publication information is provided above and the interested reader is referred to the original published papers. As part of the assessment, co-author statements have been made available to the assessment committee and are also available at the Faculty of Engineering and Science, Aalborg University.

Acknowledgement

First of all, I would like to express my sincere appreciation to my supervisor Prof. Zhe Chen for all the invaluable suggestions, professional guidance and kind encouragement throughout the whole PhD study.

The Department of Energy Technology in Aalborg University (ET.AAU) and the China Scholarship Council (CSC) are gratefully acknowledged for the financial support of this research project.

I am very grateful to Professor Shaorong Wang and Associate Professor Haishun Sun from Huazhong University of Science and Technology in China, and Professor Xiaoru Wang from Southwest Jiaotong Univeristy in China. I would also like to thank my colleagues in our research group, especially Fujin Deng, Yunqian Zhang, Chi Su, Weihao Hu, Chengxi Liu, Xiongfei Wang, Jiakun Fang for lots of help in my life and work. Many thanks also go to the experts in the Alston Grid, Stafford, UK for their help and support during my external study period.

At last but not least, I would like to thank my parents and my wife for their love and constant support.

Zhou Liu

Aalborg, Denmark

October, 2013

Abstract

This thesis concerns the development of wide area special protection and emergency control scheme that can provide effective countermeasures against long term voltage instability induced cascading events and blackouts in power system. Most past cascaded blackouts are caused by unexpected backup relay operations due to low voltage or overload state in the post stage of N-1 (or N-k) contingency. If such state could be sensed and adjusted appropriately before those relay actions, the system stability might be sustained. So it is of great significance to develop a suitable protection scheme to identify and adjust those emergency states in advance before a cascaded blackout.

In order to identify the diverse emergency states in the post fault stage, the distributed distance relays with upgraded settings, which take the capability limits into account, will be utilized in this thesis. Moreover, according to the variations of power system operation, an overload prediction algorithm based on impedance sensitivity is proposed here to distinguish the emergency states from a remote fault. These methods combined together, which can give a fast identification of the emergency states and a clear mapping of critical relays in the post fault stage.

For the purpose of adjusting the identified emergency states timely and preventing the unexpected relay operations, a fast optimal control algorithm is proposed here to find the most effective control locations and reasonable control amount, which is based on sensitivity analysis and the extent of specific emergency states. At the same time, load restoration dynamics is taken into account to compensate sensitivity calculation and correct the control algorithm. Such control methods provides a direct and simple way from problems to solutions, which is suitable for real time implementation.

On the other hand, with the aim of executing the control methods timely and implementing the whole protection strategy suitably, multi-agent system (MAS) with hierarchical structure is designed here. The distributed relays and controllers work as device agents in the lowest level of MAS. And the agents in higher levels will be used to build an effective cooperation environment. Therefore, those distributed agents can be systematically organized by MAS to effectively achieve the global goal on preventing the post fault emergency states and subsequent cascading events.

Moreover, in order to handle some unexpected failures of control methods' execution or some unexpected disturbances when the power system is already operated in an emergency situation, the process control strategy is designed in this thesis to manage the execution progress of whole protection strategy in real time. If there is an unexpected situation emerging, the specific agents in higher level will be activated to solve this problem. Such methods improve the reliability of the proposed protection strategy to cope with more complex emergency situations than planned.

Finally, in order to realize and testify the proposed protection strategy in this thesis, a real time simulation platform based on Real Time Digital Simulator (RTDS) and LabVIEW is built. In this platform, the cases of cascaded blackouts are simulated on the test system simplified from the East Denmark power system. For the MAS based control system, the distributed power system agents are set up in RTDS, while the agents in higher level are designed by LabVIEW toolkits. The case studies and simulation results demonstrate the effectiveness of real time application of the proposed MAS based special protection and emergency control scheme against the cascaded blackouts.

Dansk Abstrakt

Denne afhandling omhandler udviklingen af en omfattende beskyttelse og kontrolordning, der kan levere effektive modforanstaltninger mod længerevarende ustabilitet af netspændingen, der fremtvinger mørklægninger i elsystemet. De fleste tidligere mørklægninger er forårsaget af uventede backup relæoperationer på grund af lav spænding eller uforudsete overbelastninger i tidligere tilstande af N-1 (eller N-k). Hvis en sådan tilstand vil kunne detekteres og justeres hensigtsmæssigt inden disse relæoperationer, kan systemets stabilitet opretholdes. Så det er af stor betydning for at udvikle en passende beskyttelsesordning at identificere og tilpasse disse nødsituationer på forhånd, før en mørklægning.

For at identificere de forskellige nødsituationer i de tidligere fejltilstande vil de distribuerede afstandsrelæer med opgraderede indstillinger, som tager højde for kapacitetsbegrænsninger benyttes i denne afhandling. På grund af variationer af elsystemet er en overbelastningsestimeringsalgoritme baseret på impedansfølsomhed udviklet for at skelne fejltilstande fra en ekstern fejl. Disse metoder kombineret kan give en hurtig identifikation af undtagelsestilstande og en klar kortlægning af de kritiske relæer i de tidligere fejltilstande.

Med henblik på at justere de identificerede nødsituationstilstande rettidig og forhindre uventede relæoperationer er en hurtigt optimal kontrolalgoritme foreslået for at finde de mest effektive kontrollokationer og rimelige kontrolomfang, som er baseret på sensitivitetsanalyse og omfanget af specifikke nødstilstande. Samtidig er dynamikken i genetableringsbelastningen medtaget for at kompensere for følsomhedsberegninger og korrektioner i styringsalgoritmen. Sådanne metoder giver en direkte og enkel måde fra problemer til løsninger, der er egnet til tidstro implementering.

På den anden side, med det formål at udføre kontrolmetoderne rettidigt og gennemføre hele strategien for beskyttelsen er et multi-agent system (MAS) med hierarkisk struktur designet. De distribuerede relæer og styringer arbejder som enhedsagenter i laveste niveau af MAS. Agenter i højere niveauer, vil bruges til at bygge et effektivt interaktionsmiljø. Derfor kan de distribuerede agenter, systematisk organiseret af MAS, effektivt nå det globale mål om forebyggelse af fejltilstande og derved forhindre en efterfølgende dominoeffekt.

Desuden, for at håndtere nogle uventede fejl pga. kontrolmetodernes udførelse eller uventede forstyrrelser, når elsystemet bringes i en nødssituation, er kontrolstrategien i denne afhandling at styre udførelsen i real tid. Hvis en uventet situation opstår, vil agenterne i på det højere niveau aktiveres for at løse problemet. Sådanne metoder forbedrer pålideligheden af den foreslåede beskyttelsesstrategi til at håndtere mere komplekse nødsituationer end planlagt.

Endelig, for at realisere og teste den foreslåede beskyttelsesstrategi i denne afhandling, er en realtidsplatform baseret på Real Time Digital Simulator (RTDS) og LabVIEW bygget. I denne platform, er de tilfælde af dominoeffekter simuleret på testsystemet; dog begrænset til øst Danmark. For de MAS baserede styresystemer, er de distribuerede systemagenter oprettet i RTDS, mens agenter på højere niveauer er designet af LabVIEW toolkits. Casestudierne og simuleringsresultaterne demonstrerer effektiviteten af tidstro anvendelse af den foreslåede MAS-baserede beskyttelse og kontrolanordninger mod mørklægninger

Glossary of terms

WAMS	Wide Area Measurement System
PMU	Phasor Measurement Unit
MAS	Multi-agent System
SPECS	Special Protection and Emergency Control Scheme
RTDS	Real Time Digital Simulator
RSCAD	Real Time Digital Simulator Computer Aided Design
LTC	Load Tap Changer
LabVIEW	Laboratory Virtual Instrument Engineering Workbench
EMS	Energy Management System
SCADA	Supervisory Control And Data Acquisition
UVLS/LS	Under Voltage Load Shedding/Loading Shedding
UFLS	Under Frequency Load Shedding
FCL	Field Current Limiter
SCL	Stator Current Limiter
SCC/ CC / LCC	Supervisory Control Center/Control Center/Local Control Center
NERC	North American Electric Reliability Council
PSS	Power System Stabilizer
GR	Generator Reschedule
ILTC	Inverse Load Tap Control
PI	Performance Index
RAS	Relay Agent Society
LTAS	Load Tap Agent Society
LSAS	Load Shedding Agent Society

GAS	Generator Agent Society
DSC	Data Logging and Supervisory Control
NI PSP	National instrument Publish Subscribe protocol
RTOS	Real Time Operation System
HMI	Human Machine Interface

Table of contents

Chapter 1

Introduction

This chapter firstly presents the background and the motivations of the thesis. Secondly, problem statement and project objectives are briefly introduced. The scopes and limitations of this thesis are described in the third place. And finally, the outline of this thesis is presented.

1.1 Project background and motivations

In 1831, Michael Faraday discovered electromagnetic induction, which ushered a brand new era of electrical technology. And the first complete electric power system, which included a generator, cable, fuse, meter, and loads, was established by Thomas Edison in 1882 [1] [2]. Up to now, in order to meet the requirements of human society's development, the power system becomes a wide area distributed and fast dynamic responded system with a complex structure and numbers of components. Monitoring and maintenance over such a big system are indeed challenging problems.

Also, due to the requirements for the faster industrial and economic development, today's power system is operated closer to planed limits of safe operation [3]. Consequently, in order to insure a secure and reliable delivery of power energy, the traditional protective relay system, which is built locally and dispersedly to protect the power system components from faults, is designed with faster reaction speed, better selectivity, higher sensibility and reliability [4]. However, from the view point of whole system, the stability and integrity of today's power system in the post contingency stage become urgent problems, even though the power systems are designed with consideration of N-1 contingency sometimes [5].

In the post contingency stage, the power system becomes more vulnerable and may enter into an emergency operation situation. If this emergency situation cannot be timely adjusted, any small disturbance caused by an unexpected control will induce further deterioration of system operation condition [6]. When the critical relays are triggered by this worsen operation condition, the system will split up and collapse inevitably, which is so called cascaded blackout. It not only brings huge economic losses to electrical industry

but also makes a great influence on human's daily life. There were many cascaded blackouts occurred in the past, such as the western U.S. blackout in 1996, the Brazil blackout in 1999, the North America blackout in 2003, the southern Sweden and eastern Denmark blackout in 2003, Europe blackout in 2006 and England blackout in 2009, etc [6]- [9]. A simplified progress of cascaded blackout is shown in Fig. 1.1.

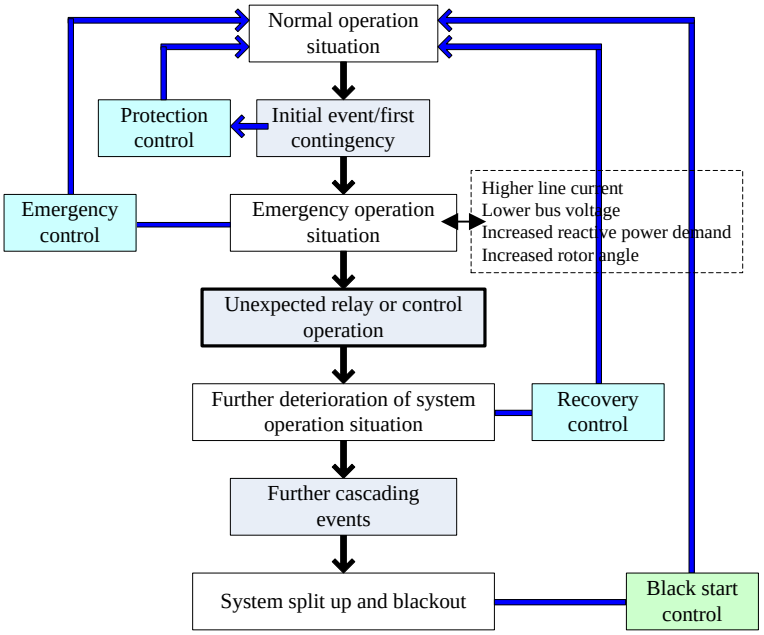

Fig. 1.1 The progress of cascading events and related protective controls

So far, many research efforts have been taken to analyze the past blackouts and search the solutions against cascading events. The main concerns are focused on two aspects. One is advanced communication tools for wide area information monitoring, and the other is improved protective control algorithms for analyzing and resolving the complex situations in cascading events.

With the development of communication and computer technology, phasor measurement units (PMUs) based wide area measurement system (WAMS) is proposed and developed with great significance, which can support a real time wide area monitoring on the varying system operation conditions [2]. Based on WAMS, the hidden failures and unexpected operations of relays and controls can be identified and traced more easily. Meanwhile, many intelligent algorithms are developed to improve the behaviors of traditional protections and controls against cascading events, such as fuzzy logic, expert system, artificial neural network, multi-agent system and etc [11]-[14]. Based on these intelligent algorithms, the protection and control system can be built with

smarter functions and flexible structures, e.g. the different control schemes (protection control, emergency control, recovery control and black start control) are designed suitably for diverse stages during the whole progress of cascading events in Fig. 1.1 [15].

1.2 Statement of the problems and project objectives

Under the circumstance described in the previous section, it would have been very valuable to have an advanced protection and control system against cascading events in power system. Such system can real time monitor and identify the emergency operation condition during cascading events, and timely supply a suitable control solution to adjust the related emergency operation condition. Thereby, the unexpected relay operations and cascading events can be prevented timely and successfully.

In order to achieve the overall purpose of this PhD project, several sub objectives are defined:

- To improve the traditional distance relay functions during voltage instability induced cascading events.
- To develop methods for emergency states detection and identification of overloaded states from Normal state and faulty state.
- To develop methods for fast analyzing the system wide operation state, while defining the relationships between vulnerable relays and other power system components under the emergency operation states.
- To develop the special protection and emergency control strategies for timely adjusting the identified emergency states.
- To build a real time hybrid simulation platform for the simulation of cascading events and the implementation of proposed special protection and emergency control scheme.
- To improve proposed protection and control scheme based on multi-agent system and process control.

1.3 Scopes and limitations

The scopes and limitations of this research are as follows:

- The long term voltage instability induced cascading events are mainly concerned; the angle instability, frequency instability and short term voltage instability have not been considered.
- As for the design of traditional relay system, the Zone 3 distance relay is mainly considered, Zone 1, Zone 2 distance relay and other types of protective relay are not the focus in this thesis.
- The sensitivity analysis based control strategy is fast enough but not that accurate when the specific system operation point cannot be reliably obtained or the operation state of power system is close to point of voltage collapse.
- Inverse tap changer control, load shedding, generator reschedule are mainly adopted as special protection and control strategies, other strategies together with black start control schemes in Fig. 1.1 are not considered in this thesis.
- Power system models are mainly developed in RTDS. Many standard models and functions in RTDS library have been used, e.g. distance relay, LTC and etc. Multi-agent based control system are mainly developed in LabVIEW based platform, also many standard functions have been used, e.g. data acquisition and analysis.
- The communication of power system is assumed to be well developed in this thesis, the communication network and time day is less discussed.

1.4 Thesis organization

This PhD thesis is categorized into seven chapters and organized as follows:

Chapter 1 Introduction

The background, motivations, main objectives and limitations of this PhD project are briefly introduced in this chapter.

Chapter 2 Literature review

This chapter gives a literature review of related project objectives, which includes power system voltage stability, some past blackouts in power system, the behaviors of traditional protective relays in blackouts, basic processes of cascading events, applications of special protection and emergency control.

Chapter 3 Emergency state detection for overloading situations

Power system modeling is presented firstly in this chapter. Then the local detection of emergency states based on improved relay functions is introduced. Also, the fundamental identification of emergency states and basic processes during the progress of cascading events are described at first glance.

Chapter 4 Sensitivity analysis for emergency states

The sensitivity analysis based emergency state analysis method is proposed in this chapter. The sensitivity analysis is based on impedance principle, and then the system wide vulnerable relays and sensitive controllers can be grouped and mapped according to sensitivities and their performance indexes. Moreover, the emergency states caused by line outage and unexpected LTC operations can also be predicted and identified based on system wide sensitivity information.

Chapter 5 Special protection and emergency control scheme design for emergency state prevention

The proposed special protection and emergency control scheme (SPECS) is designed and presented in this chapter. As for the identified emergency states, the corresponding emergency control strategies will be defined to adjust those emergency states. The priorities of control strategies are defined by integrated sensitivity and the related state signals.

Chapter 6 Implementation and improvement of SPECS

In this chapter, MAS technology will be introduced firstly. Then implementation of SPECS based on MAS is presented. A real time hybrid simulation platform based on RTDS and LabVIEW is introduced to simulate the cascading events in power system and realize the MAS based SPECS. Moreover, the process control concept is adopted to improve the SPECS's capability in dealing with possible control failures.

Chapter 7 Conclusion and perspective

The main contributions and conclusions of this thesis are given in this chapter. The topics of future work are also discussed.

List of publications

The scientific articles published during the course of this PhD project are listed.

Appendix

The detailed models and parameters of test system are listed in the appendix section, together with the pictures of control algorithms and simulation platform.

Chapter 2

Literature review

This chapter details the long term voltage instability induced cascaded blackouts in the history. The definitions related to power system stability are presented firstly. And then the classic blackouts caused by voltage instability are briefly introduced. The behaviors of traditional protection relays in blackouts are highlighted and analyzed thirdly. And finally, basic ideas and solutions for preventing this kind of cascaded blackouts are presented in brief.

2.1 Definitions of power system stability

The classic definition of power system stability is proposed and given by IEEE/CIGRE Joint Task Force on Stability Terms and Definitions in 2004 [17], which is widely accepted in the field of power system research and used in the following chapters:

"*Power system stability is the ability of an electric power system, for a given initial operating condition, to regain a state of operating equilibrium after being subjected to a physical disturbance, with most system variables bounded so that practically the entire system remains intact.*"

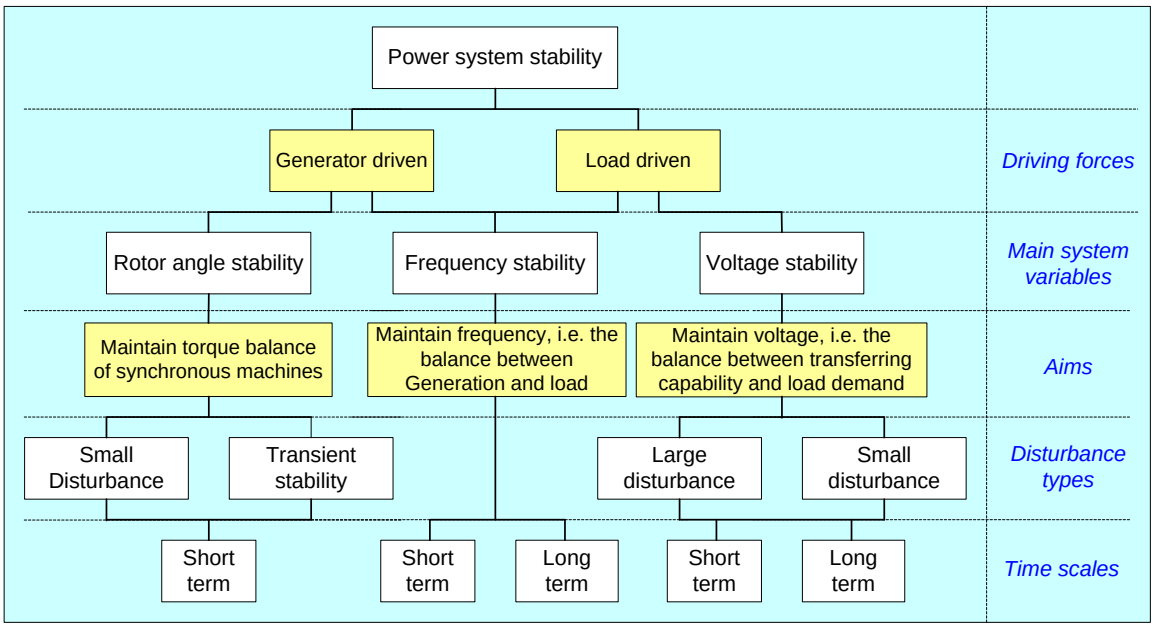

Fig. 2.1 The classic categories of power system stability [17]

Based on the definition, power system stability is essentially a single problem [1]. However, when a complex power system experiences a physical disturbance, the single problem will generate many derivatives, which could be combined with each other and turn intro complex problems. Due to different causes, aims and manifestation patterns, the classic categories of power system stability can be depicted in Fig. 2.1.

It can be seen from Fig. 2.1, the manifestation patterns of stability, which are expressed by different main system variables, are different due to the different driving forces. If the aims to maintain the equilibrium between opposing forces cannot be achieved, the instability will be induced [9]. The unbalance between synchronizing torque and damping torque, which is mainly at generator side, will induce rotor angle instability problems. The unbalance between transferring capability and load demand, which is mainly initiated from load side, will induce voltage instability problems. And the unbalance between active powers of generation and load, which could be initiated from generator side or load side, will induce frequency instability problems.

Also, due to the sizes of disturbances and response speeds of system components, the three main categories can be divided into several subcategories, as shown in Fig. 2.1.

For the large disturbance stability analysis, the detailed system model and its performance under a set of specified disturbances are required to be assessed. For the research and analysis on small disturbance stability, the linearized model of system around a system operation point is sufficient [16]. Normally, the large disturbance rotor angle stability is named transient stability, which is used to distinguish it from “steady state stability”.

When the disturbances occur in the power system, the electromechanical dynamics is mainly referred with rotor angle stability in typically several seconds. Also the dynamical characteristics of excitation systems, turbine and governor system is in the same time scale. So the related stability is regarded as short term stability.

In the post disturbance stage, when the system survived short term dynamics induced oscillation in several seconds, the system would experience long term dynamics, such as behaviors of transformer tap changers, generator limiters, boilers, etc., which is more related to frequency stability and voltage stability.

2.1.1 Definition of voltage instability

In this paper, the voltage stability problems will be mainly focused. The definition of voltage instability is proposed and discussed in Thierry Van Cutsem and Costas Vournas's book in 1998 [16]:

"*Voltage instability stems from the attempt of load dynamics to restore power consumption beyond the capability of the combined transmission and generation system.*"

Based on this definition, the key factors of voltage instability can be inferred:

- Load dynamics is the main driving force of voltage instability, which breaks the balance between load and combined transmission and generation system.
- The unbalance between load consumption and combined transmission and generation system is the total effect made by both of them.
- The transmission system has a limited capability to support the power transferring from generation to load consumption.
- The generation system also has a limited capability to supply the power demand at the load side. The limiters should be considered in the modeling.

As an important concept related to voltage instability, the term "voltage collapse" is frequently used in different phases to explain the progress of voltage instability. In early days of voltage stability research, voltage collapse and voltage instability almost had the same meaning and were used interchangeably [9] [18]. In the end of 20th century, many efforts were made to further investigate the voltage stability problems, an importance mathematic theory - bifurcation analysis are adopted in this field. The voltage collapse was no longer present the voltage instability or system wide spread voltage instability, but it is defined as a sudden catastrophic voltage transition [16] [18].

Based on voltage stability analysis in [16] [19], except the voltage collapse, the long term slow decrement of voltage could also be one final outcome of voltage instability, which is defined by dynamic characteristics of system components, especially load dynamics. The related component behaviors and phenomenon with time scales are shown in Fig. 2.2. The underline of each phenomenon represents the related time scale. The phenomenon in red box represents load side dynamic behaviors while the one in blue box represents the dynamic behavior at the side of combined generation and transmission system side.

In this thesis, the long term voltage instability induced cascading events will be focused, so the related dynamic models and behaviors will be carefully investigated.

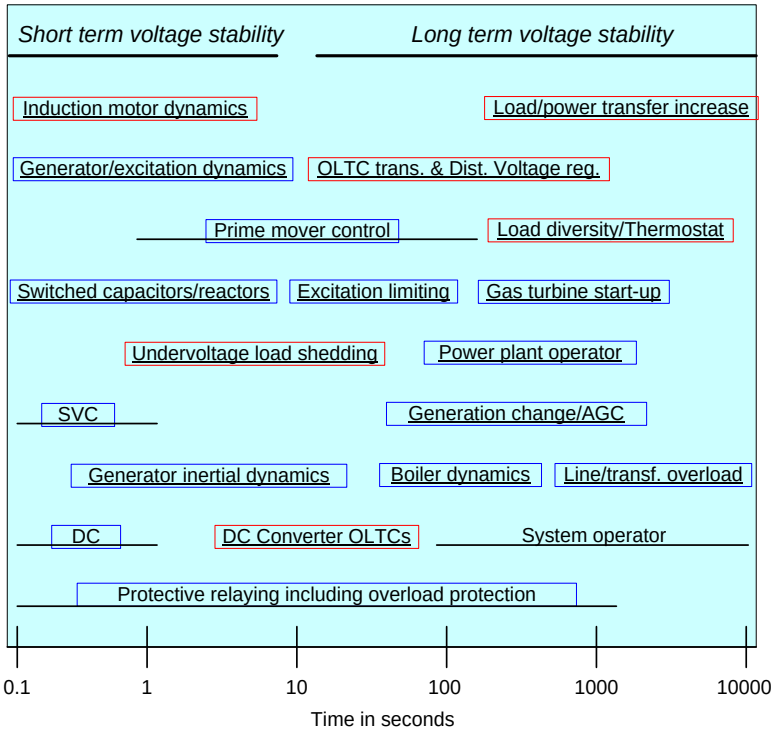

Fig. 2.2 Diverse time response of voltage stability related phenomenon [9]

2.2 Voltage instability induced blackouts in Power Systems

The power system blackouts are regarded as devastating disasters for the power system operators and customers. The India blackout in July 2012 affected over 620 million people, about half of India's population, and spread across 22 states in Northern, Eastern, and Northeast India [20]. The overload operation condition caused by load flow transferring in the post fault stage, and related unexpected backup relay operations are regarded as the main reasons of this huge event. Actually there are many blackouts occurred over the world in the past years, some of them during 1987-2012 are shown in Table 2.1 [6]-[9] [20]-[30].

Some of them collapse very fast, e.g. Europe blackout 2006 collapsed in about 20 seconds; some took longer time to whole blackout, e.g. U.S. and Canada blackout 2003 collapsed after one hour following the initiated event [31]. For analyzing the causes and progress of these blackouts, two problems may be involved. One is that plenty of detectors and recorders are required in the critical places to catch the emergency

operation conditions. The other is to distinguish between different causes which induce those emergency conditions, such as short term voltage instability and transient angle instability, or long term voltage instability and remote fault [31]. Normally, these problems will be combined and triggered each other to compose the whole progress of a cascaded blackout.

Table 2.1 Blackouts in the history

AREA	BLACKOUT EVENTS
U.S. and Canada	Western U.S. blackout 1996, U.S. and Canada blackout 2003 [6]
European	Southern Sweden and eastern Denmark blackout 2003 [21], Italy 2003 [22], Europe blackout 2006 [23]
Oceania	Australian blackout 2007 [24], New Zealand 2009 [25]
Asia	Tokyo 1987 [26], India blackout 2011, 2012 [20]
Southern America	Brazil blackout 1999 [27], 2007 [28], Colombia 2007 [29]
Africa	Tanzania 2008 [30]

In this thesis, in order to investigate the relationships between cascaded events caused by long term voltage instability. Two classic voltage instability induced cascaded blackouts are presented with time frames.

2.2.1 U.S. and Canada blackout in 2003

The U.S. and Canada blackout on August 14th, 2003 affected about 50 million people in eight states of U.S. and two provinces of Canada. About 531 generator units and 400 transmission lines were tripped off line, and approximately 63GW of load was lost. The progress and phenomenon of cascading events in this blackout are shown in Fig. 2.3 and Table 2.2 [6].

A major power outage simultaneously hit major cities in the United States and Canada shortly after 4 p.m. ET on Thursday. Blackouts struck New York City, Cleveland, Detroit, Toronto and Ottawa, as well as dozens of smaller cities and towns.

Fig. 2.3 Regions affected by U.S. and Canada blackout of Aug. 14, 2004 [32]

Based on the U.S. and Canada Power System Outage Task Force report [8] [32], the critical event leading to fast propagated cascading was the event 5 at 4:05:57 pm, i.e. tripping of the Sammis-Star line by Samis end Zone 3 relay. This unexpected relay operation and consequent cascaded blackout could have been prevented by load shedding in northeast Ohio prior to the tipping time. Also, if the Energy Management System (EMS) is reliable, the emergency condition could have been corrected earlier in the second event.

Table 2.2 The progress of U.S. and Canada blackout in 2003

	EVENTS	PHENOMENON
1	**1:31 pm 5 generation units trip and shut down**	Several remote and local generators were generating high level of reactive power. 5 voltage regulator tripped to manual mode because of over excitation limits
2	**3:05:41 pm-3:57:35 pm, three 345kV lines trip due to contact with trees**	This overloaded the underlying 138kV system and depressed voltages. No proper operational actions due to EMS failure.
3	**3:39:17-4:08:59 pm, 16 138kV lines trip due to overloading situation**	The loss of 138kV lines overloaded the Sammis-Star line
4	**4:05:57 pm, the Sammis-Star line tripped by Sammis end Zone 3 relay**	Further overload and trips were induced on the additional lines in Ohio and Michigan by operations of Zone 3 relays or Zone 2 relays set similar to the followed Zone 3 relays.
5	**4:08:59 pm, Galion-Ohio and Central Muskinghun 345kV lines trip on Zone 3**	This Caused major power swings through New York and Ontario and into Michigan. Low voltage/high load conditions propagated through the system.
6	**4:13 pm, most of the North East of U.S. and parts of Canada blackout.**	There were only a few islands which remain operating.

2.2.2 The blackout case in Sweden and Denmark 2003

The basic progress of this blackout is shown in Fig. 2.4 and Table 2.3 [10]. Before the blackout, the Nordel power system was operated in a secure and stable scope. Two 400-kV lines and the HVDC links connecting Nordel system with continental Europe were out of service due to scheduled maintenance activities. However, the system loading situation was still not stress even considering these scheduled outages.

At 12.30 pm of September 23, the first contingency occurred. A 1200 MW nuclear unit was lost due to mechanical failure, which induced some load flow transferring in northern Nordel system. Then the system was resumed and operated in a stable operation

condition within a minute. However at 12.35 pm, a double bus bar fault occurred, which resulted in the loss of two nuclear units and several transmission lines along the west coast of southern Sweden. These outages triggered a heavy power oscillation and a big load flow transferring from north to south on the remaining lines. Due to some existing frequency based control measures, such as under frequency load shedding, the system frequency recovered into the secure scope within two minutes. But in the main loading areas of southern Sweden, the voltages decreased, which induced a number of load tap changers (LTC) activated to recover the distribution side voltages. Then the voltages at the transmission side decreased further inevitably.

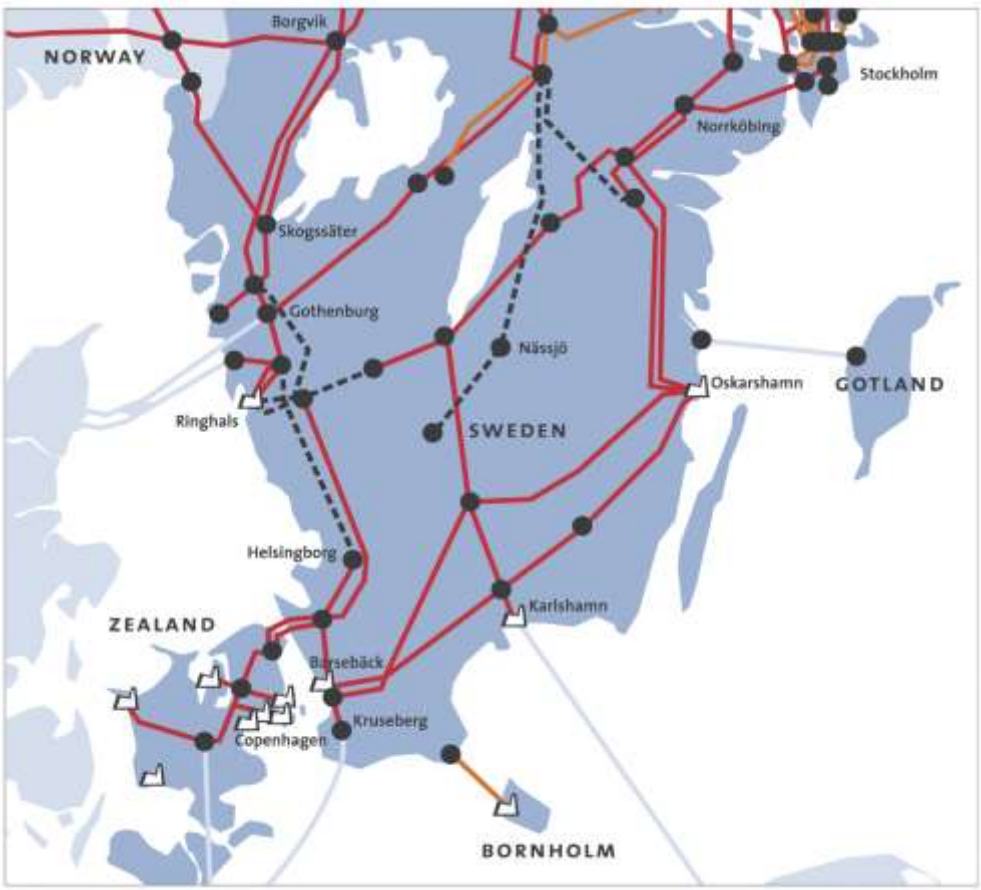

Fig. 2.4 The blackout in Sweden-Denmark in 2003 [33]

Thereafter, the distance relays on the remaining transmission lines detected the heavily overload condition violating the impedance criteria, and unexpectedly tripped the breakers in the critical grid section between central and south Sweden. Then the whole grip split up into two parts. The upside part including north and central Sweden was recovered soon and kept intact. The downside part, comprising southern Sweden and

eastern Denmark, experienced further cascading trips due to a massive inadequacy of generation. And this subsystem collapsed within seconds both on voltage and frequency.

In this blackout, the total loss of supply was about 1850 MW in Denmark and 4500 MW in Sweden. Moreover, it took about 7 hours to restore all the power equipments in this part of Nordel power system. The total non-supplied demand due to this blackout was about 8 GWh in Denmark and 10 GWh in Sweden.

Table 2.3 The progress of Sweden and Denmark blackout in 2003

	EVENTS	PHENOMENON
1	**12:30 pm, 1200 MW nuclear unit outage**	The system resumed to stable operating conditions within less than a minute.
2	**12:35 pm, a double bus bar fault occurred**.	Two nuclear units (1750MW) and several transmission lines along the west coast of southern Sweden were lost, which induced a big load flow transferring from north to south.
3	**12:35:20, action of numerous load tap changers**	The load demand recovered around the capital city of Stockholm, but the voltage decreased further on the 400 kV grids to critical levels (320kV).
4	**12:36 pm, distance relays trip lines in the critical grid.**	The heavily overload conditions violated the impedance criteria on the lines between central and south Sweden. Then the whole grid split up into two parts. The upside part was recovered soon and kept intact.
5	**12:37 pm, voltage collapse in downside subsystem**	The downside part, comprising southern Sweden and eastern Denmark, experienced further cascading trips due to a massive inadequacy of generation. And within seconds, this subsystem collapsed on voltage and frequency.

2.2.3 The anatomy of voltage instability induced blackouts

Based on those classic cases of voltage instability induced cascading events in the past blackouts, some common involved mechanism and basic processes can be observed in Fig. 2.5, which are derived from [18] [34] [35].

2.2.3.1 Common mechanism

Normally, before the voltage instability related problem emerging, the power system is in a normal operation condition but gets weaken due to some scheduled maintenances or normal fault clearing induced outages. The EMS and communication failure can be also regarded as an extra weaken operation condition, such as the situation in the case of U.S. and Canada blackout in 2003. The weaken conditions represent less margin in system voltage stability, i.e. generators are operated close to its capability limits, and transmission system is close to its loadability limit [1]. When the system is operated

under the weaken conditions, a tiny initial event is more likely to trigger enough load flow transferring and drive some system components cross the capability limits for maintaining the system voltages, which is the occurrence of voltage instability, based on definition of voltage instability in the yellow block in Fig. 2.5.

As for the system components which already hit their capability limits, they are operated in overloading situation with higher currents, lower voltages and increased reactive power demand, etc. The controllers on these system components would be triggered to protect the related components or restore the load demand and load side voltage as their normal functions, e.g. current limitation of generators, thermostatic load restoration and load tap changer operation (when long term voltage stability is concerned). These normal functions of controllers would deteriorate the overloading situation further. Moreover, if the backup relays on these components detect overloading situation violating its settings and trip the related components, then the system structure will be changed and normally a big load flow will be transferred to the neighboring area and remaining system components. These operations of controllers and relays are obviously unexpected when the system is in overloading situation.

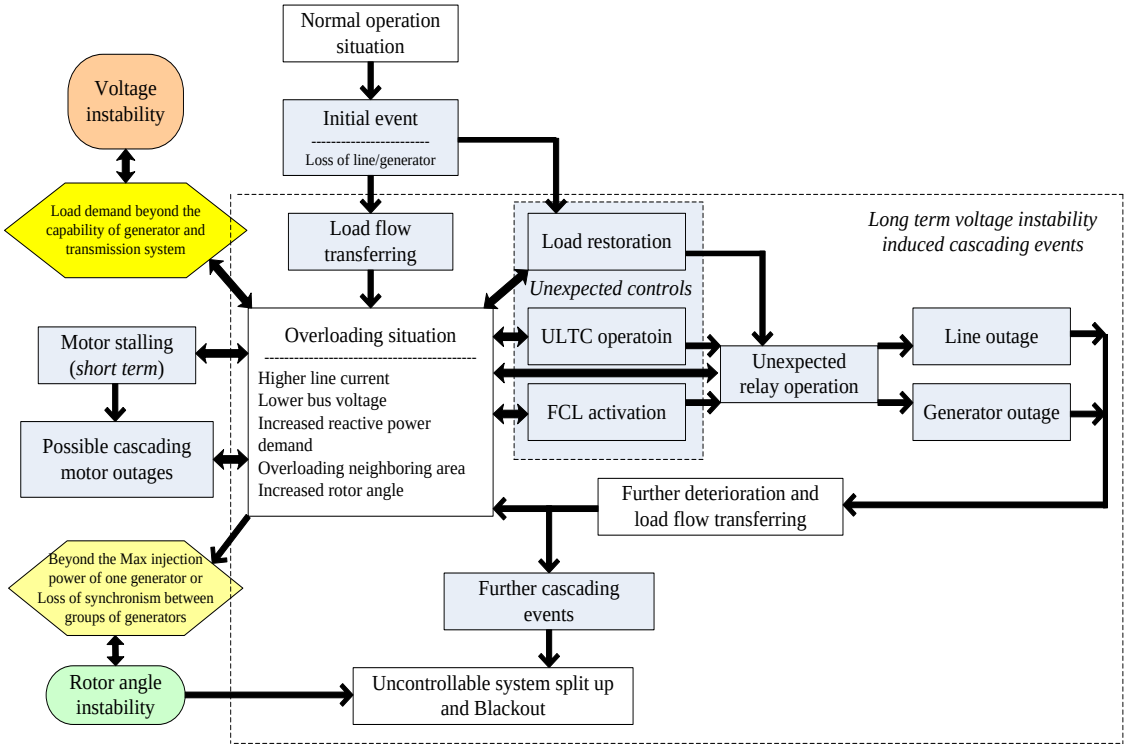

Fig. 2.5 The basic progress and mechanism of cascading events

When overloading situation is propagated from local to system wide, more unexpected operations of controllers and relays will be involved subsequently, and the system will be split up uncontrollably, which is so called cascading events. If there is no reliable and timely regulation control during this propagation progress, the blackout will occur inevitably.

Besides, the rotor angle instability and frequency instability problems could be triggered during cascading events when the overloading situation induces the rotor angle and frequency approaching the related limits. They also contribute to cascaded blackout apparently but not the primary cause of voltage instability induced cases, which are consequently not in the research scope of this thesis.

2.2.3.2 Basic processes

Based on above discussions, it can be found that the causes of cascading events leading to cascaded blackouts are diverse, which normally involve faults, unexpected relay operations, controller malfunctions, power component failures, communication problems, operation errors and etc [36]. The complexity of those causes makes it difficult to catch and predict the exact sequence of cascading events. But in the progress of cascading events, the basic patterns with specific characteristics, which may trigger other events, can be easily identified and benefit for monitoring the whole progress of the cascading events [37]-[39]. In this thesis, in order to link the cause-effect relationship between different events, the basic processes of cascading events considering the long term dynamics are list similarly, as follows:

- Transmission Line or generator tripping due to faults

As we know, the traditional protective relay system is indispensable for system operation security and should reliably trip the breakers on related components to clear the fault timely. But those actions will unplanned weaken the original power system to a maybe N-1 or N-k condition, and make it vulnerable to endure one more disturbance, which will help to make a “breeding ground” for cascading events.

- Overload due to line or generator outage induced load flow transferring

Due to the unplanned outages of transmission lines and generators, the load flow will be redistributed to the remaining lines and generators. If there are no predesigned suitable regulation methods, the large amount of load flow transferring will be a big challenge for the loadability limit of related lines, generators and protective relays.

- Overload due to load side voltage control induced load increment

Sometimes, in the post fault stage, the outage induced load flow transferring doesn't cause any emergency state but makes the voltage lower, which will induce load side voltage control operation, such as LTC operation and load restoration characteristics in the blackout cases mentioned in the former section. The continual LTC operations and load restoration characteristics will strengthen the trend of load flow transferring and induce the long term voltage instability.

- Transmission line or generator tripping due to overloading

Owing to load flow transferring induced overloading situations, namely, the loading level of transmission lines or generators violates loadability limits or capability limit settings, these overloading situations could cause transmission line tripping or generator tripping unexpectedly.

- Generator tripping due to abnormal frequency

When some important inter-area transmission lines get tripped, the power system will be unexpectedly separated into several islands, which may induce a big power unbalance in those islands. Then both voltage and frequency will be deviated from a normal level to an emergency level. Some important generator groups will be tripped under this situation which will deteriorate islanded power systems and finally induce whole system collapse.

- Under frequency and voltage load shedding

The normal under frequency load shedding (UFLS) and under voltage load shedding (UVLS) scheme may be triggered when the system frequency and voltage fall below the preset values to prevent the frequency instability and voltage instability. But the traditional UFLS and UVLS sometimes cannot give a sensitive and precise reaction to the system frequency and voltage deviation, which could make a big amount of load lost and also a big disturbance to the local system.

In this thesis, the UVLS scheme and voltage related regulations during the long term voltage instability induced cascading events will be mainly focused.

2.3 The behaviors of traditional protective relays in blackouts

2.3.1 Traditional protective relays

The traditional protective relays are normally set with each distributed power system component for detecting faults and abnormal states and initiating trip of related circuit

breakers in order to prevent possible component damage [4]. The protective device is usually comprised by several elements that are designed to detect system condition, make decisions and take actions as required, which is depicted in Fig. 2.6 [4].

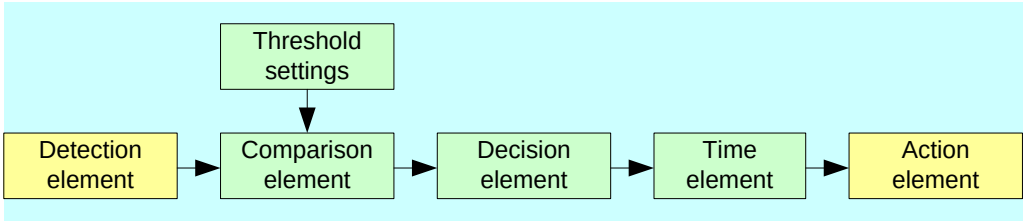

Fig. 2.6 Protective device functional elements

The local protective system firstly measures certain system variables, such as voltages and currents; and compares these system variables or their derivatives with preset threshold settings. If the comparison indicates a violation condition, the decision element will be initiated with time element to determine the related condition and time delay. Finally, when the time delay is run out and violation condition is still hold, the action element will be released to operate, i.e. the related circuit breakers are ordered to trip the related component from network [40].

With development of protection technology, the protective relays can be categorized into many types based on protected objects, detection methods, detected system variables, characteristics of threshold settings, comparison methods, decision algorithms and hardware conditions [40]. In this thesis, due to research requirement and the obvious performances in historical cascading events, the zoned distance relay with direction circle characteristics [4] will be adopted as the study example in this thesis. The Relay 1 on the transmission line *ij* between Bus *i* and Bus *j* in Fig. 2.7 is chosen as a research object. The classic characteristic circles of a three zone distance relay can be observed in this figure.

The first Zone of Relay 1, designated as Zone 1, is set to trip the related line immediately with no time delay. Zone 1 is set for approximately 80-90% of the related line impedance in order to avoid unnecessary trips for the faults occurred beyond the remote bus *j*. Zone 2 is set to protect 100% of the protected line with adequate margin, i.e. extra length about 50% of the shortest adjacent line, and is set with time delay T2. T2 is typically set to about 15-30 cycles. Technically, Zone 3 of Relay 1 is applied as a local backup for Zone 1 and Zone 2 of Relay1 and a remote backup for Zone 1 and Zone 2 of Relay 3 on the adjacent line *jk*. Zone 3 is set to reach through 100% of the impedance of

two lines and 25% of the third line *kl*. The time delay T3 for Zone 3 is normally set to about 25-90 cycles [4] [41]. The application of the timers, such as T2 and T3, provide coordination time intervals for the relay operation in the end zone of each line.

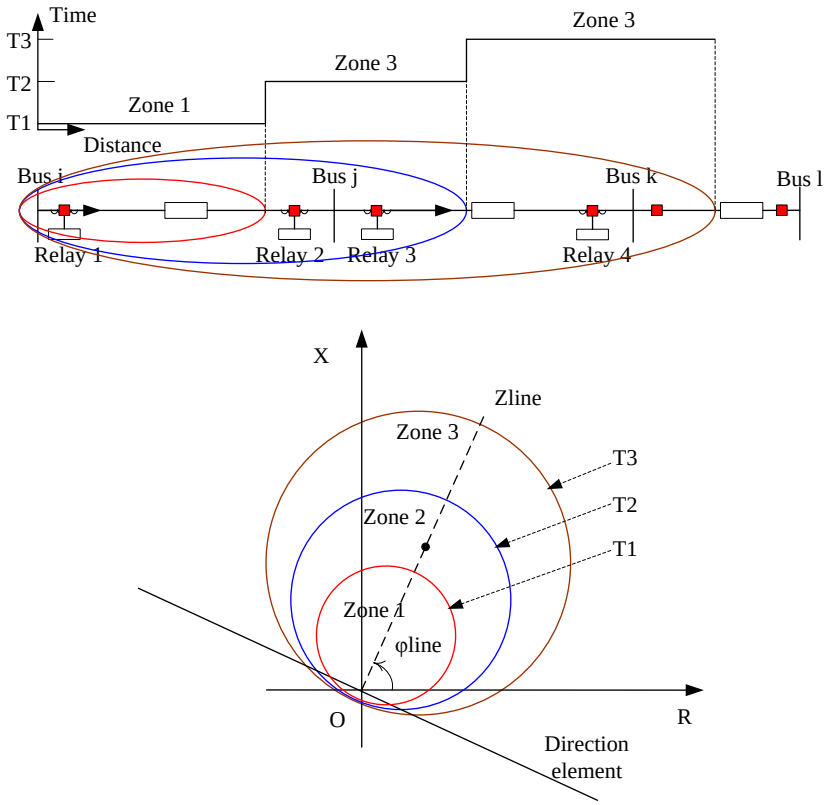

Fig. 2.7 Step time and impedance zones for distance relays

The measured impedance of Relay 1 will depend on the load flow on the transmission line *ij*. And the permitted line loading is defined by thermal ratings and voltage instability criteria of the related power components [42]. Then the possible loci of the measured impedance in the first quadrant of impedance plane can be depicted by two red curves in Fig. 2.8, when the apparent load power is fixed to two specific values. Z_{aij} is one measured point of impedance, φ_{ij} is the power factor angle of load flow. It can be inferred that the radius of red curve gets smaller when the load power gets larger; meanwhile, the measured impedance will move in the d1 direction when the power factor gets decreased and the magnitude of load flow is fixed. When the power factor is fixed, the Z_{aij} will move in d2 direction with constant φ_{ij} as the load flow power gets larger.

Also based on the deduction in [38] [42], when the active load power is fixed, Z_{aij} will move in d4 direction (along the blue circle) as the reactive power of load flow gets

increased. Similarly with fixed reactive power, Z_{aij} will move in d3 direction as the active power gets increased. Therefore, any increment in real or reactive power may induce those vulnerable distance relays to operate unexpectedly.

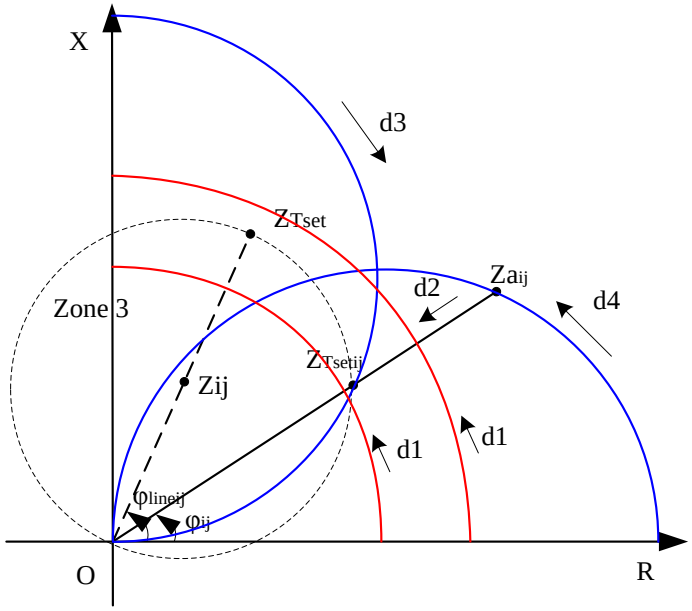

Fig. 2.8 The possible loci of measured impedance during load power variations

2.3.2 The behaviors of distance relays in cascading events

It can be easily found in those past blackouts, Zone 3 distance relay played an important role in the propagation progress of cascading events and overloading condition, as shown in Fig. 2.9. The overloading situation would be detected by Zone 3 distance relay firstly, and this situation will be propagated quickly to neighboring area if Zone 3 relay trips the related power component. Then the Zone 3 relays in neighboring area will detect the overloading situation and start a new round of cascading trips. Hereby, some researchers even suggested to completely eliminating the Zone 3 relay, to remove the possibility of the unexpected Zone 3 relay operations forever [41]. However, as a backup to zone 1 and zone 2 protections, Zone 3 relay with higher setting and longer reach is an indispensible part of zoned distance protection to protect transmission and distribution lines. Whether it should be replaced by other relays needs to be carefully evaluated.

However, from the view point of cascading events prevention, the Zone 3 relay can be a sensitive detector for system stability under stressed operation conditions when its

settings are designed considering the stability boundaries [43]. Furthermore, if the Zone 3 functions can be make immune to tripping under overloading situations, then Zone 3 relay will not be an “accomplice” to cascading events any more, and it can be a good “assistant” to prevent cascading events.

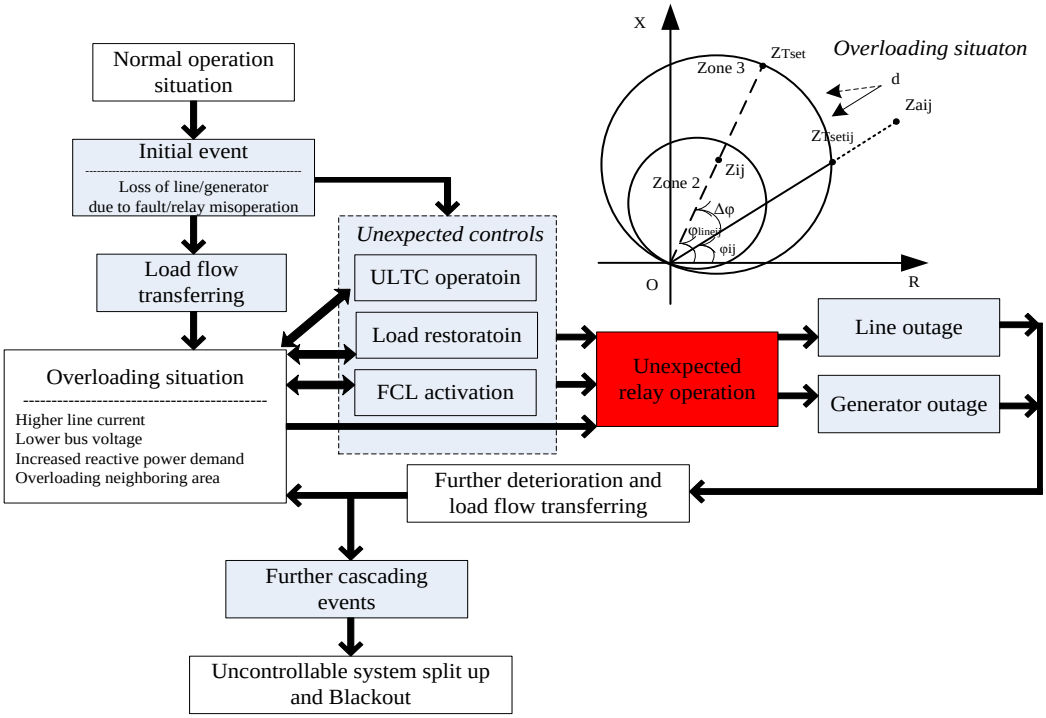

Fig. 2.9 The flowchart of voltage instability induced cascading blackouts

So, if in the early stage of cascading events, the distance relays could online differentiate those overloading situations from short circuits, then those unexpected relay operations can be blocked for a short period which will give time for execution of emergency controls. Meanwhile, according to identified different overloading situations, the corresponding emergency control strategies can be defined more specifically. In this way, the cascading relay operations will not be triggered unexpectedly, and the total blackout can be effectively prevented.

2.4 Solutions for voltage instability induced cascading events

In order to prevent the voltage instability induced problems, there are two aspects can be considered [9].

- Considering the voltage stability in the construction of power system network

Namely, in the power system planning level, the reactive power dispatching is required to be considered together with active power. The increasing remote power demand with slow transmission system construction or maintenance should be tried to avoid. Also the emergency reactive reserve and related compensators may be planed considering the situation of N-2 contingency. Direct current (DC) network may become an important part in future power system with less voltage problems.

- Considering the voltage stability in the operation and control of power system

Since most of power systems with traditional protection and control devices are already built up and operated, the new technologies are required to improve the functions of supervisory, protection and control on the power systems in a wide area, such as wide area measurement system (WAMS) based on phasor measurement units (PMU), special protection and emergency controls against specific voltage instability problems, etc.

In this thesis, the design of special protection and control strategy in the second consideration is the main focus.

2.4.1 Wide area measurement system

Since the 1970s, synchronized-measurement technology (SMT) has been developed, and then wide area measurement system (WAMS) starts to emerge [2]. Unlike traditional measurement systems, the phasor measurement units (PMU), which are the key elements of WAMS, provide accurate measurement of system dynamics in real time based on global positioning system (GPS) and SMT. With the precise and fast measurements with synchronized time stamps, the Control center is able to initiate proper response timely and protect a system wide network from big disturbances [36].

As a development trend of WAMS' application in power system [44][45], a multilayer structure is adopted to build the WAMS based system wide monitor, protection and control system, as shown in Fig. 2.10.

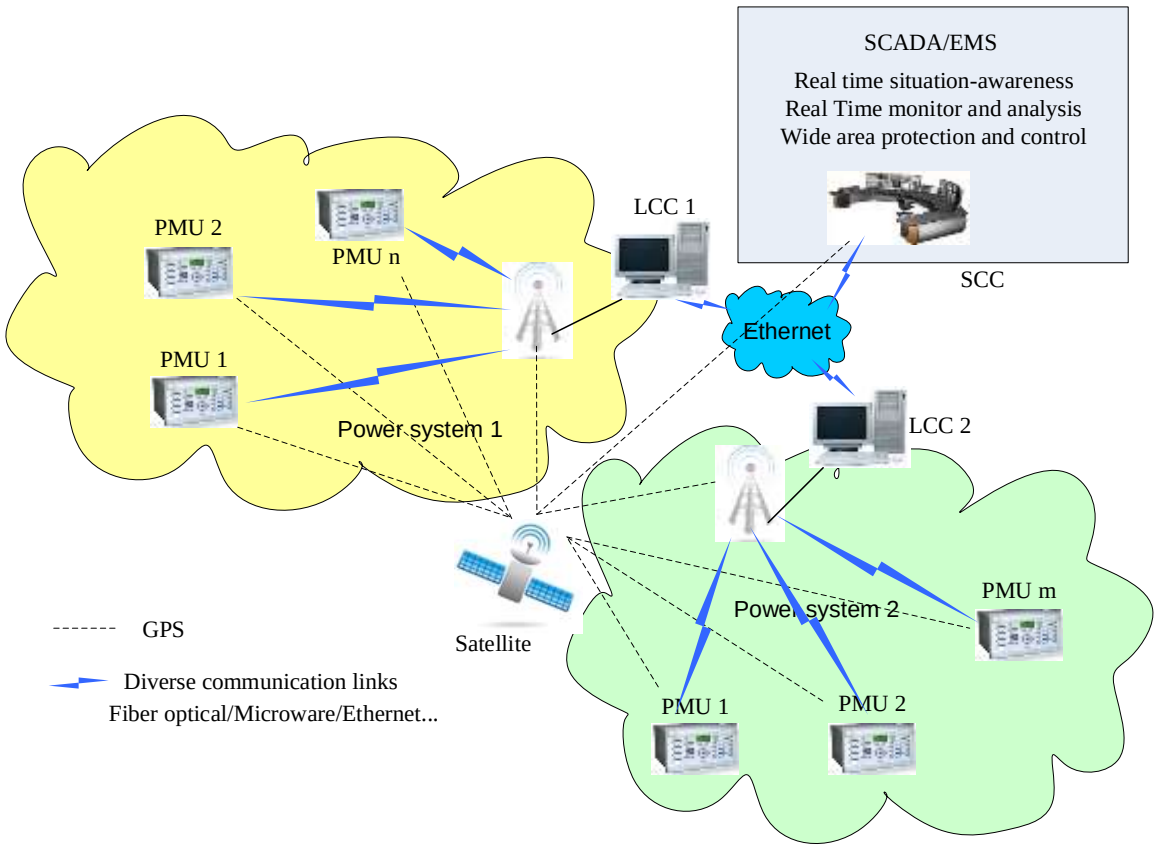

Fig. 2.10 WAMS based system wide monitor, protection and control system

The PMUs or PMUs with protection and control functions compose the bottom layer. The middle layer consists of several local Control centers (LCCs) which protect and control local power system and PMUs. The System Control center is in the top level and behaviors as the coordinator for all the elements in the lower layers. Actually there is a wide range of WAMS' application, some important research fields are list as follows:

- Real time situation awareness of power systems [46][47]
- Advanced early warning system [48]
- Dynamic security assessment [49]
- Real time state estimation [50][51]
- Real time congestion management [52]
- Real time protection and control strategy [53][54]
- Others [53][55]

Some applications could have been contained in original functions of supervisory control and data acquisition system (SCADA) and energy management systems (EMS). Typical SCADA and EMS have slow data update rate and cannot meet the requirement of

cascading events prevention [44]. Based on WAMS, the traditional monitor, protection and control functions in different time scale can be improved and cooperate with each other, which can help to define the suitable system wide protection and control strategies against cascaded blackouts [56]-[58]. The relationship between WAMS in protection and SCADA/EMS can be observed in Fig. 2.11.

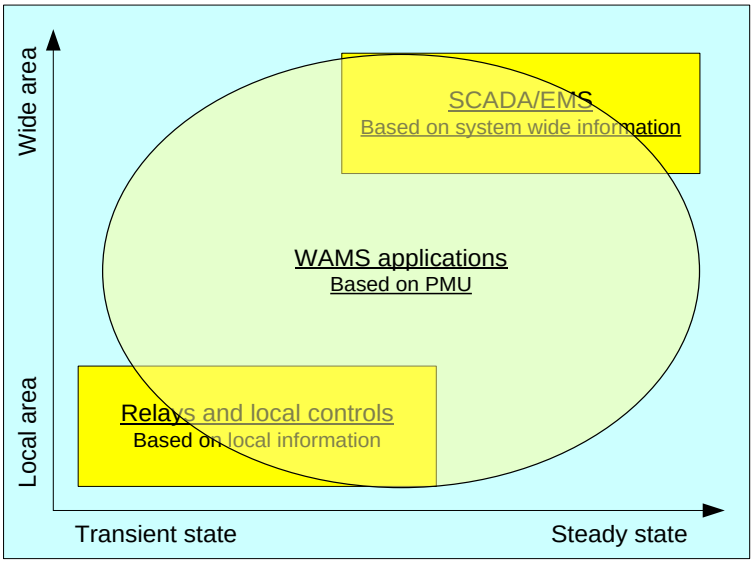

Fig. 2.11 WAMS application in power system

In those local information based protection and controls, the communication delay is very small and can be neglected normally. But when system wide information is concerned, the communication delay sometimes cannot be neglected, which is depend on communication modes and medium. Considering a remote signal used in feedback control, the communication delay time may be varied from several milliseconds to above hundreds of milliseconds, which could be a problem in a transient situation. In U.S BPA power system, the communication delay of fiber optical system is about 38ms, and microwave communication delay time is above 80ms [59]. Furthermore, considering the feedback signal to the remote device or Control center, it will be delayed by diverse measurement devices, routers in the network, waiting for signal synchronizing and mass data processing, the actual communication delay time is generally more than 100ms [60].

2.4.2 Special protection and emergency control

Since 2004, the U.S- Canada Power System Outage Task-Force has been established to investigate the causes of the blackouts and the solutions to prevent the possible blackouts [8]. The related recommendations were made and gave a development direction

of cascaded blackout prevention. Except the related operation standards and policies, "employing special protection" and "resolving issues related to Zone 3 relays" are strongly recommended, which belongs to strategy improvements in protection control level, emergency control level and recovery control level in Fig. 1.1.

As for resolving issues related to Zone 3 relays, one idea is to adjust the settings of those involved relays to match power system conditions in real time. The information from wide area measurement system (WAMS) could be utilized for this idea realization [61][62]. The other idea is to prevent cascaded events by identify potential unexpected relay operations ahead of time. In [63][64], a Fuzzy Inference System (FIS) based method was proposed to identify successive line and generator outage events due to those unexpected relay operations in the post contingency stage. Also, many fast identification algorithms were developed based on dc load flow sensitivities, including line outage distribution factor (LODF) and generator shift factor (GSF). The method predicted the component outage caused by load flow transferring and distinguished the overload situation [65]. Moreover, the variation of system state variables during transient period after an outage has also been studied over the whole system [66] [67] or by local measured information [68]. However, those dc load flow based predicting methods only consider the flow of active power and assume bus voltages and reactive power flow being constant, which is not the case in real situation, especially in the cascading events. Moreover, these methods related to Zone 3 relay may fail when the system is already operated close to the collapse point. So, further investigation in this area is very necessary.

On the other side, special protection system and emergency control strategy are recommended to detect the emergent system state (which may result in the unexpected relay operations), adjust the abnormal state and keep the system operated in the stable region. According to North American electric Reliability Council (NERC) planning standard [69], Special protection system can be defined as:

"*A special protection system (SPS) or remedial action scheme (RAS) is designed to detect abnormal system conditions and take preplanned, corrective action (other than the isolation of faulted elements) to provide acceptable system performance.*"

And the emergency control represents the related control strategy against power system emergency which is a condition or state of system operation characterized by one or more system inequality constraints [36]. The most common SPS and emergency

control schemes against long term voltage instability induced cascading events include phase angle regulator, control area interchange, capacitors, generator reschedule, load shedding, LTC emergency control and etc [37] [70]-[73].

Moreover, based on WAMS based system wide information, the basic event patterns or processes of cascading events can be identified and traced timely [61]; the composition and progress of cascading events in a blackout can be easily figured out. Then the combined protection and control strategies will be accordingly designed for different patterns to timely prevent the propagation of cascading events and mitigate the whole catastrophic outages.

2.5 Summary

This chapter reviews the relevant topics in the literature, including the power system stability, classic blackouts in the history, the common mechanism of voltage instability induced cascaded blackouts, the behaviors of traditional protective relays in cascading events, wide area measurement system, SPS and emergency controls.

Chapter 3

Emergency state detection for overloading situations

3.1 Introduction

In order to finally find the suitable solutions against the voltage instability induced cascaded blackouts, the first step is to model the critical system components and simulate the progress of voltage instability induced cascading events. Then the detection methods for those overload emergency states will be investigated subsequently.

In this chapter, the modeling of key power system components will be firstly introduced, which contains generation system (including its controllers), restoration load model, load tap changer model and distance relay models. Based on the reviews of past voltage instability induced cascaded blackouts, the power system of eastern Denmark, which experienced a blackout in 2003, is suitable and adopted for simulating the cascading blackouts. Then, the simulated scenarios of the long term voltage instability induced cascading events based on real time digital simulator (RTDS) are presented.

On the other side, based on distance relay models with the consideration of loadability, the detection of emergency states is primarily designed to sense the emergency states locally. As for complex situations, i.e. cascading events, the basic process identification based on system wide information is briefly introduced.

3.2 Power system modeling

In this thesis, modeling work of power system is mainly conducted in RTDS [75], which can simulate the whole progress of cascaded blackouts and help execute effective control measures in real time.

3.2.1 Generation system

As a primary source of active power and reactive power in the power system, synchronous generators are mainly responsible for maintaining the bus voltages and system frequency. Their characteristics, capabilities and limitations define the strength of

power system to a large extent. The excitation system and governor/turbine system are normally installed together with synchronous generators to control the bus voltages and system frequency in a secure scope [1], as show in Fig. 3.1 (a). P, Q, V and I are active power, reactive power, voltage and current respectively which are sent from the related generator to the system network. T_m and P_m are mechanic torque and power, E_{fd} and I_{fd} are excitation voltage and current, P_0 and w_0 are specific set points of active power and generator speed respectively.

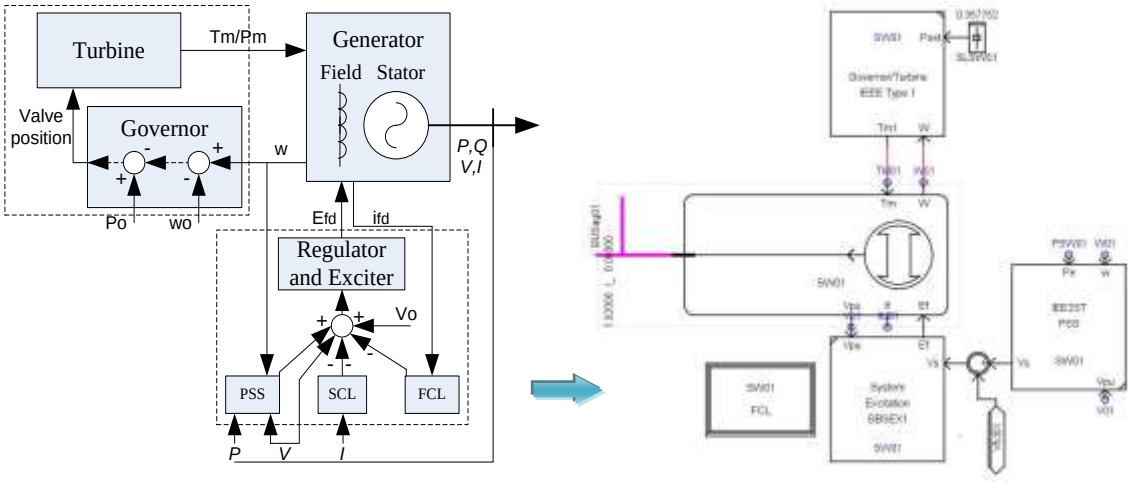

(a) Generator and related controls (b) The generator and control models in RSCAD/RTDS

Fig. 3.1 Field thermal capability and over excitation limit

The synchronous generator is modeled by standard RTDS model with two Q-axis rotor windings, the governor and turbine system in the dashed box are modeled by IEEE type 1 speed governor and steam turbine model [76]. While, the excitation systems, including exciter and regulator, power system stabilizer (PSS), stator current limiter (SCL) and field current limiter (FCL) are modeled by standard RTDS models together with user defined models (i.e. FCL), as show in Fig. 3.1 (b).

3.2.1.1 Governor and turbine system

The role of governor is to realize the frequency control, which keeps the related generator run closely to the nominal speed (w_0) and produce preset active power (P_0). In Fig. 3.1, it can be seen when the difference between the rotating speed and the nominal one has been detected by governor, it will adjust the steam or water input (valve position) to the Turbine. As a primary frequency control, the governor will keep the frequency locally and P_0 is a constant set point.

If the system experiences a big disturbance, such as a line or generator outage, the primary frequency control as a local control method may be not enough to keep the scheduled power transferring between areas. Moreover, in the post stage of N-1 or N-k contingency, a large power transferring may drive the transmission system closer to its loadability limits, which will cause the problem of voltage instability. In order to strength the ability of governor system to compensate the system power unbalance or regulate the power transferring within system loadability limits, the set point of active power will be adjusted by an upper controller, which use system power differences as inputs. This kind of control scheme can be regarded as one kind of fast generator reschedules (GR) at the second frequency control level [1], which will be discussed in Chapter V and VI.

3.2.1.2 Excitation control system

The excitation systems normally include exciter and regulator, PSS, SCL, FCL and load compensator. The load compensator is not considered in this thesis for the sake of simplicity. The exciter and regulator are modeled by Brown Boveri Static Exciter model (BBSEX1) in RTDS [1]. It is responsible to provide and quickly adjust the field current of synchronous generator to maintain the generator terminal voltage when the output varies due to outside disturbances. The excitation power of the static exciter is provided by a transformer connected to the local bus or an auxiliary bus, and the DC power required by the generator is produced through a thyristor-controlled rectifier.

The PSS is modeled by IEE2ST model in RTDS [77]. It is a compensation circuit providing additional input signal to the exciter, which aims to damp power system oscillations. In the test system used in this thesis, all the generators are equipped with governors and PSS with normal gain and response time, which is important to obtain more stable and fast-damped system frequency in the simulation cases of voltage instability induced cascaded blackouts.

The SCL is modeled inside the exciter model. It is used to prevent excessive current in the generator stator winding. Normally, the stator winding with larger thermal inertia allows overload to some extent and sends an alarm (the operator will decrease the output of reactive power or sometimes active power), which will be regarded as a detection method for overloading situations in the later contents.

The FCL is modeled by basic functions in RTDS, and the schematic diagram and functional characteristics are shown in Fig. 3.2 [1]. The FCL typically detects the high

field current and limits it to a pre-set value after a time delay. The FCL produces a voltage signal that is added to the main summing junction of the exciter. In normal operation states, this signal is equal to zero; when FCL activates, the signal will participate the exciter control to limit the field current. In Fig. 3.2, the higher setting I_{fdmax2} provides an instantaneous limiting action when full load current becomes 1.6 times. A lower setting I_{fdmax1} provides a limiting action with time delay, which is a ramp time function of the detected actual field current [78]. In this way, the limitation mechanism is run in two layers with different time responses which make generator with the ability to endure the temporary overloading situation.

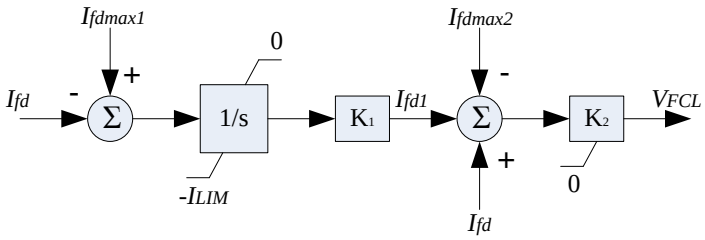

(a) FCL block diagram

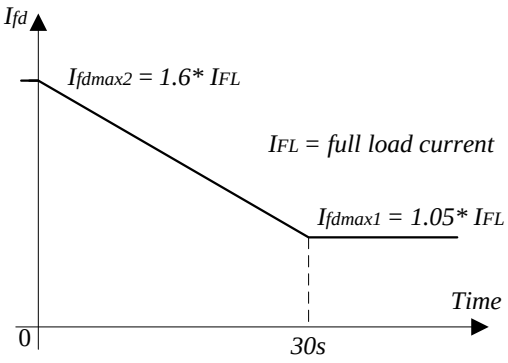

(b) Functional characteristics of FCL

Fig. 3.2 Block diagram and functional characteristics of FCL

If the FCL fails to limit the excessive field current in a long time delay, according to the ANSI standard C50.13-1977 reproduced in Fig. 3.3 [79], the limiter will initiate an exciter field breaker trip and a generator unit trip. The detailed parameters can be found in Appendix. A.1.

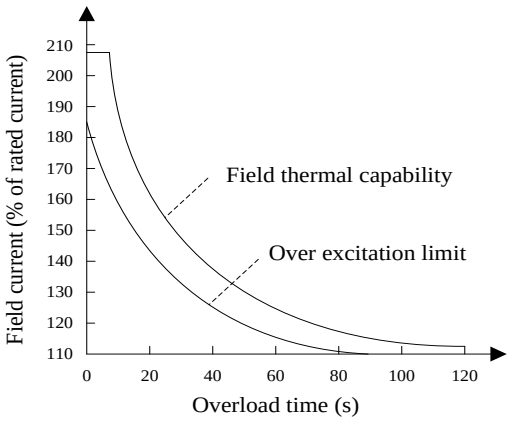

Fig. 3.3Field thermal capability and over excitation limit

3.2.2 Restoration load

In this thesis, the lumped restoration dynamics of load for long term voltage stability study is modeled as follows [16]:

$$P_L = z_P \, P_{L0} \left(\frac{V}{V_0}\right)^{\alpha_t} \tag{3.1}$$

$$Q_L = z_Q \, Q_{L0} (\frac{V}{V_0})^{\beta_t} \tag{3.2}$$

$$T_P \dot{z}_P = (\frac{V}{V_0})^{\alpha_s} - z_p (\frac{V}{V_0})^{\alpha_t} \tag{3.3}$$

$$T_Q \dot{z}_Q = \left(\frac{V}{V_0}\right)^{\beta_s} - z_Q \left(\frac{V}{V_0}\right)^{\beta_t} \tag{3.4}$$

where P_L, Q_L are the active and reactive power of the load respectively; P_{L0}, Q_{L0} are the active and reactive power respectively at the nominal voltage V_0 ; z_P , z_Q are dimensionless state variables associated with load dynamics; α_t, β_t represent the transient load exponents respectively, and α_s, β_s are the steady state ones; T_P, T_Q are the load restoration time constant respectively. In steady state, the voltage characteristics can be given by (3.5) and (3.6):

$$P_{Ls} = P_{L0} \left(\frac{V}{V_0}\right)^{\alpha_s} \tag{3.5}$$

$$Q_{Ls} = Q_{L0} (\frac{V}{V_0})^{\beta_s} \tag{3.6}$$

The classic parameters are adopted normally: $\alpha_s = \beta_s = 0$, $\alpha_t = \beta_t = 2$ and $T_P = T_Q = 100s$ [16]. And this load model is initialized with $z_P = z_Q = 1$.

When a big voltage variation is experienced on the load bus *i*, the load will firstly respond with its transient characteristics (3.1) (3.2), and then slowly recover based on (3.1)-(3.4). Finally the load will reach its steady state characteristics (3.5) (3.6). This restoration load represents the aggregate behavior of a number of voltage controlled loads or the consumer reaction following a disturbance, e.g. switching on more devices to compensate for the reduced power supplied.

3.2.3 Load tap changer

As one of the key mechanisms in long term load restoration, the load tap changers (LTC) are modeled on some critical load side transformers in the test systems; which can be mathematically expressed by (3.7) and (3.8) [16].

$$t_{k+1} = t_k + \Delta T_k, \qquad k = 0, 1, \ldots \tag{3.7}$$

$$r_{k+1} = \begin{cases} r_k + \Delta r & \text{if} \quad V_2 > V_2^{max} + d \ \text{ and } r_k < r^{max} \\ r_k - \Delta r & \text{if} \quad V_2 < V_2^{min} - d \ \text{ and } r_k > r^{min} \\ r_k & \text{else} \end{cases} \tag{3.8}$$

where the tap ratio of LTC transformer is $r{:}\,1$, the size of each tap step is denoted by Δr, ΔT_k is the time delay to perform the tap change, V_2^{max} and V_2^{min} are the upper and lower limits of voltage V_2 at the distribution side of related transformer, d is half the LTC dead band, r^{max} and r^{min} are the limits of related tap.

If the inverse tap control function is activated, the equation (3.8) will be changed into (3.9), namely, the LTC will be changed to control and restore the transmission side voltages rather than the load side voltages. V_1^{max} and V_1^{min} are the upper and lower limits of voltage V_1 at the transmission side of related transformer.

$$r_{k+1} = \begin{cases} r_k - \Delta r & \text{if} \quad V_1 > V_1^{max} + d \ \text{ and } r_k < r^{max} \\ r_k + \Delta r & \text{if} \quad V_1 < V_1^{min} - d \ \text{ and } r_k > r^{min} \\ r_k & \text{else} \end{cases} \tag{3.9}$$

The initial time delay ΔT_0 is usually longer than ΔT_k, and then the tap changes continually at constant time intervals (i.e. ΔT_k) until the voltage is recovered or the tap

limits are reached. ΔT_0 will not be counted in the case of inverse tap control. The detailed parameters can be found in Appendix. A.1.

3.2.4 Distance relay considering Loadability

In this thesis, in order to better analyze the behaviors of distance relays during cascading events, the distance relays are modeled based on classic three zone characteristics, and with the consideration of loadability of related power components.

3.2.4.1 Zoned distance relay for transmission line

(a) Loadability and operation margin of distance relay

The loadability of transmission line is generally used as a concept for developing a fully understanding of power transfer capability which is influenced by voltage level and line length [1]. In order to make sure that the unexpected Zone 3 relay trips will not occur due to extreme loading conditions, NERC guidelines [80] in 2006 specified that the relays should not operate at or below the line emergency rating of the line. And the "extreme" emergency loading was defined as 150% of emergency load rating of a line as S_{max}, assuming a 0.85 per unit relay voltage V_{min} and a load power factor angle φ of 30°. Thus, the relay loadability limit can be easily obtained, taking Relay 1 in Fig. 3.4 as an example. $V_i, V_j, \theta_i, \theta_j$ represent the bus voltage magnitudes and phase angles respectively; $Z_{ij}\angle\varphi_{lineij}$ is the impedance of line ij; $Z_{aij}\angle\varphi_{ij}$ is the measured impedance by Relay 1; Z_{Tset}, Z_{Tsetij} are the values of relay settings at the impedance angle φ_{lineij} and power factor angle φ_{ij} respectively.

Assuming the power factor angle $\varphi_{ij} = \varphi_{max}$, the loadability limit of this relay can be given by (3.10), and the reach of Zone 3 can be obtained accordingly by (3.11).

$$Z_{Tsetij} = \frac{V_{imin}^2}{S_{maxij}} \tag{3.10}$$

$$Z_{Tset} = \frac{Z_{Tsetij}}{cos(\varphi_{lineij} - \varphi_{max})} \tag{3.11}$$

where $S_{maxij}, V_{imin}, \varphi_{lineij}, \varphi_{max}$ represent the emergency rating of the related line, low voltage limit of the bus, impedance angle of the line and maximum allowed power factor angle respectively.

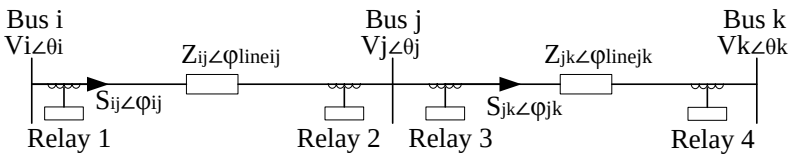

(a) Transmission lines with zoned distance relays

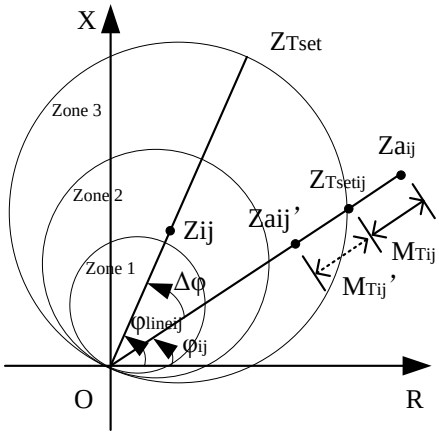

(b) The distance relay with three zone characteristics

Fig. 3.4 Traditional Zoned distance relays on transmission lines

In order to evaluate the extent of emergency load conditions to violate the Zone 3 relay, it is not sufficient to merely detect the time when the limit boundary is touched. The relay operation margin, which represents the distance from an observed operating point to its corresponding loadability limit, can be an effective indicator [57]. At power factor angle φ_{ij}, the operation margin of Relay 1 can be expressed as:

$$M_{Tij} = Z_{aij} - Z_{Tsetij} \tag{3.12}$$

where

$$Z_{aij} \approx \frac{Z_{ij}V_i}{\sqrt{\left(V_i - V_j cos\theta_{ij}\right)^2 + \left(V_j sin\theta_{ij}\right)^2}} \tag{3.13}$$

In normal operation states, the measured impedance Z_{aij} should be located outside the Zone 3 area and the operation margin is positive as expressed by M_{Tij} in Fig. 3.4 (b). If Z_{aij} enters the Zone 3 area and come to Z'_{aij}, Relay 1 will be initiated to trip the line with a preset delay. At this situation, the sign of operation margin (M'_{Tij}) is negative. If this negative margin is caused by the post fault overloading situation, this trip will be

regarded as unexpected one because it will weaken the stressed transmission system further and might result in cascaded trips.

(b) Operation margin for distance relays with the load blinders

Technically, relay engineers must ensure that a distance relay does not trip under heavy load conditions in order to give system operator enough time to mitigate the related system wide disturbances. Therefore, many efforts have been taken to improve the loadability of distance relay to ride through the extreme loading conditions. There are several methods to increase loadability of distance relay locally [80]:

- Increase the angle of maximum torque
- Change the distance relay characteristics form a circle to a lens
- Add blinders to the characteristics to limit reach along the real axis
- For remote Zone 3 protection, use an distance relay offset into the first quadrant
- For a quadrilateral characteristics, reset the relay
- Enable the load encroachment function of the relay

All these method try to adjust the operation region of Zone 3 distance relay, so the margin will be also adjusted. For an example in Fig. 3.5, the Zone 3 operation region of Relay 1 in Fig. 3.4 is restrained by load encroachment element formed by two lines and one circle, where φ_{setij}, φ_{setij}' and Z_{Tsetij}' are the settings of load encroachment element. The setting value of them can be easily obtained based on NERC report [80], with consideration of voltage instability criteria [42].

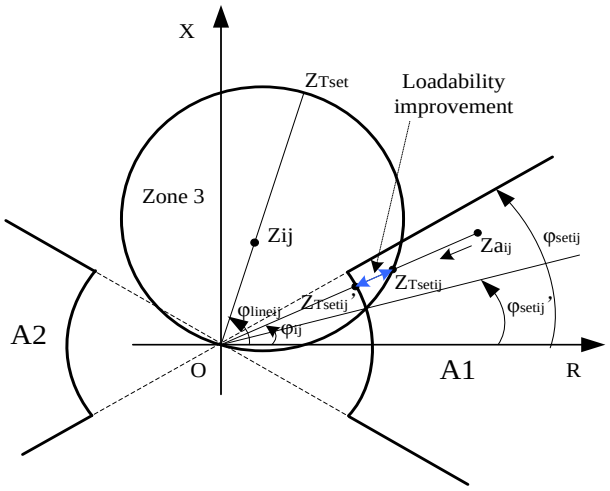

Fig. 3.5 Zone 3 distance relay with load encroachment function

Obviously, it can be seen from Fig. 3.5, the operation region of Zone 3 is changed from original Zone 3 to $\text{Zone 3} \cap \overline{\text{A1} \cup \text{A2}}$, where the blinding area A1 and A2 are given by (3.13) and (3.14).

$$A1 = \{cos\varphi_{ij} \geq cos\varphi_{setij}\} \cap \{Z_{aij} \geq Z'_{Tsetij}\} \tag{3.14}$$

$$A2 = \{cos\varphi_{ij} \leq -cos\varphi_{setij}\} \cap \{Z_{aij} \geq Z'_{Tsetij}\} \tag{3.15}$$

where

$$cos\varphi_{ij} \approx \frac{(V_i - V_j cos\theta_{ij})cos\varphi_{lineij} + V_j sin\theta_{ij} sin\varphi_{lineij}}{\sqrt{(V_i - V_j cos\theta_{ij})^2 + (V_j sin\theta_{ij})^2}} \tag{3.16}$$

Then the operation margin can be defined according to different parts of the revised operation region at the specific power factor angle φ_{ij}. Suppose the power flow is positive on Relay 1, then in the first quadrant of R-X plane, the M_{Tij} of Zone 3 of Relay 1 can be expressed as:

$$M_{Tij} = \begin{cases} Z_{aij} - Z_{Tsetij}, & \varphi_{ij} \geq \varphi_{setij} \; and \; \varphi_{ij} \leq \varphi'_{setij} \\ Z_{aij} - Z_{Tsetij}', & \varphi_{setij} \geq \varphi_{ij} \geq \varphi'_{setij} \end{cases} \tag{3.17}$$

where φ'_{setij} is the angle of intersection point between the circle element and Zone 3 border in the first quadrant. Obviously, if the settings of load encroachment elements are set suitably, the loadability of Zone 3 can be improved in the region containing normal power factor angles of power flow, which is shown with blue arrows in Fig. 3.6.

3.2.4.2 The distance backup relay for generator

Technically, the protection system of generators is complex and based on diverse principles [81]. In this thesis, the distance backup relay on generator is chosen to be studied, which is convenient for the system wide impedance criteria analysis. A distance backup relay for the generator has been shown in Fig. 3.6, Relay 3 is the concerned generator backup relay. The outmost backup setting curve of Relay 3 in R-X plane is transferred from capability curves of the synchronous generator, which are field current limit curve (FCL) and stator current limit curve (SCL) [82]. These two curves intersect at the points with the rated power factor angle φ_{ir}. And the solid parts of the two limit curves with $V_{min} = 0.9pu$ in Fig. 3.6 (b) and (c) are chosen as setting curve of Relay 3, while the limits with the rated voltage are depicted with dashed curves.

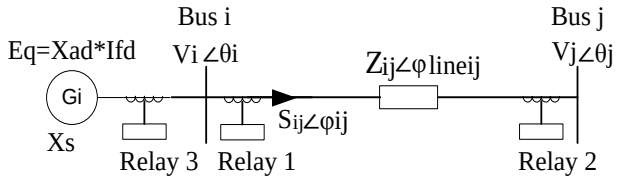

(a) Relays on generator and transmission line

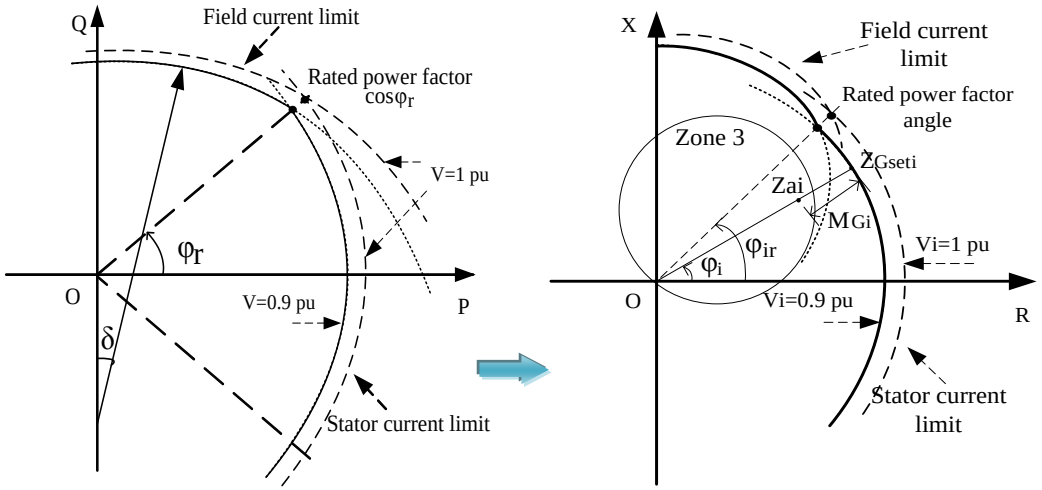

(b) Capability curves of generator (c) Setting values of backup relay

Fig. 3.6 Impedance backup relay on Synchronous generator

At the power factor angle φ_i, $Z_{ai}, Z_{Gseti}$are the measured impedance and setting value of the backup relay; then the operation margin of this relay can be expressed as:

$$M_{Gi} = Z_{ai} - Z_{Gseti} \tag{3.18}$$

Also according to the classic generator equations of active power and reactive power (P_{gi} and Q_{gi}), as expressed by:

$$P_{gi} = V_i I_{si} cos\varphi_i = \frac{V_i X_{adi} I_{fdi}}{X_{si}} sin\delta_i \tag{3.19}$$

$$Q_{gi} = V_i I_{si} sin\varphi_i = \frac{V_i X_{adi} I_{fdi}}{X_{si}} cos\delta_i - \frac{{V_i}^2}{X_{si}} \tag{3.20}$$

Then Z_{ai} can be given by:

$$Z_{ai} = \frac{{V_i}^2}{\sqrt{P_{gi}^2 + Q_{gi}^2}} = \frac{X_{si} V_i}{\sqrt{{X_{adi}}^2 {I_{fdi}}^2 + {V_i}^2 - 2 V_i X_{adi} I_{fdi} \cos\delta_i}} \tag{3.21}$$

where X_{si}, X_{adi} are synchronous impedance and mutual reactance of the generator i; I_{fdi} and I_{si} are the field current and stator current; δ_i and φ_i are the load angle and power factor angle.

In Fig. 3.6 (c), due to the transformation of FCL and SCL, the setting curve of Relay 3 has two parts divided by the point with related power factor angle φ_{ir}, which is the intersection point of FCL and SCL. So Z_{Gseti} at φ_i can be given by:

$$Z_{Gseti} = \begin{cases} Z_{fcli}, & \varphi_i > \varphi_{ir} \\ Z_{scli}, & \varphi_i \leq \varphi_{ir} \end{cases} \tag{3.22}$$

where

$$Z_{fcli} \approx \frac{X_{si} V_{imin}}{\sqrt{(E_{fdimax})^2 + {V_{imin}}^2 - 2V_{imin}E_{fdimax}\, cos\, \delta_{is}}} \tag{3.23}$$

$$Z_{scli} = V_{imin}/I_{simax} \tag{3.24}$$

Z_{fcli} and Z_{scli} represent the setting values on the FCL and SCL respectively; φ_{ir} are rated power factor angle; $E_{fdimax}\left(= X_{adi} i_{fdimax}\right)$, I_{fdimax}, I_{simax} represent the maximum values of field voltage, field current and stator current respectively; δ_{is} is the load angle if the generator active power P_{ig}, the low voltage limit V_{imin} and E_{fdimax} are specified according to classic generator power equations [1].

3.2.5 Eastern Denmark power system

In this thesis, the 19-bus test system model which is simplified from eastern Denmark is built in RTDS with two racks and depicted in Runtime/RTDS, as shown in Fig. 3.7. This model contains 19 buses with voltages from 0.7 kV to 400 kV, four central power plants and their control (G01, G11, G21 and G22), a Static VAR compensator (SVC), several consumption centers modeled by constant power load, a lumped equivalent of local wind turbines and an equivalent of a large offshore wide farm [83]. The wind farms are equipped with fixed-speed conventional asynchronous generators. The generation and load consumption level can be observed in Table A.1 and Table A.2 in Appendix.

All the four central power plants have applied the governor/turbine model and the excitation model (including PSS, SCL and FCL models), which are already introduced in the beginning of this chapter. The generators' capability limit curves are also modeled as

backup relay settings in the impedance plane, which are used to initiate alarms to Control center and will be explained concretely in the following content. The FCL settings apply $I_{fd01max} = I_{fd11max} = I_{fd21max} = 2.68\,pu$, $I_{fd22max} = 2.85\,pu$ and $V_{min} = 0.9\,pu$. The restoration load model is applied for consumption center Load 1 and Load 2. And Load 3 and Load 4 are modeled by constant power load. The LTCs are modeled on transformer TX0811 (between bus 8 and bus 11) and TX0912 (between bus 9 and bus 12). The power components are named based on node numbers, e.g. TL0607a represent one of the two lines between bus 6 and bus 7. The detailed parameters can be found in Appendix.

It should be noted that the SVC (±50Mvar) is placed at bus 16 with the aim to hold the voltage at bus 13, which is the connection point between main power system and wind farm system. If the SVC is operated in normal control scope, the load variation in main power system will not influence the operation of wind farm system. But if the SVC hits its capability limit during an overloading situation, it will behavior as same as a capacitor bank, which will deteriorate the overloading situation.

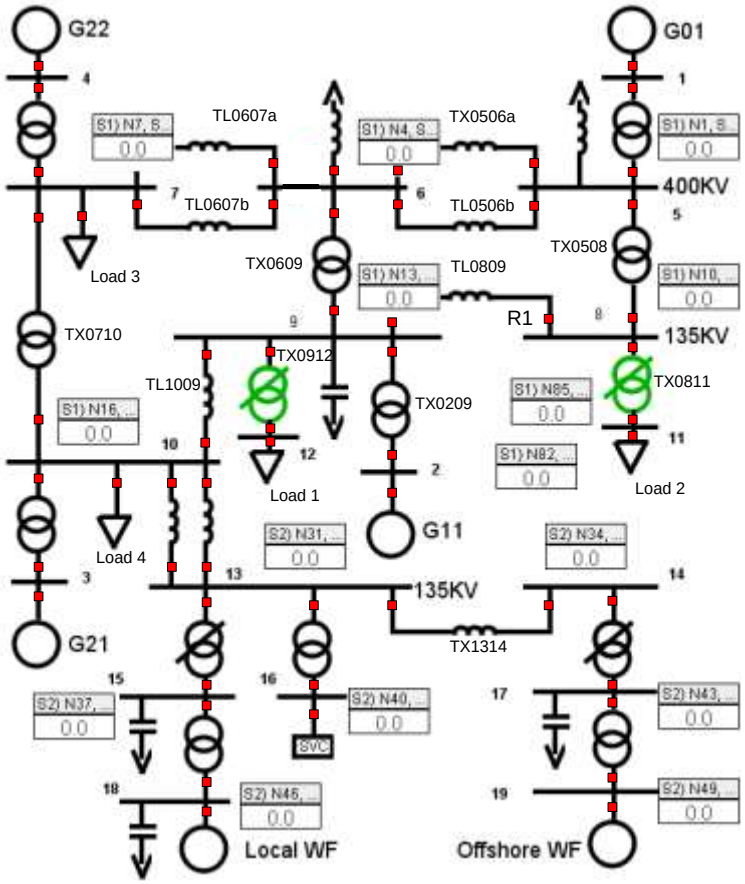

Fig. 3.7 The simplified eastern Denmark system model in Runtime/RSCAD

3.3 Detection of overloading situation in cascading events

3.3.1 Emergency state detection

In order to detect the long term voltage stability associated overloading situations without disturbing the normal functions of relays, the diverse operation states will be defined hereby, which can be explained by Fig. 3.8.

As for the generator back up relay, the impedance plane in the first quadrant can be divided into four areas, which are labeled as Normal area, Urgent area, Zone 3 area and Zone 12 area respectively. Zone 3 area is the operation region of Zone 3 element in well-known zoned distance relays. Similarly, Zone 12 area is the operation regions of Zone 1 and Zone 2 elements. Normal area represents the Normal state that no limits of the generator are reached, and the area between Normal area and Zone 3 area is named Urgent area where the generator reaches its capability limit.

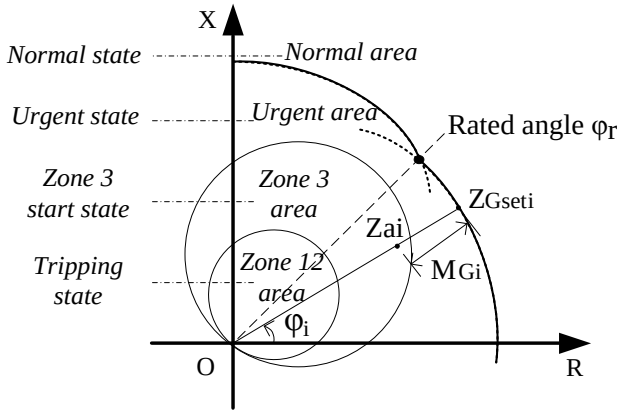

Fig. 3.8 Areas for operation states of an distance relay on a generator

Comparing the measured Z_{ai} with the setting values of zone circles and capacity limit curves, five states can be defined by the relay state signals named D_{g1i}, D_{g2i}, D_{g3i} and breaker state signal named D_{bi} as follows:

- Normal state, if Z_{ai} is in the Normal area, $M_{Gi}>0$, $D_{g1i}= D_{g2i}=D_{g3i}=0$, $D_{bi}=1$.
- Urgent state, if Z_{ai} is in the Urgent area, $M_{Gi}\leq 0$, $D_{g1i}=D_{g2i}=0$, $D_{g3i}=1$, $D_{bi}=1$.
- Zone 3 start state, if Z_{ai} is in the Zone 3 area, $M_{Gi}<0$, $D_{g1i}=0$, $D_{g2i}=D_{g3i}=1$, $D_{bi}=1$.
- Tripping state, if Z_{ai} is in the Zone 12 area, $M_{Gi}<0$, $D_{g1i}= D_{g2i}=D_{g3i}=1$ and $D_{bi}=1$.
- Tripped state, if $D_{bi}=0$.

For a distance relay on transmission line *ij*, the R-X plane can be similarly divided into four areas, i.e. Zone 12 area, Zone 3 area, Urgent area and Normal area. Due to the different blinders or loadability curves, the urgent area will be different. For an example, the distance relay with load encroaching element is shown in Fig. 3.9. In the first quadrant of impedance plane, the area circled by blue lines is named as Urgent area in which the loading condition is still normal but it is already inside the original Zone 3 area and very close to the loadability limit. So in the Urgent area, the trip signal of Zone 3 relay will be blocked. Three relay state signals named D_{L1ij}, D_{L2ij}, D_{L3ij} will be generated together with one breaker state signal named D_{bij}. So there are also five states for the relay on transmission line can be defined accordingly, i.e. Normal state, Urgent state, Zone 3 start state, Tripping state and Tripped state.

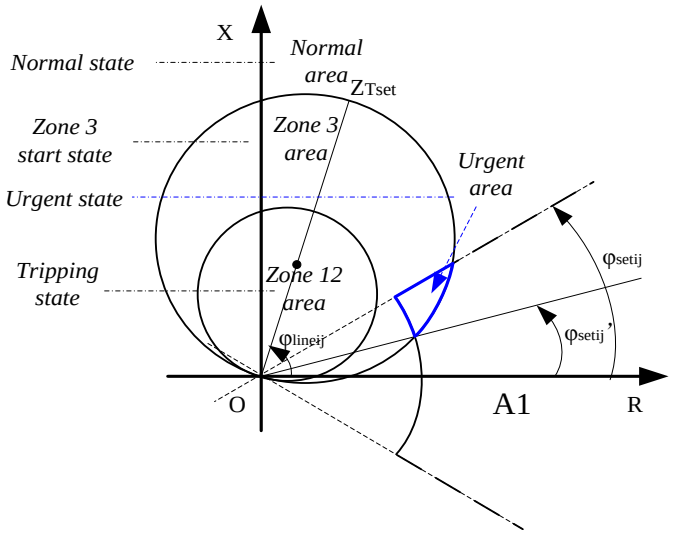

Fig. 3.9 Areas for operation states of an distance relay on a transmission line

Obviously, the Urgent state and Zone 3 start state will be easier to be initiated under the overloading situations. These two states, which are defined as emergency states in this thesis, will be mainly focused in following chapters.

3.3.2 Complex situations related to cascaded blackouts

All the blackouts initially occurred from some local failures, such as power component failures, unexpected protection and control operation, and etc. After the initial event, when the system becomes weaker and gradually loses its operation equilibrium which will be represented by abnormal voltage and frequency over the system, then the local component failures will be propagated from one to another, and a final blackout will

occur if no suitable prevention measures are taken in time. This kind of disaster is so called cascading events and more complex than local ones. In order to easily analyze the cascading events and find the solutions to prevent the whole blackouts, the long term voltage instability induced cascading events have been simulated in RTDS with above described 19-bus test system.

3.3.2.1 Voltage instability induced blackout scenarios

As for the 19-bus test system in Fig. 3.10, a severe case of post fault voltage instability was initiated by a three phase short circuit fault applied on bus 6 at about 11s. The local relays cleared the fault within 0.1s immediately tripping all the lines and transformers connected to bus 6. The red cubes represent the breakers are on, and the blue ones are off. Then, this system survives an oscillation within about 24s. Due to load restoration by the loads and the LTC on transformer TX0912, the stressed network cannot support the continually load demand increment. Depending on the diverse states of relay system, the two different scenarios can be obtained as follows:

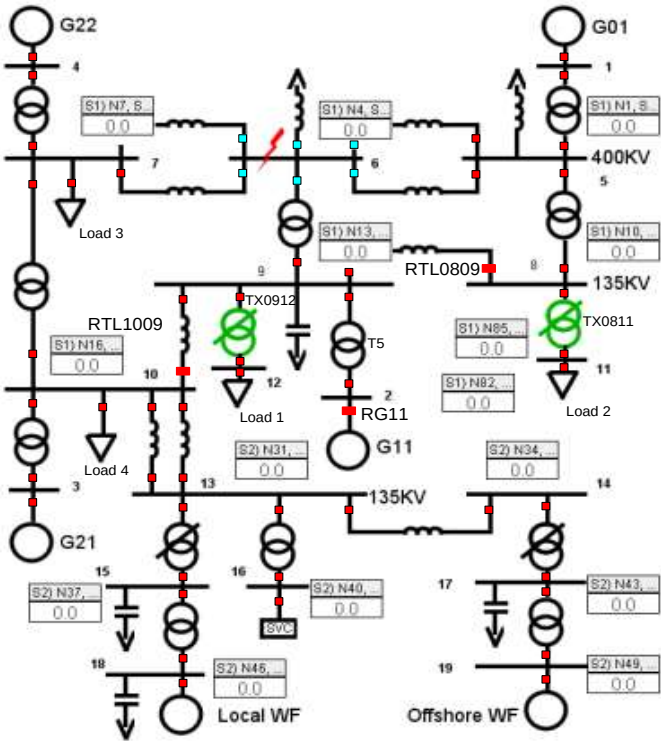

Fig. 3.10 The 19-bus test system for cascading events simulation

(a) Voltage collapse scenario with relay blocked

The voltage collapse progress with all the Zone 3 relays blocked in the post fault stage can be observed Fig. 3.11. In this scenario, when the traditional relays were blocked

in the post fault stage, the normal LTC operations on TX0912 were started to operate at about 65s, which tried to recover the voltage on bus 12. Meanwhile, the restoration load (described in section 3.2.2) at bus 12 also tried to recover itself. Then after a long time voltage decreasing, voltage collapse still occurred at about 210s since all the generators hit the capability limits to support prevailing load flows.

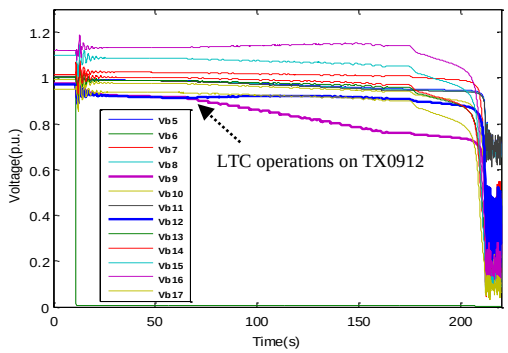

(a) Bus voltages

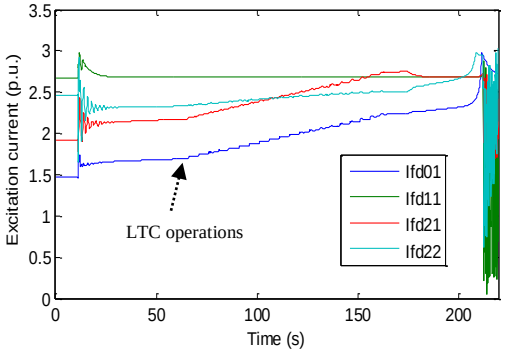

(b) Field currents of synchronous generators

Fig. 3.11 Voltage collapse scenario with relays blocked in the post fault stage

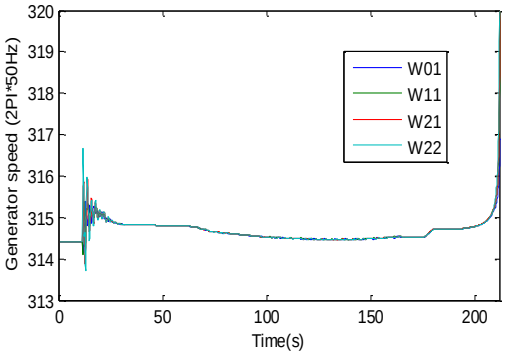

(a) The rotor speeds of synchronous generator

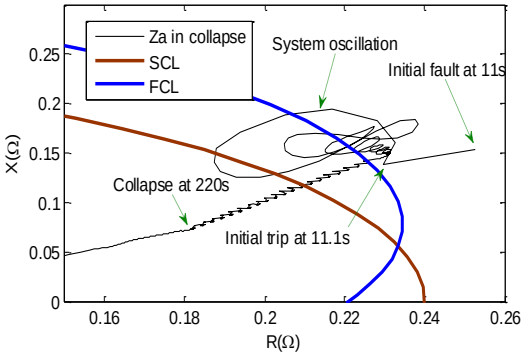

(b) Impedance locus of relay R_{G11} on G11

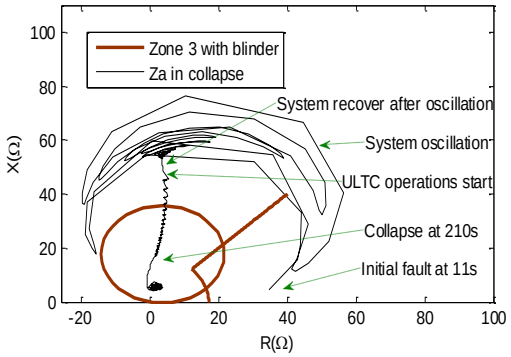

(b) Impedance locus of relay R_{TL0809} on TL0809

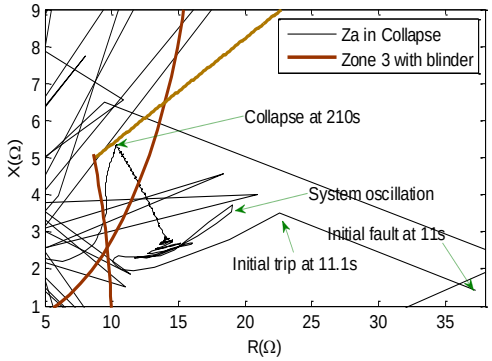

(d) Impedance locus of relay R_{TL1009} on TL1009

Fig. 3.12 Speeds of generator, impedance loci of critical relays during voltage collapse

From Fig. 3.12 (a), the speeds of generators are around its nominal values, but voltage waveforms in Fig. 3.11 have bigger derivations. When voltage collapse occurred, the rotors of generator also run away, which is a classic phenomenon of long term voltage instability induced rotor angle instability.

From Fig. 3.12 (b)-(d), the behaviors of critical relays can be observed. In the beginning of post fault stage, G11 was still in the normal region but almost run out of its reactive power reserve; the impedance locus was close to its FCL (blue circle in Fig. 3.12 (b)). During continual LTC operation and load restoration, G11 firstly hit its FCL and the state of R_{G11} was changed from Normal state (0001) to Urgent state (0011) immediately, when voltage collapsed, Zone 3 start state was also triggered with state signal as "0111".

The relay R_{TL0809} on transmission line TL0809 was triggered secondly when impedance locus entered Zone 3 area at about 86s. From Fig. 3.12 (b), the power factor changed a lot compared with the one in the pre fault stage, so the load encroachment blinder in brown color could not block this kind of load restoration. The state of R_{TL0809} was changed directly from Normal state (0001) to Zone 3 start state (0101).

When loading level got deteriorated, the relay R_{TL1009} on transmission line TL1009 was triggered thirdly when the impedance locus entered its Zone 3 circle. The power factor angle on TL1009 was still small, so the blinder could block the load increment until the voltage collapsed. So the state of R_{TL1009} was changed from Normal state (0001), then Urgent state (0011) to Zone 3 start state (0111).

(b) Voltage collapse scenarios with relay activated

When the traditional relay system is activated in the post fault stage, the different voltage collapse progress with cascaded trips can be observed in Fig. 3.13 and Fig. 3. 14.

In the post fault stage, since load restoration and LTC operations started at about 65s, the Zone 3 distance relay R_{TL0809} on the line between bus 8 and bus 9 was triggered at about 86s to trip this important line at 87s unexpectedly. Then the part Area 1 (including bus 1, bus 5 and bus 8) was separated from whole network and survived. Thereafter, due to about 70% of total load in Area 2, a large amount of power flow was transferred from Area 3 (including bus 3, 4, 7, 10, 13, 14, 15, 16, 17, 18, 19) to Area 2 (bus 2, 9, 12) through the line (TL1009) between bus 10 and bus 9 to meet the power difference and load restoration demand, TL1009 was thus heavily overloaded and tripped by the backup relay R_{TL1009} at about 93s, then the remaining network split into Area 3 and Area 2. Due

to big unbalance between generation and consumption in Area 3 and Area 2, frequency and voltage collapsed together in these two areas.

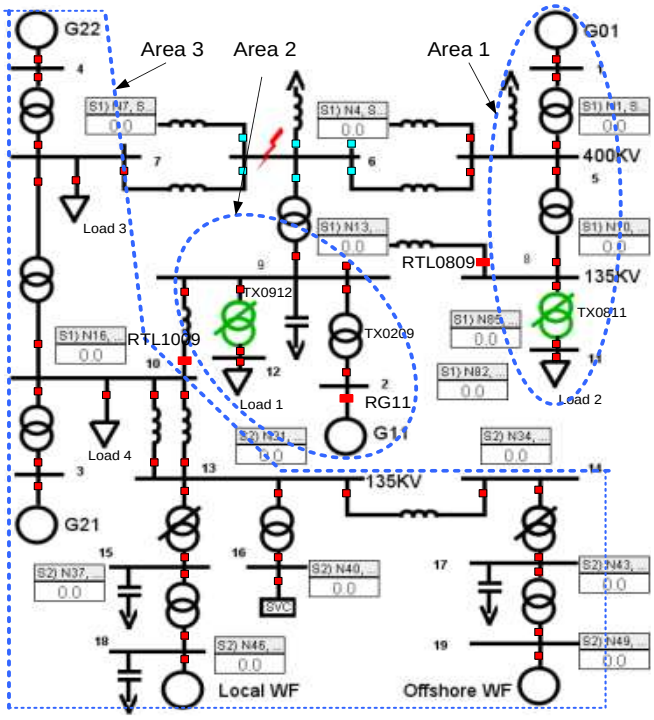

Fig. 3.13 The test system during cascading events

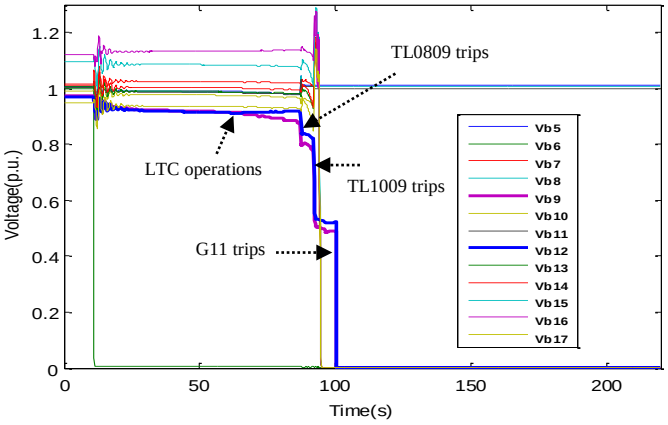

Fig. 3.14 Voltage collapse scenario with relays activated in the post fault stage

The bus voltages are shown in Fig. 3.14. Apparently, due to the deteriorating effect of those unexpected relay operations, the voltage collapsed much faster than the former scenario. The relay R_{G11} on G11 firstly hit its capability limit (FCL), which would send alarm state signal to Control center. Also, it had been set with about 5s delay when it enters Zone 3 start state. So the relay R_{TL0809} and R_{TL1009} tripped the related transmission

lines TL0809 and TL1009 firstly. If there was no timely execution of emergency controls, G11 in the islanded part Area 2 was tripped finally at about 100s.

From the waveforms of excitation currents in Fig. 3.15 (a), except G11, other generator could output more reactive powers in the post fault stage. But unexpected relay operations accelerated the speed of voltage collapse. And the rotors of all the generators ran away from nominal values in different directions firstly when the system separated into islands, finally ran far away and get cut when voltage collapsed, which can be observed in Fig. 3.15 (b).

The impedance loci of critical relays can be seen in Fig 3.15 (c)-(e). The loci in blue color represent the cascaded blackout scenario. R_{TL0809} tripped TL0809 firstly when impedance entered Zone 3 area. R_{TL1009} was triggered secondly and it could sense the effect of the line TL0809 outage, which is shown in Fig. 3.15 (e). The outage of TL0809 induced the impedance locus of R_{TL1009} change the direction a little at 88s, and then the locus quickly entered Zone 3 circle beyond the blinder, which made R_{TL1009} change into Zone 3 start state and tripped the line TL1009 unexpectedly. Based on the blue locus of R_{G11} in Fig. 3.15 (c), the effects of R_{TL0809} and R_{TL1009} operations can be also observed.

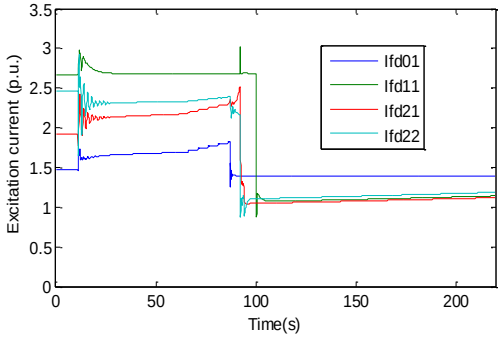

(a) Field currents of generators

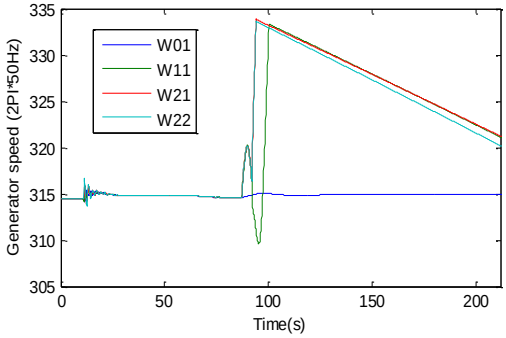

(b) The rotor speeds of generators

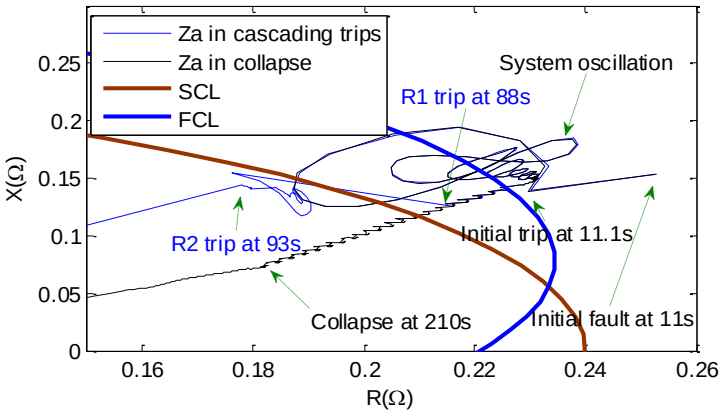

(c) Impedance locus of relay R_{G11} on G11

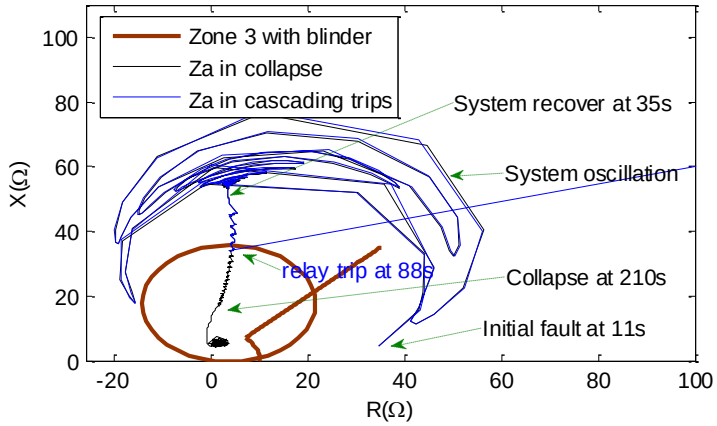

(d) Impedance locus of relay R_{TL0809} on TL0809

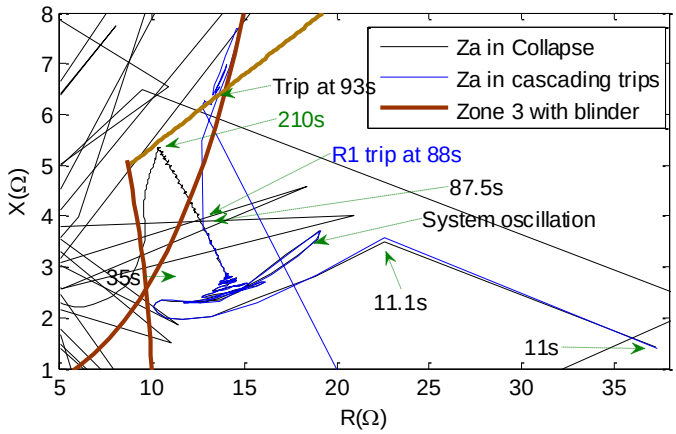

(e) Impedance locus of relay R_{TL1009} on TL1009

Fig. 3.15 The critical system variables during voltage collapse

Under the extreme loading situations, these relay operations affect each other and make the system condition deteriorated further, which finally form the cascaded blackouts. Moreover, the blinder sometime doesn't work when the power factor change a lot. In order to find more effective methods to prevent the overload induced unexpected relay operations, the relationships between these cascaded operations need to be carefully investigated.

3.3.2.2 Basic processes of cascading events

Based on the simulated cascading events and the practical blackouts discussed in former chapters, it can be found that the causes of cascading events leading to blackouts are diverse, but the basic process seems easy to be identified. The concerned basic processes of long term voltage instability induced cascading events are list as follows:

- Transmission Line or generator tripping due to faults or temporary maintenance

The state signals of related relays on the faulty components will be changed from "0001" (Normal state) to "1111" or "1101" (Tripping state) and finally to "XXX0" (tripped state, X means "1" or "0"). Or the state signals will be directly changed from "0001" to "0000" when the temporary maintenance is required. This basic process belongs to the normal operation of relay system, which will be collected and recorded in Control center for updating the network data.

- Overload due to line or generator outage induced load flow transferring

If the amount of load flow transferring is not that big, then the system can be still run in a normal situation. However, if the load flow transferring is big enough to induce the related power components and relays violating their setting or loadability limits, then this process, which causes the overloading situation and could trigger the cascading trips, should be identified. The state signals of related relays will be changed from "0001" (Normal state), to "0011" (Urgent state) or even "0111" or "0101" (Zone 3 start state), sometimes even to "1111" or "1101" (Tripping state).

These transitions of state signals can be used for state confirmation and emergency control initiation in Control center. Sometimes, when the related relay gets into Zone 3 start state or Tripping state very fast, it is hard to tell this situation caused by an outage induced load transferring or a fault. Then the more accurate identification method should be developed to quickly differentiate the overloads from the fault, which will be discussed further in next chapter.

- Overload due to load side voltage control induced load increment

In this process, the overloading situation is caused by long term load side voltage control, i.e. LTC operation and long term load restoration dynamics. The transition of state signals will be similar to the former one, except with slow time responses. Together with the former process, these two load flow transferring induced overloading situations can be seen in Fig. 3.16, the basic events are denoted with black letters while the processes are denoted with red letters, and the impedance locus of R_{TL1009} in blue color reflects the processes (red arrows). Before it got tripped at 93s, there were several scenarios of load flow transferring. It can be seen that the outage induced load flow transferring is faster than LTC induced load increment, and the outage induced load flow transferring from 11.1s to 35s did not caused any violation of relays, which belongs to normal process but not overload processes.

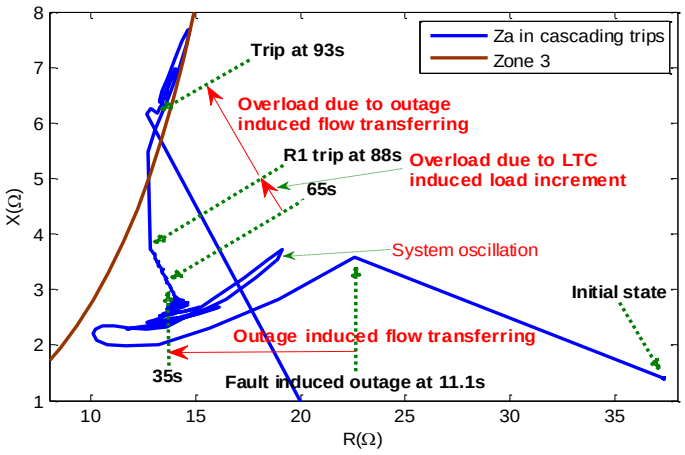

Fig. 3.16 Basic processes on the impedance locus of relay R_{TL1009}

- Transmission line or generator tripping due to overloading situation

This process were the result of the former two overload processes, and the result of this process will induce further load flow transferring if no emergency control gets executed. The state signals will be changed from "0011" (Urgent state), "0111" or "0101" (Zone 3 start state) to "0010" or "0110" (Tripped state). The example based on former simulation case is shown in Fig. 3.17. The state signal of R_{TL1009} was changed from "0111" to "0110" at 93s.

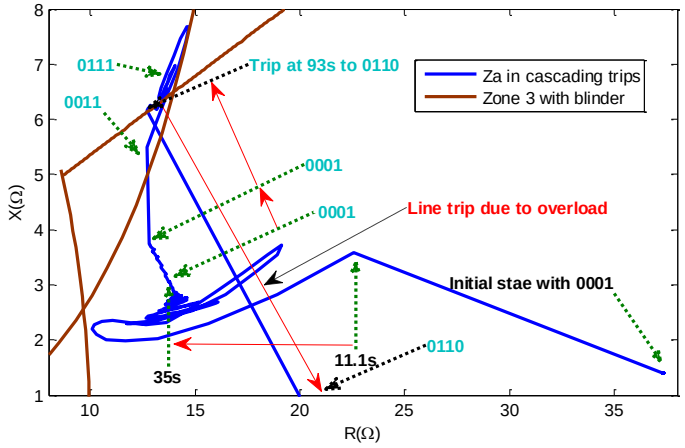

Fig. 3.17 State signals and Basic processes on the impedance locus of relay R_{TL1009}

- Generator tripping due to abnormal voltage and frequency

This process can also be regarded as a result of overload processes, if the load is more than generation in the island. However, if the generation is more than load in the island, then this situation will not belong to voltage instability case. The over frequency relay

will be responsible for this situation in the simulation, and state signals of this kind of relay can be similarly defined. Since the frequency or angle stability issues are out of the scope of this thesis, so it will not be mainly focused.

Based on identification and analysis of these basic processes of cascading events, the composition and progress of whole cascading events in a blackout can be easily figured out, as well as the cause-effect relationships between these basic processes can be clarified and visualized. Then the related emergency analysis can be taken in different stages to produce the early warning information for next event, as well as the suitable protection and control strategy will be accordingly designed for those overload processes and timely prevent the propagation of cascading events.

3.4 Summary

In order to have an in-depth analysis and understanding on cascading events, the practical 19-bus eastern Denmark test system have been modeled in RTDS, the detailed models of those concerned power components are described, such as FCL model, LTC model, restoration load model, distance relay model and etc. Due to the contribution of distance relays on cascading events, the loadability of distance relay has been discussed. The relay operation margin on impedance plane and related state signals are used as effective indicator to express the loadability level locally.

Based on the appropriate design of test system together with relay system, the emergency states of local components can be easily identified by improved distance relays. As for the complex situations of cascading events, the basic simple processes are used to decompose the whole progress of cascading events and find the cause-effect relationships between them. Hereafter, the suitable assessment and preventive protection strategy can be implemented in place.

The load blinder is used in the line distance relay to prevent overload situation, which is not that dependable if power factor angle changes a lot. Moreover, in order to effective trace the progress of cascaded blackout, identification of those overload induced unexpected relay operation is very necessary. So the discrimination of overload situations from three phase short circuit becomes a critical problem.

Chapter 4

Sensitivity analysis for emergency states

4.1 Introduction

In Chapter 3, two defects of load blinders for distance relay can be found:

- Although the load blinders can improve loadability of Zone 3 relay to some extent; the sensitivity of Zone 3 relay as a remote backup protection element will be sacrificed at the same time.
- If a large amount of reactive power is transferred to the critical transmission line in the post stage of N-1 (or N-k) contingency, then the power factor angle may not always be a dependable indicator to distinguish a heavy load situation from a faulty situation.

In this chapter, in order to better identify the emergency overloading situations in the whole system, a sensitivity method will be adopted to online analysis the system operation states. The impedance margin sensitivity is proposed to discover the vulnerable relays and sensitive controllers under different operation states, which will help online monitor system operation states and timely define the effective emergency control measures. Also based on the impedance sensitivity, the related identification and prediction methods are proposed to fast differentiate load flow transferring induced emergency states from the faulty state, i.e. effectively identify the unexpected relay operations under the emergency overloading situation.

The sensitivity method will be briefly introduced in next section; based on impedance sensitivity, the emergency state analysis including detection, prediction and identification will be described in section 4.3; the case study on the blackout scenarios will be given in section 4.4; and finally, the conclusion is made in section 4.5.

4.2 Brief discussion of sensitivity method

4.2.1 Sensitivity in Power system

4.2.1.1 Definition of sensitivity

Assume that the power system in a steady state can be described by a set of algebraic equations in a function form as [84]:

$$\boldsymbol{\sigma}(\boldsymbol{u},\boldsymbol{p})=\mathbf{0} \tag{4.1}$$

where $\boldsymbol{u}$ is an n dimension vector of algebraic variables, $\boldsymbol{p}$ represents a vector of parameters. If the system is operated at a specific point $(\boldsymbol{u_0},\boldsymbol{p_0})$, then (4.1) can be rewritten as:

$$\boldsymbol{\sigma}(\boldsymbol{u_0},\boldsymbol{p_0})=\mathbf{0} \tag{4.2}$$

When there is a variation on system operation state, the operation point will be changed from $(\boldsymbol{u_0},\boldsymbol{p_0})$ to $(\boldsymbol{u_0}+\Delta\boldsymbol{u},\boldsymbol{p_0}+\Delta\boldsymbol{p})$, then the equations can be expressed as:

$$\boldsymbol{\sigma}(\boldsymbol{u_0}+\Delta\boldsymbol{u},\boldsymbol{p_0}+\Delta\boldsymbol{p})=\mathbf{0} \tag{4.3}$$

The (4.3) can be expanded at the operation point $(\boldsymbol{u_0},\boldsymbol{p_0})$ in the form of Taylor series as (4.4), where the terms in high order have been omitted, which is so called linearization.

$$\boldsymbol{\sigma}(\boldsymbol{u_0},\boldsymbol{p_0})+\frac{\boldsymbol{\partial\sigma}}{\boldsymbol{\partial u}}\Delta\boldsymbol{u}+\frac{\boldsymbol{\partial\sigma}}{\boldsymbol{\partial p}}\Delta\boldsymbol{p}\approx\mathbf{0} \tag{4.4}$$

Introducing (4.2) into (4.4) yields:

$$\frac{\boldsymbol{\partial\sigma}}{\boldsymbol{\partial u}}\Delta\boldsymbol{u}+\frac{\boldsymbol{\partial\sigma}}{\boldsymbol{\partial p}}\Delta\boldsymbol{p}\approx\mathbf{0} \tag{4.5}$$

The equation (4.5) is the basis of sensitivity analysis, and the coefficient matrices $\boldsymbol{\partial\sigma/\partial u}$ and $\boldsymbol{\partial\sigma/\partial p}$ are so called Jacobian matrices.

Based on equation (4.5), assuming $\boldsymbol{\partial\sigma/\partial u}$ is nonsingular, then

$$\Delta\boldsymbol{u}=-\left(\frac{\boldsymbol{\partial\sigma}}{\boldsymbol{\partial u}}\right)^{-\mathbf{1}}\frac{\boldsymbol{\partial\sigma}}{\boldsymbol{\partial p}}\Delta\boldsymbol{p}=\boldsymbol{\mathcal{L}}\Delta\boldsymbol{p} \tag{4.6}$$

where $\boldsymbol{\mathcal{L}}=-(\boldsymbol{\partial\sigma/\partial u})\text{^}(-\mathbf{1})*\boldsymbol{\partial\sigma/\partial p}$, is denoted as sensitivity matrix between variable $\boldsymbol{u}$ and parameter $\boldsymbol{p}$.

Due to the sensitivity information, the direct relationship between $\boldsymbol{u}$ and $\boldsymbol{p}$ can be approximately quantified in the steady states [1]. Based on theories and analysis in [16], the long term voltage instability scenarios before the point of collapse commonly present the quasi-steady state characteristics. Since the WAMS based data collection and model verification is fast enough, the "early warning" on long term voltage instability based on sensitivity analysis can be anticipated.

4.2.1.2 Power flow sensitivity

Firstly, the related concepts of power flow sensitivity in the area of power system are introduced. According to Kirchhoff's circuit laws [85], the injecting current on bus *i* can be expressed as:

$$I_i = \sum_{j=1}^{n} Y_{ij} V_j \tag{4.7}$$

where V_j is the voltage at bus *j*, Y_{ij} represents the related element of bus admittance matrix, *n* is the number of buses. This equation can be expressed in polar form:

$$I_i = \sum_{j=1}^{n} |Y_{ij}||V_j| \angle \varphi_{ij} + \theta_j \tag{4.8}$$

where φ_{ij} is the voltage angle difference when current flow through Y_{ij}, θ_j is the voltage phase angle at bus *j*. Then according to the formula (4.9) and (4.10) of complex power at bus *i*, the active power P_i and reactive power Q_i can be given by (4.11) and (4.12) respectively, where θ_i is the voltage phase angle at bus *i*.

$$P_i - jQ_i = V_i^* I_i \tag{4.9}$$

$$P_i - jQ_i = |V_i| \angle -\theta_i \sum_{j=1}^{n} |Y_{ij}||V_j| \angle \varphi_{ij} + \theta_j \tag{4.10}$$

$$P_i = \sum_{j=1}^{n} |V_i||V_j||Y_{ij}| cos(\varphi_{ij} - \theta_i + \theta_j) \tag{4.11}$$

$$Q_i = -\sum_{j=1}^{n} |V_i||V_j||Y_{ij}| sin(\varphi_{ij} - \theta_i + \theta_j) \tag{4.12}$$

As for a power system, a set of nonlinear algebraic equations can be composed by (4.11) and (4.12), which are classic power flow equations for power system analysis. Similar to (4.4), this set can be expanded in Taylor's series and linearized as:

$$\begin{bmatrix} \Delta P_1 \\ \vdots \\ \Delta P_n \\ \Delta Q_1 \\ \vdots \\ \Delta Q_n \end{bmatrix} = \begin{bmatrix} P_1 - P_1^0 \\ \vdots \\ P_n - P_n^0 \\ Q_1 - Q_1^0 \\ \vdots \\ Q_n - Q_n^0 \end{bmatrix} = \begin{bmatrix} \frac{\partial P_1}{\partial \theta_1} & \cdots & \frac{\partial P_1}{\partial \theta_n} & \frac{\partial P_1}{\partial |V_1|} & \cdots & \frac{\partial P_1}{\partial |V_n|} \\ \vdots & \ddots & \vdots & \vdots & \ddots & \vdots \\ \frac{\partial P_n}{\partial \theta_1} & \cdots & \frac{\partial P_n}{\partial \theta_n} & \frac{\partial P_n}{\partial |V_1|} & \cdots & \frac{\partial P_n}{\partial |V_n|} \\ \frac{\partial Q_1}{\partial \theta_1} & \cdots & \frac{\partial Q_1}{\partial \theta_n} & \frac{\partial Q_1}{\partial |V_1|} & \cdots & \frac{\partial Q_1}{\partial |V_n|} \\ \vdots & \ddots & \vdots & \vdots & \ddots & \vdots \\ \frac{\partial Q_n}{\partial \theta_1} & \cdots & \frac{\partial Q_n}{\partial \theta_n} & \frac{\partial Q_n}{\partial |V_1|} & \cdots & \frac{\partial Q_n}{\partial |V_n|} \end{bmatrix} \begin{bmatrix} \partial \theta_1 \\ \vdots \\ \partial \theta_n \\ \Delta |V_1| \\ \vdots \\ \Delta |V_n| \end{bmatrix} \tag{4.13}$$

where the variables or parameters with superscript "0" represent initial values of related variables or parameters, and in short form, it can be written as:

$$\begin{bmatrix} \Delta \boldsymbol{P} \\ \Delta \boldsymbol{Q} \end{bmatrix} = \begin{bmatrix} \boldsymbol{J_1} & \boldsymbol{J_2} \\ \boldsymbol{J_3} & \boldsymbol{J_4} \end{bmatrix} \begin{bmatrix} \Delta \boldsymbol{\theta} \\ \Delta |\boldsymbol{V}| \end{bmatrix} = \begin{bmatrix} \frac{\boldsymbol{\partial \Delta P}}{\boldsymbol{\partial \theta}} & \frac{\boldsymbol{\partial \Delta P}}{\boldsymbol{\partial V}} \\ \frac{\boldsymbol{\partial \Delta Q}}{\boldsymbol{\partial \theta}} & \frac{\boldsymbol{\partial \Delta Q}}{\boldsymbol{\partial V}} \end{bmatrix} \begin{bmatrix} \Delta \boldsymbol{\theta} \\ \Delta |\boldsymbol{V}| \end{bmatrix} \tag{4.14}$$

where the submatrices $\boldsymbol{J_1, J_2, J_3, J_4}$ represent derivative matrices of $\Delta \boldsymbol{P}, \Delta \boldsymbol{Q}$ to $\Delta \boldsymbol{\theta}, \Delta |\boldsymbol{V}|$ respectively. Then the classic power flow Jacobian (i.e. power flow sensitivity matrix) is denoted as:

$$\boldsymbol{J} = \begin{bmatrix} \boldsymbol{J_1} & \boldsymbol{J_2} \\ \boldsymbol{J_3} & \boldsymbol{J_4} \end{bmatrix} \tag{4.15}$$

There are several simplification methods for power flow Jacobian calculation, such as decoupled method, direct current method and etc [85]. If the more accurate information under the overloading situation is the aim to be pursued, the basic calculation method expressed by (4.14) is better but with slower calculation speed than those simplified methods.

4.2.2 Impedance margin sensitivity to power system variables

4.2.2.1 Sensitivity of relay margin to bus voltage

(a) Sensitivity of relay operation margin on transmission lines

According to equation (3.12) and the linearization method, the sensitivity of transmission line relay operation margin to bus voltages can be given by (4.16) and (4.17),

based on power flow of the current operation point. C_{Tij} is the sensitivity vector including the sensitivities of the relay margin M_{Tij} to related bus voltages (θ_i, θ_j, V_i, V_j).

$$\Delta M_{Tij} = C_{T\theta i}\Delta\theta_i + C_{T\theta j}\Delta\theta_j + C_{Tvi}\Delta V_i + C_{Tvj}\Delta V_j \tag{4.16}$$

$$\begin{aligned} C_{Tij} &= [C_{T\theta i} \quad C_{T\theta j} \quad C_{Tvi} \quad C_{Tvj}] \\ &= \left[\frac{\partial M_{Tij}}{\partial \theta_i} \quad \frac{\partial M_{Tij}}{\partial \theta_j} \quad \frac{\partial M_{Tij}}{\partial V_i} \quad \frac{\partial M_{Tij}}{\partial V_j}\right] \end{aligned} \tag{4.17}$$

So at a specific operation point, taking all the concerned relays into consideration, the linearized sensitivity of relay operation margin can be given in matrix form as (4.18), where $\boldsymbol{C_{T\theta}}$ and $\boldsymbol{C_{TV}}$ are submatrices of sensitivity matrix $\boldsymbol{C_T}$ related to the relays on transmission lines.

$$\Delta \boldsymbol{M_T} = \boldsymbol{C_T}\begin{bmatrix}\Delta\boldsymbol{\theta}\\ \Delta\boldsymbol{V}\end{bmatrix} = [\boldsymbol{C_{T\theta}} \quad \boldsymbol{C_{TV}}]\begin{bmatrix}\Delta\boldsymbol{\theta}\\ \Delta\boldsymbol{V}\end{bmatrix} \tag{4.18}$$

(b) Sensitivity of relay operation margin on generators

Similarly, sensitivity calculation can be taken on generator backup relay operation margin. Based on the analysis in the section 3.2.4.2, the generator relay operation margin is mainly related to bus voltages together with some other variables, such as i_{fdi} and δ_i. For the operation margin sensitivity of the relays on synchronous generators, there are two situations to be considered according to the equations (3.18)-(3.24). Also, the active power and reactive power of the generator *i* can be expressed as:

$$P_{gi} = V_i I_{si} cos\varphi_i = \frac{V_i X_{adi} I_{fdi}}{X_{si}} sin\delta_i \tag{4.19}$$

$$Q_{gi} = V_i I_{si} sin\varphi_i = \frac{V_i X_{adi} I_{fdi}}{X_{si}} cos\delta_i - \frac{{V_i}^2}{X_{si}} \tag{4.20}$$

- Under field current limiter

When $\varphi_i > \varphi_r$, the FCL is the first constraint to be violated under the overloading situation, so the generator relay margin M_{Gi}^{fcl} can be given by (4.21). Then the linear relationship and sensitivity vector C_{Gi}^{fcl} of the relay operation margin are given by (4.22) and (4.23), where $\Delta V_i, \Delta I_{fdi}, \Delta\delta_i$ are variations of the related voltage, field current and power angle respectively; $C_{GVi}^{fcl}, C_{Ifdi}^{fcl}, C_{G\delta_i}^{fcl}$ are the sensitivities of M_{Gi}^{fcl} to the variables V_i, I_{fdi}, δ_i respectively.

$$M_{Gi}^{fcl} = Z_{ai} - Z_{fcli} \tag{4.21}$$

$$\Delta M_{Gi}^{fcl} = C_{GVi}^{fcl}\Delta V_i + C_{Ifdi}^{fcl}\Delta I_{fdi} + C_{G\delta_i}^{fcl}\Delta\delta_i \tag{4.22}$$

$$C_{Gi}^{fcl} = \begin{bmatrix} C_{GVi}^{fcl} & C_{Ifdi}^{fcl} & C_{G\delta_i}^{fcl} \end{bmatrix} = \begin{bmatrix} \frac{\partial M_{Gi}^{fcl}}{\partial V_i} & \frac{\partial M_{Gi}^{fcl}}{\partial I_{fdi}} & \frac{\partial M_{Gi}^{fcl}}{\partial \delta_i} \end{bmatrix} \tag{4.23}$$

When the generator i hits the FCL, i.e. $i_{ifd} = i_{ifdmax}$ and $M_{Gi}^{fcl} \leq 0$, suppose the active power P_{gi} is constant, then from (4.19), the angle δ_i is a function of V_i. Also from (4.20), Q_{gi} will also change with V_i, so this type of node can be regarded as PIf node [86]. Considering $i_{ifd} = i_{ifdmax}$ in a long run, i.e. $\Delta I_{fdi} = 0$, the equation (4.22) can be accordingly simplified as (4.24). The related sensitivity $C_{GVi}^{fcl'}$ given by (4.25), indicates that this generator is mainly related to bus voltage in the prevailing state; $C_{G\delta_i Vi}^{fcl}$ is the sensitivity of δ_i to V_i.

$$\Delta M_{Gi}^{fcl} = C_{GVi}^{fcl}\Delta V_i + C_{G\delta_i}^{fcl}\Delta\delta_i = C_{GVi}^{fcl'}\Delta V_i \tag{4.24}$$

$$C_{GVi}^{fcl'} = C_{GVi}^{fcl} + C_{G\delta_i}^{fcl} * C_{G\delta_i Vi}^{fcl} = \frac{\partial M_{Gi}^{fcl}}{\partial V_i} + \frac{\partial M_{Gi}^{fcl}}{\partial \delta_i} * \frac{\partial \delta_i}{\partial V_i} \tag{4.25}$$

- Under stator current limiter

When $\varphi_i \leq \varphi_r$, the SCL will be the first constraint to be hit during load restoration. Based on (4.19) and (4.20), the stator current can be expressed as:

$$I_{si} = \frac{\sqrt{X_{adi}{}^2 I_{fdi}{}^2 + V_i{}^2 - 2V_i X_{adi} I_{fdi}\cos\delta_i}}{X_{si}} \tag{4.26}$$

Then the measured impedance Z_{ai} and relay margin M_{Gi}^{scl} can be given by (4.27) and (4.28) respectively. Similarly, the linear relationship and sensitivity vector C_{Gi}^{scl} of the relay operation margin are given by (4.29) and (4.30), where ΔV_i and ΔI_{si} are variations of the related voltage and stator current respectively; C_{GVi}^{scl} and C_{Isi}^{scl} are the sensitivities of M_{Gi}^{scl} to the variables V_i and I_{si} respectively.

$$Z_{ai} = V_i / I_{si} \tag{4.27}$$

$$M_{Gi}^{scl} = Z_{ai} - Z_{scli} \tag{4.28}$$

$$\Delta M_{Gi}^{scl} = C_{GVi}^{scl}\Delta V_i + C_{Isi}^{scl}\Delta I_{si} \tag{4.29}$$

$$C_{Gi}^{scl} = [C_{GVi}^{scl} \quad C_{Isi}^{scl}] = \left[\frac{\partial M_{Gi}^{scl}}{\partial V_i} \quad \frac{\partial M_{Gi}^{scl}}{\partial I_{si}}\right] \tag{4.30}$$

When the generator hits the SCL, i.e. $M_{Gi}^{scl} \leq 0$, $I_{si} = I_{simax}$, $\Delta I_{si} = 0$; and its linear form to the variables (V_i and I_{si}) can be similarly simplified as:

$$\Delta M_{Gi}^{scl} = C_{GVi}^{scl}\Delta V_i + C_{Isi}^{scl}\Delta I_{si} = C_{GVi}^{scl}\Delta V_i \tag{4.31}$$

So in the Normal state, taking all the concerned relays into consideration, the sensitivity of relay operation margin can be given in matrix form as (4.32), where $\boldsymbol{C_{GV}}$, $\boldsymbol{C_{GIfd}}$, $\boldsymbol{C_{GIs}}$, $\boldsymbol{C_{G\delta}}$ are submatrices of sensitivity matrix $\boldsymbol{C_G}$ related to the relays on generators. Also, with the division angle φ_r, sensitivity matrices will be calculated differently with superscript ***fcl*** or ***scl***.

$$\Delta \boldsymbol{M_G} = \begin{cases} \boldsymbol{C_G^{fcl}}\begin{bmatrix}\Delta \boldsymbol{V} \\ \Delta \boldsymbol{I_{fd}} \\ \Delta \boldsymbol{\delta}\end{bmatrix} = \begin{bmatrix}\boldsymbol{C_{GV}^{fcl}} & \boldsymbol{C_{GIfd}^{fcl}} & \boldsymbol{C_{G\delta}^{fcl}}\end{bmatrix}\begin{bmatrix}\Delta \boldsymbol{V} \\ \Delta \boldsymbol{I_{fd}} \\ \Delta \boldsymbol{\delta}\end{bmatrix}, & \boldsymbol{\varphi > \varphi_r} \\ \boldsymbol{C_G^{scl}}\begin{bmatrix}\Delta \boldsymbol{V} \\ \Delta \boldsymbol{I_s}\end{bmatrix} = \begin{bmatrix}\boldsymbol{C_{GV}^{scl}} & \boldsymbol{C_{GIs}^{scl}}\end{bmatrix}\begin{bmatrix}\Delta \boldsymbol{V} \\ \Delta \boldsymbol{I_s}\end{bmatrix}, & \boldsymbol{\varphi \leq \varphi_r} \end{cases} \tag{4.32}$$

But in those emergency operation states, the linear form of $\boldsymbol{M_G'}$ and sensitivity $\boldsymbol{C_G'}$ on generators could be simplified from (4.24) and (4.31) to (4.33).

$$\Delta \boldsymbol{M_G'} = \boldsymbol{C_G'}\Delta \boldsymbol{V} = \begin{cases} \boldsymbol{C_{GV}^{fcl'}}\Delta \boldsymbol{V}, & \boldsymbol{\varphi > \varphi_r} \\ \boldsymbol{C_{GV}^{scl}}\Delta \boldsymbol{V}, & \boldsymbol{\varphi \leq \varphi_r} \end{cases} \tag{4.33}$$

4.2.2.2 Sensitivity of relay margin to injection power

Suppose that the power flowing into the bus is positive. Based on load flow Jacobian $\boldsymbol{J}$, the sensitivities of relay margins to bus powers can be derived from (4.34) and (4.35) at the current operation point, where $\boldsymbol{H_T}$, $\boldsymbol{H_G}$ are sensitivity matrices of impedance margins of relays on transmission lines and generators respectively; $\boldsymbol{H_{TP}}$, $\boldsymbol{H_{TQ}}$ are the submatrices of $\boldsymbol{H_T}$; $\boldsymbol{H_{GP}}$, $\boldsymbol{H_{GQ}}$ are submatrices of $\boldsymbol{H_G}$; $\Delta \boldsymbol{P}$, $\Delta \boldsymbol{Q}$ are the variations of active and reactive powers; $\boldsymbol{J_T^{-1}}$ and $\boldsymbol{J_G^{-1}}$ are submatrices of $\boldsymbol{J^{-1}}$.

$$\Delta \boldsymbol{M_T} = \boldsymbol{H_T}\begin{bmatrix}\Delta \boldsymbol{P} \\ \Delta \boldsymbol{Q}\end{bmatrix} = \begin{bmatrix}\boldsymbol{H_{TP}} & \boldsymbol{H_{TQ}}\end{bmatrix}\begin{bmatrix}\Delta \boldsymbol{P} \\ \Delta \boldsymbol{Q}\end{bmatrix} \tag{4.34}$$

$$\Delta \boldsymbol{M_G} = \boldsymbol{H_G}\begin{bmatrix}\Delta \boldsymbol{P} \\ \Delta \boldsymbol{Q}\end{bmatrix} = \begin{bmatrix}\boldsymbol{H_{GP}} & \boldsymbol{H_{GQ}}\end{bmatrix}\begin{bmatrix}\Delta \boldsymbol{P} \\ \Delta \boldsymbol{Q}\end{bmatrix} \tag{4.35}$$

where

$$\boldsymbol{H_T = C_T J_T^{-1}} \tag{4.36}$$

$$\boldsymbol{H_G = C_G' J_G^{-1}} \tag{4.37}$$

If the injection powers are with constant power factor $\boldsymbol{cos\emptyset}$ and the node types are neglected, then based on (4.34)-(4.37) and online data of injection powers, the sensitivity matrix $\boldsymbol{H_S}$ between the relay margins $\boldsymbol{M}$ and the apparent injection powers $\boldsymbol{S}$ can be deduced by (4.38).

$$\begin{aligned} \Delta \boldsymbol{M} &= \boldsymbol{H}\begin{bmatrix}\Delta \boldsymbol{P}\\ \Delta \boldsymbol{Q}\end{bmatrix} = \begin{bmatrix}\boldsymbol{H_P} & \boldsymbol{H_Q}\end{bmatrix}\begin{bmatrix}\Delta \boldsymbol{P}\\ \Delta \boldsymbol{Q}\end{bmatrix} = \boldsymbol{H_P}\Delta \boldsymbol{P} + \boldsymbol{H_Q}\Delta \boldsymbol{Q} \\ &= \left(\boldsymbol{H_P cos\emptyset} + \boldsymbol{H_Q sin\emptyset}\right)\Delta \boldsymbol{S} = \boldsymbol{H_S}\Delta \boldsymbol{S} \end{aligned} \tag{4.38}$$

where $\boldsymbol{H}$ is the sensitivity matrix of impedance margin $\boldsymbol{M}$ to $\boldsymbol{P}$ and $\boldsymbol{Q}$; $\boldsymbol{H_P}$ and $\boldsymbol{H_Q}$ are the submatrices of $\boldsymbol{H}$. $\Delta \boldsymbol{P}$ and $\Delta \boldsymbol{Q}$ can be injection power variations of generators or the ones of loads.

4.2.2.3 Sensitivity of relay margin to tap ratio

Assume the variation of tap ratio on a transformer is Δr, if other control parameters keep unchanged, then the bus voltages will change as well as line currents, so the measured impedances by relays will change. Then the sensitivity matrix $\mathcal{L}_{\boldsymbol{Mr}}$ between load bus voltages $\boldsymbol{V}$ and tap ratios $\boldsymbol{r}$ can be given by:

$$\Delta \boldsymbol{V} = \mathcal{L}_{\boldsymbol{Mr}}\Delta \boldsymbol{r} \tag{4.39}$$

As for the branch *ij* with a tap changing transformer, as shown in Fig. 4.1, when the tap ratio r is at the nominal value, the transformer is represented by a series impedance $z_t(= 1/y_t)$. With an off nominal ratio, the impedance on this branch is different due to the effect of the off nominal ratio [1].

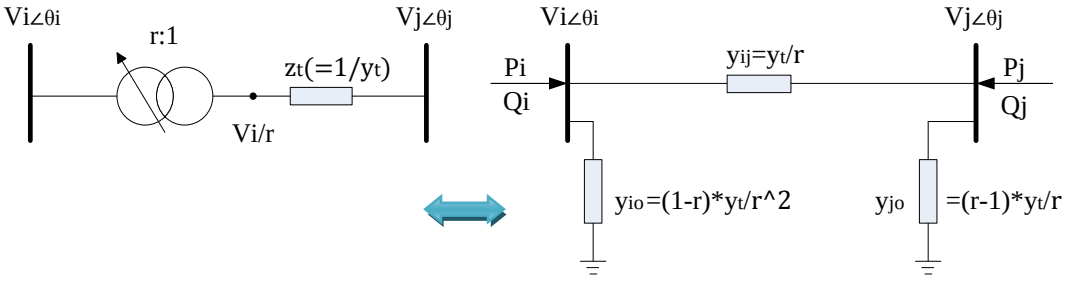

(a)Transformer with tap ratio r:1 (b) Equivalent circuit for tap changing transformer

Fig. 4.1 A transformer branch with tap changer

The **Π** model equivalent circuit considering the off nominal tap ratio is shown in Fig. 4.1 (b). The parameters of **Π** model equivalent circuit are expressed as:

$$\begin{cases} y_{ij} = \dfrac{y_t}{r} \\ y_{i0} = \dfrac{(1-r)y_t}{r^2} \\ y_{j0} = \dfrac{(r-1)y_t}{r} \end{cases} \qquad tap\ side \tag{4.40}$$

When the tap ratio is changed by Δr, the node admittance matrix $\boldsymbol{Y}$ will be changed, and power flow on this branch will be changed accordingly, which induce the injection powers at related nodes change. Assume $y_{ij}\angle\varphi_{ij} = g_{ij} + jb_{ij}$, then based on power equations (4.11) (4.12), the sensitivities $\boldsymbol{\mathcal{L}_{Sr}}$ of injection powers to tap ratios can be expressed as:

$$\boldsymbol{\mathcal{L}_{Sr}} = \begin{cases} \dfrac{\partial P_i}{\partial r} = -\left(\dfrac{2}{\mathrm{r}^3}\right)V_i^2 g_{ij} + \left(\dfrac{1}{\mathrm{r}^2}\right)V_i V_j\left(g_{ij}cos\theta_{ij} + b_{ij}sin\theta_{ij}\right) \\ \dfrac{\partial Q_i}{\partial r} = \left(\dfrac{2}{\mathrm{r}^3}\right)V_i^2 g_{ij} - \left(\dfrac{1}{\mathrm{r}^2}\right)V_i V_j\left(b_{ij}cos\theta_{ij} - g_{ij}sin\theta_{ij}\right) \\ \dfrac{\partial P_j}{\partial r} = \left(\dfrac{1}{\mathrm{r}^2}\right)V_i V_j\left(g_{ij}cos\theta_{ij} - b_{ij}sin\theta_{ij}\right) \\ \dfrac{\partial Q_j}{\partial r} = -\left(\dfrac{1}{\mathrm{r}^2}\right)V_i V_j\left(b_{ij}cos\theta_{ij} + g_{ij}sin\theta_{ij}\right) \\ \dfrac{\partial Q_k}{\partial r} = 0 \qquad (k \neq i, k \neq j) \end{cases} \tag{4.41}$$

where $\theta_{ij} = \theta_j - \theta_i$, bus *i* is at the tap side.

If there are n tap changing transformer branches in the system, then

$$\begin{bmatrix} \Delta \boldsymbol{P} \\ \Delta \boldsymbol{Q} \end{bmatrix} = \boldsymbol{\mathcal{L}_{Sr}}\Delta \boldsymbol{r} = \begin{bmatrix} \boldsymbol{\mathcal{L}_{Pr1}} & \cdots & \boldsymbol{\mathcal{L}_{Prn}} \\ \boldsymbol{\mathcal{L}_{Qr1}} & \cdots & \boldsymbol{\mathcal{L}_{Qrn}} \end{bmatrix} \begin{bmatrix} \Delta r_1 \\ \vdots \\ \Delta r_n \end{bmatrix} \tag{4.42}$$

where $\boldsymbol{\mathcal{L}_{Pr1}} \ldots \boldsymbol{\mathcal{L}_{Prn}}$ and $\boldsymbol{\mathcal{L}_{Qr1}} \ldots \boldsymbol{\mathcal{L}_{Qrn}}$ are the submatrices of $\boldsymbol{\mathcal{L}_{Sr}}$.

From equations (4.41) and (4.42), the $\boldsymbol{\mathcal{L}_{Sr}}$ is a sparse matrix, there are at most two non-zero elements in each column, which is related to the nodes of tap changing transformer branch.

Therefore, according to the equations (4.34) and (4.35), the linear form of $\Delta \boldsymbol{M}$ to tap ratios can be given by:

$$\Delta \boldsymbol{M} = \boldsymbol{H}\begin{bmatrix}\Delta \boldsymbol{P} \\ \Delta \boldsymbol{Q}\end{bmatrix} = \boldsymbol{\mathcal{L}_{Mr}}\Delta \boldsymbol{r} \tag{4.43}$$

and the related sensitivity matrices can be obtained by:

$$\boldsymbol{\mathcal{L}_{Mr}} = \boldsymbol{H}\boldsymbol{\mathcal{L}_{Sr}} \tag{4.44}$$

4.3 Emergency state analysis

4.3.1 Detection of vulnerable relays

Detection of vulnerable areas and main supply paths in a power system is very significant for power system secure operation, which is a precondition for an effective implementation of special protection and emergency control.

Based on online sensitivity analysis between relay operation margins and power system variables, the sensitive relays and related main supply sets to critical loads can be quickly and easily defined. Also in Chapter III, the backup setting of distance relay is designed with the consideration of loadability, so the dispersed relays can provide prompt and accurate information locally related to overload emergency situations.

4.3.1.1 The supply sets to critical loads

(a) Critical load searching

Since the load variations on different load buses will make different effects on the margins of dispersed relays, in order to search the critical loads which have bigger effects, a performance index related to load effect on relay is proposed here.

Suppose all the distributed relays in a power system are collected as set A, power components are collected as set *B* (in which B_G denotes the set of generators, B_T denotes the set of transmission lines and B_L denotes the set of loads). Based on prevailing system data, a performance index PI_{BL} is defined by (4.45) to evaluate the total effect of a variation of load *i* on all the relays in the positive direction.

$$PI_{BLi} = \sum_{j \in \mathrm{A}^+} w_j H_{MBLij} \tag{4.45}$$

where PI_{BLi} is the performance index of load i ($i \in B_L$); H_{MBLij} is the impedance margin sensitivity between load i and relay j; A^+ represents the all the relays in the positive direction; and w_j is the related weight of relay j, which is expressed as:

$$w_j = \left(|M_j| \Big/ \sum_{k \in \mathrm{A}^+} |M_k| \right)^{-1} \tag{4.46}$$

In (4.46), M_j is the operation margin of relay j, and M_k is the operation margin of relay k, $j, k \in \mathrm{A}^+$. Obviously, the weight of relay j is inverse proportional to its prevailing relay operation margin. Based on the performance indexes PI_{BL}, the critical loads which have bigger influences on impedance margins can be found and grouped as B'_L with a preset threshold ξ_2.

(b) The supply sets to critical loads

Then according to the equation (4.38), the sensitivity matrix $\boldsymbol{H_{MB'L}}$ between all related relay operation margins $\boldsymbol{M_A}$ and selected load powers $\boldsymbol{S_{B'L}}$ of loads in B'_L can be obtained by:

$$\Delta \boldsymbol{M_A} = \boldsymbol{H_{MB'L}} \Delta \boldsymbol{S_{B'L}} \tag{4.47}$$

Based on $\boldsymbol{H_{MB'L}}$, the related sensitive relays (with the absolute value of sensitivity bigger than a selection threshold ξ_1) to the load points in B'_L can be easily found and grouped as a set A_L. Then the corresponding set of transmission lines $B_{TL}$is the set of main power flow paths to the critical loads.

Meanwhile, also based on equation (4.38), the sensitivity matrix $\boldsymbol{H_{ALG}}$ between the critical relay margins $\boldsymbol{M_{AL}}$ in A_L and the apparent generator powers $\boldsymbol{S_G}$ can be given by:

$$\Delta \boldsymbol{M_{AL}} = \boldsymbol{H_{ALG}} \Delta \boldsymbol{S_G} \tag{4.48}$$

Based on $\boldsymbol{H_{ALG}}$, the relative sensitive generators (with a selection threshold ξ_3) to the relays in A_L can be found subsequently and grouped as B_{GL}, which is the set of main sources supplying the load flow. In this way, the sensitive maps (which are built by links from critical loads, through sensitive transmission lines and related relays, to generators) can be depicted directly and easily, as shown in Fig. 4.2.

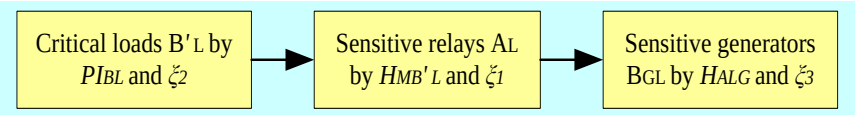

Fig. 4.2 Sensitive map between loads, relays and generators

4.3.1.2 Vulnerable relay detection

(a) Performance indexes of relays

Based on the definition of sensitivity, the margin sensitivities of relays to those critical loads represent the variation speed of margins to load variations. Moreover, the distance from measured apparent impedance to the setting, i.e. the margin of relay *i* (M_i), is already a useful index to show whether this relay and related power component are operated close to their loadability limit in a Normal state. Also in the emergency states, the margin represents the distance to be recovered to Normal state. So in order to discover the relays which are more vulnerable to load variations, a performance index considering both margin and sensitivity is given by:

$$PI_{rj} = \frac{\sum_{i\in B_L'} w_i H_{MB'Lij} / |M_j|}{\max_n \left\{ \sum_{i\in B_L'} w_i H_{MB'Lij} / |M_1|, \cdots, \sum_{i\in B_L'} w_i H_{MB'Lij} / |M_n| \right\}} \tag{4.49}$$

where PI_{rj} is the performance index of relay *j* in A_L; $H_{MB'Lij}$ is the margin sensitivity of relay j to the critical load i in B_L'; M_j is the online measured margin of relay *j; n* represents the number of all the related sensitive relays in A_L; and w_i is the related weight of load i, which is expressed as:

$$w_i = |PI_{BLi}| \Big/ \sum_{k\in B_L'} |PI_{BLk}| \tag{4.50}$$

PI_{BLi} represents the performance index of load *i*, PI_{BLk} is the performance index of load k in critical load set B_L'. The load with bigger w_i means relay margins will be more vulnerable to this load. Since the power injected into bus node is assumed positive, only the relays in the positive direction with positive sensitivities are considered here under overloading situations.

It can be seen from equation (4.49), if the relay *j* has bigger $H_{MB'Lij}$ and smaller $|M_i|$, the PI_{rj} will be bigger, which means this relay are more vulnerable to the load increments; otherwise, the related relay is less vulnerable. Based on PI_{rj}, the *n* relays in A_L can be classified into two sets with a threshold ξ_1', i.e. high vulnerable set and low vulnerable set, which is important for emergency state monitoring and emergency control defining under emergency situations.

(b) State signals of each relay

Based on the design of distance relay in Chapter III, according to state signals of relays and breakers, the Control center (CC) can sense the critical relays in emergency states immediately. From Fig. 4.3, the five states can be detected according to the prevailing position of Z_{ai} and breaker states; and the detailed meanings of signal codes for different states can be found in the section 3.3.1.

In the Normal state (0001) or tripping state (1111 or 1101), the CC will do nothing but keep its monitoring function. Those relays in Urgent state (0011) and Zone 3 start state (0111 or 0101) will be grouped into set A'_L, which will be selected to do sensitivity analysis and preparation for related emergency control strategy defining. If the relay is already in tripped state (XXX0) with the breaker signal set to "0", the CC will register this state and update the system network data.

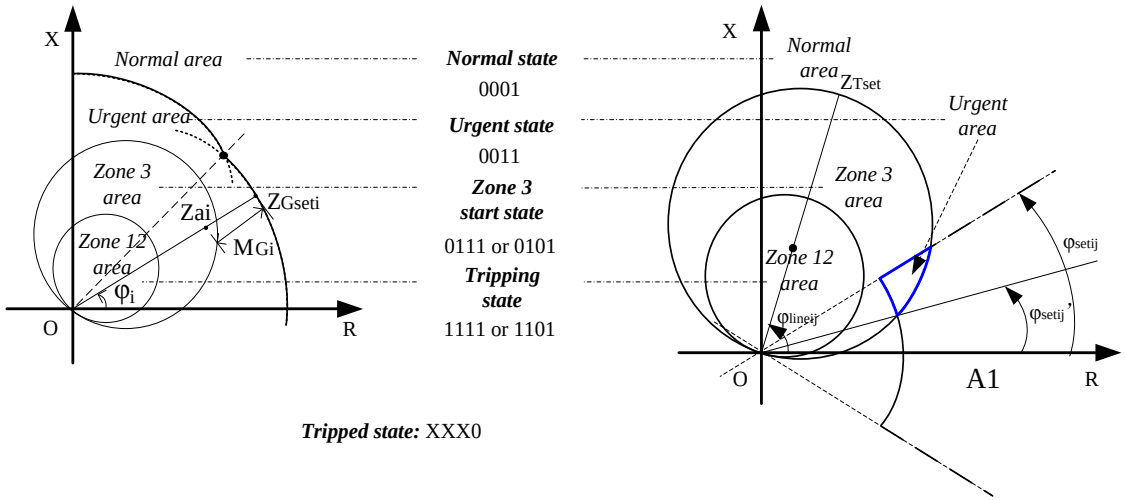

Fig. 4.3 Diverse operation states and related state signals detected by relays

This method is more direct and fast than the sensitivity method, but the sensitivity analysis can supply more information for both normal and emergency situations.

(c) Vulnerable relay detection

Based on the methods discussed above, the flowchart of vulnerable relay detection combining both two methods can be depicted in Fig. 4.4.

By virtue of WAMS, the sensitivity analysis in this thesis, which includes sensitivity calculation, vulnerable relay detection and related supply sets formation, can be done in Control center. On the other side, the local relays can do their local measurements and decisions on which states they are in; meanwhile they can share their data and state

signals with Control center in the environment based on MAS (detailed explanations are made in Chapter VI). Then the vulnerable relays in both normal operation situation and overloading situation can be accurately detected by the MAS based control system, according to local detected state signals and system wide sensitivity information.

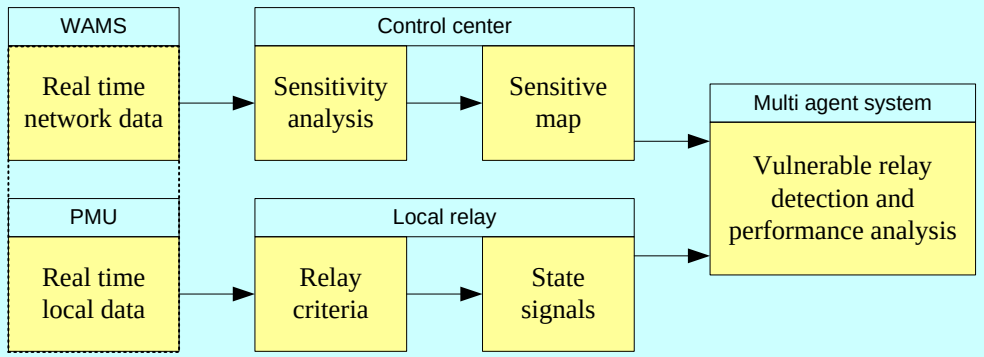

Fig. 4.4 Vulnerable relay detection

4.3.2 Detection of sensitive controllers

In order to timely adjust the emergency states and prevent the unexpected relay operations, three control measures (i.e. the load shedding, generator reschedule and inverse load tap changer control) will be mainly adopted. Take the overload induced Zone 3 start state for an example, the emergency load shedding and generator reschedule would be adopted as main control measures. Before the execution of control measures, the effective controllers can be found out based on sensitivity information.

The sensitivities $\boldsymbol{H_{A'LS}}$ between critical relays in A'_L and injection powers are then adopted here to search the sensitive control points, as given by (4.51). If the generators and loads are located on different buses, also the generators or loads on the same bus are integrated into one generator or load, then $\boldsymbol{H_{A'LS}}$ can be easily divided into two submatrices $\boldsymbol{H_{A'LSG}}$ and $\boldsymbol{H_{A'LSL}}$, which are the sensitivity matrices of $\boldsymbol{M_{A'L}}$ to generator and load powers ($\boldsymbol{S_G}$ and $\boldsymbol{S_L}$) respectively, and given by (4.52).

$$\Delta \boldsymbol{M_{A'L}} = \boldsymbol{H_{A'LS}} \Delta \boldsymbol{S} \tag{4.51}$$

$$\Delta \boldsymbol{M_{A'L}} = \mathrm{H}_{\boldsymbol{A'LS}} \Delta \boldsymbol{S} = [\boldsymbol{H_{A'LSG}} \quad \boldsymbol{H_{A'LSL}}] \begin{bmatrix} \Delta \boldsymbol{S_G} \\ \Delta \boldsymbol{S_L} \end{bmatrix} \tag{4.52}$$

If one generator and one load on the same bus i need to be considered separately, the related element ($H_{A'LSi}$) in $\boldsymbol{H_{A'LS}}$ will exist in $\boldsymbol{H_{A'LSG}}$ and $\boldsymbol{H_{A'LSL}}$ at the same time, which

can be expressed by (4.53), with the assumption that only one critical relay is detected in the set A_L':

$$[\boldsymbol{H}_{\boldsymbol{A'LSG}} \quad \boldsymbol{H}_{\boldsymbol{A'LSL}}] = [\dots, H_{A'LSi}, \dots, \quad \dots, H_{A'LSi}, \dots] \tag{4.53}$$

Obviously, at this situation, the dimension of $[\boldsymbol{H}_{\boldsymbol{A'LSG}} \quad \boldsymbol{H}_{\boldsymbol{A'LSL}}]$ will be bigger than $\mathrm{H}_{\boldsymbol{A'LS}}$. And the bus *i* can be used as a control point for both LS and GR.

In this way, the relationships between critical relays in A_L' and those injection powers (generators in B_G and loads in B_L) are defined by sensitivity matrices. According to $\boldsymbol{H}_{\boldsymbol{A'LSG}}$ and $\boldsymbol{H}_{\boldsymbol{A'LSL}}$, the sensitive control points for GR and LS can be easily obtained and classified. Actually for a critical relay, only few control points with larger absolute values of sensitivities have the significant effects on the relay operation margin.

(a) Performance indexes of controllers

Normally except the related sensitivities, the control effects of both LS and GR controllers will be limited by many other factors, such as the control orders from CC, prevailing operation states of controllers and their regulation limits. Here consider regulation limits and related sensitivities, the performance indexes of these controllers can be given by:

$$PI_{ci} = \frac{\sum_{j\in A_L'} w_j \left|H_{A'LSij}\right| \Delta S_{imax}}{\max\limits_{n} \left\{\sum_{j\in A_L'} w_j \left|H_{A'LS1j}\right| \Delta S_{1max}, \cdots, \sum_{j\in A_L'} w_j \left|H_{A'LSnj}\right| \Delta S_{nmax}\right\}} \tag{4.54}$$

where PI_{ci} is the performance index of controller *i*; $H_{A'LSij}$ is the margin sensitivity of relay *j* in A_L' to the control point *i* (generator or load); *n* represents the number of all the related sensitive control points; ΔS_{imax} is the regulation limits of control point *i*; and w_j is the related weight of relay *j*, which is expressed as:

$$w_j = \left|M_j\right| \Big/ \sum_{k\in A_L'} |M_k| \tag{4.55}$$

In the emergency states, the margins of relays in A_L' are negative, so when $\left|M_j\right|$ is bigger, the relay *j* is harder to be recovered, which is different with the normal situation.

Based on related PI_{ci}, the effective generator and load controllers will be selected as set $B_{LA'L}$ and $B_{GA'L}$ with threshold ξ_2' and ξ_3' respectively. Then sensitive map and inclusion relationship between those sensitive and vulnerable sets can be observed in Fig. 4.5. Normally, $A_L' \subset A_L$, $B_{GA'L} \subset B_{GL}$.

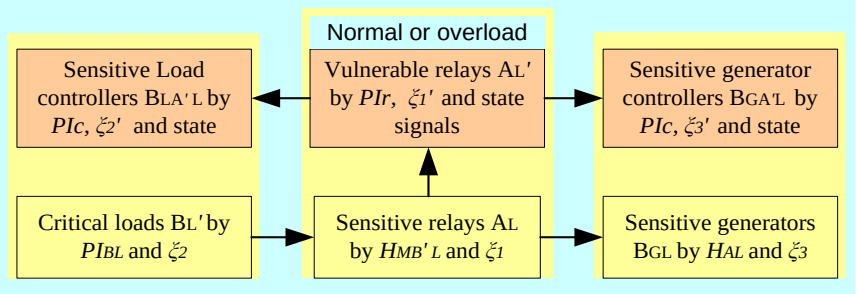

Fig. 4.5 Sensitive map and inclusion relation between sensitive sets

4.3.3 Emergency state prediction and identification

Based on the vulnerable relay detection methods proposed above, not only the specific states can be detected, but also sensitive relationships between related relays and power components can be defined. However in the complex situation, i.e. cascading events, the reasons inducing an emergency state may be very diffident. If the unexpected relay operation cannot be identified and blocked, those sensitivity based analysis methods and subsequent emergency controls will be meaningless. So identification and prediction are significant for overload emergency states after outage contingencies or those unexpected control operations.

4.3.3.1 Load flow transferring due to line outage

(a) N-1 situation

Line outage induced load flow transferring to overload, as a basic process of cascading events, may trigger the unexpected relay operations. With the aim of finding the influence factors between relay measured impedance and load flow transferring, the sensitivity method can also be applied here. The impedance seen by Relay 1 in Fig. 4.6 can be rewritten with (4.56)-(4.58).

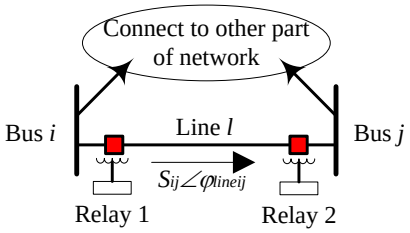

Fig. 4.6 Traditional distance relay on Line *l*

$$\overline{Z_{aij}} = R_{aij} + jX_{aij} \tag{4.56}$$

$$R_{aij} \approx \frac{V_i\left(G_{ij}V_j cos\theta_{ij} + B_{ij}V_j sin\theta_{ij} - G_{ij}V_i\right)}{\left(B_{ij}^2 + G_{ij}^2\right)\left(V_i^2 + V_j^2 - 2V_iV_j cos\theta_{ij}\right)} \tag{4.57}$$

$$X_{aij} \approx \frac{V_i\left(B_{ij}V_j cos\theta_{ij} - G_{ij}V_j sin\theta_{ij} - B_{ij}V_i\right)}{\left(B_{ij}^2 + G_{ij}^2\right)\left(V_i^2 + V_j^2 - 2V_iV_j cos\theta_{ij}\right)} \tag{4.58}$$

where $\overline{Y_{ij}} = \overline{Z_{ij}}^{-1} = G_{ij} + jB_{ij}$, Z_{ij} is the impedance of Line l ignoring the susceptance to the ground.

- Impedance sensitivity to system operation variables

Similar to impedance margin sensitivity formula (4.16) (4.17), the linearized form of (4.57) (4.58) is given by (4.59) (4.60).

$$\Delta R_{aij} = C_{R\theta i}\Delta\theta_i + C_{R\theta j}\Delta\theta_j + C_{Rvi}\Delta V_i + C_{Rvj}\Delta V_j \tag{4.59}$$

$$\Delta X_{aij} = C_{X\theta i}\Delta\theta_i + C_{X\theta j}\Delta\theta_j + C_{Xvi}\Delta V_i + C_{Xvj}\Delta V_j \tag{4.60}$$

$$C_{ij} = \begin{bmatrix} C_{Rij} \\ C_{Xij} \end{bmatrix} = \begin{bmatrix} C_{R\theta i} & C_{R\theta j} & C_{Rvi} & C_{Rvj} \\ C_{X\theta i} & C_{X\theta j} & C_{Xvi} & C_{Xvj} \end{bmatrix}$$

$$= \begin{bmatrix} \frac{\partial R_{aij}}{\partial \theta_i} & \frac{\partial R_{aij}}{\partial \theta_j} & \frac{\partial R_{aij}}{\partial V_i} & \frac{\partial R_{aij}}{\partial V_j} \\ \frac{\partial X_{aij}}{\partial \theta_i} & \frac{\partial X_{aij}}{\partial \theta_j} & \frac{\partial X_{aij}}{\partial V_i} & \frac{\partial X_{aij}}{\partial V_j} \end{bmatrix} \tag{4.61}$$

where C_{ij} is the sensitivity matrix including the sensitivities of impedance (R_{aij}, X_{aij}) to related bus voltages $(\theta_i, \theta_j, V_i, V_j)$, C_{Rij} and C_{Xij} are submatrices of C_{ij}.

Taking all the concerned relays into consideration, the sensitivity of impedance can be expressed in the matrix form as (4.62) (4.63); also based on load flow Jacobian $\boldsymbol{J}$, the sensitivity $\boldsymbol{H}$ of impedance to injection powers can be derived from (4.64), where $\boldsymbol{C_{R\theta}}, \boldsymbol{C_{RV}}, \boldsymbol{C_{X\theta}}$and $\boldsymbol{C_{XV}}$ are submatrices of $\boldsymbol{C}$; $\boldsymbol{H_{RP}}, \boldsymbol{H_{RQ}}, \boldsymbol{H_{XP}}$and $\boldsymbol{H_{XQ}}$are submatrices of $\boldsymbol{H}$.

$$\begin{bmatrix} \Delta \boldsymbol{R_a} \\ \Delta \boldsymbol{X_a} \end{bmatrix} = \boldsymbol{C}\begin{bmatrix} \Delta \boldsymbol{\theta} \\ \Delta \boldsymbol{V} \end{bmatrix} = \begin{bmatrix} \boldsymbol{C_{R\theta}} & \boldsymbol{C_{RV}} \\ \boldsymbol{C_{X\theta}} & \boldsymbol{C_{XV}} \end{bmatrix}\begin{bmatrix} \Delta \boldsymbol{\theta} \\ \Delta \boldsymbol{V} \end{bmatrix} \tag{4.62}$$

$$\begin{bmatrix} \Delta \boldsymbol{R_a} \\ \Delta \boldsymbol{X_a} \end{bmatrix} = \boldsymbol{H}\begin{bmatrix} \Delta \boldsymbol{P} \\ \Delta \boldsymbol{Q} \end{bmatrix} = \begin{bmatrix} \boldsymbol{H_{RP}} & \boldsymbol{H_{RQ}} \\ \boldsymbol{H_{XP}} & \boldsymbol{H_{XQ}} \end{bmatrix}\begin{bmatrix} \Delta \boldsymbol{P} \\ \Delta \boldsymbol{Q} \end{bmatrix} \tag{4.63}$$

where

$$\boldsymbol{H = CJ^{-1}} \tag{4.64}$$

- Flow transferring prediction and identification

In order to predict the post outage load flow transferring based on pre outage system data, the simulation method of line outage is shown in Fig. 4.7. Fig. 4.7 (a) is a network

operated in normal situation without line outage. Suppose line *l* from bus *m* to bus *n* was tripped by circuit breakers due to some kind of fault, as shown in Fig. 4.7 (b). A line outage may be modeled by adding two virtual power injections ($\Delta P_m, \Delta Q_m, \Delta P_n, \Delta Q_n$) to the network, one at each end of the line to be tripped [84], which is shown in Fig. 4.7 (c). At the situation of Fig. 4.7 (c), the line is still kept in the network, and the effects of its being tripped are modeled by the virtual injections.

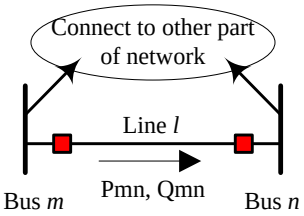

(a) Network before line *l* outage

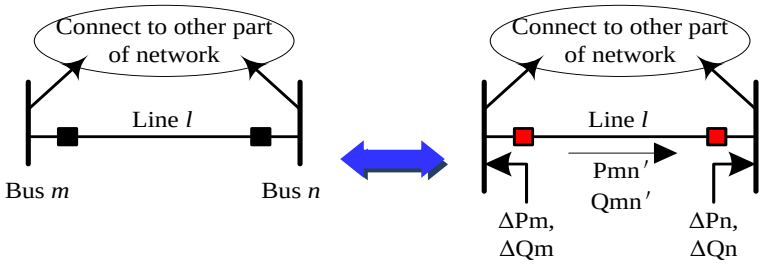

(b) Network after line l outage (c) Modeling the outage by injections

Fig. 4.7 Line outage simulation in power network

With the aim of making these two situations have the equal effect, the virtual power flow on line *l* is only supplied by the virtual power injections in Fig. 4.7 (c), i.e. the necessary requirements about the active power and reactive power on line *l* (considering the susceptance to the ground) should be satisfied as:

$$P'_{mn} = P_{mn} + \Delta P_{mn} = \Delta P_m = -\Delta P_n \tag{4.65}$$

$$\begin{aligned} Q'_{mn} &= Q_{mn} + \Delta Q_{mn} = \Delta Q_m + \frac{b}{2} V'^2_m \\ &= -\Delta Q_n + \frac{P'^2_{mn} + Q'^2_{mn}}{V'^2_m} X_{mn} - \frac{b}{2} V'^2_n \end{aligned} \tag{4.66}$$

where

$$V'_m = V_m + \Delta V_m \tag{4.67}$$

$$V'_n = V_n + \Delta V_n \tag{4.68}$$

P_{mn}, Q_{mn}, V_m, V_n represent the line flows and node voltages in the pre fault state; $P'_{mn}, Q'_{mn}, V'_m, V'_n$ represent these variables in the post fault state; $\Delta P_{mn}, \Delta Q_{mn}, \Delta V_m$ and ΔV_n represent the variations of these variables when the virtual injections have been applied, *b* is the susceptance of line *l* to ground.

In this way, it can be assumed that line *l* is isolated from the remainder of the network even though the breakers are closed. Compared the situation in Fig. 4.7 (c) with Fig. 4.7 (a), the variations are mainly expressed by those virtual injections. So if the $\Delta P_m, \Delta Q_m$ and $\Delta P_n, \Delta Q_n$ can be obtained, the variation of impedances in the relays of rest lines can be easily deduced by (4.63) based on pre fault system data.

- Virtual injection powers calculation

The line flows P_{mn}, Q_{mn} of the line *l* can be expressed as:

$$P_{mn} = V_m V_n (G_{mn} cos\theta_{mn} + B_{mn} sin\theta_{mn}) - G_{mn} V_m^2 \tag{4.69}$$

$$Q_{mn} \approx -V_m V_n (G_{mn} sin\theta_{mn} - B_{mn} cos\theta_{mn}) - B_{mn} V_m^2 \tag{4.70}$$

Then the linear relationship between line flow and these virtual injection powers can be expressed as:

$$\begin{bmatrix} \Delta P_{mn} \\ \Delta Q_{mn} \end{bmatrix} = D_{mn} \begin{bmatrix} \Delta\theta_m \\ \Delta\theta_n \\ \Delta V_m \\ \Delta V_n \end{bmatrix} = L_{mn} \begin{bmatrix} \Delta P_m \\ \Delta P_n \\ \Delta Q_m \\ \Delta Q_n \end{bmatrix} \tag{4.71}$$

$$L_{mn} = D_{mn} {J_{mnmn}}^{-1} \tag{4.72}$$

where D_{mn} is the sensitivity matrix including the sensitivities of line flow to the bus voltages $(\theta_i, \theta_j, V_i, V_j)$, L_{mn} is the sensitivity matrix of line flow to virtual injections. J_{mnmn} is the submatrix of load flow Jacobian $\boldsymbol{J}$.

According to load flow sensitivities in the pre fault state, ΔV_m and ΔV_n can be also expressed by $\Delta P_m, \Delta Q_m, \Delta P_n, \Delta Q_n$, then based on equations (4.65)-(4.72), $\Delta P_m, \Delta Q_m$, $\Delta P_n, \Delta Q_n$ can be calculated easily.

- Sensitivity based relay impedance prediction

When the virtual injection variations $\Delta P_m, \Delta Q_m$ and $\Delta P_n, \Delta Q_n$ are obtained, the impedances seen by relays in the post fault state can be previously calculated based on

the pre fault sensitivities. Based on equation (4.63), the predicted impedance variations (ΔR_{aij}^{Pl}, ΔX_{aij}^{Pl}) on any transmission line *ij*, after line *l* is tripped, can be calculated by:

$$\begin{bmatrix} \Delta R_{aij}^{Pl} \\ \Delta X_{aij}^{Pl} \end{bmatrix} = C_{ij} {J_{ijmn}}^{-1} \begin{bmatrix} \Delta P_m \\ \Delta P_n \\ \Delta Q_m \\ \Delta Q_n \end{bmatrix} = H_{ijmn} \begin{bmatrix} \Delta P_m \\ \Delta P_n \\ \Delta Q_m \\ \Delta Q_n \end{bmatrix} \tag{4.73}$$

where J_{ijmn} is the submatrix of load flow Jacobian $\boldsymbol{J}$, and H_{ijmn} is the submatrix of $\boldsymbol{H}$ defined by (4.64).

- Flow transferring identification

After the line l is tripped by the related relay to clear the fault, the practical impedance can be real time measured by the relays on the remaining transmission lines, named by Z_{aij}^{M}; and the predicted one can be named by Z_{aij}^{P}. It can be inferred that in those outage induced load flow transferring cases, Z_{aij}^{P} and Z_{aij}^{M} will be approximately same; while in the cases of internal faults, this condition cannot be satisfied. In order to distinguish the load flow transferring from internal faults, the identification criterion can be written as:

$$\left| Z_{aij}^{M} - Z_{aij}^{P} \right| < \varepsilon_1 \left| Z_{aij}^{P} \right| \tag{4.74}$$

where

$$Z_{aij}^{M} = R_{aij}^{M} + jX_{aij}^{M} \tag{4.75}$$

$$\begin{aligned} Z_{aij}^{P} &= R_{aij}^{P} + jX_{aij}^{P} \\ &= R_{aij}^{0} + \Delta R_{aij}^{P} + \mathrm{j}(X_{aij}^{0} + \Delta X_{aij}^{P}) \end{aligned} \tag{4.76}$$

R_{aij}^{0} and $X_{aij}^{0}$are measured impedance in the pre fault state; ΔR_{aij}^{P} and ΔX_{aij}^{P} are predicted variation of the impedance in the post fault state; ε_1 represents the threshold of error caused by linearization and neglecting transient characteristics of components. If the criterion holds, this relay will define this trigger caused by line outage induced flow transferring. It should be blocked or extend the delay settings until this line reached its thermal limit, and the emergency countermeasures should be taken to eliminate the overload situation. Otherwise, if the criterion cannot hold, the relay system will define this situation as an internal fault and trip the line according to traditional functions. The workflow chart of this algorithm can be depicted in Fig. 4.8.

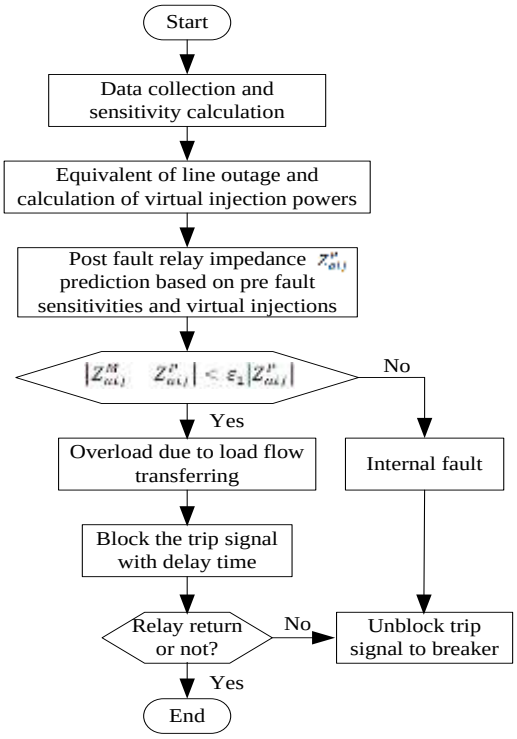

Fig. 4.8 Flowchart of N-1 line outage induced load flow transferring identification

- Transient period consideration

So far in the identification and predication method, the network structure and all other node injections have been assumed unchanged. However, during transient period in the post fault stage, node injection powers are not constant, especially the reactive powers of generators, which is the main reason of error production. Assume that the load model applies static constant power load, the variation of generator node injection should be only considered then. So, according to superposition principle, the final predicted relay impedance variation ($\Delta R_{aij}^{P}, \Delta X_{aij}^{P}$) on line *ij*, after line *l* is tripped, can be expressed as:

$$\begin{bmatrix} \Delta R_{aij}^{P} \\ \Delta X_{aij}^{P} \end{bmatrix} = \begin{bmatrix} \Delta R_{aij}^{Pl} \\ \Delta X_{aij}^{Pl} \end{bmatrix} + \begin{bmatrix} \Delta R_{aij}^{Pg} \\ \Delta X_{aij}^{Pg} \end{bmatrix} \tag{4.77}$$

where

$$\begin{bmatrix} \Delta R_{aij}^{Pg} \\ \Delta X_{aij}^{Pg} \end{bmatrix} = C_{ij} {J_{ijg}}^{-1} \begin{bmatrix} \Delta P_{g1} \\ \vdots \\ \Delta P_{gn} \\ \Delta Q_{g1} \\ \vdots \\ \Delta Q_{gn} \end{bmatrix} = H_{ijg} \begin{bmatrix} \Delta P_{g1} \\ \vdots \\ \Delta P_{gn} \\ \Delta Q_{g1} \\ \vdots \\ \Delta Q_{gn} \end{bmatrix} \tag{4.78}$$

J_{ijg} and H_{ijg} are the submatrices of $\boldsymbol{J}$ and $\boldsymbol{H}$ respectively, which represent the sensitivities of node voltages and relay impedances to generator node injections. $\Delta P_{g1}, \Delta Q_{g1} \cdots \Delta P_{gn}$, ΔQ_{gn} represent the variations of *n* generator node injections.

Actually, the sensitivity matrix $\boldsymbol{H}$ between impedances and injection powers is a high order matrix and the values of most elements in each line are quite small, which means for specific branch in the network, few node injections have the significant influence on the relay measured impedances. So in order to decrease the measurement points in the post fault stage, the generator nodes with bigger performance index will be chosen to be considered in the prediction algorithm.

(b) N-k situation

If the N-k outage is composed by one after one N-1 outage, then the N-1 outage identification method can still be effective. However, if the N-k outage occurs at one time, then this method is hard to be realized due to calculation complexity of virtual injection powers, e.g. 5 branches got cut by the relays due to a bus bar fault in the blackout scenario on 19-bus test system.

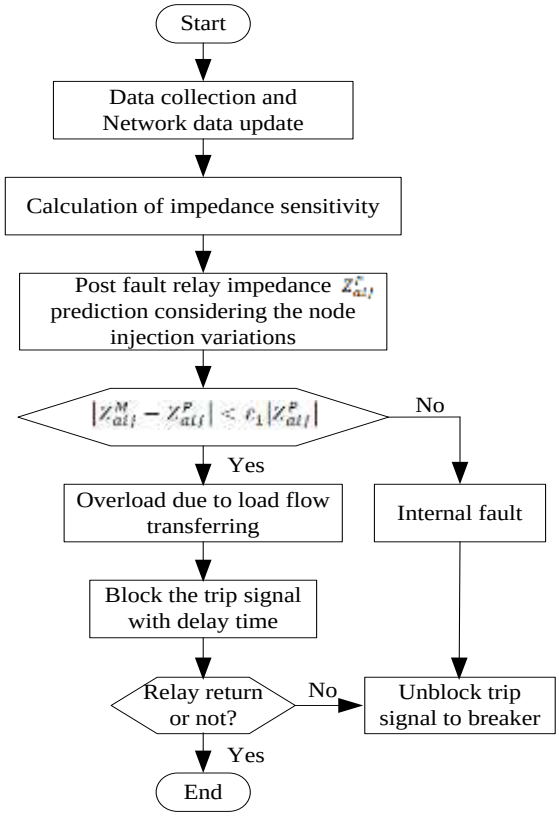

Fig. 4.9 Flowchart of N-k line outage induced load flow transferring identification

In the case of one time N-k outage, the communication based on MAS environment and WAMS will be mainly relied on. The online state signals of relays on the related components will be collected firstly once the N-k outage occurs, and then related impedance sensitivity matrix will be calculated based on updated system wide information. Meanwhile the variation of generator nodes and load nodes will be considered as well. In this way, the impedance variation ($\Delta R_{aij}^{P}, \Delta X_{aij}^{P}$) on any line *ij* in the post N-k outage can be predicted as well. The workflow chart can be seen in Fig. 4.9.

4.3.3.2 Load flow transferring due to LTC operations

Based on the analysis on the blackout scenarios in Chapter 3, the normal LTC operation under heavy loading situation is also regarded as an unexpected control operation which could induce overloading situation and trigger the unexpected relay operations. In order to identify this kind of overload, similarly, sensitivity based prediction and identification method can be defined.

- Impedance sensitivity to tap ratios

The equivalent circuit and impedance margin sensitivity model for transformer with tap changer are already given in 4.2.2.3, similarly, according to the equations (4.43), the linear form of impedances to tap ratios can be given by:

$$\begin{bmatrix}\Delta \boldsymbol{R_a}\\ \Delta \boldsymbol{X_a}\end{bmatrix} = \boldsymbol{H}\begin{bmatrix}\Delta \boldsymbol{P}\\ \Delta \boldsymbol{Q}\end{bmatrix} = \boldsymbol{\mathcal{L}_{Zr}}\Delta \boldsymbol{r} \tag{4.79}$$

where $\boldsymbol{\mathcal{L}_{Zr}}$ is the sensitivity matrix between measured impedances and tap ratios, and given by:

$$\boldsymbol{\mathcal{L}_{Zr}} = \boldsymbol{H}\boldsymbol{\mathcal{L}_{\mathrm{Sr}}} \tag{4.80}$$

- Sensitivity based relay impedance prediction

Base on the sensitivity model, the impedances seen by relays can be previously calculated before every next step of LTC operations. Then based on the equation (4.81), the predicted impedance variations ($\Delta R_{aij}^{Plt}, \Delta X_{aij}^{Plt}$) on any transmission line *ij* after next step of LTC operations, can be expressed as:

$$\begin{bmatrix}\Delta R_{aij}^{Plt}\\ \Delta X_{aij}^{Plt}\end{bmatrix} = \boldsymbol{\mathcal{L}_{Zr.ijk}}\begin{bmatrix}\Delta \mathrm{r}_1\\ \vdots\\ \Delta \mathrm{r}_k\end{bmatrix} \tag{4.81}$$

Here assume *k* LTCs change their taps by one step at the same time, if all their operations are at the different time, then there could be only one element in the matrix $\Delta \boldsymbol{r} = [\Delta \mathrm{r}_1 \quad ... \quad \Delta \mathrm{r}_k]^{\boldsymbol{T}}$. $\boldsymbol{\mathcal{L}_{Zr.ijk}}$ is the submatrix of $\boldsymbol{\mathcal{L}_{Zr}}$.

- LTC operation identification

Similarly, in order to identify the unexpected LTC operation induced overloading situation, the identification criterion based on measured data Z_{aij}^{M} and predicted data Z_{aij}^{P} can be given by:

$$\left|Z_{aij}^{M} - Z_{aij}^{P}\right| < \varepsilon_2 \left|Z_{aij}^{P}\right| \tag{4.82}$$

where

$$Z_{aij}^{M} = R_{aij}^{M} + jX_{aij}^{M} \tag{4.83}$$

$$\begin{aligned} Z_{aij}^{P} &= R_{aij}^{Plt} + jX_{aij}^{Plt} \\ &= R_{aij}^{0} + \Delta R_{aij}^{Plt} + \mathrm{j}\left(X_{aij}^{0} + \Delta X_{aij}^{Plt}\right) \end{aligned} \tag{4.84}$$

R_{aij}^{0} and $X_{aij}^{0}$are measured impedance before every next step of tap operation; ΔR_{aij}^{Plt} and $\Delta X_{aij}^{Plt}$are predicted variation of the impedance after every next step; ε_2 is the threshold of errors.

The identification rules are almost the same with the case of load flow transferring induced overload, except the block signal will be also sent to related LTC controllers to stop their continually unexpected operation. The flowchart of this identification method is shown in Fig. 4.10.

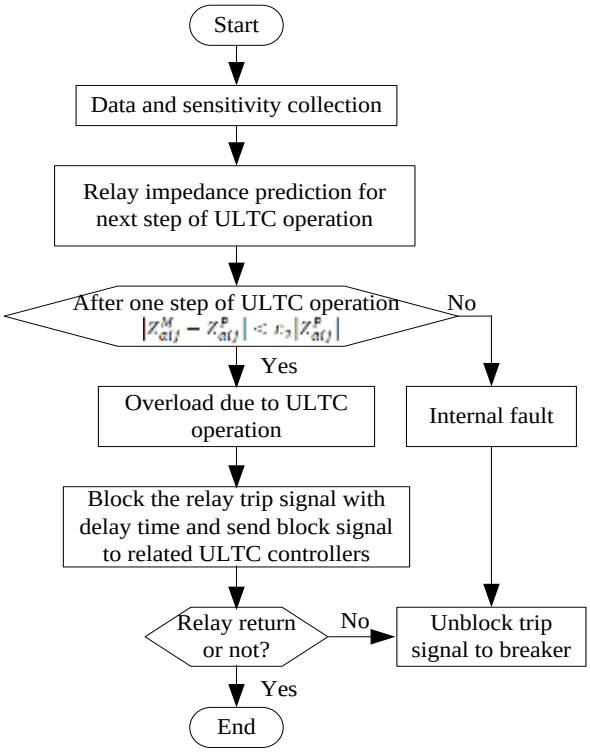

Fig. 4.10 Flowchart of LTC operation induced overload identification

4.4 Case study

4.4.1 Sensitivity analysis

Take the 19-bus test power system in Fig. 3.7 for an example; the sensitivity analysis can be conducted based on the former descriptions.

4.4.1.1 Initial normal situation

In a normal operation state, the status information of generation and load consumption level can be observed in Table A.1 and Table A.2 in Appendix. A.1. Firstly, based on the physical structure and blackout scenario analysis (in former chapter), the test system can be divided into four areas, and it can be easily found the biggest load consumption center (Load 1) is at Bus 12 in Area 2 and take up about 70% of total load, and all the generators in the whole system supply the power to this load. The load set B_L is given by $B_L = \{\text{Load 1}, \text{Load 2}, \text{Load 3}, \text{Load 4}\}$.

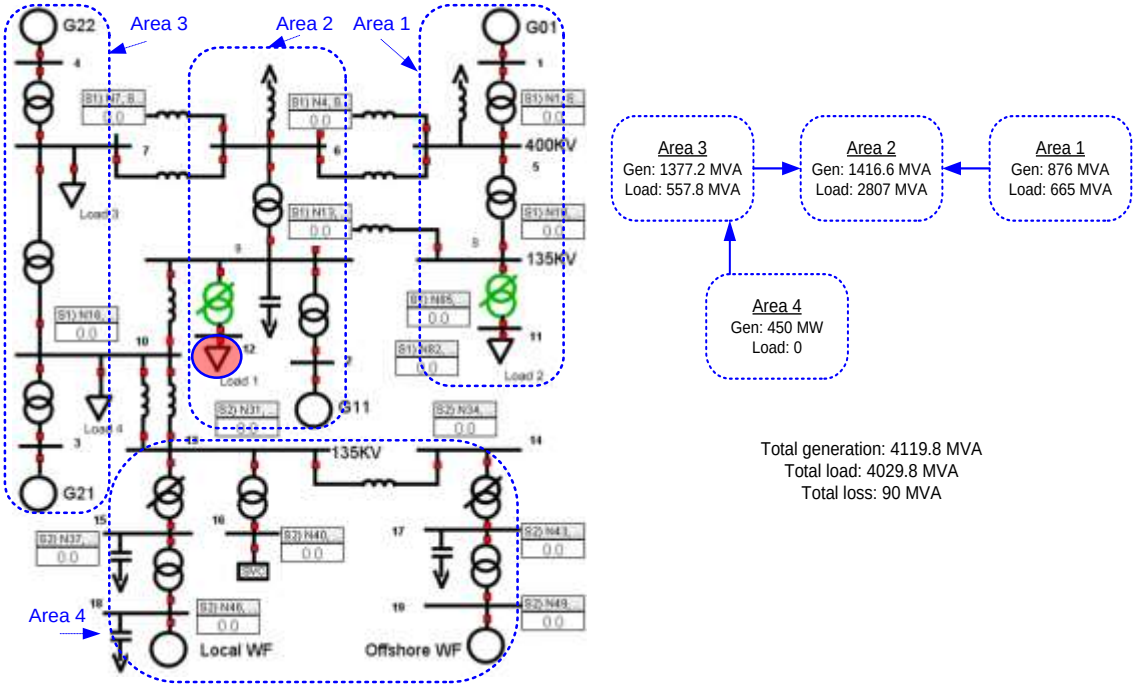

Fig. 4.11Power data and physical areas in eastern Denmark system

Then, the sensitivities $\boldsymbol{H_{MBL}}$ between all distance relays and loads in this normal operation state can be calculated quickly, as shown in Table 4.1. The performance indexes PI_{BL} of four loads are also given in the table with green color. By virtue of directional characteristics considered in the distance relay settings, the relays in the

negative direction are neglected because they won't be easy to be affected by overloading operation conditions. Based on PI_{BL}, the critical load set can be easily obtained: $B_L' =$ {Load 1}, the threshold is set as $\xi_2 = 3$, considering the size and type of the loads.

Also since the SVC (±50Mvar) at Bus 16 is set to control the voltage of Bus 13 (135kV), and only wind generators are in Area 4 with limited capacities, the distance relays in this area are not easy to be influenced by load variations, except the case when the SVC hits its limit and the voltages in Area 4 decreased a lot. So in the Normal state of SVC operation, the relays in this area with their sensitivities in olive green color in Table 4.1 are not considered in the sensitivity analysis.

Table 4.1 Performance index $\boldsymbol{PI_{BL}}$ of loads and sensitivities $\boldsymbol{H_{MBL}}$ of relays to loads

	S7	S10	S11	S12
$\boldsymbol{PI_{BL}}$	-1.3776	2.309	1.23	3.1392
R_{G01}	-0.019	0.014	0.0077	**0.0105**
R_{G11}	-0.00453	0.0137	0.0029	**0.0213**
R_{G21}	-0.0135	0.0297	0.0048	**0.0096**
R_{G22}	-0.0174	0.0141	0.0066	**0.0098**
R_{TL0605}	-0.0763	-0.0668	-9.00E-05	**-0.0049**
R_{TL0706}	-0.0245	-0.0172	0.0006	**-0.0032**
R_{TL0809}	-0.0009	0.0163	0.0007	**0.0337**
R_{TL1009}	-0.0019	-0.016	0.0008	**0.0116**
R_{TX0105}	-0.0024	0.0018	0.001	**0.0013**
R_{TX0508}	-0.0037	-0.0002	0.0033	**0.0008**
R_{TX0209}	-0.0004	0.0011	0.0002	**0.0018**
R_{TX0310}	-0.002	0.0044	0.0007	**0.0014**
R_{TX0407}	-0.0033	0.0027	0.0013	**0.0019**
R_{TX0609}	-0.0255	-0.0082	-0.0252	**0.003**
R_{TX1007}	0.0218	-0.0251	0.0199	**0.0028**
R_{TX0811}	-0.0008	0.0013	0.0236	**0.0014**
R_{TX0912}	-0.0004	0.0003	8.80E-05	**0.0016**
R_{TL1310}	-0.0025	0.0175	0.0017	0.0085
R_{TL1413}	-0.0037	0.0258	0.0025	0.0126
R_{TX1513}	-0.0037	0.0082	0.0013	0.0026
R_{TX1613}	-0.0459	0.3245	0.031	0.0198
R_{TX1815}	-0.0005	0.0011	0.0002	0.0004
R_{TX1714}	-0.0051	0.0357	0.0034	0.0174
R_{TX1917}	-0.006	0.0423	0.004	0.0207

Based on the sensitivity data of relays on generators (in the pink color), transformers and transmission lines (in the blue color), the relative sensitive relays can be easily selected and underlined in Table 4.1. The relay R_{G01} on G01, R_{G11} on G11, R_{G21} on G21, R_{G22} on G22, R_{TL0809} on transmission line TL0809 between Bus 8 and Bus 9,

R_{TL1009} on transmission line TL1009 between Bus 10 and Bus 9 are the sensitive relays with bigger sensitivities (the threshold ξ_1 is set to 0.005), and grouped as A_L. The related transmission lines can be grouped as B_{TL}. This is the first step.

$$A_L = \{R_{G01}, R_{G11}, R_{G21}, R_{G22}, R_{TL0809}, R_{TL1009}\}$$

$$B_{TL} = \{TL0809, TL1009\}$$

Then, in the second step, the sensitivities of these selected relays to apparent generator powers can be deduced based on equation (4.48), as shown in Table 4.2

Table 4.2 Sensitivities $\boldsymbol{H_{ALG}}$ of relays to Generators

$\boldsymbol{H_{ALG}}$	S1 (G01)	S2 (G11)	S3 (G21)	S4 (G22)	S18 (LWF)	S19 (OWF)
R_{G01}	0.0063	0.0001	0.0021	-0.0006	-0.0008	-0.0009
R_{G11}	-3.4E-06	0.0056	3.2E-05	-8.2E-05	-1.3E-03	-1.8E-03
R_{G21}	0.0018	9.5E-05	0.0189	0.0006	-0.0139	-0.015
R_{G22}	3.5E-03	1.0E-04	3.3E-03	0.0078	-4.3E-03	-4.6E-03
R_{TL0809}	-0.0186	2.07E-05	-0.009	-0.0133	-0.0027	-0.0022
R_{TL1009}	-0.0063	3.28E-05	-0.0226	-0.007	-0.0173	-0.0162

It can be seen from Table 4.2, the relative more sensitive generators to the relays in A_L are underlined. Then the set of main sources, which mainly supply the load flows through the sensitive relays in A_L can be defined (the threshold ξ_3 is set to 0.003): $B_{GL} = \{B_{GL1}, B_{GL2}, B_{GL3}, B_{GL4}, B_{GL5}, B_{GL6}\} = \{\{\mathrm{G01}\}, \{\mathrm{G11}\}, \{\mathrm{G21}\}, \{\mathrm{G22}\}, \{\mathrm{G01}, \mathrm{G21}, \mathrm{G22}\}, \{\mathrm{G01}, \mathrm{G21}, \mathrm{G22}, \mathrm{LWF}, \mathrm{OWF}\}\}$.

Meanwhile, based on the physical connection relationship between these elements as shown in Fig. 4.11 (a), the sensitive map can be easily obtained, which can be depicted in Fig. 4.12 (b). It can be seen that there are four supply paths to Load 1, three of them are more sensitive in the preset Normal state, and the one through transformer TX0609 are less sensitive. Based on the sensitive map, it can be inferred that in the normal operation state, variation of critical loads in load set B_L'will mainly influence the margins of relays in relay set A_L, and the variation of output power in generator set B_{GL}.

Also it can be seen that in the normal operation state, R_{G01} and R_{TL0809} are serially connected in one supply path, R_{TL1009} are serially connected with R_{G21} and R_{G22}in the other supply path, and R_{G11} is the third supply path. Based on sensitivity values in Table 4.1, the R_{TL0809}, R_{TL1009} and $R_{G11}$are with bigger sensitivities, which could represent the three different supply paths.

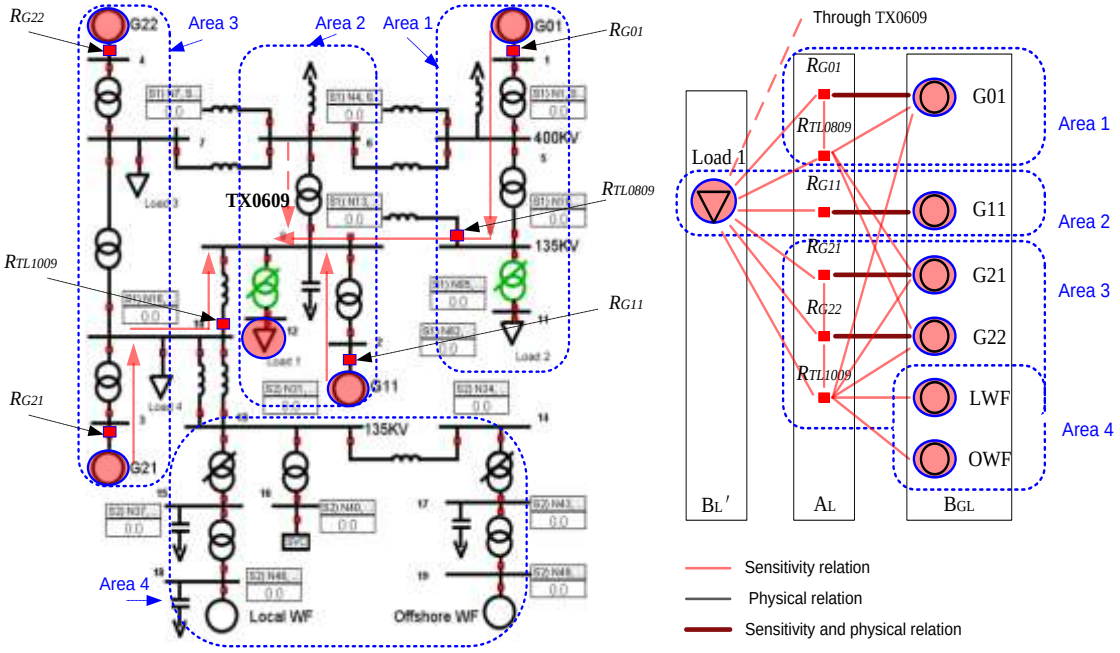

(a) Physical connection relationship (b) Sensitive map

Fig. 4.11 Critical load, sensitive relays and sensitive generators in the system

4.4.1.2 Emergency situations

(a) Detection of vulnerable relays

Here we further take the blackout scenario (the one with relay activated) on the 19-bus system in Chapter 3 for an example. The initial Normal state is the same as the one described above. The three phase fault, which occurred on bus 6 at about 11s, induced an N-5 contingency. From 11s to about 65s, the system survived an oscillation and got temporary stable under the N-5 situation, as shown in Fig. 4.12. However, the load restoration and LTC operations firstly induced backup relay R_{G11} on G11 hit its field current limit at about 70s, and then the Zone 3 relay on TL0809 operated at 86s to trip this line with one second delay. Thereafter, the system entered into a fast voltage collapse together with cascading trips.

In the post fault N-5 situation, the sensitivities at 62s (before the first LTC operation) and 86.5s (R_{TL0809} in a Zone 3 start state) are adopted as examples to be analyzed, as shown in Table 4.3 and Table 4.4. Similarly, the relays in the negative direction are neglected, as well as the relays in Area 4 due to SVC operating in a normal condition.

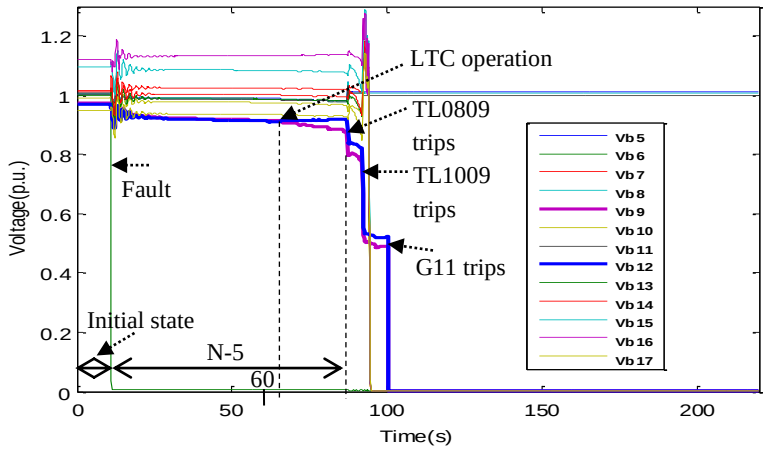

Fig. 4.12 Blackout scenario of cascading events on 19-bus system

Table 4.3 $\boldsymbol{PI_{BL}}$ and $\boldsymbol{H_{MBL}}$ in the N-5 situation

	Normal state under N-5 at 62s				R_{TL0809} in Zone 3 start state at 86.5s			
	S7	S10	S11	S12	S7	S10	S11	S12
$\boldsymbol{PI_{BL}}$	-5.9481	-2.048	1.022	4.6563	-7.3688	-3.4926	0.7324	5.5462
R_{G01}	-0.0076	0.0098	0.0134	**0.0152**	-0.0097	-0.0054	0.0174	**0.0089**
R_{G11}	-0.0189	-0.00936	0.00176	**0.0194**	-0.0126	-0.0122	0.0019	**0.017**
R_{G21}	-0.0367	-0.0176	0.0053	**0.0091**	-0.0258	0.0104	0.0003	**0.0038**
R_{G22}	-0.0539	0.0033	0.0004	**0.0049**	-0.0507	0.0043	0.0001	**0.0015**
R_{TL0809}	-0.0403	-0.02	-0.0005	**0.0409**	-0.0222	-0.013	3.14E-05	**0.0256**
R_{TL1009}	-0.012	-0.0082	0.0004	**0.0057**	-0.0108	-0.0085	0.0004	**0.005**
R_{TX0105}	-0.0008	0.0019	0.0144	**0.0162**	-0.001	-0.0006	0.0018	**0.0082**
R_{TX0508}	0.0013	0.0025	0.0097	**0.0102**	-0.0006	0.0004	0.0064	**0.0075**
R_{TX0209}	-0.003	-0.0005	0.0002	**0.0022**	-0.0019	-0.0011	0.0002	**0.002**
R_{TX0310}	-0.0056	0.0014	0.0002	**0.002**	-0.0033	0.0013	4.17E-05	**0.0005**
R_{TX0407}	-0.012	0.0007	1.00E-04	**0.0011**	-0.011	0.0009	2.95E-05	**0.0003**
R_{TX0710}	-0.0328	0.0007	1.00E-04	**0.001**	-0.0315	0.0004	9.54E-05	**0.0011**
R_{TX0811}	-0.001	-0.0006	2.30E-02	**0.0007**	-0.0012	-0.0007	2.38E-02	**0.0008**
R_{TX0912}	-0.0009	-0.0005	1.00E-04	**0.0023**	-0.0006	-0.0004	5.61E-05	**0.0013**

From Table 4.3, in the Normal state under N-5 situation, the sensitive relays (A_L) to the critical load (Load 1) can be selected with the threshold $\xi_1 = 0.005$. Then the related B_{TL} as well as B_{GL} based on Table 4.4 with the threshold $\xi_3 = 0.003$ can be given by

$$A_L = \begin{cases} \{R_{G01}, R_{G11}, R_{G21}, R_{TL0809}, R_{TL1009}, R_{TX0105}, R_{TX0508}\} & \text{Normal state} \\ \{R_{G01}, R_{G11}, R_{TL0809}, R_{TL1009}, R_{TX0105}, R_{TX0508}\} & \text{Zone 3 start state} \end{cases}$$

$$B_{TL} = \begin{cases} \{TL0809, TL1009\} & \text{Normal state} \\ \{TL0809, TL1009\} & \text{Zone 3 start state} \end{cases}$$

$$B_{GL} = \begin{cases} \{\{\text{G01}\}, \{\text{G11}\}, \{\text{G21}\}, \{\text{G01}, \text{G22}\}, \{\text{G21}, \text{G22}, \text{LWF}, \text{OWF}\}, \{\text{G01}\}, \{\text{G01}\}\} & \text{Normal state} \\ \{\{\text{G01}\}, \{\text{G11}\}, \{\text{G01}\}, \{\text{G21}, \text{G22}, \text{LWF}, \text{OWF}\}, \{\text{G01}\}, \{\text{G01}\}\} & \text{Zone 3 start state} \end{cases}$$

Table 4.4 Sensitivities $\boldsymbol{H_{ALG}}$ of relays to loads in the N-5 situation

$\boldsymbol{H_{ALG}}$	Normal state under N-5 at 62s					
	S1 (G01)	S2 (G11)	S3 (G21)	S4 (G22)	S18 (LWF)	S19 (OWF)
R_{G01}	0.0065	6.25E-06	-3.32E-06	-3.22E-05	-3.22E-05	-3.22E-05
R_{G11}	-4.18E-05	0.0056	-5.28E-05	-5.12E-04	-5.12E-04	-5.12E-04
R_{G21}	-1.27E-05	0.0004	0.0047	-7.43E-04	-7.18E-04	-7.18E-04
R_{TL0809}	-0.0281	2.10E-03	-0.0015	0.0093	-0.0012	-0.0012
R_{TL1009}	-6.68E-06	1.59E-05	-0.0074	-0.0048	-0.0044	-0.004
R_{TX0105}	-0.01	6.94E-07	-3.68E-07	0.0028	-3.32E-06	-3.34E-06
R_{TX0508}	-0.0096	6.56E-07	-3.48E-07	-0.0005	-3.14E-06	-3.16E-06
	R_{G11} in Urgent state and R_{TL0809} in Zone 3 start state at 86.5					
	S1 (G01)	S2 (G11)	S3 (G21)	S4 (G22)	S18 (LWF)	S19 (OWF)
R_{G01}	0.037	4.39E-04	2.61E-04	2.13E-04	1.96E-04	1.81E-04
R_{G11}	3.07E-04	0.0128	2.40E-04	4.47E-04	4.18E-04	4.07E-04
R_{TL0809}	-0.011	1.15E-04	-6.30E-05	-0.0007	-0.0007	-0.0007
R_{TL1009}	-6.08E-06	1.35E-05	-0.0065	-0.0039	-0.0036	-0.0032
R_{TX0105}	-0.008	5.56E-07	-3.05E-07	-3.57E-06	-3.37E-06	-3.39E-06
R_{TX0508}	-0.0066	4.65E-07	-2.55E-07	-2.99E-06	-2.83E-06	-2.84E-06

Similarly, the sensitive map under these two states can be depicted respectively, as shown in Fig. 4.13.

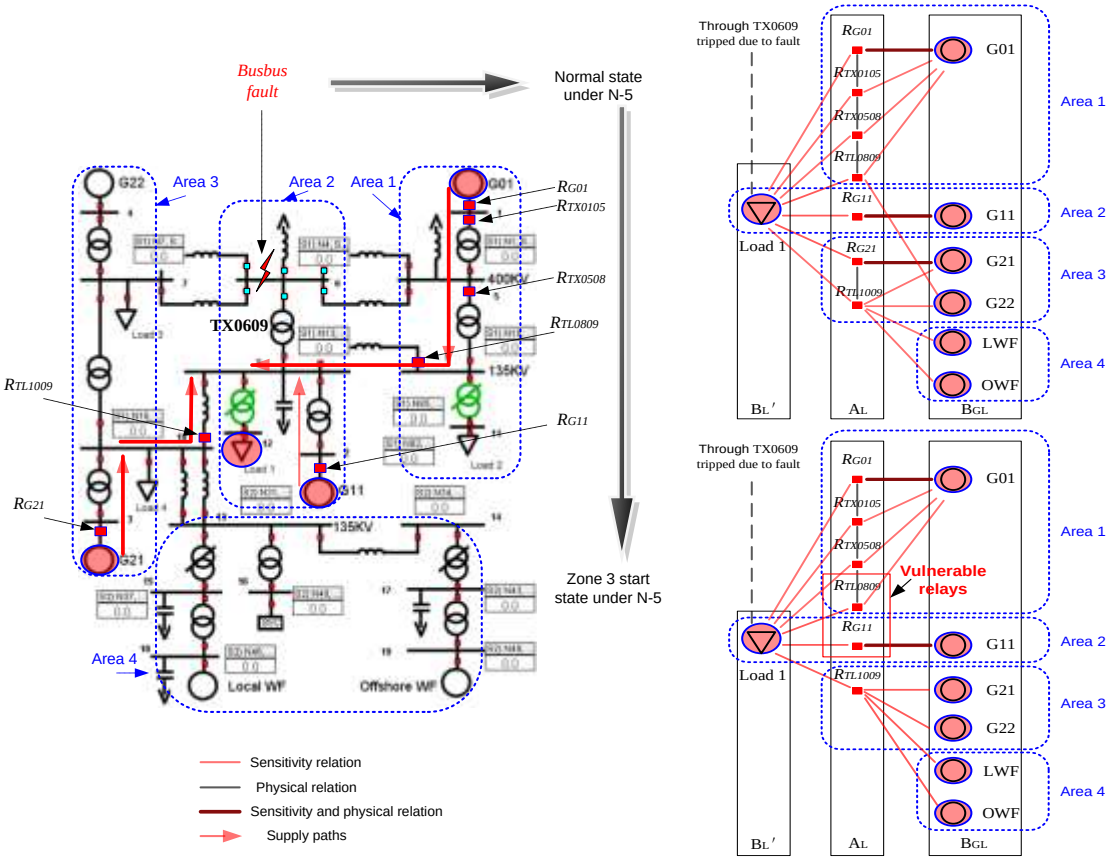

Fig. 4.13 Physical system and sensitive maps

By virtue of local measured impedances at 62s and 86.5s, the margins and performance indexes of the relays can be obtained as shown in Table 4.5 together with the data in the pre fault stage. It can be seen that the margins of R_{G11} and R_{TL0809} were negative and with high PI at 86.5s. When the measured impedance violated the relay settings, the state signals of R_{G11} and R_{TL0809} were given with "0011" and "0101" respectively, which can be selected from A_L and grouped as vulnerable relay set A'_L with threshold $\xi'_1 = 0.2$:

$$A'_L = \{R_{G11}, R_{TL0809}\}$$

Table 4.5 The margins and performance indexes of the relays

	Initial state			**Normal state under N-5**			**Zone 3 start state under N-5**		
	M (p.u.)	$H_{MB'_L}/\|M\|$	PI	M (p.u.)	$H_{MB'_L}/\|M\|$	PI	M (p.u.)	$H_{MB'_L}/\|M\|$	PI
R_{G01}	0.0797	0.1317	0.0866	0.0675	0.2251	0.0536	0.0575	0.1548	0.0331
R_{G11}	0.014	1.5214	**1**	0.005	4.2	**1**	**-0.0053**	3.238	**0.694**
R_{G21}	0.0773	0.1243	0.0818	0.0658	0.1384	0.033	0.0523	0.0727	0.0156
R_{G22}	0.0625	0.1568	0.1032	0.055	0.0891	0.0212	0.049	0.0306	0.0066
R_{TL0809}	0.1108	0.304	**0.2**	0.0878	0.4659	**0.1109**	**-0.0055**	4.6656	**1**
R_{TL1009}	0.1701	0.0682	0.0449	0.0137	0.4155	0.0989	0.0077	0.8679	0.139
R_{TX0105}	0.0888	0.0146	0.0096	0.079	0.2051	0.0488	0.066	0.1242	0.0266
R_{TX0508}	0.0889	0.009	0.0059	0.0775	0.1316	0.0313	0.0695	0.1079	0.0231
R_{TX0209}	0.029	0.062	0.0408	0.0275	0.08	0.019	0.0115	0.1739	0.0373
R_{TX0310}	0.0923	0.0152	0.01	0.0808	0.0248	0.0059	0.0673	0.0074	0.0016
R_{TX0407}	0.0831	0.0229	0.0151	0.0831	0.0132	0.0032	0.077	0.0039	0.0008
R_{TX0710}	0.2443	0.0115	0.0075	0.0433	0.0231	0.0055	0.037	0.0297	0.0064
R_{TX0811}	0.0658	0.0213	0.014	0.0619	0.0113	0.0027	0.0619	0.0129	0.0028
R_{TX0912}	0.0149	0.1072	0.0705	0.0127	0.1807	0.043	0.0061	0.2116	0.0453

Actually, in the initial state and normal operation state under N-5 situation, R_{G11} and R_{TL0809} already had high PIs, which can be an early warning that they are more vulnerable than other relays. Based on the local detected state signals at 86.5s, R_{TL0809} was in Zone 3 start state (0101) which was more dangerous than R_{G11} (0011) in Urgent state. The PIs also showed a same trend at 86.5s, i.e. PI of R_{TL0809} was higher than R_{G11} because the measured impedance just crossed the Zone 3 setting of R_{TL0809}. But at this moment, R_{TL1009} on the last supply path was in Normal state but close to its loadability limit, which means this supply path between Area 3 and Area 3 still has some remained margin to take more load flow. This margin reserve regulation between supply paths could be considered in the design of control strategies which will be in next Chapter.

Based on these data in Table 4.5, the sensitivity chart and performance indexes chart can be depicted as Fig. 4.14 (a) and (b) respectively. The trend of margin sensitivities and relay PIs can be observed more clearly.

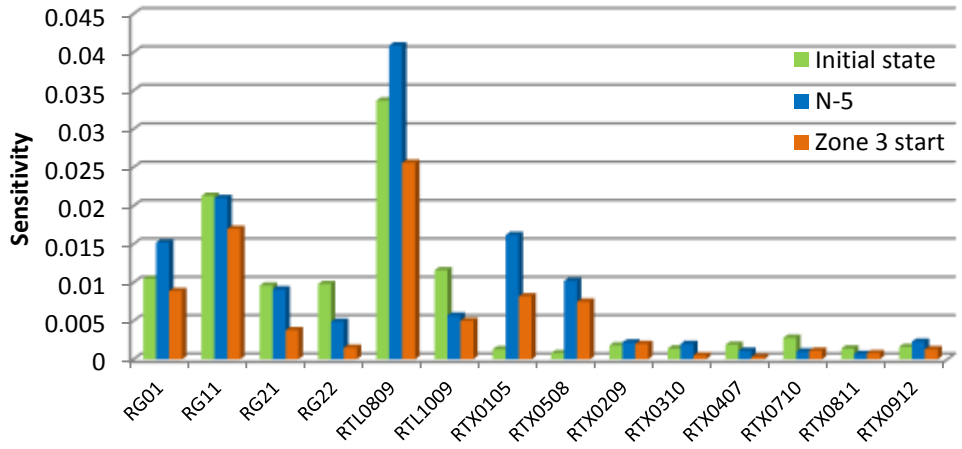

(a) Sensitivity chart of relays to critical load

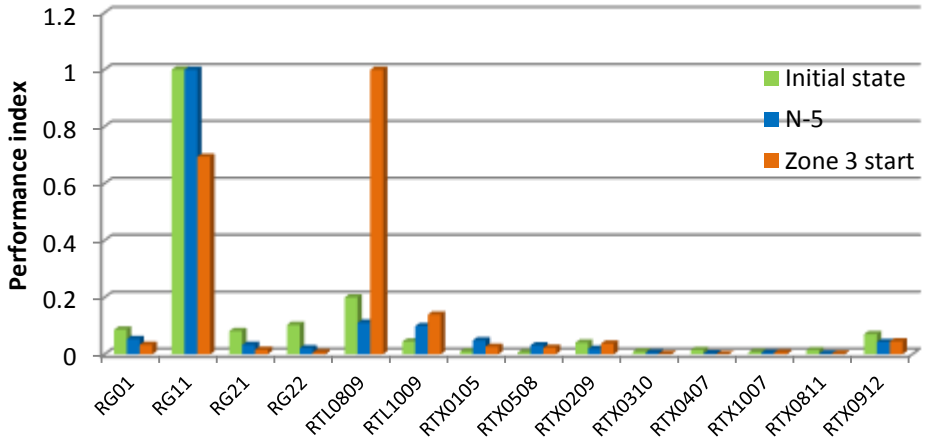

(b) Performance index chart of relays to critical load

Fig. 4.14 Sensitivity and performance index charts

(b) Detection of sensitive controllers

Based on the former results, at 86.5s, $A'_L = \{R_{G11}, R_{TL0809}\}$, the sensitivities $\boldsymbol{H_{A'LSL}}$ (to loads) and $\boldsymbol{H_{A'LSG}}$ (to generators) can be obtained as shown in Table 4.6 and Table 4.7.

Table 4.6 The sensitivities of relay in A'_L to load powers

$\boldsymbol{H_{A'LSL}}$	At 86.5s			
	S7	S10	S11	S12
R_{G11}	-0.0126	-0.0122	0.0019	0.017
R_{TL0809}	-0.0222	-0.013	3.14E-05	0.0256

Table 4.7 The sensitivities of relay in A'_L to generator powers

$\boldsymbol{H_{A'LSG}}$	At 86.5s (R_{G11} in Urgent state, R_{TL0809} in Zone 3 start state)					
	S1 (G01)	S2 (G11)	S3 (G21)	S4 (G22)	S18 (LWF)	S19 (OWF)
R_{G11}	3.07E-04	0.0128	2.40E-04	4.47E-04	4.18E-04	4.07E-04
R_{TL0809}	-0.011	1.15E-04	-6.30E-05	-0.0007	-0.0007	-0.0007

Suppose the regulation limit of controllers is 20% of total capacity for each load or generator, then the performance index PI_{ci} can be calculated based on equation (4.54), as shown in Table 4. 8.

Table 4.8 Performance indexes of the LS and GR controllers

	S7	S10	S11	S12	S1	S2	S3	S4	S18	S19
PI_{ci}	0.0325	0.094	0.0107	1	0.2236	0.162	0.0021	0.0016	0.0013	0.0004

It can be seen from performance indexes of the controllers, LS controller on Load 1 at bus 12 is the most effective controller to adjust the emergency states on R_{G11} and R_{TL0809}, the threshold can be set: $\xi_2' = 0.5$. Meanwhile, the signs of sensitivities should be considered for the controller selection, e.g. the LS controller with negative sensitivity may not be adopted since loads should not be increased under an overloading situation. Also, G01 at bus 1 and G11 at bus 2 are the more effective GR controllers with $\xi_3' = 0.1$.

Obviously, the PIs will be changed when the operation state and control amount limits change. The control strategy design will be concretely introduced in next chapter.

4.4.2 Prediction and identification of emergency states

4.4.2.1 Line outage induced overloading situation

(a) N-1 situation

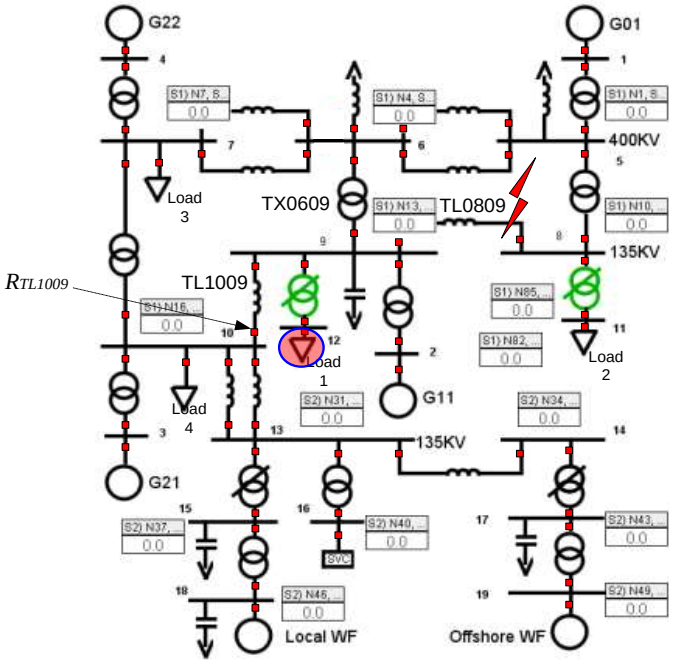

Fig. 4.15 TL0809 outage induced by a three phase fault

In order to investigate the N-1 line outage induced overloading situation, suppose at 3s, a three phase permanent short circuit fault occurred on the line TL0809 in the 19-bus test system, and then this line was tripped 0.1s later. The Zone 3 relays on the line TL1009 and transformer TX0609 were overloaded due to load flow transferring, the relay R_{TL1009} on TL1009 is chosen as a studied example, which is shown in Fig. 4.15. The line flow and measured impedance seen by R_{TL1009} can be observed in Fig. 4.16.

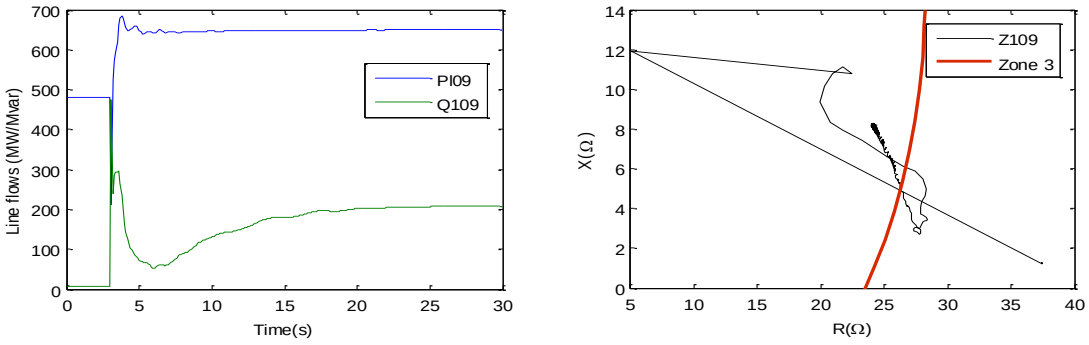

(a) Line flow (b) Impedance locus of relay R_{TL1009}

Fig. 4.16 Line flow and impedance seen by R_{TL1009}

When the proposed prediction and identification algorithm is taken into effect, the virtual injections and the sensitivities based on pre fault system data can be obtained by equation (4.71), as shown in Table 4.9. Then based on the impedance sensitivity method described in section 4.3.3.1, the related sensitivities and the predicted impedance variation can be obtained, as shown in Table 4.10.

Table 4.9 Virtual injections and related sensitivities

For Line TL0809 Outage between Bus 9 and Bus 8	
Sensitivity matrix D_{89}	***Virtual Injections (p.u.)***
$\begin{matrix} 53.3641 & -53.3641 & 15.9851 & -5.7506 \\ -5.6143 & 5.6143 & 54.8958 & -54.6597 \end{matrix}$	$\begin{bmatrix} \Delta P_8 \\ \Delta P_9 \\ \Delta Q_8 \\ \Delta Q_9 \end{bmatrix} = \begin{bmatrix} 11.8 \\ -11.8 \\ -0.0035 \\ 1.87 \end{bmatrix}$
Sensitivity matrix L_{89}	
$\begin{matrix} 0.0090 & -0.5486 & 0.0141 & -0.0148 \\ 0.0071 & 0.0058 & 0.1168 & -0.2042 \end{matrix}$	

Table 4.10 Impedance prediction on TL1009

For Line TL1009 between Bus 10 and Bus 9	
Sensitivity matrix C_{109}	***Predicted impedance (ohm)***
$\begin{matrix} -1.1346 & 1.1346 & -0.0312 & 0.0318 \\ -0.0310 & 0.0310 & 1.1422 & -1.1621 \end{matrix}$	$\begin{bmatrix} R^0_{a109} \\ X^0_{a109} \end{bmatrix} = \begin{bmatrix} 37.45 \\ 1.25 \end{bmatrix}$
Sensitivity matrix H_{10989}	$\begin{bmatrix} \Delta R^{Pl}_{a109} \\ \Delta X^{Pl}_{a109} \end{bmatrix} = \begin{bmatrix} -13.3589 \\ 0.0365 \end{bmatrix}$
$\begin{matrix} 0.0001 & 0.0064 & 0.0006 & 0.0005 \\ -0.000 & -0.0009 & -0.0007 & -0.0057 \end{matrix}$	

With the consideration of node injection variation, if the delay of communication takes 5 circles, the prediction calculation can be started after 10 circles, namely 0.2s after the fault. Here the nodes of generator G01, G11, G21 and G22 will be chosen to be monitored. The injection variations of these nodes can be seen in Fig. 4.17.

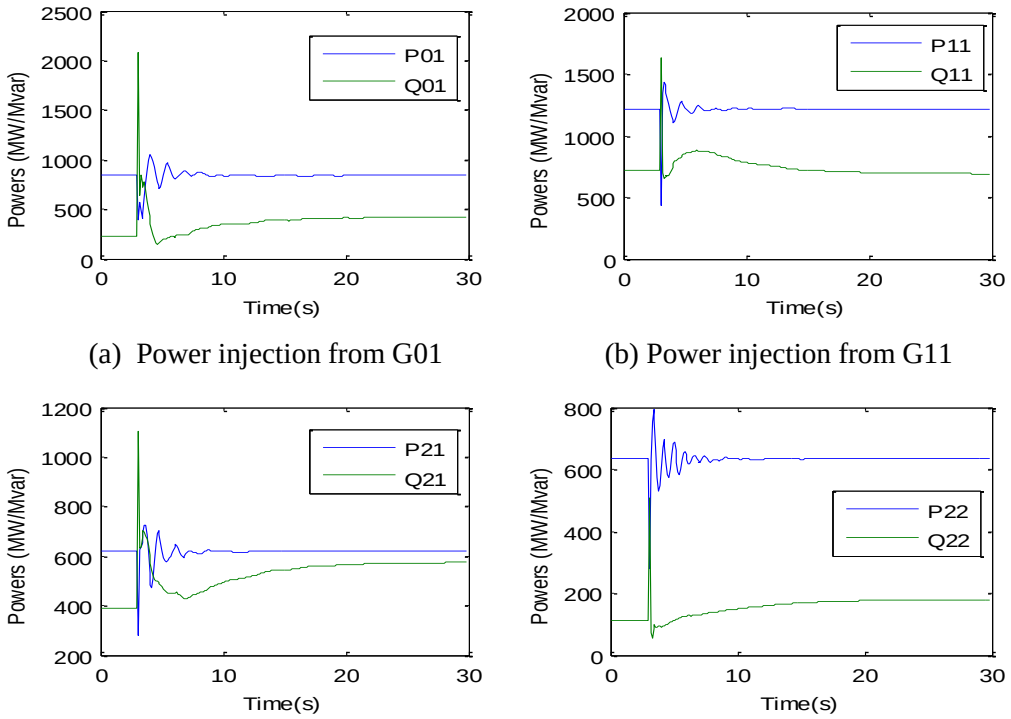

(a) Power injection from G01 (b) Power injection from G11

(c) Power injection from G21 (d) Power injection from G22

Fig. 4.17 Generator injection variations

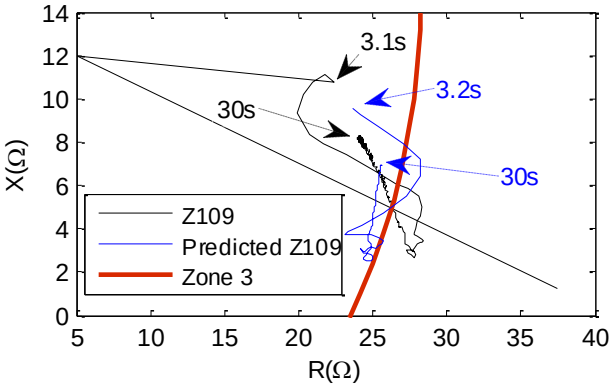

Fig. 4.18 Predicted impedance locus of relay R_{TL1009}

From Fig. 4.18, the predicted impedance locus in blue color can be observed. The biggest error about 12% between predicted impedance and measured impedance (black locus) appeared just after the fault was cleared. But in about 500ms, the error decreased into 8%. So the threshold of identification criterion (4.74) can be set as $\varepsilon_1 = 8\%$. Then

this N-1 line outage induced load flow transferring together with the load flow transferring induced relay operation can be predicted and identified by the proposed protection strategy.

(b) N-k situation

The former cascaded blackout scenario on the 19-bus test system is adopted here as the research object. Since a three phase permanent short circuit fault occurred on the Bus 6 at 11s, then an N-5 contingency happened due to fault clearing, as shown in Fig. 4.19. The relay R_{TL0809} is chosen as a studied example. The line flow and measured impedance seen by R_{TL0809} from 0s to 50.1s can be observed in Fig. 4.20.

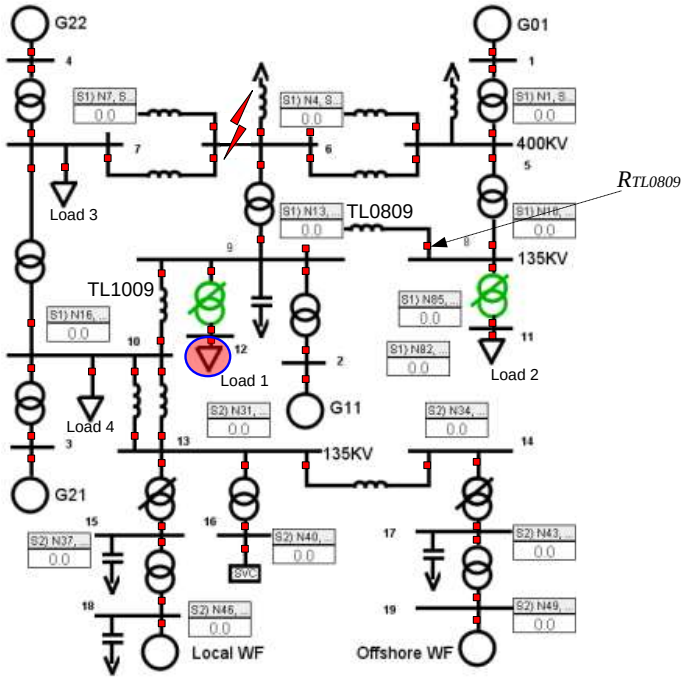

Fig. 4.19 Overload of RTL0809 induced by ULTC operations

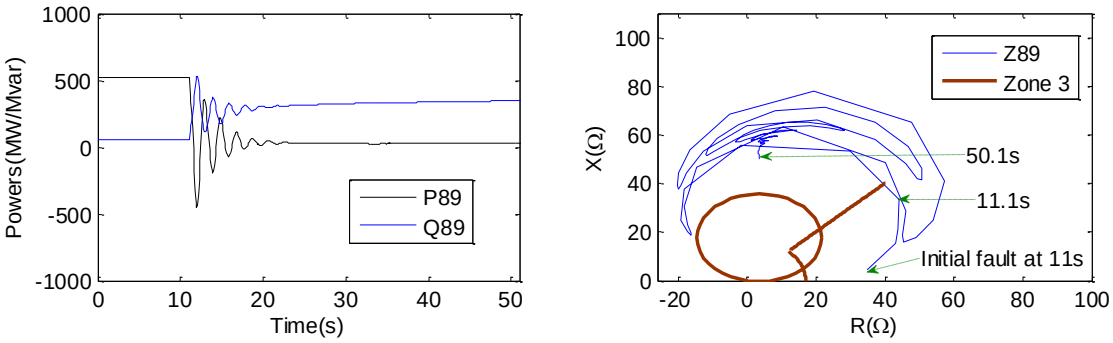

(a) Line flow (b) Impedance locus of relay

Fig. 4.20 Line flow and impedance seen by RTL1009

Assume the nodes of main generator G01, G11, G21 and G22 will be chosen to be monitored. The injection variations can be seen in Fig. 4.21. If the communication delay takes 5 circles, the impedance sensitivity calculation can be started after 10 circles, namely 0.2s after the fault. Then based on collected injection variations and the calculated sensitivities at 11.2s, the predicted impedance locus can be calculated and depicted in Fig. 4.22. The predicted impedance locus is in red color while the measured impedance locus is in blue color.

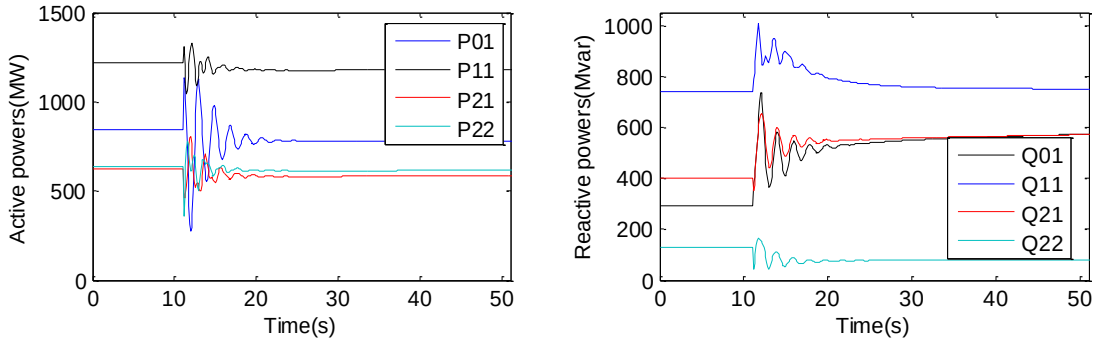

Fig. 4.21 Injection variations of generators

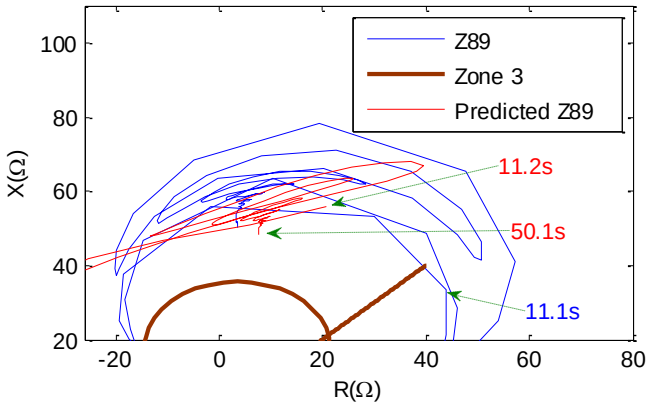

Fig. 4.22 Predicted impedance locus of relay R_{TL1009}

During the oscillation period, the error is quite big due to the strong nonlinear characteristics and not considering the other injection variations (such as loads). The sensitivities cannot represent accurate relationships between system variables in this period. When the oscillation died out and system became stable, the error between predicted impedance and measured impedance became smaller consequently. Fortunately, in this case, the oscillation did not drive any impedance violating the Zone 3 settings. More precise methods are required to identify this kind of events involved with oscillation and block the possible relay operation under oscillation, which are beyond the scope of this thesis.

4.4.2.2 ULTC operation induced overloading situation

In order to identify the ULTC operation induced overloading situation, here the case of cascaded blackout on the 19-bus test system is still adopted as the research object. If a three phase permanent short circuit fault occurred on the Bus 6 at 5s, then in the post N-5 contingency stage, the ULTC on TX0912 started to operate at about 60s. Due to continue tap changer operations, the Zone 3 relay R_{TL0809} on TL0809 was tripped firstly. And the system would experience cascading events and collapse finally, as shown in Fig. 3.14. The relay R_{TL0809} is still chosen as a studied example; here assume all the tripping signals are blocked in the post fault stage, the line flow and impedance seen by R_{TL0809} are shown in Fig. 4.23.

The impedance loci from 55s to 100s will be focused. When the proposed identification method is applied, assume $r^0 = 1$ and $\Delta r = 0.01$, the related sensitivities and predicted impedance of R_{TL0809} at the first step are shown in Table 4.13. Similarly, the predicting calculation can be started at 0.2s after every step of ULTC operation. The injection variations and impedance curves are shown in Fig. 4.24.

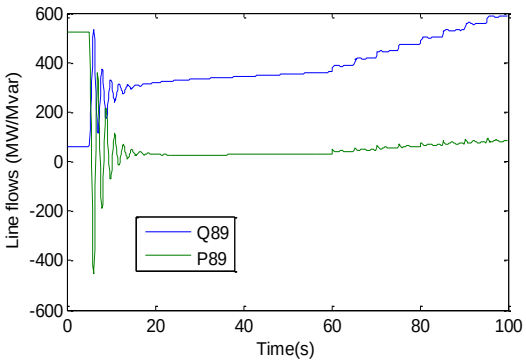

(a) Line flow in 100s

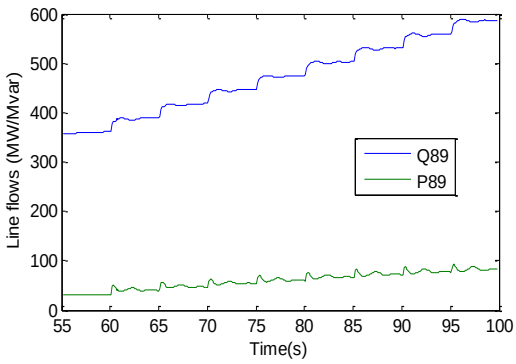

(b) Line flow from 55s to 100s

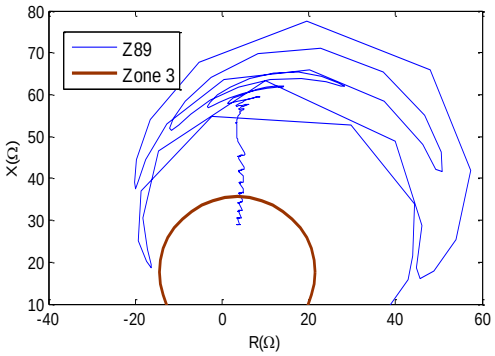

(c) Impedance locus of R_{TL0809}

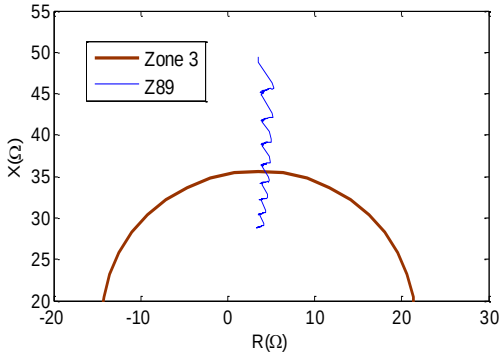

(d) Impedance locus from 55s to 100s

Fig. 4.23 Line flow and impedance seen by R_{TL0809}

Table 4.13 Impedance prediction on TL0809 and related sensitivities at the first step

$\mathcal{L}_{Sr129}$ *of powers to tap ratio*	$0.5025 \quad -0.5025 \quad 91.9816 \quad 91.9816$
C_{89} *of impedance of* R_{TL0809} *to local voltages*	$-3.1630 \quad 3.1630 \quad -0.1787 \quad 0.1928$ $-0.1765 \quad 0.1765 \quad 3.2034 \quad -3.4546$
H_{89129} *of impedance of R2 to powers on transformer TX0912*	$0.0637 \quad 0.0637 \quad -0.0064 \quad 0.0003$ $-0.0073 \quad -0.0067 \quad 0.0567 \quad 0.0015$
Predicted impedance (ohm)	$\begin{bmatrix} R^0_{a109} \\ X^0_{a109} \end{bmatrix} = \begin{bmatrix} 3.56 \\ 48.81 \end{bmatrix}$ $\begin{bmatrix} \Delta R^{Plt}_{aij} \\ \Delta X^{Plt}_{aij} \end{bmatrix} = \begin{bmatrix} -1.0264 \\ -9.2497 \end{bmatrix}$

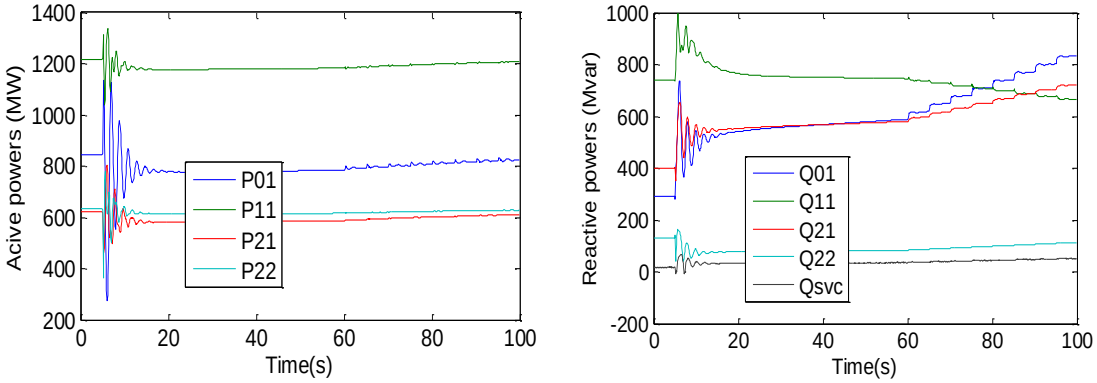

(a) Active power of generators (b) Reactive power of generators

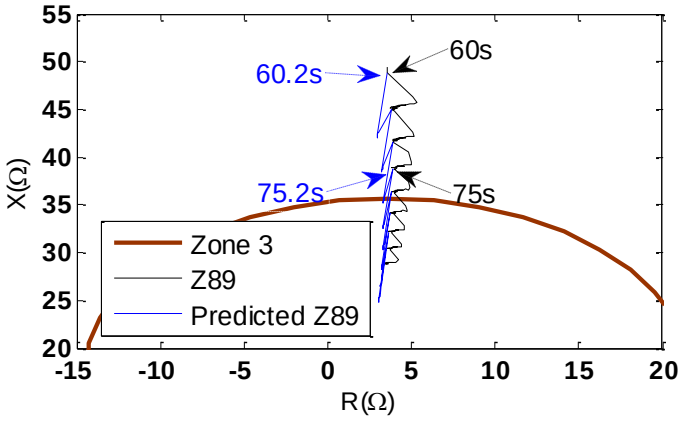

(c) Impedance loci of relay R2

Fig. 4.24Generator powers and impedance loci seen by TL0809

It can be seen from Fig. 4.24 (c), the biggest error is about 80% between predicted impedance (blue locus) and measured impedance (black locus). So the threshold of identification criterion can be set as $\varepsilon_2 = 80\%$. It should be noted that, the variations of

load power was not considered in this case, that is why the predicted error here is a little bigger. Also, it can be seen that the predicted impedance violates the Zone 3 before it really happens which may give an early alarm to Control center. Then emergency control strategies, such as the ULTC blocking or inverse controlling, can be applied timely and effectively to adjust this overloading situation.

4.5 Summary

A sensitivity method is adopted in this chapter to online analyze the relationship between relay-measured impedances and the system operation variables. Based on online calculation of sensitivities and performance indices, the vulnerable relays and sensitive controllers can be quickly detected under different operation states. The sensitive map and sensitive supply paths can be also depicted easily, which give effective indicators to define suitable emergency controls for diverse emergency states.

Meanwhile, based on impedance sensitivity, the overloading situations caused by line outage and LTC operations, as basic processes of cascading events, can be predicted and identified effectively. In this way, the Zone 3 relay can differentiate the load flow transferring induced emergency states from a fault state, and the unexpected relay operations can be blocked timely, which gives time for emergency controls to adjust the emergency states to the Normal state finally.

Chapter 5

Special protection and emergency control design for emergency state prevention

5.1 Introduction

In this chapter, the design of protection and control strategies will be mainly focused. Based on sensitivity analysis in former chapters, the detailed control algorithms will be presented. Also according to the specific emergency state identified by the methods described in the last chapter, the diverse protection and control strategies will be suitably placed to adjust the corresponding emergency state.

Since the control methods are mainly placed on load side, the optimal control algorithm will be applied to minimize the total load loss in the protection and control strategies. On the other hand, the load dynamic restoration characteristics in the post fault stage needs be considered to ensure the secure relay margin in a long run since this kind of loads reaches its steady state characteristics slowly.

The case studies are based on former described cascading events on 19-bus test system in RTDS, simulation results demonstrate the developed protection and control strategies can prevent the unexpected relay operations and adjust the related emergency states successfully.

5.2 Control strategy design for emergency states

Since distance relays are mainly considered in this thesis, the states of these critical relays and the causes of the related states will be the basis of control strategy defining. The state signals of emergency states will be used to initiate the corresponding control strategies when Control center receives these emergency state signals. The related controllers will then execute the defined control strategies to adjust the emergency states. Whether the emergency states have been adjusted to Normal state successfully will be

reflected by apparent impedance loci, which are checked by dispersed relays again. The control structure corresponding to identified states can be depicted in Fig. 5.1.

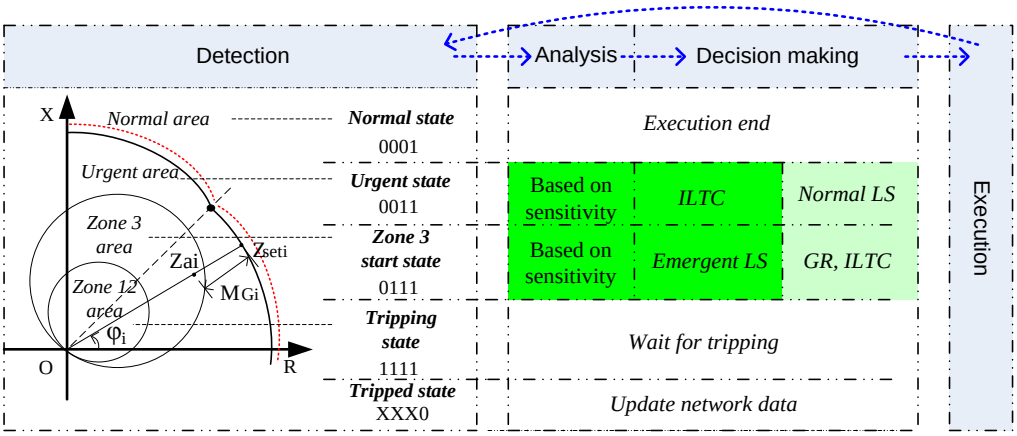

Fig. 5.1 The basic structure of control strategy design

From Fig. 5.1, the distance relay margin is an importance index in the design of control strategy; also, the required relay margin M_i^{req} is defined as the $0.05Z_{seti}$ (red dotted line) to ensure that the loadability margin is no less than the required 5% [80]. As for the critical relay *i* in emergency state, the expected increment ΔM_i^{exp} can be given by:

$$\begin{aligned}\Delta M_i^{exp} &= M_i^{req} - M_i = 5\%Z_{seti} - (Z_{ai} - Z_{seti}) \\ &= (1+5\%)Z_{seti} - Z_{ai}\end{aligned} \tag{5.1}$$

Based on former analysis, the overload emergency states include Urgent state and Zone 3 start state. When the Urgent state has been detected, the inverse load tap changer control (ILTC) will be adopted as main countermeasure to adjust system state, meanwhile the normal load shedding (LS) will be used as a backup strategy [87]. When Zone 3 start state has been identified, the related trip signal will be blocked for several seconds, and the emergency LS will be chosen as main countermeasure in order to adjust this state timely before the unexpected relay trips, while the generator reschedule (GR) and inverse tap changer control (ILTC) will be used as a backup strategy. In Tripping state, the Control center will do nothing but let the traditional function of the critical relay to deal with it. And the Normal state will be regarded as a secure operation state or a return state after the control execution. The final aim of all the protection and control strategies is to keep and adjust the states of power system components into the Normal states.

5.2.1 Inverse tap changer control

The inverse tap changer control (ILTC) is adopted as main control strategy to adjust the identified Urgent states which are detected by dispersed relays. When Control center detects the Urgent state signals-"0011", the following procedures will be executed.

5.2.1.1 Selection of control points

Firstly, the control points for ILTC will be selected based on sensitivities between relay margins and tap ratios. Based on equations (4.39) to (4.44), for the critical backup relay *i*, the linear form of operation margin M_i to the ratio of related tap changers can be given by:

$$\Delta M_i = \sum_{k \in l} \mathcal{L}_{Mrik} \Delta r_k \tag{5.2}$$

where $\Delta r_k = n\Delta r$, n is a integer, Δr is the step size of tap changer, l represents the number of all the related transformers with load tap changers, $\mathcal{L}_{Mrik}$ represents the sensitivity of relay margin M_i to any tap changer k ($\in l$). According to $\mathcal{L}_{Mrik}$ and the available regulation limit of tap changer Δr_{maxk}, the similar performance index PI_{ltck} of tap changer k can be given by:

$$PI_{ltck} = \frac{|\mathcal{L}_{Mrik}|\Delta r_{maxk}}{\max\limits_{l}\{|\mathcal{L}_{Mri1}|\Delta r_{max1}, \cdots, |\mathcal{L}_{Mril}|\Delta r_{maxl}\}} \tag{5.3}$$

A suitable threshold ξ_4 can be set to divide all the related tap changers into two groups with different priorities: the tap changers with higher $PI_{ltc}(\geq \xi_4)$ will be classified to the first group, and all the related tap changers will constitute the second group.

Then, in the progress of inverse tap changer control, the tap changers in the first group with higher PI_{ltc} will be blocked firstly to prevent the possible unexpected operations, then the detailed control amount will be defined based on these tap changers, and finally these tap changers will be changed to the inverse control mode and execute the defined control amounts. Normally, the tap changers with high PI_{ltc} will be relatively less, so if the Urgent states cannot be adjusted only based on first group, then more control points from the second group will be considered to strength the control effect, and finally realize the aim to adjust the Urgent state to Normal state.

5.2.1.2 Determination of control amounts

Suppose the first group for ILTC is denoted as B_{ltc1}, then the control amount Δr_k ($k \in B_{ltc1}$) can be solved out based on the following objective function (5.4) with the consideration to minimize the total control amount T_r. ΔM_i^{exp} represents the expected increment of relay margin defined by (5.1).

$$\begin{aligned} &min\ T_r = min\left\{\sum_{k\in B_{ltc1}} \Delta r_k\right\} \\ &s.t. \quad \Delta M_i^* \geq \Delta M_i^{exp}; \\ &V_{j1max} \geq V_{j1}^* \geq V_{j1min}; \\ &|\Delta r_{maxk}| \geq |\Delta r_k| \geq 0; \end{aligned} \tag{5.4}$$

where ΔM_i^* is the achieved increment of related relay margin, and V_{j1}^* is achieved voltage magnitude at the transmission side of controlled transformer j ($j \in B_{ltc1}$). These two variables can be expressed by (5.5) and (5.6). V_{j1max} and V_{j1min} represent the maximum value and minimum value of V_{j1}, V_{j1}^0 represents the initial value of V_{j1} before the initiation of ILTC, $\mathcal{L}_{Vrjk}$ represents the sensitivity of bus voltage V_{j1} to tap changer k, which can be calculated based on $\boldsymbol{J^{-1}}$ and $\boldsymbol{\mathcal{L}_{Sr}}$.

$$\Delta M_i^* = \sum_{k\in B_{ltc1}} \mathcal{L}_{Mrik} \Delta r_k \tag{5.5}$$

$$V_{j1}^* = V_{j1}^0 + \Delta V_{j1}^* = V_{j1}^0 + \sum_{k\in B_{ltc1}} \mathcal{L}_{Vrjk} \Delta r_k \tag{5.6}$$

The first constraint in (5.4) is used to achieve secure positive margin of critical relays, the second one is the specific limitations for voltage magnitudes at transmission sides of controlled transformers in the selected group, and the third one represents specific limitations for the possible control amounts on the controllable tap changers ($j, k \in B_{ltc1}$).

Since the control amount Δr_k on tap changer k will be normally realized step by step, the consuming time will depend on how many steps required and the delay time ΔT_k for each following step. Also, if there are more sensitive tap changing controllers can be controlled together, then the consuming time will be less. The chart of workflow can be depicted in Fig.5.2.

It should be noted that, under Urgent states, the normal three-step under voltage load shedding strategy is very important as a backup strategy for ILTC to prevent the unacceptable low voltage at the load side or possible failure of ILTC control strategy.

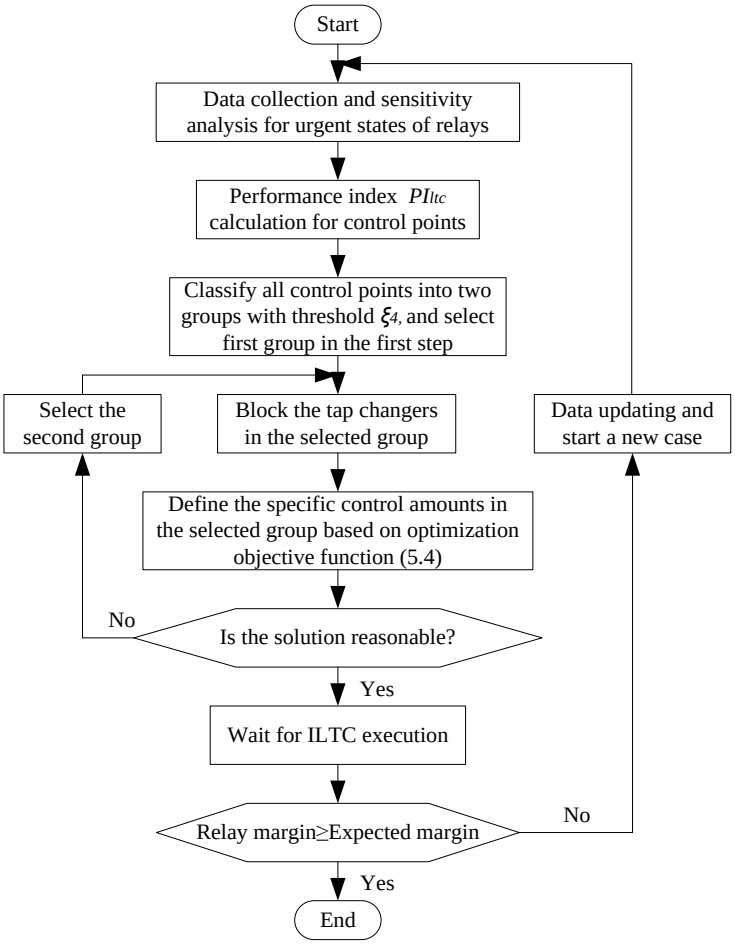

Fig. 5.2 Workflow of ILTC for overload induced Urgent states

5.2.2 Load shedding

When Zone 3 start state is detected by a relay, meanwhile this emergency state is identified as the one caused by overloading conditions, then the trip of this relay and related breaker will be regarded as an unexpected operation which could deteriorate system structure and stability. In order to adjust this kind of emergency states as soon as possible, emergency load shedding scheme (LS) as the best choice will be adopted. The detailed procedures are described as follows:

5.2.2.1 Selection of critical relays

When the overloading situation induces the measured impedance violate the Zone 3 setting, some generator backup relay may already detect the Urgent state, e.g. in the case of cascaded blackout in section 4.4.1.2, the relay R_{G11} on G11 hit its field current limit firstly, and then the Zone 3 relay R_{TL0809} on TL0809 got violated subsequently. Based on performance index analysis shown in Fig. 4.14, the R_{TL0809}'s PI_r (=1) is higher than R_{G11}'s PI_r (=0.694), also the Zone 3 start state is more dangerous than Urgent state, but according to definition of PI_r, the violated relay with negative margin and low PI_r will be harder to be recovered. So only considering the relay in Zone 3 start state may be not enough to adjust the overloading situation in the system. In order to adjust all the emergency states, all the relays in the emergency states including Zone 3 start state and Urgent state should be selected as critical relays in A_L' to define the LS control strategy.

5.2.2.2 Selection of control points

In order to find effective control points, the sensitivities $H_{A'LS}$between relay margins and apparent load powers will be utilized. Based on the analysis in section 4.3.2, the control points can be selected based on performance indexes (PI_{ci}) defined by equation (4.54) with a suitable threshold ξ_2'.

Similar to ILTC strategy, based on PI_{LScj} for load shedding points, all the LS controllers can be divided into two groups. The first group will include the LS controllers with higher $PI_{LSc}(>\xi_2')$ to all the relays in A_L', and the second group will include all the LS controllers in the system. When emergency LS strategy is triggered by the identification of Zone 3 start state, the detailed strategy will be defined firstly based on the controllers in the first group. And the second group will be the backup if the emergency states cannot be adjusted only based on the first group.

5.2.2.3 Determination of control amounts

Assume the first group of control points for emergency LS is denoted as B_{LS1}, then in order to minimize the total shedding amount on the selected loads, an optimal load shedding strategy is applied with the following objective function:

$$\begin{aligned} &minS_{LS} = min\{\textstyle\sum_{j\in B_{LS1}} \Delta S_{Lj}\}, \\ &s.t. \quad \Delta M_i^* \geq \Delta M_i^{exp},\ i \in A_L' \\ &|\Delta S_j|_{max} \geq |\Delta S_j| \geq 0 \end{aligned} \tag{5.7}$$

where $|\Delta S_j|_{max}$ represents the limit of LS controller j, ΔS_{Lj} is the shedding amount on the related load j, ΔM_i^* is the achieved increment of related relay margin on relay i, which can be expressed as (5.8). $H_{A'LSLij}$ is the margin sensitivity of relay i in A_L' to the selected controllable load j.

$$\Delta M_i^* = \sum_{j \in B_{LS1}} H_{A'LSLij} \Delta S_{Lj} \tag{5.8}$$

5.2.2.4 The work flow of emergency LS control strategy

According to the content discussed above, the work flowchart of the proposed LS strategy can be depicted by Fig. 5.3.

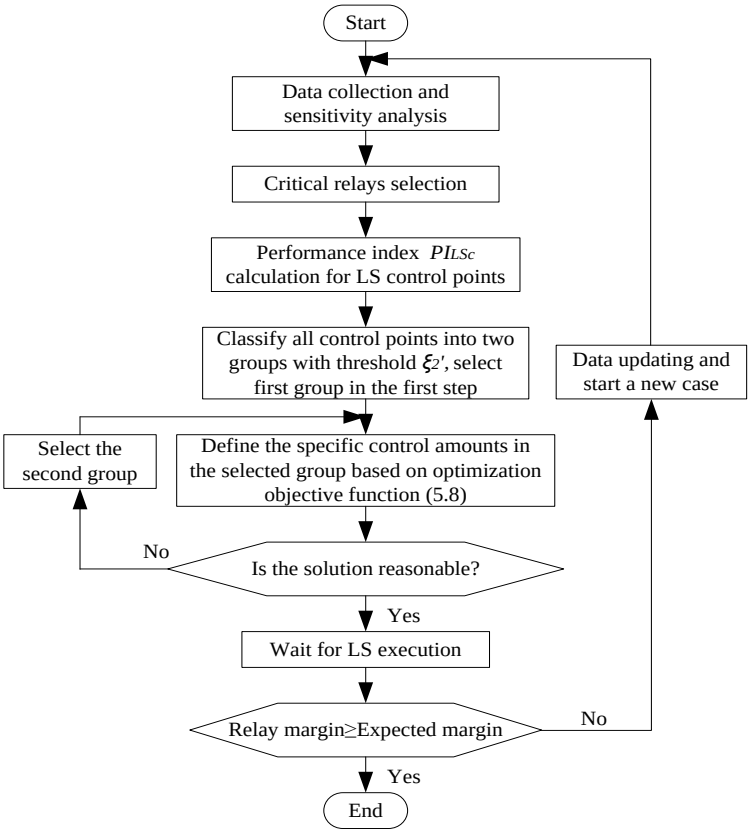

Fig. 5.3 Flowchart of proposed LS strategy

5.2.3 Generator reschedule

In the overloading situations, the control measures on the sensitive loads will be more effective than those on the sensitive generators. Also since the governor system normally take the responsibility to do primary frequency control, the active power difference will be compensated after execution of emergency LS strategy. But if the LS amount is too

big beyond the regulation capability of governors, the system may encounter the angle stability problem. So in order to suitably compensate the active power unbalance, a sensitivity based generator reschedule (GR) control is designed in place to modify the active power reference in the governor, which can be regarded as one kind of secondary frequency control [1].

Besides, by decreasing the active power output, the local generator can send more reactive power to support the voltage and prevent the overloading situation. So here the GR control can be utilized as an auxiliary control strategy, which will be executed at the same time with emergency LS control strategy. Also it will make effects on operation margins of critical relays, which is required to be considered in the progress of relay margin adjusting.

5.2.3.1 Selection of control points

Consider GR control as an ancillary control for LS control strategy, the local sensitive GR controllers which are more close to critical loads will be the most effective controllers, because it can not only compensate the active power unbalance but also can send more reactive power at the same time to support the voltage. The sensitive map and related sensitivities defined in section 4.3.1.1 will be utilized to selected GR control points. Based on $\boldsymbol{H_{ALG}}$ and threshold ξ_3, the more sensitive generators will be selected as the first group B_{GR1}, the other sensitive generators will be the second group B_{GR2}.

5.2.3.2 Determination of control amounts

Then in order to determinate control amount of GR strategy combined with LS strategy, the objective function can be given as:

$$\begin{gathered} minS_{LS} = min\{\textstyle\sum_{j\in B_{LS1}} \Delta S_{Lj}\}, \\ s.t. \quad \Delta M_i^* \geq \Delta M_i^{exp},\ i \in A_L' \\ |\Delta S_y|_{max} \geq |\Delta S_y| \geq 0 \\ \sum_{j\in B_{LS1}} \Delta S_{Lj} cos\emptyset_{Lj} = -\sum_{x\in B_{GR1}} \Delta S_{Gx} cos\emptyset_{Gx} \end{gathered} \tag{5.9}$$

where $|\Delta S_y|_{max}$ represents the regulation limit of LS or GR controller y ($y \in B_{LS1} \cup B_{GR1}$), ΔS_{Lj} is the shedding amount on $Load\ j$, ΔS_{Gx} is the reschedule amount on the

sensitive generator x, $cos\emptyset_{Lj}$ and $cos\emptyset_{Gx}$ are power factors of related load and generator respectively.

The last constraint in (5.9) is for active power balance between LS and GR, the meanings of the first and second ones are same with (5.7), except the ΔM_i^* needs to consider the effect of GR control, which is given by (5.10).

$$\Delta M_i^* = \sum_{j \in B_{LS1}} H_{A'LSLij} \Delta S_{Lj} + \sum_{x \in B_{GR1}} H_{A'LSGix} \Delta S_{Gx} \tag{5.10}$$

where $H_{A'LSLij}$ is the margin sensitivity between critical relay i in A_L' and $Load\ j$, $H_{A'LSGix}$ is the margin sensitivity between critical relay *i* and sensitive generator x.

5.2.3.3 The modified work flow of combined LS and GR strategy

Based on the above discussion, the modified work flow of combined LS and GR control strategy can be depicted as:

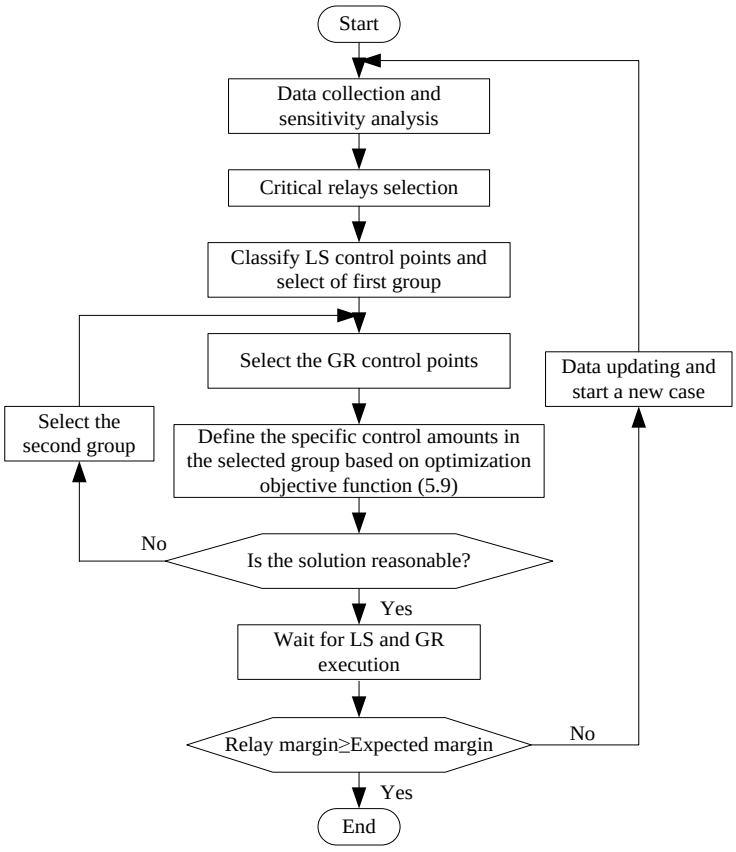

Fig. 5.4 Flowchart of proposed LS and GR strategy

5.3 Integrated optimization and compensation strategy

5.3.1 Integrated sensitivity

Based on the control strategies described above, all the controllers (i.e. tap changers, LS controllers and GR controllers) can be utilized to effectively regulate the critical relay margins. If all the effects of these controllers have been considered together, the integrated sensitivities can be utilized and obtained based on linear superposition principle. Then the variation of relay margins can be expressed by (5.11), where the n, m, l are the number of related controllers in the related first groups. It can also be written as a matrix form, which is given by (5.12).

$$\Delta M_i^* = \sum_{j=1}^{n} H_{A'LSLij}\Delta S_{Lj} + \sum_{x=1}^{m} H_{A'LSGix}\Delta S_{Gx} + \sum_{k=1}^{l} \mathcal{L}_{Mr,ik}\Delta r_k \tag{5.11}$$

$$\begin{aligned}\Delta \boldsymbol{M}_{\boldsymbol{A'L}} &= \boldsymbol{H}_{\boldsymbol{A'LSL}}\Delta \boldsymbol{S}_{\boldsymbol{L}} + \boldsymbol{H}_{\boldsymbol{A'LSG}}\Delta \boldsymbol{S}_{\boldsymbol{G}} + \boldsymbol{\mathcal{L}}_{\boldsymbol{Mr}}\Delta \boldsymbol{r} \\ &= [\boldsymbol{H}_{\boldsymbol{A'LSL}} \quad \boldsymbol{H}_{\boldsymbol{A'LSG}} \quad \boldsymbol{\mathcal{L}}_{\boldsymbol{Mr}}] \begin{bmatrix} \Delta \boldsymbol{S}_{\boldsymbol{L}} \\ \Delta \boldsymbol{S}_{\boldsymbol{G}} \\ \Delta \boldsymbol{r} \end{bmatrix}\end{aligned} \tag{5.12}$$

Then the integrated sensitivity matrix $\boldsymbol{I}_{\boldsymbol{A'L}}$ can be obtained by (5.13), where the sub matrix of it can be deduced by (4.52) (4.53) and (5.2) respectively.

$$\boldsymbol{I}_{\boldsymbol{A'L}} = [\boldsymbol{H}_{\boldsymbol{A'LSL}} \quad \boldsymbol{H}_{\boldsymbol{A'LSG}} \quad \boldsymbol{\mathcal{L}}_{\boldsymbol{Mr}}] \tag{5.13}$$

5.3.2 The priority of control strategies

Due to different emergency state, the main control strategy and backup control strategy will be different. Moreover, the time responses of different control strategies are diverse. The emergency LS strategy is required to be executed and adjust the Zone 3 start state as soon as possible, and ILTC may take tens of seconds to adjust the Urgent state by continuous tap changing.

5.3.2.1 The priority of control strategies for different emergency states

As we know, the state signals of relays are designed based on different emergency states, i.e. Urgent state (D_{g1i}=D_{g2i}=0, D_{g3i}=1, D_{bi}=1) and Zone 3 start state (0111 or 0101).

Based on the values of D_{g2i}, D_{g3i} (of generator relay) or D_{L2ij}, D_{L3ij} (of transmission line relay), the achieved margin ΔM_i^* can be expressed as:

$$\Delta M_i^* = D_{2c}\left(\sum_{j=1}^{n} H_{A'LSLij}\Delta S_{Lj} + \sum_{x=1}^{m} H_{A'LSGix}\Delta S_{Gx}\right) + \overline{D_{2c}}D_{3c}\sum_{k=1}^{l}\mathcal{L}_{Mr,ik}\Delta r_k \tag{5.14}$$

where D_{2c} and D_{3c} represent the state signals D_{g2i}, D_{g3i} or D_{L2ij}, D_{L3ij} of the most critical relay in A'_L.

Actually, the most critical relay will be featured with highest performance index, so the state of the relay in A' with highest PI_r decide which state the system is in now.

If the Control center just detects the Urgent states of some relays, i.e. $D_{2c} = 0, D_{3c} = 1$, then the first part multiplied with D_{2c} in the right side of (5.14) will be eliminated, and the second part multiplied with $\overline{D_{2c}}D_{3c}$ will be kept for the determination of control amount. The equation becomes the same with (5.5) in ILTC control. Or if the Control center detects the Zone 3 start states of some relays, i.e. $D_{2c} = 1, D_{3c} = 1 or\ 0$, then the first part in the right side of (5.14) is kept and the second part will be eliminated. At this time the equation becomes the same with (5.12) which is the emergency LS and GR control.

In this way, the different control strategy can be combined together with different priorities to prevent related emergency states.

5.3.2.2 The priority of control strategies for one emergency state

As we designed in the beginning of this chapter, when the Urgent state is detected, the ILTC will be the main control strategy with normal LS as backup, which is already introduced above. And the normal LS strategy is designed based on the standard model described in [87], which is not discussed here.

If the Control center detects the Zone 3 start state, the emergency LS strategy will be the main control strategy, GR control will be the ancillary control for active power balance, and the ILTC could be the backup strategy initiated to share the LS burden and

keep the voltage at transmission side. As a backup control, the ILTC will be mainly used to keep the voltage level at transmission side, and margin sensitivity analysis will not be considered in this backup ILTC control.

5.3.3 Load restoration characteristics consideration

So far, all the control strategies are based on online sensitivity analysis at the prevailing system operation point, and the load powers are default regarded as constant power load. However, based on the equations (3.1)-(3.6), the load with restoration characteristics is varying with the variations of voltage and time.

In this thesis, the restoration load will apply the classic parameters: $\alpha_s = \beta_s = 0$, $\alpha_t = \beta_t = 2$, $T_P = T_Q = 100s$, z_P and z_Q are initialized with 1 [16]. The $cos\emptyset_{Li}$ will keep constant during load restoration. Then this kind of load will firstly respond with its transient characteristics (i.e. impedance load characteristics) when a big voltage variation is experienced on the load bus *i*. Thereafter it will slowly restore based on its time characteristics (3.3) (3.4). Finally the load will reach its steady state characteristics (i.e. constant power load). Since the post fault load restoration is normally associated with continually LTC actions and emergency controls, all the sensitivity based control algorithms are defined based on the measured load power in transient characteristics.

So in order to predict the possible restoration amount of loads, we suppose the execution of LS is at time *t*, due to the variation of voltage V_i at the load bus *i*, there will be inevitable load restoration (e.g. ΔP_{Li}^{res}) according to the load dynamics, which can be given by (5.15). Also suppose the V_i recovers from V_{it} to at least the low voltage limit (i.e. $V_{min} = 0.9pu$), D_{Pi} is the sensitivity of active load power P_{Li} to bus voltage, P_{Li} is defined by (3.1), then the restored active power can be approximately given by:

$$\Delta P_{Li}^{res} = D_{Pi}(V_{min} - V_{it}) = D_{Pi}\Delta V_i \tag{5.15}$$

where

$$D_{Pi} = \partial P_{Li}/\partial V_i \tag{5.16}$$

This load restoration may make the achieved margin M_A^*, become smaller and even negative again to trigger the backup relays. In order to prevent the unexpected relay trips all at once, this part of load restoration amount should be predicted and added into LS amount in advance. Then the total LS amount ΔP_{Li}^{tot} can be corrected and obtained by:

$$\Delta P_{Li}^{tot} = \Delta P_{Li}^{sen} + \Delta P_{Li}^{res} \tag{5.17}$$

where $\Delta P_{Li}^{sen} (= \Delta S_{Li}^{sen} cos\emptyset_{Li})$ is the active power part of calculated LS amount, ΔS_{Li}^{sen} is the calculated LS amount based on online sensitivity analysis, $cos\emptyset_{Li}$ is the load power factor.

Similarly, considering constant load power factor, the apparent LS amount can be also defined by:

$$\Delta S_{LI}^{tot} = \Delta S_{Li}^{sen} + \Delta S_{Li}^{res} \tag{5.18}$$

Then the work flow chart of emergency controls can be modified with consideration of control priorities and load restoration dynamics, which is given by Fig. 5.5.

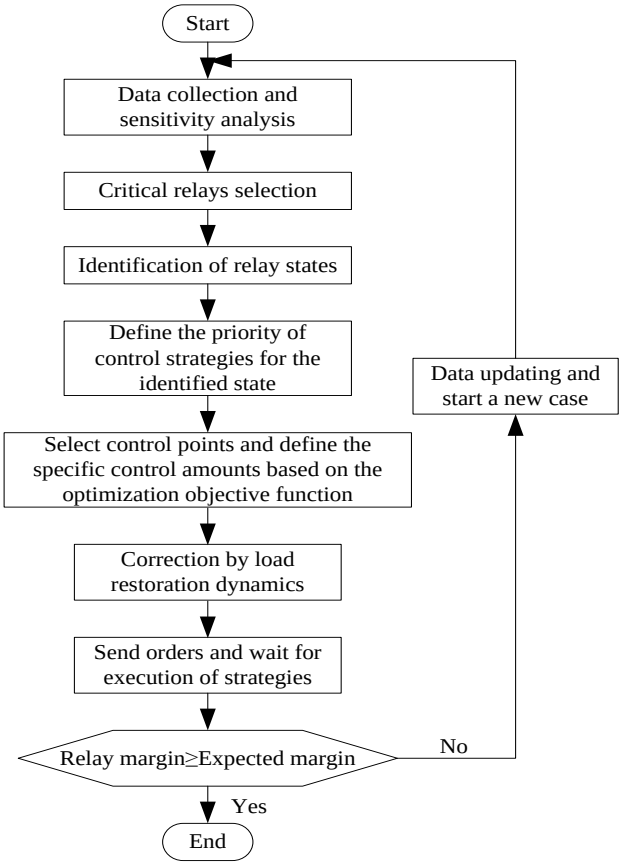

Fig. 5.5 Flowchart of control strategy considering priority and load restoration

5.3.4 Basic processes of protection and control strategies

Based on the control strategies presented so far, the work flowchart of the proposed protection and control scheme can be depicted in Fig. 5.6.

This work flowchart can be compared with the Fig. 5.1. Firstly, the workflow will go into Detection area, which includes vulnerable relay detection and specific relay state

confirmation. The function chart of vulnerable relay detection can be seen Fig. 4.4 based on the local detection together with sensitivity analysis in Control center. Secondly, the work flows into the Analysis area, which includes the prediction and identification of overloading emergency states and has been discussed in section 4.3.3. The third area is Decision making area, which includes the detailed emergency control strategy defining. The flowchart of emergency LS and GR strategy can be seen in Fig. 5.4, and the ILTC strategy can be observed in Fig. 5.2. The fourth area is the Execution area in which the distributed controllers will execute the defined control strategies. Then workflow will go back to Detection area to check if all the relays have been recovered into Normal state, or else, another round of work flow will be conducted similarly.

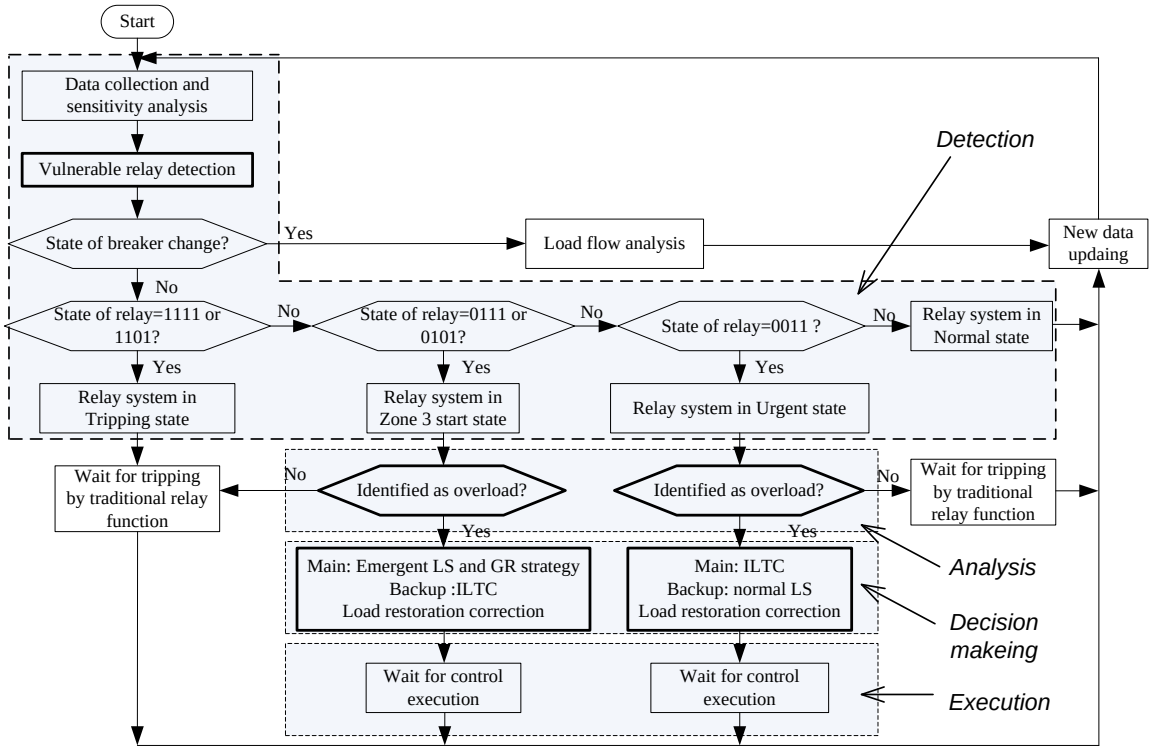

Fig. 5.6 Work flowchart of proposed protection and control scheme

According to the work flow chart in Fig. 5.6, the basic processes of emergency control and protection system can be categorized as:

- State detection based on relay system
- Analysis and decision making in Control center according to detected states from relay system

- Execution of defined control strategy by distributed controllers following the orders from Control center

Besides, wait for tripping can be also regarded as one of defined strategies. When the protection and control strategies are taken into effect to prevent the case of cascaded blackouts, these control processes will interrupt and regulate the basic processes of cascading events. Sometimes, if the regulations fail, the basic event processes will be mixed with the control processes and make the progress of cascading events even more complex. How to deal with this situation will be discussed in following chapter.

5.4 Case study

5.4.1 Urgent state prevention

In the cascaded blackout case described in Chapter 3, after the bus bar fault happened, the unexpected LTC operation started at about 65s which further decreased the voltage at the load side. 5s later, the local generator G11 hit its field current limiter and the state signal of R_{G11} is changed from "0001" (Normal state) to "0011" (Urgent state) immediately. According to the work flow in Fig. 5.6, when Control center receive these Urgent state signals and identify the system state as an urgent overloading situation, the ILTC will be initiated as main control strategy with $D_{2c} = 0$ and $\overline{D_{2c}}D_{3c} = 1$. The related sensitivities and performance indexes are shown in Table 5.1, the ξ_4 can be set as 0.5. The control amounts considering the load restoration are given in Table 5.2. In this case, the tap changer controller on load transformer TX0912 is in the first control group B_{ltc1}.

It can be seen that the tap changer should be inversely controlled by 6 steps when load restoration dynamics is considered. With the successful execution of ILTC, the bus voltage variations, tap position variations and impedance loci seen by R_{G11} can be observed in the following Fig. 5.7, Fig. 5.8 and Fig. 5.9.

Table 5.1 Sensitivities and performance indexes of LTC controllers

	For LTC on TX0912	**For LTC on TX0811**
$\mathcal{L}_{Mr}$	-0.18866	-0.03702
Δr_{maxk}	0.2 (20stepsX0.01)	0.2
PI_{ltc}	1	0.19621

Table 5.2 Expected relay margin increment and related control amounts

For LTC on TX0912			
ΔM_2^{exp}	0.00325 p.u.	Δr_{TX0912}	-0.0172 (ILTC two steps)
V_{min} of LTC	0.92 p.u.	ΔV	0.018 p.u.
$\mathcal{L}_{Vr}$	1.022	Δr_{TX0912}	-0.0176
Load restoration consideration			
D_{L1}	49.5871	D_{L2}	11.0451
ΔS_{L12}^{res}	1.021 p.u.	Δr_{TX0912}^{res}	-0.0335 (ILTC four steps)

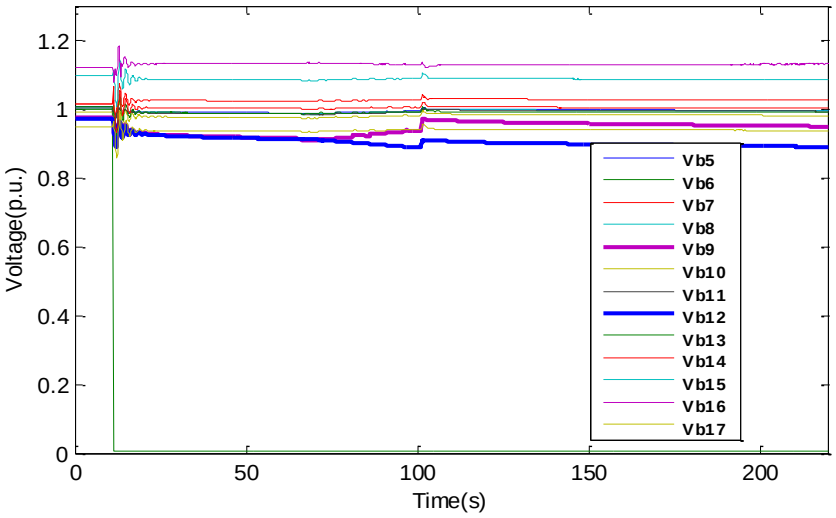

Fig. 5.7 System bus voltages with control strategy activation

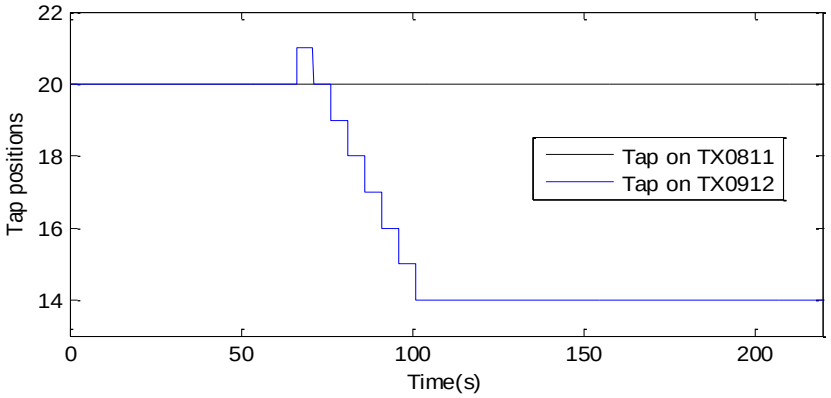

Fig. 5.8 Variation of tap positions during ILTC

The first step of ILTC is started at 75s, considering 5s delay after blocking the normal LTC operation. The normal LS is initiated when voltage is lower than 0.9 p.u. with 15s delay. In this case, the normal LS shed the load at 101s with preset 10%. It can be seen that after the successful execution of the control strategy, all the voltages return beyond the 0.9 p.u., and the Urgent state (0011) of R_{G11} has been adjusted into Normal state

(0001). In Fig. 5.9, the red locus represents the situation with successfully ILTC and normal LS execution, and the blue locus represents the cascaded blackout. Obviously, the basic process of cascading events, which is overload due to load side voltage control induced load increment, has been corrected into a new process which drives the system into Normal state.

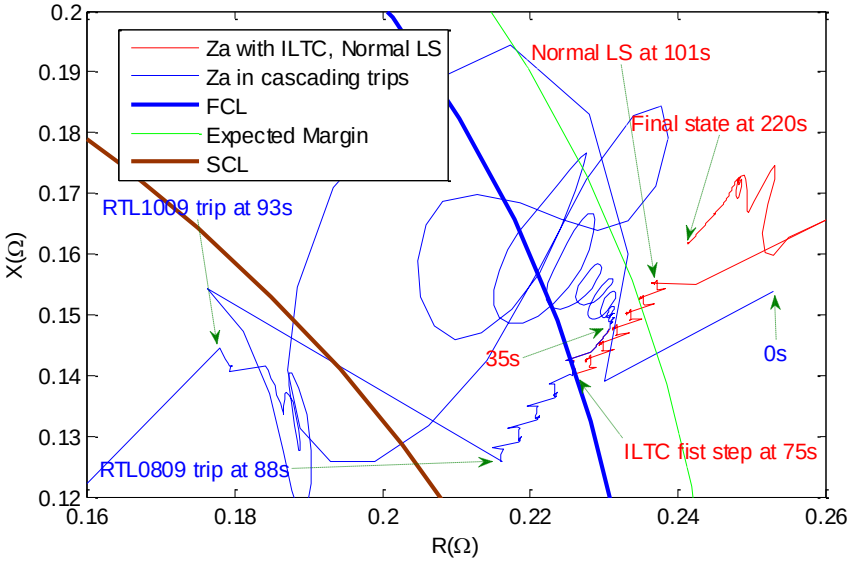

Fig. 5.9 Impedance loci seen by R_{G11}

5.4.2 Zone 3 start state prevention

In order to validate the LS and GR strategy against Zone 3 start state, the studied cascaded blackout case is simulated without initiation of ILTC control and normal LS control when G11 hit its field current limiter. Thereafter, at about 87s, the relay R_{TL0809} on transmission line TL0809 was triggered when impedance locus entered Zone 3 area. The state of R_{TL0809} was changed from Normal state (0001) to Zone 3 start state (0101) directly. When Control center receive these state signals and identify the system state as an overloading situation induced Zone 3 start state, the emergency LS and GR control will be initiated as the main control strategy with $D_{2c} = 1$ and $\overline{D_{2c}} D_{3c} = 0$, based on equation (5.14) and work flow in Fig. 5.6.

According to the sensitivity analysis in section 4.4.1.2, the relay R_{TL0809} and R_{G11} should be identified as vulnerable relays in A'_L, even though R_{TL0809} showed a higher PI_r, which is already given in Table 4.5 and Fig. 4.14. Also based on sensitivities and performance indexes of related controllers given in Table 4.6-4.8, the LS controller on

Load 1 is selected into first LS group $B_{LS1}$with threshold $\xi_2' = 0.5$. And the GR controller on G11 will be selected as an auxiliary controller, which is the closest one to Load 1. Then according to the linear programming algorithm and the objective function (5.9), the related control amount considering load restoration dynamics can be obtained, as shown in Table 5.3 and Table 5.4. The base MVA adopted in this thesis is 100 MVA.

Table 5.3 Expected relay margin increment and related control amounts

	Expected margin $\Delta \boldsymbol{M^{exp}}$ $(\boldsymbol{p.u.})$	**$\Delta \boldsymbol{S}$ $(\boldsymbol{p.u.})$on Load 1**
R_{TL0809}	0.0189	0.54
R_{G11}	0.0076	2.027

Table 5.4 Total LS and GR amount considering restoration

For Load 1 and G11		**For Load 2 and G01**	
D_{L1}	57.6461	D_{L2}	13.0974
ΔS_{12}^{res}	3.157	ΔS_{11}^{res}	0.0712
ΔS_{12}^{ses}	2.027	ΔS_{11}^{ses}	0
ΔS_{12}^{tot}	5.184	ΔS_{11}^{tot}	0.0712

Based on effective and fast communication, the distributed controllers will receive the orders from Control center and execute them immediately. It can be seen from Fig. 5.10, that after timely execution at 87.5s, the bus voltages were recovered to a safe level over 0.9pu. Also in Fig. 5.11, the impedance loci between 35s and 220s have been depicted, the critical relays were reset back when measured impedance in red color moved into Normal area (the black loci represent the collapse situation with relays being blocked in the post fault stage, and the blue loci represent the collapse situation with relays activated). The state signals of R_{G11} were changed from "0011" to "0001", as well as the ones of R_{TL1009}. And R_{TL0809}'s state signals were changed from "0101" to "0001".

It should be noted that the LTCs did not participate in the adjustment of the emergent states in this case due to their long time delay, and their state signals were reset to zero level immediately after execution of LS and GR. In this way, the proposed wide area protection strategy can timely and successfully adjust the system state, prevent the unexpected trips and recover the system voltage.

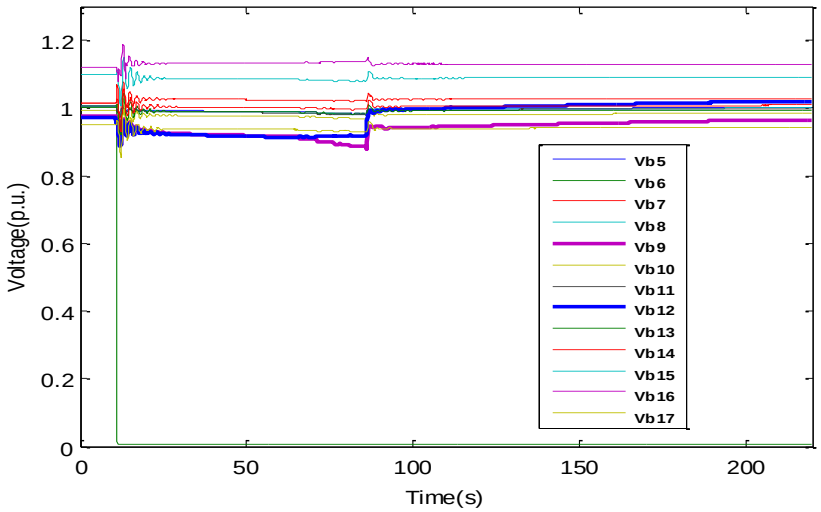

Fig. 5.10 Bus voltages with protection strategy activated

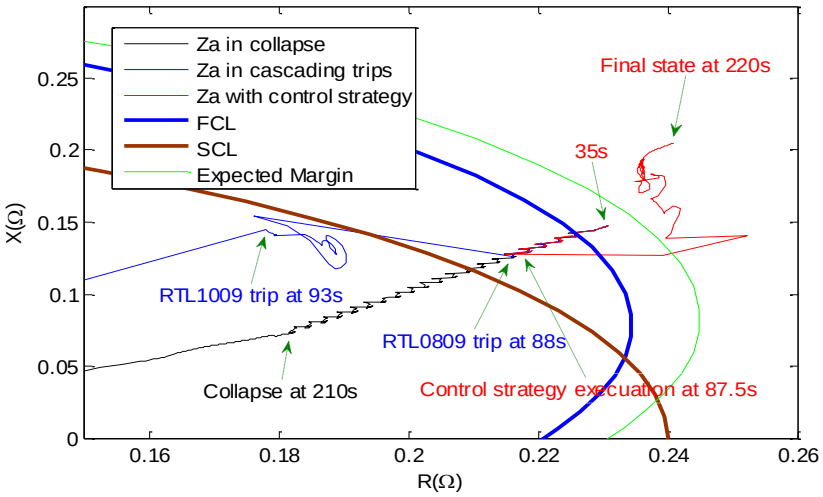

(a) Impedance loci of relay R_{G11}

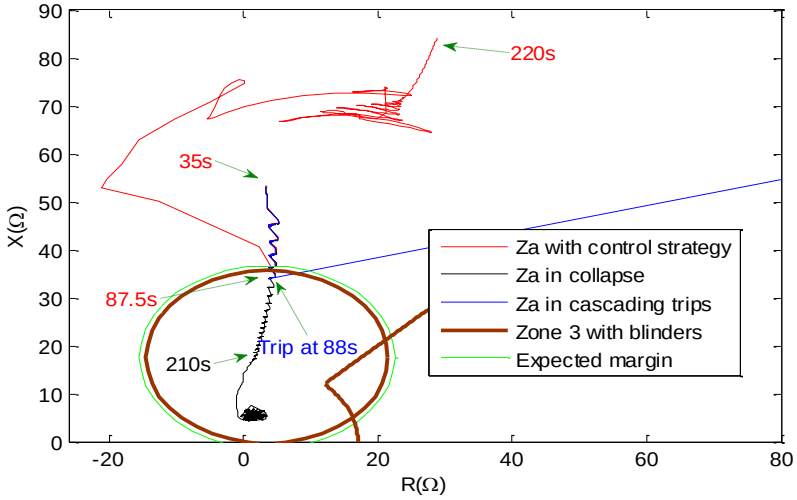

(b) Impedance loci of relay R_{TL0809}

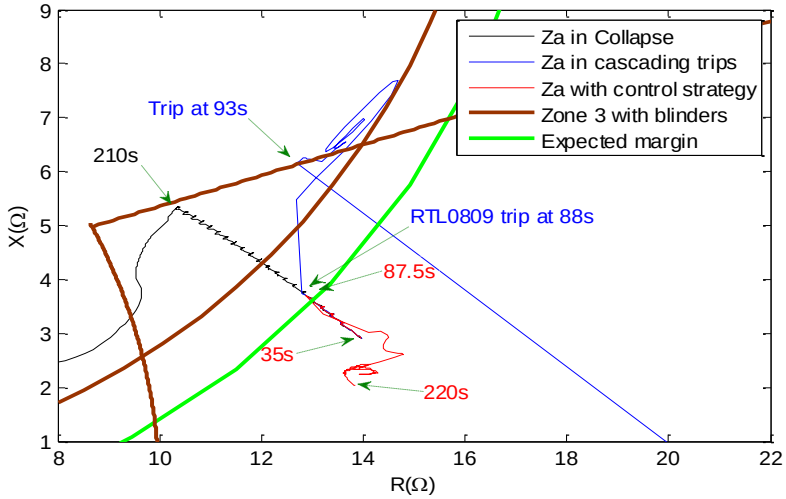

(c) Impedance loci of relay R_{TL1009}

Fig. 5.11 Impedance loci measured by critical relays

By virtue of successful execution of the proposed control strategies, the progress of cascading events has been effectively prevented. The basic processes of cascading events have been stopped and adjusted, such as transmission line tripping due to overloading situation in this case. In this way, the control strategies successfully change the original development progress of cascading events into a healthy progress and keep the normal operation of power systems.

5.5 Summary

In this chapter, the sensitivity based special protection and control strategies are presented according to the identified emergency states under overloading situation. Corresponding to Urgent state, ILTC will be adopted as the main control strategy and normal UVLS strategy will be backup strategy. When Zone 3 start state is detected, the emergency LS control will be set as main control strategy, GR regulation will be the ancillary control for LS and the ILTC will be backup strategy. The priority between different strategies can be defined by related state signals and integrated sensitivities. The case studies, based on the cascaded blackout scenario on 19-bus test system, demonstrate that the proposed special protection and control strategy (SPECS) can successfully adjust the overload emergency states and prevent those processes involved with unexpected cascading events.

Chapter 6

Implementation and improvement of SPECS

6.1 Introduction

In order to implement the proposed special protection and emergency control strategy (SPECS), multi-agent system (MAS) is adopted as a tool to build a suitable environment for emergency state detection, sensitivity analysis, control strategy defining and execution.

In this chapter, the relevant concepts and applications about MAS will be firstly introduced; then the detailed implementation of proposed SPECS based on a hierarchical MAS will be presented; real time hybrid simulation platform based on LabVIEW and RTDS will be introduced to demonstrate the MAS based SPECS. Moreover, in order to effectively monitor and regulate the mixed processes of cascading events and control strategies, the concept of process control is introduced and adopted to improve the SPECS and make it more reliable. Finally, case study based on the hybrid simulation platform will be presented to validate the effectiveness of proposed MAS based SPECS.

6.2 MAS for power system application

6.2.1 Agent technology

6.2.1.1 Definition of agent

Owing to the fast development of distributed artificial intelligence and computer network technology, the “agent”, especially “soft agent”, has been born and widely used in a number of industrial technologies. So far, there is no generally accepted definition of the term “agent”. Based on diverse application requirements, the agent will be designed with different characteristics. The paper [88] gives a comparison of those already existing definition from a computer science perspective. The definition presented by Wooldridge and Jennings [89], which is more frequently quoted, is adopted here:

"*Agent is a software (or hardware) entity, which is situated in some environment and is able to autonomously react to changes in that environment.*"

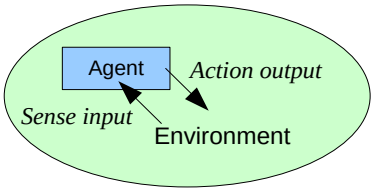

Fig. 6.1 An agent in its environment

An abstract view of an agent function can be observed in Fig. 6.1; the agent detects the requirements or variations of its environment, and produces output actions that affect the environment.

6.2.1.2 Features of agent

According to Wooldridge's definition, an entity situated in an environment can be regarded as an agent if it can act autonomously in response to environmental changes. So the *autonomy* is the primary feature of an agent, which can operate without the intervention from others and control its states by itself. Besides, as an intelligent agent, the following three features are required:

- *Sociality*

An intelligent agent is able to cooperate with humans or other agents in the common environment in order to achieve its or global tasks.

- *Reactivity*

Intelligent agents have the ability to perceive the variation of its environment (such as state changing of other agents) and respond quickly.

- *Pro-activeness*

Intelligent agents do not only response simply to its environment but also act proactively to realize some tasks. For example, if the communication fails between two agents, then these two agents will change their preset behaviors to communicate with other agents and realize the original tasks.

Normally, the intelligent agents can be categorized into three types [90]:

- Reactive type: It quickly responses to any interferences from the environment without any analysis and inference.

- Deliberative type: It can learn and analyze the detected situation, and change its states and response according to rule-based inference.
- Hybrid type: It integrates both reactive type and deliberative type, i.e. it is able to quickly response to its environment after reasonable inference.

Also it can be inferred that one agent could be a tiny hybrid system including both software and hardware. Furthermore, an agent can be mobile if necessary, such as Google map application in the mobile phone can be regarded as a mobile agent, which includes the application software together with the hardware-mobile phone.

6.2.1.3 The structure of multi-agent system

Due to the random variation of environment, single agent sometimes cannot deal with complex situation. So the multi-agent system (MAS) is built by two or more agents to handle the complex situation and realize the task targets together. MAS behaviors like a human organization or society, so the thinking way and organization structure could be similar. Under Wooldridge's definitions, the social ability is an important feature of an agent; therefore the development of communication network between agents in MAS is necessary. In this thesis, the author focuses on the application of MAS in which the communication network is well supported. Three basic structure types of MAS are as follows [91]:

- Peer to peer structure

The peer to peer structure type is shown in Fig. 6.2. All the agents are in the same layer and communicate with each other. Under this structure, the information exchanging is fast and flexible, but the communication network will be complicated if the number of agents is large.

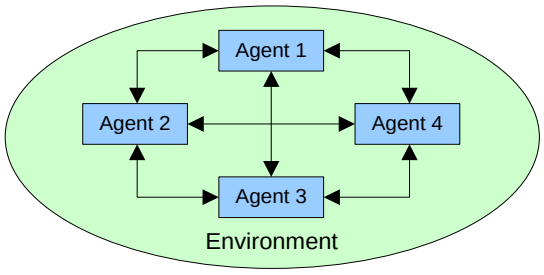

Fig. 6.2 The peer to peer structure of MAS

- Blackboard structure

The blackboard structure of MAS can be observed in Fig. 6.3. The blackboard agent is used as an information recorder to share the information between distributed agents. Also, the blackboard agent can be used as Control center in the higher layer to coordinate all the agents in the lower layer to realize some complex tasks. The information exchanging under this structure is not that directed but communication will be easy and efficient.

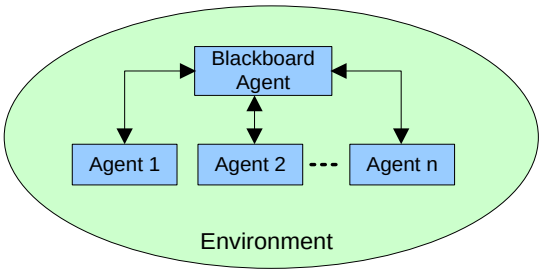

Fig. 6.3 The blackboard structure of MAS

- Alliance structure

The alliance structure is a hybrid structure composed by several blackboard structures and peer to peer structures. From Fig. 6.4, the structure of agent 1 and agent 2 in the higher layer belongs to the peer to peer structure. The agent 1.1, agent 1.2 and agent 1.n in the lower layer together with agent 1 in the higher layer compose one group, which is in the blackboard structure, as well as agent 2.1, agent 2.2 and agent 2.n together with agent 2. The alliance structure with distinct layers is suitable for a bigger system and its control strategy implementation.

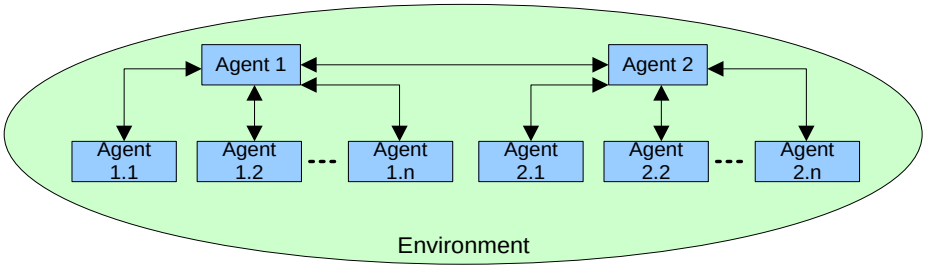

Fig. 6.4 An agent in its environment

6.2.2 Application of MAS

Based on the characteristics and structure types, MAS has its advantages on two aspects [92]. One is construction of flexible and extensible distributed software/hardware system; the other is to simulate those complex situations in the environment of real world

based on intelligent software/hardware setup systems. So MAS has been widely used in the areas of manufacturing industry, the traffic control, information management, electronic business, medical application and etc. In the power industry, the application of MAS can be briefly observed in Fig. 6.5.

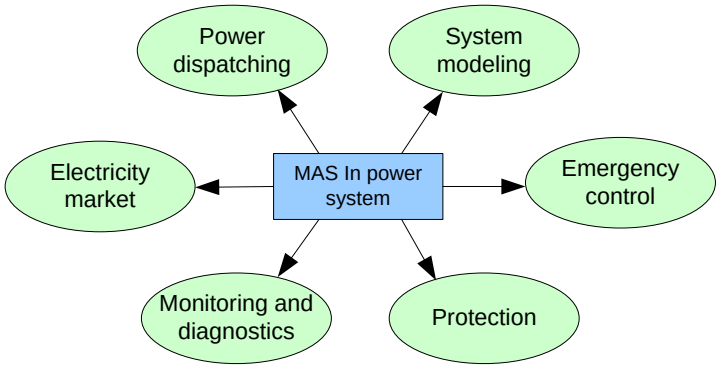

Fig. 6.5 The application of MAS in power system

Compared with traditional power system modeling tools, MAS provides an object-oriented system design, which is better to model the power system components as distributed intelligent objects. And the interaction behaviors between objects can be accordingly modeled based on unified principles. The paper in [93] proposed a multi-agent model of wind-solar power generation system, which is designed and simulated with the consideration of randomicity and complexity of climate environment. And in Greece, agent technology has been used to build Smart houses as proactive customers, which negotiate and collaborate as intelligent agents in close interaction with their external environment [94].

Also, MAS has been used to realize the complex algorithms and regulate the power system operations. The paper [95] has adopted MAS to divide the total optimal power flow function into sub functions, which is executed by dispersed agents. Then the result from each agent will be integrated to obtain the final optimal result. The paper [96] proposed a MAS based particle swarm optimization approach for optimal reactive power dispatching. Each agent represents one particle in this algorithm, i.e. one candidate solution for optimal reactive dispatching. In [97], an autonomous regional active network management system is developed based MAS to provide flexible and extensible methods for voltage control, power flow management and automatic restoration. And In [98], an Energy-Saving Generation Dispatching mode is built to be accordance with safety, energy-saving and environmental protecting characteristics.

With the development of electrical market in this century, MAS has been widely adopted to simulate the mechanism and operation rules in the electrical market. The paper [99] proposed a MAS based trading model of electrical market, which is able to help market participants make decisions based on their own benefits; meanwhile without a central controller, the minimum transmission cost of whole system can be reached. Also in [100], an electric vehicle aggregation agent has been designed as a commercial middleman between electricity market and EV owners. This agent participates with bids for purchasing electrical energy and selling secondary reserve.

In order to timely collect and manipulate the system wide information, MAS technology is also a good tool in condition monitoring and fault diagnosis [101]-[107]. In [106], a novel MAS has been integrated with a legacy SCADA interpretation system, which provides a flexible and scalable architecture to interpret digital fault recorder (DFR) record and enhance fault record retrieval from remote DFRs.

Moreover, protection engineers also try to build protective agents based on microcomputer protection devices. MAS technology, which shows its advantages on condition monitoring and fault diagnosis, also apparently can be a good platform to upgrade traditional protection schemes or develop novel schemes based on wide area information [108]-[110]. The paper [108] designed a multi-agent based adaptive wide-area current differential protection system. Based on the graph theory and expert system, predictive self-healing strategies have been proposed to prevent misoperation of the relay agent. And in paper [109], agent are used to give each protection component control ability as well as the ability to communicate with other agents, based on a simulation engine called EPOCHS (electric power and communication synchronizing simulator). This system can detect primary and remote faults, relay misoperation, breaker failures, and to compensate such problems with a much better performance than can be done in traditional schemes.

Then in order to face the ever-increasing challenge of security problems in power system, some researchers start to further investigate the capability of MAS based protection system dealing with more complicated situations, such as voltage collapse, cascading events and etc. In [111] [112], an emergency control system based on MAS is presented. The control system is designed with the ability to define a coordinated control action (load shedding, generation change), and then to prevent the power system voltage

instability problems. The paper [113] presents DefPlans, an environment envisaged to specify and validate defense plans for bulk power systems. In this software environment, it is possible to specify the emergency control functionality according to the multi-agents paradigm, and validate them by the Power System Dynamic simulator. The SPID (Strategic Power Infrastructure Defense) system proposed in the paper [114]-[116] is built to avoid catastrophic power outages through the failure analysis, vulnerability assessment, and adaptive control actions. MAS has been adopted based on bargain methods to identify the decision options to reduce the system vulnerability.

In this thesis, in order to deal with the voltage instability induced cascading events, the tasks on detection, identification, prevention and control are of the same importance. Multi-agent system technology is an effective and suitable approach to build such special protection and emergency control system with a large number of distributed autonomous agents and intelligent interactions involved.

6.3 Implementation of SPECS based on MAS

6.3.1 The targets of SPECS

Based on the working principle of proposed SPECS depicted in Fig. 5.1 and Fig. 5.6 of last chapter, the targets of this protection scheme are to adjust the overload emergency states and prevent the related unexpected relay operations. After the execution of related control strategies, all the violated relays will be hopefully adjusted from emergency states to Normal states, i.e. the impedance locus will finally moved into normal area, as shown in Fig. 6.6 with a generator relay settings as an example. The returning of relays also conversely proves the effectiveness of control strategies.

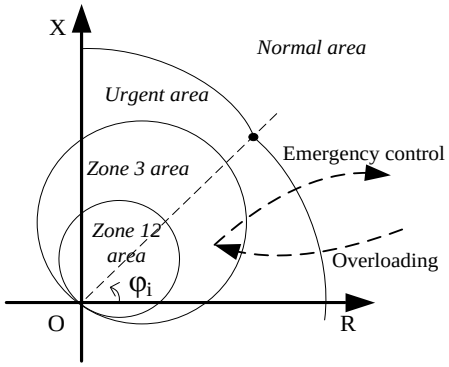

Fig. 6.6 The application of MAS in power system

6.3.2 Structure of MAS for SPECS implementation

In order to implement the proposed SPECS effectively, the structure of MAS in Fig. 6.7 is adopted, where the distributed relays and controllers work as device agents. They not only execute the normal function automatically but also can be modified to fulfill the extra functions according to external requirements. In this way, the distributed agents are organized by MAS to achieve the global targets for adjusting emergency states and preventing unexpected relay and control operations.

Every agent in this system has three basic functions. First function is for information collection, which might include local measurements of the current, voltage, and the status of related equipments; second one is to make decisions according to the prevailing state; last one is to produce output actions or information, such as breaker trip or block signals, state signals or information, control orders and etc. Moreover, this MAS based control system adopts a three-layer blackboard structure, which is comprised of distributed agent layer, cooperation society layer and central processing layer.

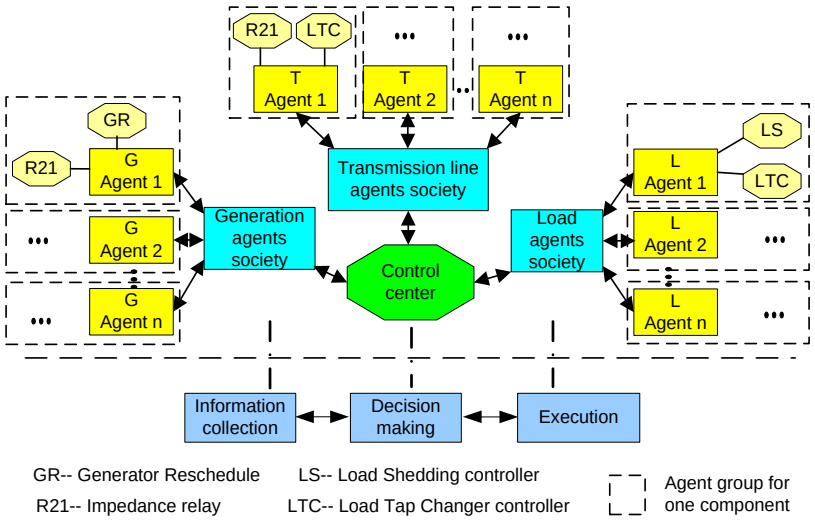

Fig. 6.7 The basic structure of MAS based SPECS

- Distributed agent layer

The distributed equipment controllers or relays are designed as the lowest layer of the MAS, including the generator controllers and relays, transmission line relays, load shedding controller, load tap changer controller and etc. Besides fulfilling their normal control and protective function independently, these agents have the ability to

communicate with the corresponding higher level agents, and then execute some extra functions accordingly.

- Cooperation society layer

The distributed agents in the lowest layer can be grouped into agent societies according to the similarity of their functions, such as generation agent society, transmission agent society, load agent society and etc. This is the middle layer which builds an effective cooperation environment between agents. At this layer, the state information of each agent can be monitored and collected if the communication network is well developed between the agents. These society agents can also communicate with higher layer agents to exchange and update the state information and control orders in a wider area.

- Central processing layer

In the highest layer of the MAS, Control center (CC) agent is designed to coordinate with all the lower level agents for collecting and sharing information, identifying system emergency state, generating and executing the control strategies. The algorithms of control strategies will be mainly fulfilled in CC, such as integrated network information processing, control strategy defining and etc.

6.3.3 Distributed agents and agent societies

6.3.3.1 Distributed agent

(a) Relay agent

All the distance relays of the generators and transmission lines are regarded as agents in the distributed layer, which are based on impedance principle and modeled with the standard distance relay model embedded in RTDS. The work flowchart of a generator relay agent can be observed in Fig. 6.8. The relays on transmission lines are similar.

The relay agent will online detect the position of *Zai* and send the related state signals to CC and other agents; based on the settings described in Section 3.3.1, the functions framed with red dashed line are new ones including cooperation and communication with other agents. The functions related to communication are with blue bold edges.

By this way, in addition to the traditional relay functions, the relay agents can help CC to collect and detect the information of equipment emergency states, such as the

position of *Zai* and related margin M_{Gi}; and then in CC a corresponding control strategy will be generated. Moreover, with the sensitivity information, the local relay agents can predict and identify the overload induced emergency states, and then the unexpected relay operations can be detected and blocked timely. The detailed workflow of the prediction and identification function can be observed in section 4.3.3. Obviously, the relay agents belong to hybrid type with those improved relay functions.

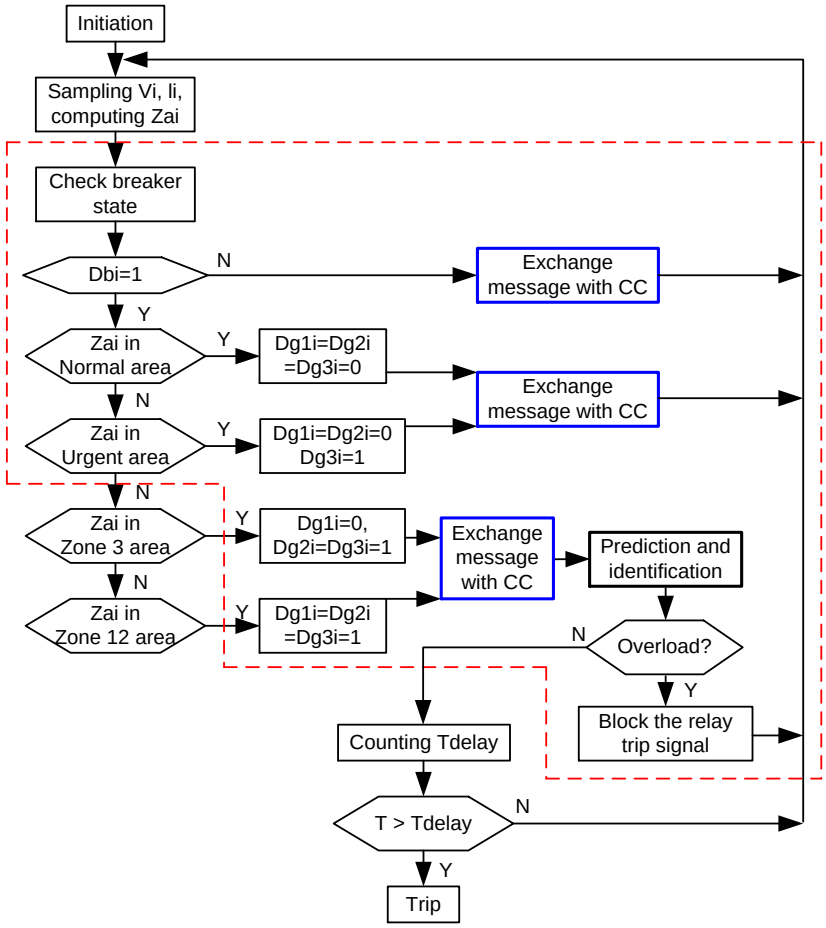

Fig. 6.8 The work flowchart of relay agent on the i^{th} generator

(b) Control agents

Based on the control strategies introduced in former chapter, LTC, LS and GR controllers will be also regarded as important agents in the distributed agent layer, which is able to perform extra functions when they receive the orders from agents in the higher layers. The workflows are shown in Fig. 6.9. The extra control function will be started when the signals of D_{tg} for the g^{th} LTC, D_{LSh} for the h^{th} LS and D_{Gn} for the n^{th} Governor are set to high level by CC. After successful execution of the related emergency controls, these signals will be reset to zero level and returned to CC for next action preparation.

Similarly, the functions framed with red dashed line are new ones for communication with other agents and execution of the related control strategies. The detailed workflow of related emergency control functions with black bold edges in Fig. 6.9 can be observed in Fig. 5.2, Fig. 5.3 and Fig. 5.4 respectively. The functions related to communication are set with blue bold edges. The defining of related control strategies is mainly conducted in CC, so basically these controllers belong to reactive agents.

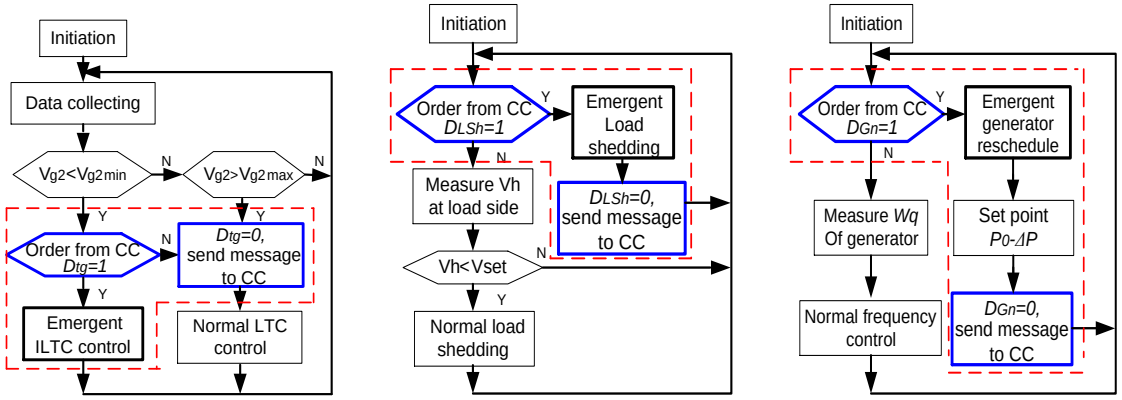

(a) LTC agent (b) LS agent (c) GR agent

Fig. 6.9 The work flowcharts of LTC agent, LS agent and GR agent

(c) CC agent

The agent of Control center in the highest layer of MAS will perform three tasks based on wide area collected information. The first task is to real time detect the vulnerable relays and collect the information of related emergency states including the changes of breaker states, and renew the state information of whole system; the second task is to do related sensitivity analysis and timely identify the emergency states caused by load flow transferring; and the third task will define reasonable control strategies to adjust the identified emergency states, and send control orders to related relay agents and controller agents. The work flowchart of CC agent is shown in Fig. 6.10.

Basically, it will firstly collect important information including the state signals from critical relay agents (D_{g1i}, D_{g2i}, D_{g3i} or D_{L1j}, D_{L2j}, D_{L3j}, and D_{bi} or D_{bj}), the state signals from LTC, LS, GR control agents (D_{Tg}, D_{LSh}, D_{Gn}) and state information of power components (node voltages and powers, status of tap changers, relay impedance and etc). Thus, the system emergency states can be detected and identified based on sensitivity analysis. When an overload Urgent state has been detected and identified, the emergency LTC control (i.e. ILTC) will be started as main control strategy. When the overload

induced Zone 3 violations have been identified, the emergency LS and GR control strategy will be initiated immediately.

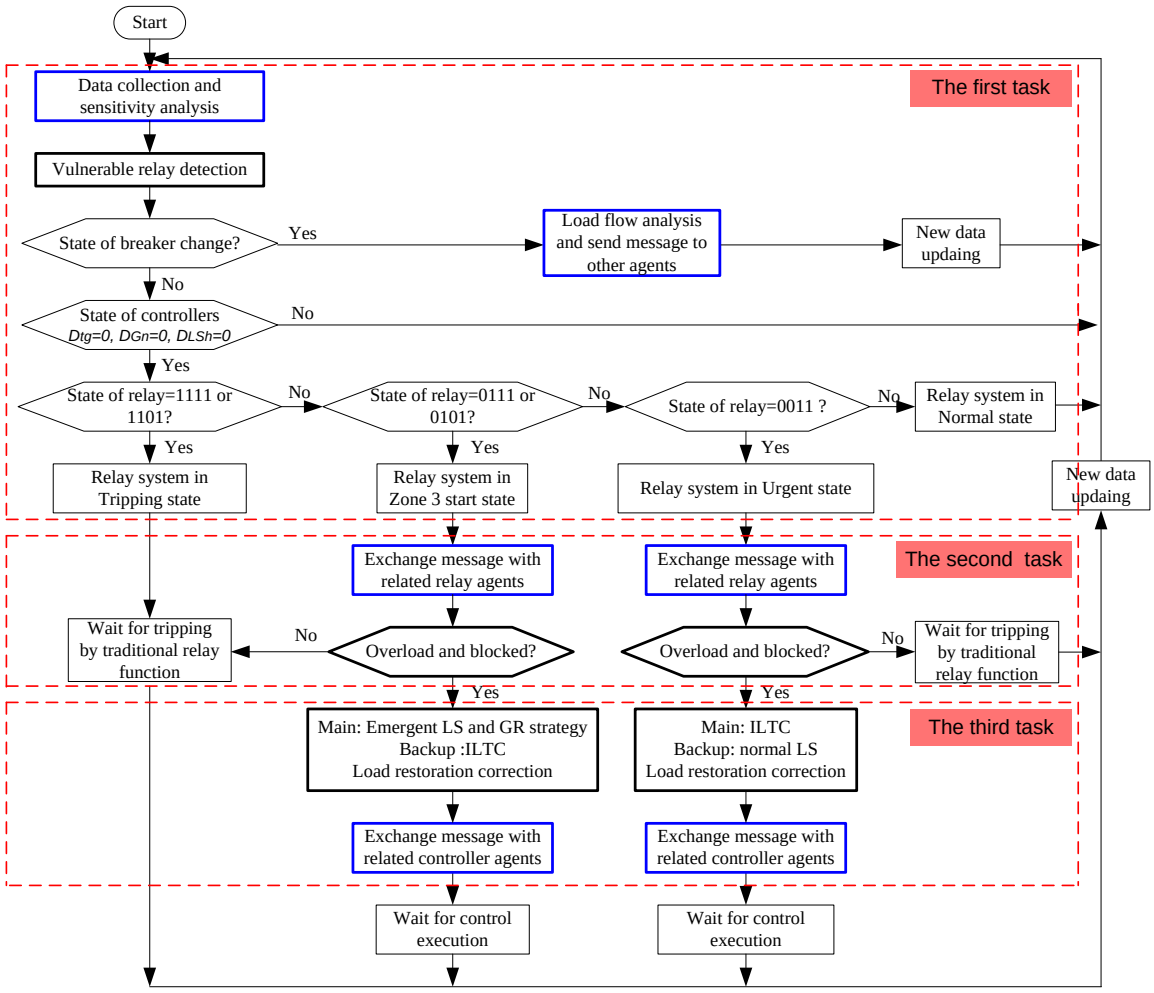

Fig. 6.10 The work flowchart of CC agent

The detailed workflow of the functions with black bold edges in Fig. 6.10 can be found in former chapters, and the communication functions are important during the workflow, which are set with blue bold edges. It should be note that the control strategies do not interrupt the traditional function of the relay, except the block function when the overloading situations are identified. So if the CC receives the information that some Zai is in Zone 12 area or the emergency states caused by faults, traditional function in relay system will cope with these situations to trip the component while the emergency control strategy will not be initiated by CC. Moreover, if the control strategies fail to adjust the related overload emergency states in the time delay period, then the critical relay will trip

the related component inevitably. Obviously, here the CC agent is an agent in hybrid type with fast reactive behaviors and specific information analysis.

6.3.3.2 Agent society

When the power system is toward a post fault long term voltage instability situation, there may be a big area with a number of relays and controllers involved. The distributed agents with similar characteristics can be grouped into one agent society. According to diverse characteristics, the related agent societies can be generated, which are relay agent society (RAS), LTC agent society (LTAS), load shedding agent society (LSAS) and generator reschedule agent society (GAS), as shown in Fig. 6.11.

Assume the communication network is well developed; the agents can communicate with each other not only within the same society, but also among different agent societies and system layers. When the power system experiences the overload emergency states at the risk of cascading events, the critical relays in RAS and most effective control locations in LTAS or LSAS can be easily identified, grouped and mapped according to the proposed sensitivity methods, which has been discussed in Chapter 4; meanwhile, the effectiveness of control strategy can be verified effectively, because the RAS can check the measured impedance on each relay directly and LSAS or LTAS will return the state of controllers after execution of related control strategies. In this way, the societies become middle agents as "blackboards" between CC and diverse societies, and then the work burden of CC can be alleviated to some extent.

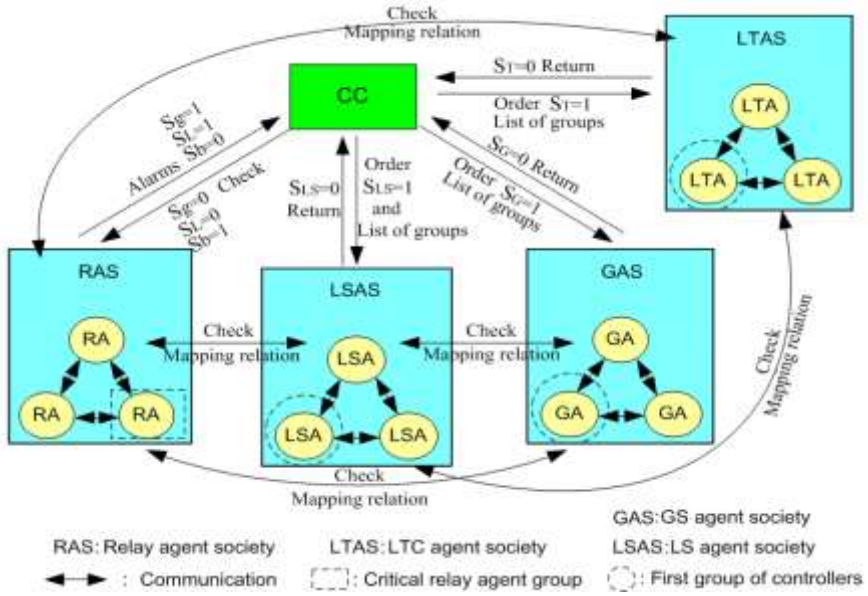

Fig. 6.11 Agent societies in the proposed MAS

Also from Fig. 6.11, the structure of propose MAS can be easily observed, the peer to peer structure is adopted to organize the agents in same layer, and the blackboard structure organizes the agents in different layers; such as the relay agents in RAS are in peer to peer structure, and the RAS and distributed relay agents are in blackboard structure. In this way, all the agents can be efficiently coordinated to realize the system wide protection and control strategies.

6.3.4 Hybrid simulation platform

6.3.4.1 Structure of hybrid simulation platform

In order to effectively simulate the cascading events and test the proposed SPECS, a real time hybrid simulation platform has been built based on RTDS and LabVIEW, as shown in Fig. 6.12. With the powerful libraries and programming environment, the intelligent agents can easily be programmed in LabVIEW by an end user [122]. Also since the power system modeling is accomplished by RTDS in this thesis, and the LabVIEW can provide a fast data transmission and communication interface with RTDS, so the proposed SPECS in former chapters can be suitably implemented in the simulation platform combining RTDS and LabVIEW.

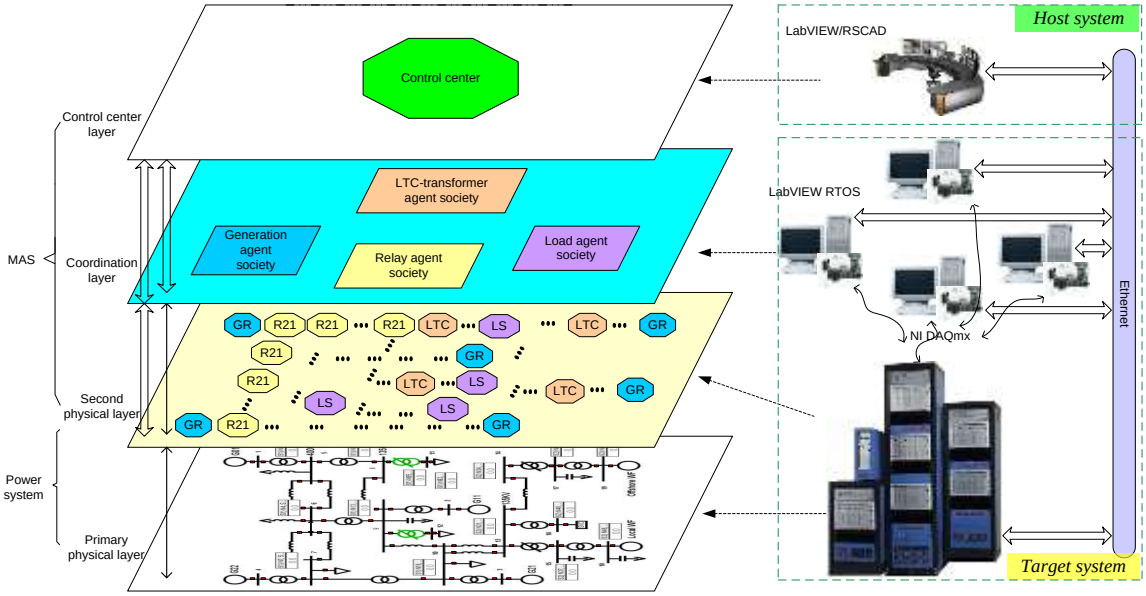

Fig. 6.12 MAS based SPECS in hybrid simulation platform

Based on the standard models in the library of RTDS, the power system model are developed, which is named as primary physical layer in Fig. 6.12; and the distributed agents relays and controllers are also modeled in RTDS together with the task of

information exchange between the agents and societies, which is named as second physical layer. The detection, selection and mapping functions of different agent societies will be modeled by LabVIEW in the real time operation system (RTOS) [123], which is denoted as coordination layer. All the functions in CC including the sensitivity based control strategies are also implemented by LabVIEW with a powerful RTOS, which is denoted as Control center layer and shown in Appendix A.2.

6.3.4.2 Communication consideration

In the hybrid simulation platform, the NI DAQmx cards (NI PCIe-6363) [124] are adopted to exchange data between LabVIEW RTOS and RTDS in real time. The maximum analog input sampling rate is 2 Mega Sampling/second, maximum analog output update rate is 2.86 MS/s, and maximum digital I/O rate is up to 10MHz. Since the normal time step of RTDS simulation is about 50 us, so real time data exchange between LabVIEW RTOS and RTDS through NI DAQmx cards can be easily realized.

Also, based on real time LabVIEW module, the real time communication network in MAS can be built, as shown in Fig. 6.12. To take advantage of parallel processing on a multiple-CPU system, many real time design and application can be done based on symmetrical multiprocessing technology [125]. The network communication and data exchanging between LabVIEW host system and target system (i.e. RTOS) can be based on three options, which are transmission control protocol (TCP), user datagram protocol (UDP) and shared variable communication in NI publish subscribe protocol (NI PSP). Since the former two communication methods in LabVIEW cannot be used in time critical control loop, i.e. they are not suitable for real time application. But the NI PSP with the characteristic of real time fast input fast output (RT FIFO) enabled is different, which provides a real time deterministic data transfer method that does not add jitter to a time-critical application in LabVIEW [126]. So the network published shared variables with RT FIFO characteristics are built in the suitable places of MAS, such as relay impedance information, results of real time sensitivity analysis and etc. Then these variables will be subscribed immediately through the shared variable engines of all the LabVIEW hosts and targets, and the real time application in different agents can obtain and access these network shared variables in real time. However, due to limited network buffering, which is used to decrease the likelihood of shared variable data loss in

applications, the number of shared variables is limited according to the capability of computer system.

As for the transmit delay of communication system in the practical power system, it can take on as 5μs/km as far as the delay of multiplexer and repeater in whole optic fiber system is considered [62]. Since the normal backup time delay from starting signal to breaker action is about 500ms, and with blocking signal set to delay several seconds, the communication tasks of proposed SPECS, i.e. those blue functions in the workflows of diverse agents, can be conducted and finished timely. Also with powerful processing ability of agents in higher layer and fast sensitivity algorithms, the final aims of SPECS can be effectively realized to prevent the unexpected relay operations and correct the system emergency states in the practical situation.

6.3.5 Process control strategy based on MAS

6.3.5.1 Introduction

As one kind of control methods, process control deals with architectures, mechanisms and algorithms for keeping the output of a specific process within a desired range [127]. It is widely used in the industrial application, such as oil refining, paper manufacturing, chemicals, power plants and many other industries [128].

So far in this thesis, the whole progress of SPECS is basically straightforward and without monitoring and regulating the possible failures in the progress. It is very important to build process monitor and regulation control for the operation reliability of proposed SPECS. Also, in order to further minimize the load loss, reserve regulation in the sensitive sets of transmission lines can be conducted by this fast supervisory process control.

Therefore, more efforts are required to develop a more secure and reliable control system for SPECS implementation.

6.3.5.2 Basic processes of proposed SPECS

In a power system, when the load demand increases beyond the supply capability of the power system, the overload states of relevant power components is hereby induced. According to the basic structure of MAS based SPECS in Fig. 6.12. The classic fluid representation for a supply chain [129] can be applied here to describe the basic processes of task flow in this MAS based protection system, as shown in Fig. 6.13. Three tanks are

used to represent the basic structure of power network (including generation, transmission and load consumption), i.e. the primary physical layer. The detectors and controllers represent the relays and power system component controllers, which are in secondary physical layer in Fig. 6.12.

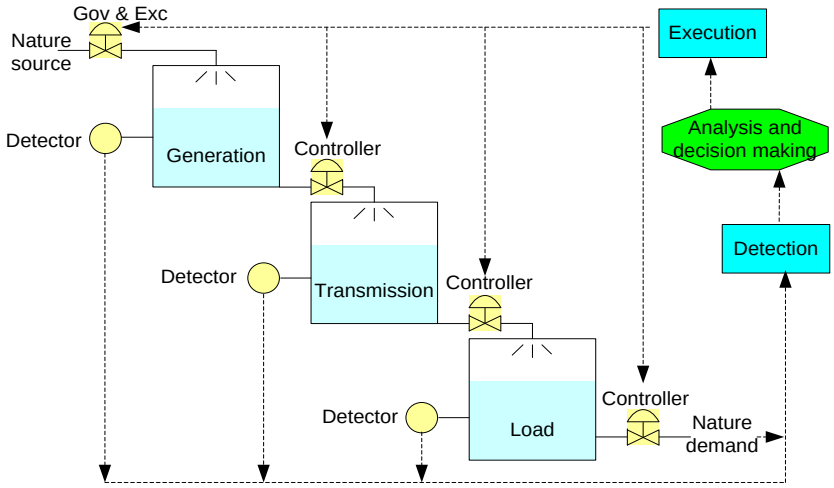

Fig. 6.13 The processes of basic task flow

The integrated detection function and execution function in turquoise blocks represent the tasks of agent societies in the coordination layer of MAS. The centre controller will fulfill the analysis and decision making tasks in the highest layer. Then power flows can be modeled using the fluid analogy, and fluid level in tank can represent the loading state of related power components. Therefore, the aim of SPECS is to maintain the levels in desired limits and keep stable power flows without interruption. In this supervisory system, the basic operation processes of MAS based SPECS can be described as follows:

- State detection based on relay system

Firstly, the overload states of power system components will be detected and identified by distributed relays.

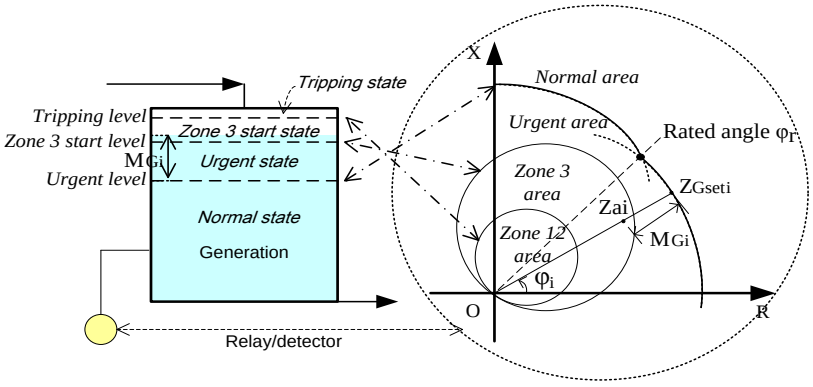

Fig. 6.14 Levels and Areas for operation states for a distance relay

Taking a distance backup relay for a generator as an example, the impedance plane in the first quadrant is divided into four areas, which correspond to four loading levels of related generator as well as the related tank.

- Analysis and decision making in Control center according to detected states from relay system

Through the cooperation societies, the detected emergency states of system are analyzed and identified by related relay agents together with CC, and the sensitivity based control strategies are accordingly produced，which is shown in Fig. 6.15.

In the Fig. 6.15, the agent societies are mainly "middleman" between CC and distributed agents of relays and controllers. Their behaviors on subscribing shared variables, grouping and mapping of critical agents will be not discussed here.

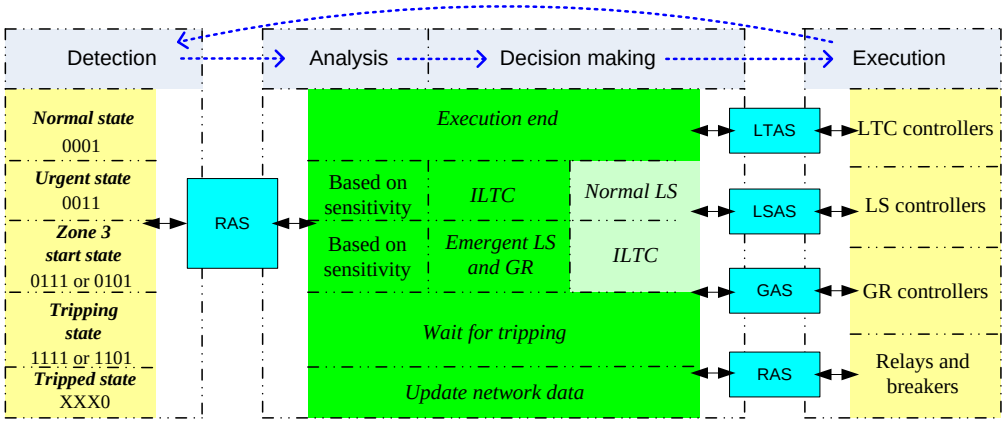

Fig. 6.15　Solutions for identified states

- Execution of defined control strategy by distributed controllers following the orders from Control center

Finally, the distributed controllers will execute the defined control strategies immediately when they receive the orders from CC. the state signals of related controllers will be sent back to CC through agent societies. The relay agents will be in turn to check if the emergency state has been adjusted successfully after execution of control strategies, and then prepare for a new round of basic task flow in SPECS.

6.3.5.3 Advanced SPECS considering the margin reserve regulation

In these basic processes of SPECS discussed above, the process of analysis and decision making will define how the control strategies will be executed, i.e. the process of control strategy execution. If the sequence or priority of control strategies is changed, then the related sensitivity analysis, control effect and process will be varied accordingly. Taking the Zone 3 start state for an example, when the MAS based control system detects this emergency state, the related control strategy will be initiated according to Fig. 6.15. The emergency LS and GR will be adopted as main control strategy while ILTC will be the backup. But GR is used as ancillary control for active power balance in the related design in Chapter 5. If the margin reserve regulation in the sensitive supply paths of transmission lines could be considered, which utilizes the remain margin of normal transmission lines and related relays to take more load flow, then GR strategy can be also selected as one of main active control strategies and not just an ancillary control. The workflow of this control strategy can be observed in Fig. 6.16.

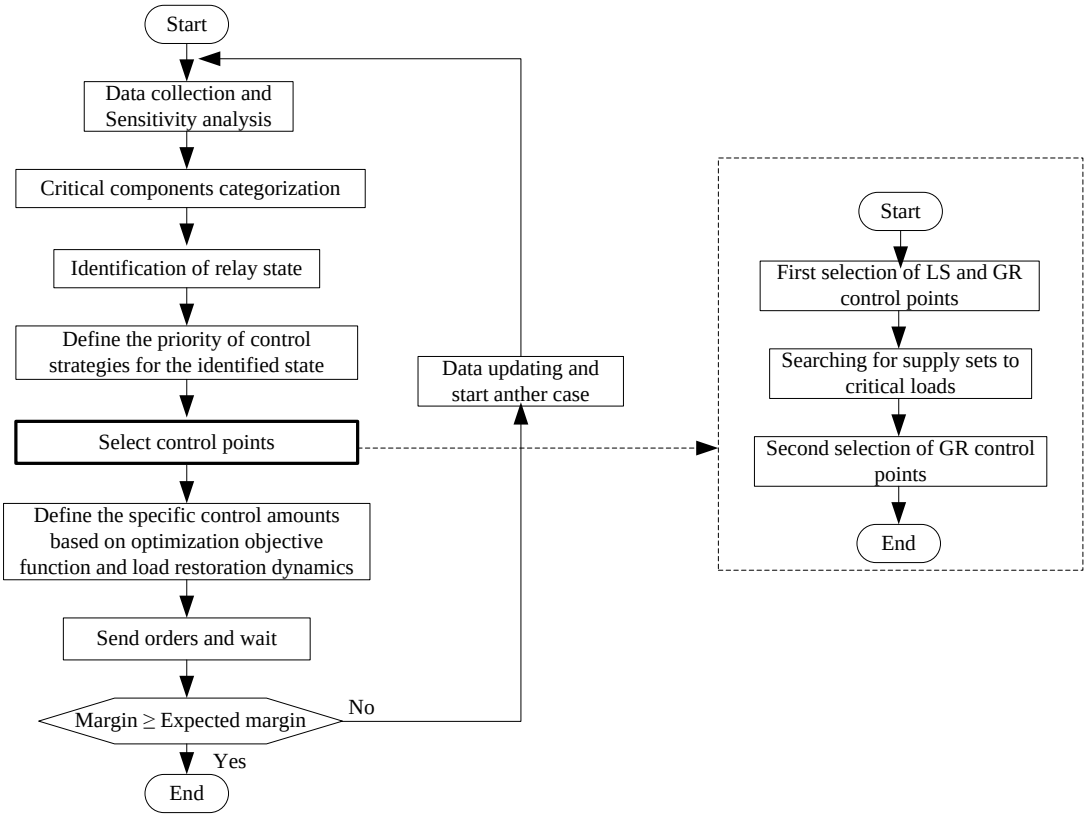

Fig. 6.16 Workflow of emergency LS and GR with considering reserve regulation

Based on online data of power network and the methods in section 4.3.1, the set of critical vulnerable relays (A_L') in the emergency states can be easily obtained. And the sensitive relationship between critical relays and injection powers can be defined based on sensitivity $\boldsymbol{H_{A'LS}}$ defined by (4.51). The set of related components may have two main subsets, i.e. critical generator set $B_{GA'}$ and critical transmission line set $B_{TA'}$. Then the procedures of control point selection can be conducted as:

- First selection of control points

Based on the sensitivity analysis in section 4.3.2, the effective controllers can be selected based on the performance indexes.

According to PI_{LScj} of LS points, all the LS controllers can be divided into two groups. The first group will include the LS controllers with higher $PI_{LSc}(> \xi_2')$ to all the relays in A_L', and the second group will include all the LS controllers in the system, which has been discussed in section 5.2.2. Based on PI_{GRcj} of GR controllers, similarly, the more effective GR control points with higher $PI_{GRc}(> \xi_3')$ will be selected as the first group, and the second group will include all the related GR controllers, which is different from GR ancillary control in section 5.2.3. Normally, the generator already in Urgent state will not be selected due to its importance role to support the load locally lest the load flow will be transferred from remote place. Then two control sets can be obtained: generator set $B_{GA'L}$ and load set $B_{LA'L}$.

- Finding the supply sets to critical loads

Secondly, according to the methods introduced in section 4.3.2, the supply sets and sensitive map can be quickly obtained. The related sensitive supply path set (including those in Normal states) to the critical load points can be easily found and grouped to a set A_{L1}. Then the corresponding set of transmission lines $B_{TL}$is the set of main power flow paths to the critical loads. Meanwhile, based on the control point selection method discussed above, the related sensitive generators to these relays in A_{L1} are defined as B_{GL}, which is the set of main sources supplying the load flow through the relays. Obviously, $A_L' \subset A_{L1}$, $B_{TA'} \subset B_{TL}$, $B_{GA'} \subset B_{GA'L} \subset B_{GL}$, the related sensitive map and inclusion relationships can be depicted in Fig. 6.17, which is similar to Fig. 4.5.

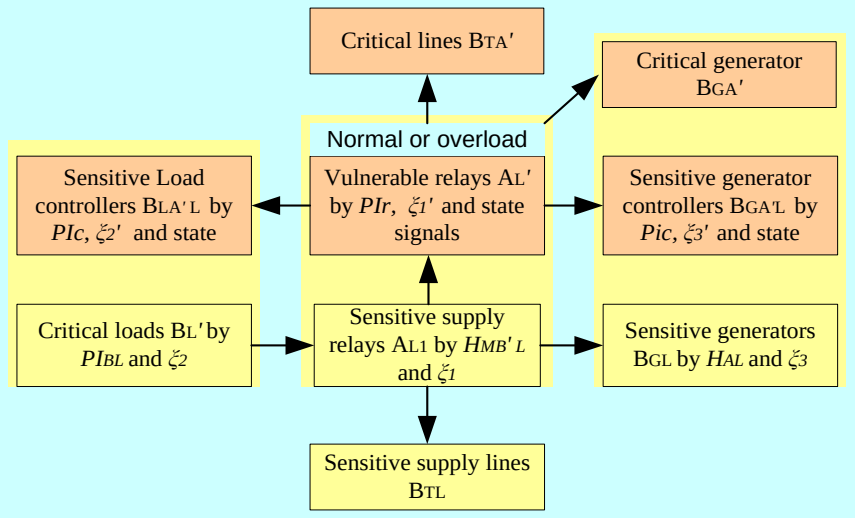

Fig. 6.17 Sensitive map and relationships based on sensitivity analysis

- Second selection of control points

Thirdly, according to the Fig. 6.17, the sets of relay A_r, transmission lines B_{Tr} and generators B_{Gr}, which are still in Normal state and have reserve margin to take more load flow, can be easily obtained by (6.1)-(6.4) respectively.

$$A_r = A_{L1} - A'_L \tag{6.1}$$

$$B_{Tr} = B_{TL} - B_{TA'} \tag{6.2}$$

$$B_{Gr} = B_{GL} - B_{GA'L} \tag{6.3}$$

Then these generators in B_{Gr} will be considered as additional control points, then the power in B_{Gr} and B_{Tr} are adjusted to send more load flow to the critical loads within their capability limits. In this way, the emergency states of components in A'_L, $B_{GA'}$ and $B_{TA'}$ will be alleviated to some extent; also, the relays in A_r won't be overloaded.

- Optimization of the control strategy

Then the achieved increment ΔM_i^* in (5.10) of former LS and GR strategy will be rewritten as:

$$\Delta M_i^* = \sum_{j \in B_{LA'L}} H_{A'LSLij} \Delta S_{Lj} + \sum_{x \in B_{GA'L}} H_{A'LSGix} \Delta S_{Gx} + \sum_{y \in B_{Gr}} H_{A'LSGiy} \Delta S_{Gry} \tag{6.4}$$

In the right part of equation (6.4), the first and second options represent effects of LS and GR in the control set $B_{LA'L}$ and $B_{GA'L}$ defined in the first step, the third option represents the effect of GR in the control set B_{Gr} considering reserve margin regulation defined in the third step. Also for the relays in A_r, the LS and GR strategy will change the margins of them, which may induce these relay into the emergency states. So the margin variations of these relays in A_r are required to be considered, the equation (6.5) can be also adopted to consider ΔM_p^* with related sensitivities ($p \in A_r$).

Therefore, the objective function in (5.9) will be rewritten as:

$$\begin{gathered} min\ S_{LS} = min\left\{\sum_{j\in B_{LA'L}} \Delta S_{Lj}\right\}, \\ s.t. \quad \Delta M_q^* \geq \Delta M_q^{exp}, \\ |\Delta S_m|_{max} \geq |\Delta S_m| \geq 0 \\ \sum_{x\in B_{GA'L}} \Delta S_{Gx} cos\emptyset_{Gx} + \sum_{y\in B_{Gr}} \Delta S_{Gy} cos\emptyset_{Gy} = -\sum_{j\in B_{LA'L}} \Delta S_{Lj} cos\emptyset_{Lj} \end{gathered} \tag{6.5}$$

The first constraint is used to achieve secure positive margin including both critical relays and those relays in reverse regulation ($q \in A_L' \cup A_r$), the second one is specific limitations for the possible control amounts on the controllable controllers ($m \in B_{GA'L} \cup B_{Gr} \cup B_{LA'L}$), and the last one is for active power balance.

6.3.5.4 Advanced MAS structure for process control

Based on the previous contents, it can be inferred that whether the emergency states can be adjusted and prevented successfully mainly depends on the fast and effective control strategy defining and execution. When the relay reserve margin regulation is considered, the progress of control execution becomes complex. If the related countermeasures fail to prevent the emergency states and subsequent trips, the system will experience a more complex situation. So in order to improve the effectiveness and reliability of this protection and control scheme, an advanced MAS based on hierarchical control structure is proposed here, as shown in Fig. 6.18.

The central agent named Supervisory Control center (SCC) is responsible for general supervision of all other agents' performances, i.e. states variations of relays, controllers and main functions in CC. Based on these real time state signals, the processes of cascading events and controls can be monitored and linked clearly. Then the related

regulation and compensation control strategies can be defined to timely adjust the processes of normal control strategies, if some possible failures occur in normal control processes. Moreover, human-machine interface (HMI) is built to support the supervisory controls by operators.

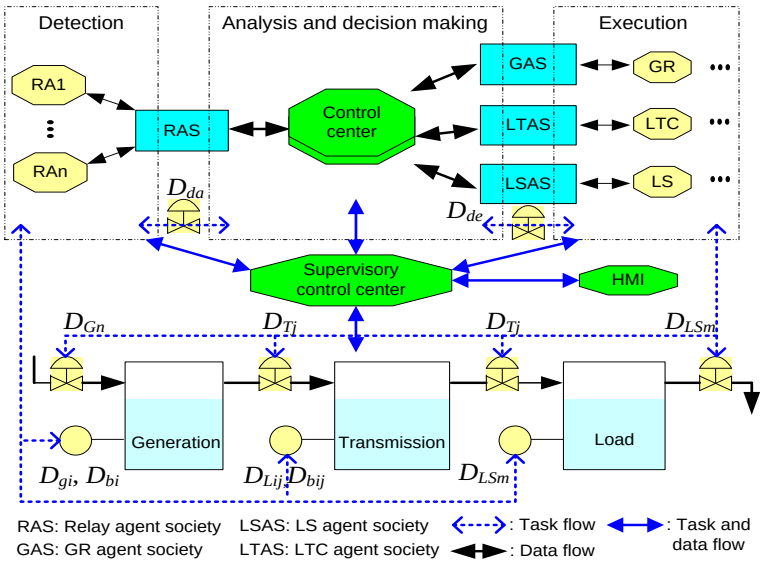

Fig. 6.18 Advanced MAS structure for process control

Besides the D_{gi}, D_{bi} (or D_{Lij}, D_{bij}) signals are already designed for the states of i^{th} relay and breaker, the signals of D_{Tj} for the j^{th} LTC, D_{LSm} for the m^{th} LS controller and D_{Gn} for the n^{th} GR controller are set to represent the states of distributed controllers, as well as D_{da} and D_{de} are set for the states of functions in CC. Moreover, D_{id} is set for overload identification function states. Zero level means an overloading situation, and high level represents a faulty situation.

(a) Supervisory control agent

The basic functions of SCC can be observed in Fig. 6.19. Except the same functions of CC as a backup, the states of relays, controllers and CC functions will be detected by the state supervisor in SCC. Also, based on principle of virtual state machine [130] and complex event processing [131], the state transitions of control and basic event processes will be traced. In this way, the Supervisory Control center can easily identify the variations of control process and the prevailing operation situation in the whole progress. Then compared with normal operation processes and initial settings, if there are abnormal processes occurring, the operation supervisor will conduct process regulations against these abnormal process variations.

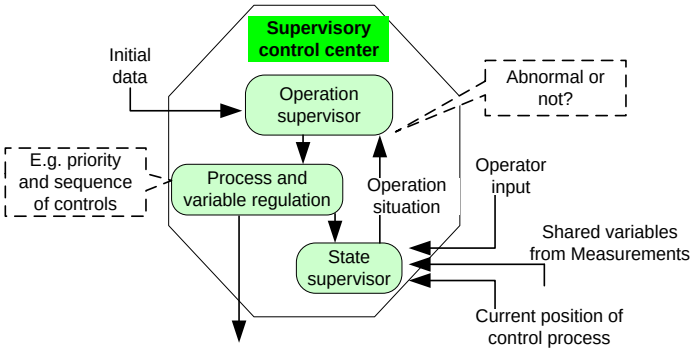

Fig. 6.19 The structure of Supervisory Control center

(b) The processes of cascading events under proposed SPECS

The basic states and basic processes under the proposed SPECS can be observed in Fig. 6.20. The basic numbered states include the event states (in yellow blocks) and control states (in green blocks). And the basic transitions, i.e. state transitions, include normal transitions (black arrows), fail transitions (red arrows) and the transitions of cascading events (bold blue arrows), etc. The state signals for each control state are composed by relay state signals, control function state signals and controller state signals.

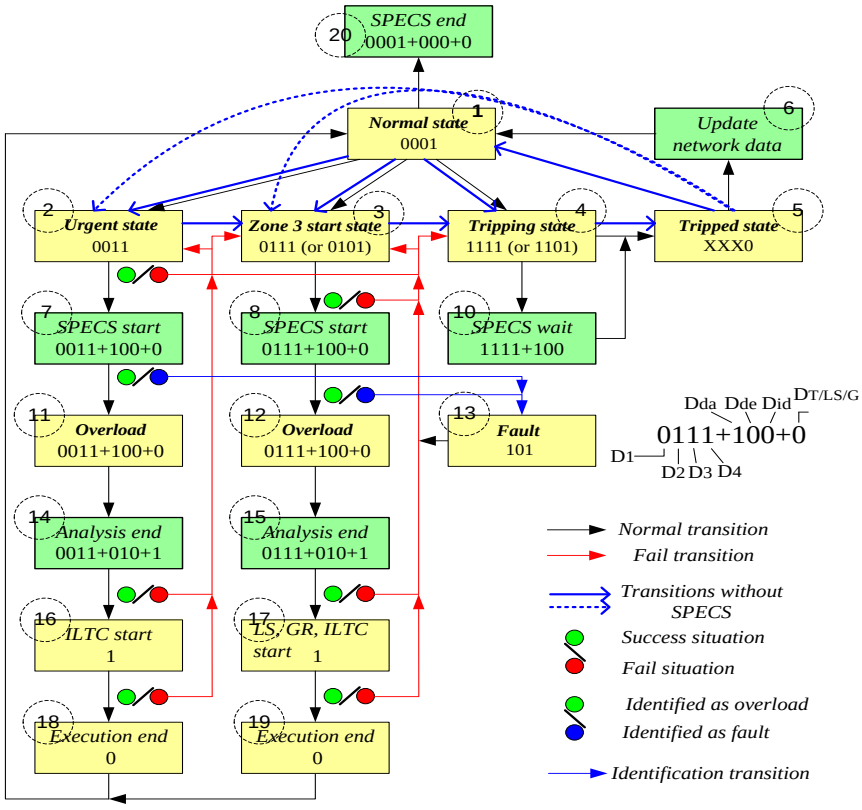

Fig. 6.20 Basic states/processes transition diagram under SPECS

According to the state diagram in Fig. 6.20, the diverse states can be identified by different combination of state signals. Also, the basic processes can be identified based on combinations of state transitions, which is given in Table 6.1.

Table 6.1 State transitions in basic processes

	Basic processes	**State transitions**
1	Power component outage due to faults or temporary maintenance	1→2/3/4/5→3/4/5→4/5→5
2	Overload due to outage induced load flow transferring	5→2→7→11 or 5→3→8→12
3	Overload due to LTC induced load flow transferring	2→7→11 or 3→8→12
4	Transmission line or generator tripping due to overloading	11→14→2/3/4→3/4/5→4/5→5 or 12→15→2/3/4→3/4/5→4/5→5
1	State detection based on relay system	1→2/3/4/5→7/8/10/6
2	Analysis and decision making in Control center according to detected states from relay system	7→11→14 or 8→12→15
3	Execution of control strategy by distributed controllers when the orders from CC is received	14→16→18 or 15→17→19

The front four processes with yellow numbers belong to event processes, while the rear three processes with green numbers belong to control processes. The control processes are responsible to prevent the development of event processes and regulate the emergency state into Normal state through normal transitions. The whole evolution progress is more complex but with clearer cause-effect relationships under SPECS, especially, when overload identification criteria are applied. When single state can be clearly identified, these basic processes can be effectively traced by sequential combination of detected signal states. The event processes with number 1, 2, 3 and all control processes belong to normal processes, and the event process 4 belongs to abnormal process..

6.3.5.5 Process regulation control based on integrated sensitivity

(a) Process regulation

Based on above process supervisory method, the state and the process transitions can be clearly traced. From the Fig. 6.20, when the fail transitions in red color occur, the emergency states will get worse, which may induce the further cascading events even under the proposed SPECS, i.e. event process 4 in Table 6.1. So when a fail transition happens, the SCC will be responsible to trace and detect it, and then the related regulation control should be initiated to prevent the deterioration of system state, or else, the cascading events will occur unstoppably.

As for the situation of CC failure in communication when the emergency states are detected, the SCC will substitute to do analysis and decision making, or just change another CC to fulfill the related tasks.

As for the situations that some controllers cannot be communicated, the SCC will firstly change the priority of existing control strategies, and then change the selection of control points. The process regulation (in brown dashed arrows) can be seen in Fig. 6.21 for this situation.

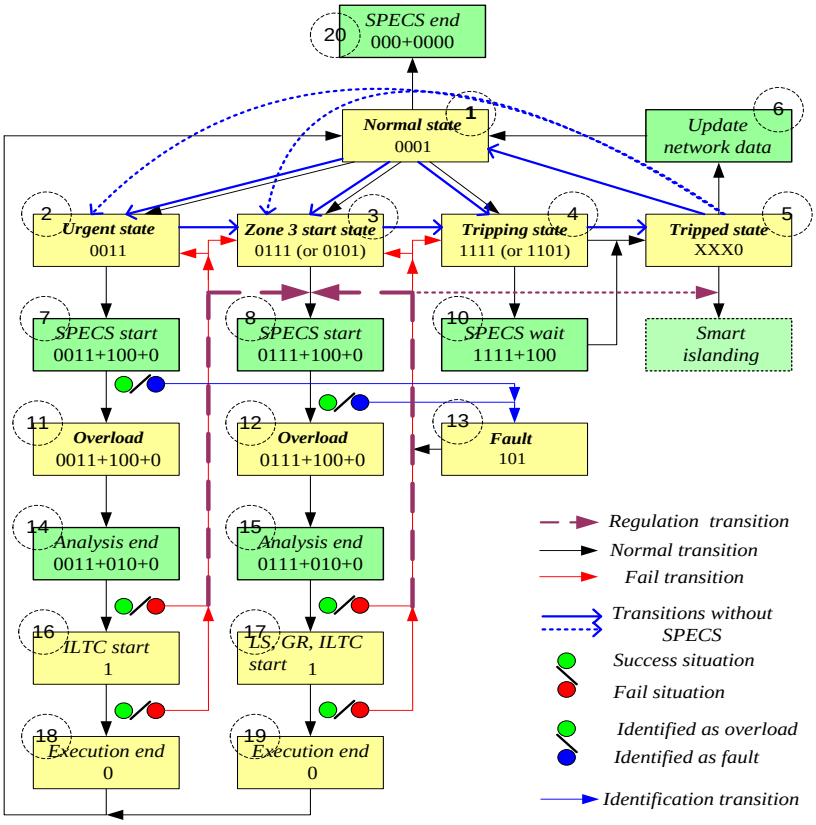

Fig. 6.21 Process regulation for controller failures

Moreover, if some controllers can be contacted but fail to execute the LS and GR control strategy, the related component may be tripped unexpectedly when time period of relay blocking has been run out, and then the regulation control should be defined immediately as a backup. At this situation, except the further LS and GR, smart islanding may be a good backup alternative to make the system survive this worse situation, which will be also conducted by SCC and not discussed in this thesis.

(b) Sensitivity based control strategy considering process control

In order to change the selection of control points, the state signals of controllers can be considered in regulation limits ΔS_{imax} of controllers, which can be expressed as:

$$\Delta S_{imax} = \bar{D_i} k S_i \tag{6.6}$$

where D_i is state signal of the controller i, k is the controllable ratio and S_i is the total capacity of controlled object.

According to process regulation discussed above, the SCC can monitor and regulate execution process of control strategies. Taking the emergency LS and GR strategy against Zone 3 start state for an example, if some LS and GR controllers are not available, the formula (6.5) will be corrected by:

$$\begin{gathered} min\ \ S_{LS} = min\left\{\sum_{j\in B_{LA'_L}} \Delta S_{Lj}\,\overline{D_{LSJ}}\right\}, \\ s.t. \quad \Delta M_q^* \geq \Delta M_q^{exp} \\ |\Delta S_m|_{max} \geq |\Delta S_m| \geq 0 \\ \sum_{x\in B_{GA'_L}} \Delta S_{Gx} cos\emptyset_{Gx} \overline{D_{Gx}} + \sum_{y\in B_{Gr}} \Delta S_{Gy} cos\emptyset_{Gy} \overline{D_{Gy}} = -\sum_{j\in B_{LA'_L}} \Delta S_{Lj} cos\emptyset_{Lj}\,\overline{D_{LSJ}} \end{gathered} \tag{6.7}$$

where ΔM_q^* can be given by (6.8) with consideration of integrated sensitivity.

$$\begin{gathered} \Delta M_i^* = D_{2c}\left(\sum_{j\in B_{LA'_L}} H_{A'_LSLij}\Delta S_{Lj}\,\overline{D_{LSJ}} + \sum_{x\in B_{GA'_L}} H_{A'_LSGix}\Delta S_{Gx}\overline{D_{Gx}} + \sum_{y\in B_{Gr}} H_{A'_LSGiy}\Delta S_{Gry}\overline{D_{Gy}}\right) \\ +\overline{D_{2c}} D_{3c} \sum_{k=1}^{l} \mathcal{L}_{Mr,ik}\Delta r_k \overline{D_{Tk}} \end{gathered} \tag{6.8}$$

In this way, when the x[th] generator cannot be regulated, the related element in (6.7) (6.8) will be eliminated due to the binary variable $\overline{D_{Gx}} = 0$. Otherwise, the related element will be accounted if $\overline{D_{Gx}} = 1$. Therefore, the control process will be regulated timely and effectively under the SCC.

6.3.5.6 Implementation of SPECS considering process control

The main functions and algorithms of SCC are implemented in host system based on the LabVIEW environment and DSC toolkit (Data logging and Supervisory Control) [132], which are shown in Fig. 6.22. The SCC is in a higher layer than CC, which is named as super center layer. Every lower agent and its behaviors will be projected as an image in SCC, so there is a mirrored image structure with three inner layers in the super

center layer, i.e. Control center image layer, agent society image layer and distributed agent image layer. In this way, the states of lower agents can be timely supervised, and the loading levels of related power system components can be monitored as well. Besides, the basic control processes can be identified based on the state transitions of control functions in the Control center while projected in the Control center image layer. Also the event processes can be identified based on combinations of state transitions of distributed agents while projected in the distributed agent image layer, e.g. the cascaded blackout scenario with processes denoted by red arrows is shown in the image layers in Fig. 6.22.

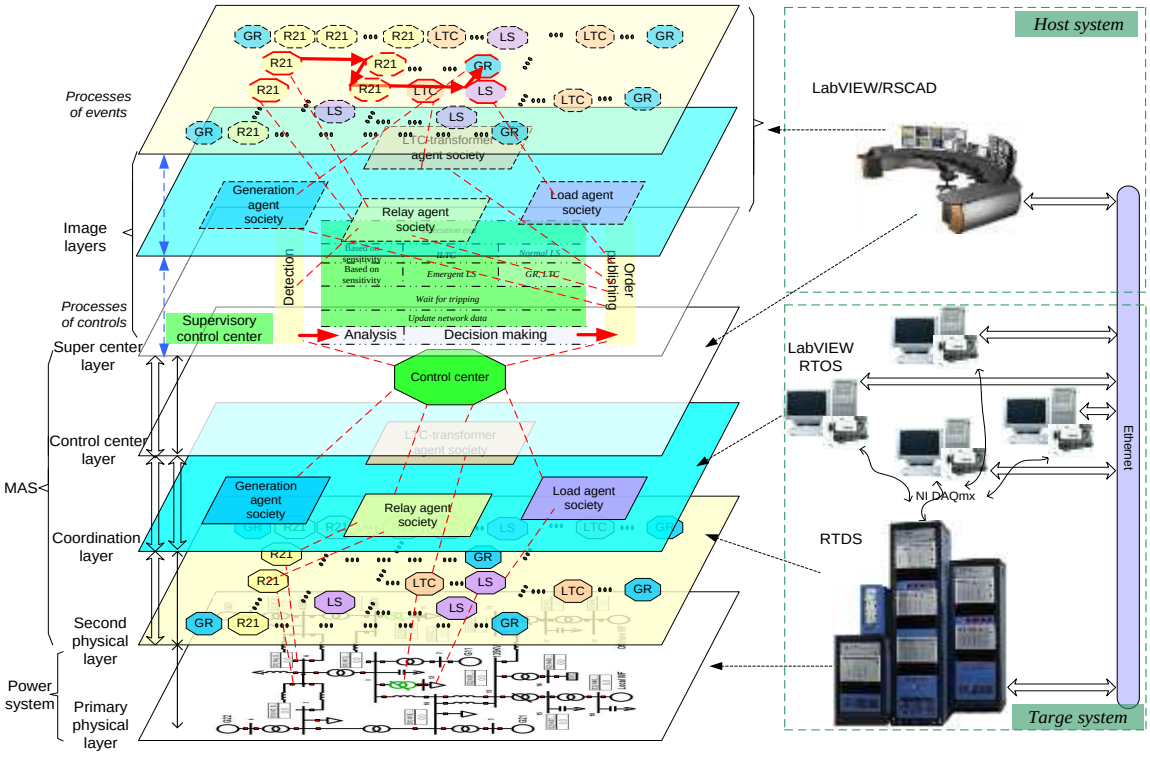

Fig. 6.22 States/processes transition tracing and regulation under SPECS

Then according to Fig. 6.21, the operation supervisor in SCC will compare the detected state and basic process with those normal processes or state transitions. If the fail transitions or event process 4 are identified, the process regulation control will be defined and initiated immediately, which has already been discussed in former contents.

6.4 Case study

In the case of cascaded blackout on 19-bus test system as shown in Fig. 6.23, if LTC agent on TX0912 and other controls failed to be execute emergency control strategy

when R_{G11} detected Urgent state (0011), then R_{TL0809} would be triggered at 87s, the Zone 3 start state and the related state or process transition (5→2→7→11 to 11→14→3) will be identified and the state signals will be shared in MAS. CC will do sensitivity analysis and define the related control strategies immediately, based on the workflow in Fig. 6.10. And SCC will identify the failing transition and regulate the control strategy to prevent the further development of this abnormal process.

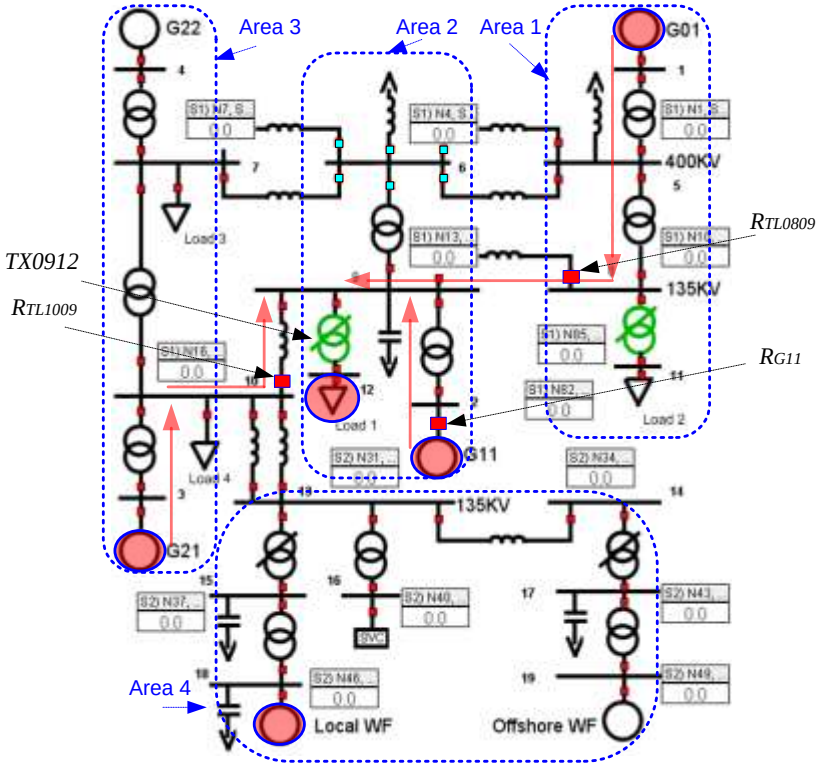

Fig. 6.23 The 19-bus test system in the post fault stage

6.4.1 Control strategies considering margin reverse regulation

- Critical components categorization

Firstly, at 87s, the critical relays R_{TL0809} (in Zone 3 start state) and R_{G11} (in Urgent state) will be detected, identified and grouped as set A_L' together with critical power components {G11, TL0809}.

- First selection of control points

According to online sensitivities calculation, the relevant sensitivities and performance indexes will be deduced immediately, which have been already given in

Table 4.6-4.8. The most effective LS and GR control sets can be obtained as: $B_{LA'_L}$= {Load 1}, $B_{GA'_L}$= {G01}. Also because G11 is already operated in an urgent overload state and close to the Load 1, so it is not selected, even though it has larger sensitivity and PI, which is different from the GR strategy considered as ancillary control in Chapter 5. Hereby, the state signal D_{G11} of GR controller on G11 will be set to high level.

- The supply sets and control points for reserve regulation

In this case, the critical load in B'_L is Load 1. According to sensitivity based method described in section 4.3.1.1**,** the relative sensitive relays to Load 1 can be easily found: A_{L1}= $\{R_{G11}, R_{TL0809}, R_{TL1009}\}$. Also, the related sets of transmission line and generators can be found: B_{TL} = { $TL0809, TL1009$ }, B_{GL} = {G01, G21, Local WF}. G22 and offshore WF (OWF) are not selected because they are already operated close to their capability limits, the state signals D_{G22} and D_{Gof} will be set to high level.

Then, based on (6.1)-(6.3), the sets of relays, transmission lines and generators with redundant reserve can be obtained: A_r= $\{R_{TL1009}\}$, B_{Tr}= { $TL1009$}, and B_{Gr}= {G21, Local WF}, which are selected secondly for GR control points.

- Optimized control strategy

In order to minimize the load loss in the LS and GR control strategy. Based on the principles and optimal objective functions described in Section 6.3.5.3, the detailed control strategy is shown in Table 6.2.

Table 6.2 Expected relay margin and control amount (p.u.)

	ΔM^{exp} (R_{TL0809})	ΔM^{exp} (R_{G11})	M_{Ar} (R_{TL1009})	ΔS (Load 1)	ΔP (G01)	ΔP (G21)	ΔP (LWF)
1	0.0076	0.0189	0.0077	5.184	-0.071	0	0
2				3.979	-1.07	0.54	0.11

The number "1" in the first column of Table 6.2 represents the original control strategy without the consideration of reserve margin regulation, and "2" represents the strategy considering the regulation of reserve margin in the supply sets. Obviously, the smaller total LS amount is achieved by this advanced protection and control strategy without compromising security and reliability, which is proved by real time simulation with results shown in Fig. 6.25.

6.4.2 Strategy execution and supervisory

In order to effectively execute and supervise the whole process of proposed SPECS, the proposed MAS based process control are taken into effect to monitor the states of agents and then regulate the reserve margins in supply sets timely.

For this case, $D_{G11} = D_{G22} = D_{Gof} = 1$ means the controllers of these components will refuse to execute orders from CC, also this worsen overloading situation is caused by LTC agent failing to be initiated. So SCC will be responsible to detect these situations, and regulate the control process. The front panel of supervisory control system built in LabVIEW can be seen in Fig. 6.24.

There are five modules in the front panel of LabVIEW, which are initiation module, detection module, analysis module, decision making and execution module, and process supervisory module. The data communication channels and settings will be initiated in initiation module. Emergency states featured in different colorful lights will be detected in detection module. Sensitivity analysis, overloading identification and critical sets grouping will be conducted by analysis module. Control regulation, optimization and execution orders will be produced by decision making and execution module. The results of execution will be checked by detection module in turn.

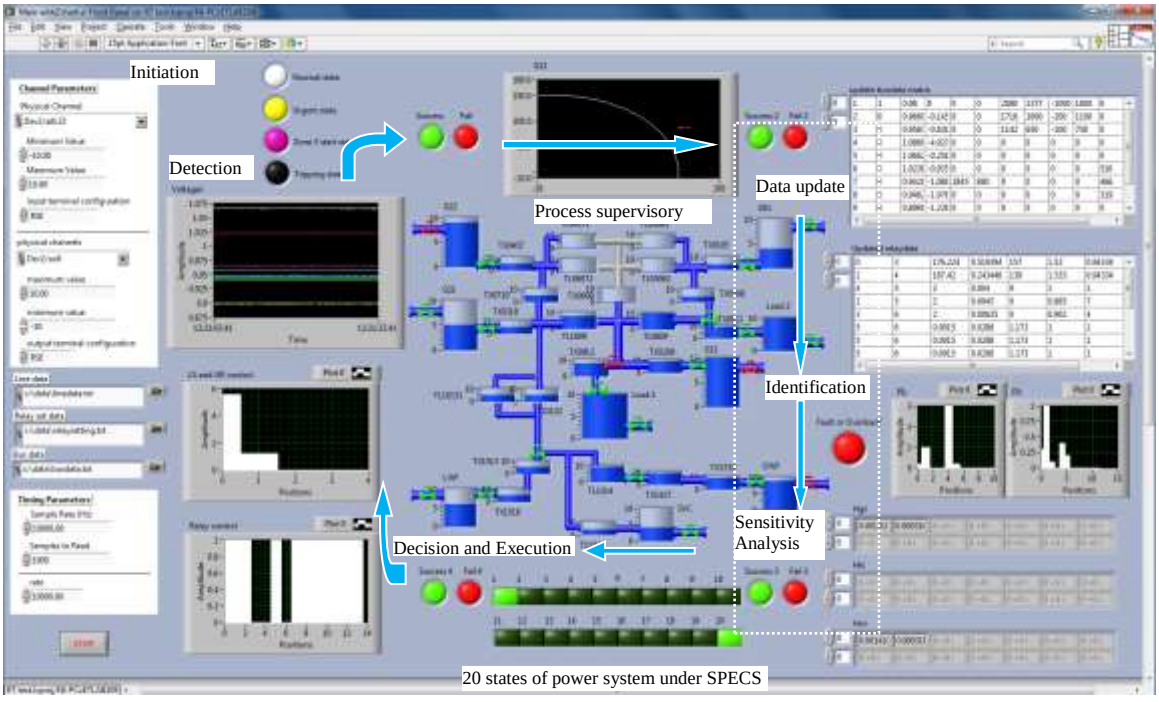

Fig. 6.24 The front panel of control system in LabVIEW

Moreover, the physic process of whole protection strategy can be supervised by the process supervisory module (i.e. SCC) in Fig. 6.24, which is conducted by DSC toolkit (Data logging and Supervisory Control) in LabVIEW. The tanks represent the power components, the pipes gives the states of breakers and the multi state valves are used to show the states of distributed controllers. According to classic fluid flow representation, the pipes and tanks which represent transmission lines, transformer and breakers around Bus 6 are blank due to the bus bar fault; then TL0809 is fully loaded, and TL1009 is still with some reserve margin; also the valves of G11, G22, OWF together with the LTC on TX0912 are set in red color which means they can't be controlled by CC in this situation. The state transitions are traced by 20 signal lights at the bottom of Fig. 6.24. So based on this LabVIEW toolkit and sensitivity method, the state information of whole power system and the processes under proposed SPECS can be supervised delicately.

Finally, the distributed controller agents execute control strategy immediately and successfully, under the effective supervisory and fast sensitivity analysis. It can be seen from Fig. 6.25 (a) and (b) that after timely execution at 87.5s, all the bus voltages are recovered to a safe level over 0.9pu. Moreover, due to better control strategy and less LS amount, the critical bus voltages V_{b9} and V_{b12} in Fig. 6.25 (b) are stabilized more quickly and recovered to a lower level compared with Fig. 6.25 (a).

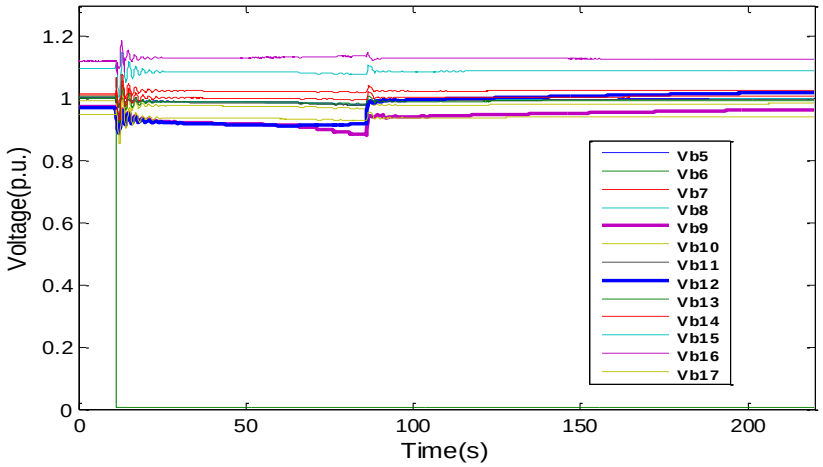

(a) Bus voltages with normal control process

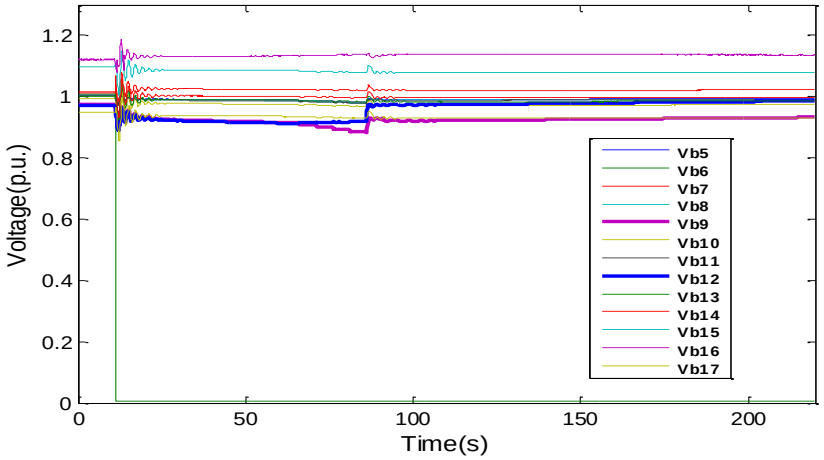

(b) Bus voltages with advanced control process

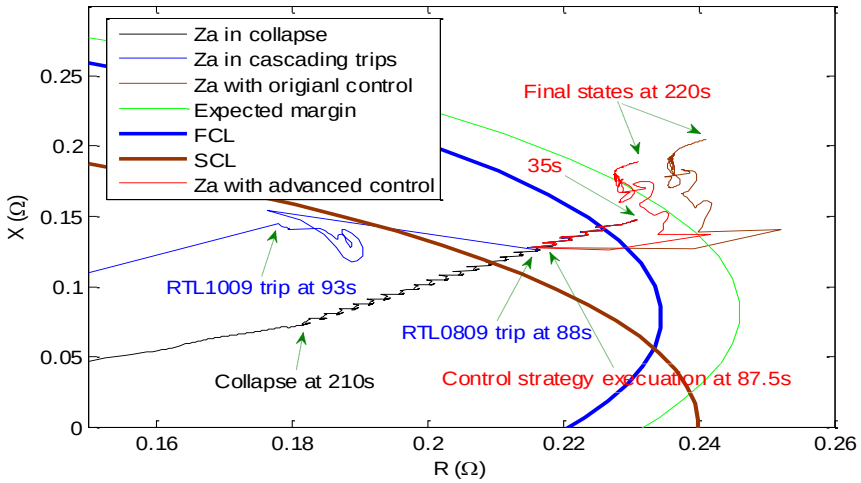

(c) Impedance loci of R_{G11} with normal and advanced control process

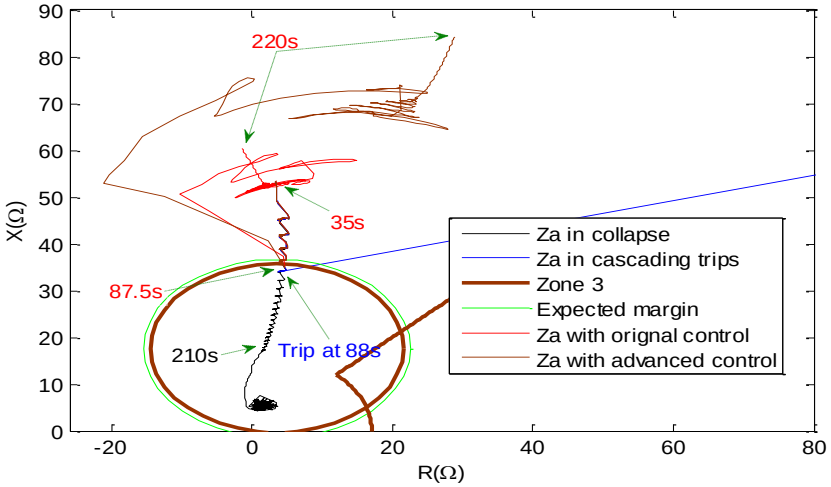

(d) Impedance loci of R_{G11} with normal and advanced control process

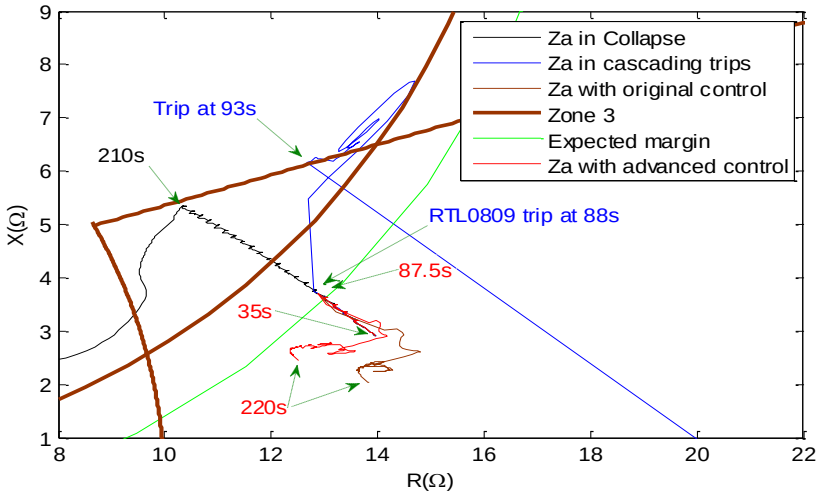

(e) Impedance loci of R_{TL1009} with normal and advanced control process

Fig. 6.25 Bus voltages and impedance loci in the normal control and the advanced control

From the figures of impedance loci, all the critical relays are reset back when measured impedances in red and brown colors move into Normal area over the expected margin. In the impedance plane, the black loci represent the collapse situation with relays being blocked in the post fault stage, the blue loci represent the collapse situation with relays activated, brown ones is under the original control strategy and red ones represent the progress with advanced control strategy considering margin reserve regulation. All the loci in four situations start at the time 35s in the post fault stage.

It also can be seen from Fig. 6.25 (c) (d) (e), with consideration of reverse margin regulation and advanced control process, the impedance loci in red color settle closer to expected margins compared with the brown ones, especially in Fig. 6.25 (e), the red impedance locus settles just beyond the expected margin, which means the TL0809, TL1009 and G11 take more loads under a better control regulation with less load shedding. Because at the time of 87s, R_{G11} and R_{TL0809} hit their relay settings due to overloading situation, but R_{TL1009} in the sensitive supply path set to Load 1 is still in normal state with some redundant reserve margin. Then in the advanced control with the reverse margin regulation, TL1009 takes more load flow nearly to its loadability limit when G21 together with LWF increase the active power output and G01 decreases the active power output. Hereafter the load flow supplied from TL0809 and G11 are decreased, the related overload states are alleviated, voltage decreasing are accordingly alleviated due to G11 and G01 supporting more reactive powers. Hereby the required total load shedding amount are decreased. After timely execution of GR and LS at the

same time, the results of real time simulation in Fig. 6.25 (b) (c) (d) (e) demonstrate the advanced process control gives a better protection strategy to prevent emergent system states and minimize the LS amount.

It should be noted that the critical LTC on TX0912 failed to be controlled in this case, so it did not participate in the adjustment of the emergent states. Also, in order to compare with the former case under normal control strategy, the process regulation control considering margin reserve regulation in this case was initiated when zone 3 relay R_{TL0809} got triggered. Actually, the process regulation could be initiated earlier when the LTC agent failure on TX0912 was detected at about 70s and before R_{TL0809} got triggered, then LS amount will be minimized further.

Based on this simulation case, it can be seen that the proposed SPECS considering process control can timely and reliably adjust those worsen situation, finally prevent the unexpected trips and recover the system operation states.

6.5 Summary

The implementation and improvement of SPECS are focused in this chapter. A multi-agent system based control structure is adopted to implement the proposed SPECS. The merits and features of MAS are presented and suitable for proposed SPECS. The detailed implementation is based on three layers, i.e. agents in the distributed layer, agent societies in the coordination layer and Control center in the center processing layer. A hybrid simulation platform based on RTDS and LabVIEW is set up to simulate the cascaded blackout and validate the SPECS in a real time environment.

The concept of process control is used to supervise the progress of cascading events prevention under SPECS, and an effective process regulation control is proposed to adjust those abnormal or failing control processes. Also the margin reserve regulation is considered in the control strategy defining, which could further minimize the load loss during control strategy execution.

The MAS structure is then improved with consideration of process control. The supervisory control agent is built in the highest level to implement the process monitor and control over all the agents. The simulation results based on hybrid simulation

platform demonstrate the advanced SPECS has the ability to successfully and reliably prevent the cascading events with less loss of load consumption.

Chapter 7

Conclusion and perspective

7.1 Conclusion

The overall purpose of this PhD project is to develop a wide area special protection and emergency control scheme that can provide effective countermeasures against long term voltage instability induced cascading events and blackouts in power system.

In order to have an in-depth analysis and understanding on the long term voltage instability induced cascading events, the simplified eastern Denmark power system has been adopted as a test system, and the detailed models of concerned power components are developed, such as FCL model, LTC model, restoration load model, distance relay model and etc. Due to the contribution of distance relays to historical cascading events, the loadability of distance relay has been discussed. The capability limit curves of generator and loadability of transmission lines have been considered in the design of relay backup settings. Then the relay operation margin in the impedance plane and related state signals are adopted as an indicator to express the loading level and emergency states locally. The scenarios of cascaded blackouts have been simulated successfully based on RTDS. The progress of cascading events has been decomposed into basic processes which is easier to be identified and analyzed.

In order to realize the system wide emergency state awareness and fast analysis, a sensitivity method has been adopted to online analyze the relationship between relay measured impedances and the system operation variables. Based on sensitive relationships and performance indexes, the vulnerable relays and sensitive power system components can be quickly detected under different operation states. The sensitive map and sensitive supply paths can be also depicted easily, which give effective indicators for defining suitable emergency controls against diverse emergency states. Meanwhile, for prevention of unexpected relay operation, impedance sensitivity based identification methods have been proposed to predict and identify overload emergency states, which are caused by the line outage and LTC operations induced load flow transferring.

Accordingly, the Zone 3 relay can effectively differentiate the load flow transferring induced emergency states from a fault state, and the unexpected relay operations can be blocked timely, which gives time for emergency controls to adjust the emergency states to the Normal state.

With aim of effectively adjusting those identified emergency states, sensitivity based special protection and control strategies have been designed, which can quickly define the detailed control points and control amounts based on the results of sensitive analysis and linear programming algorithm. Also, an integrated sensitivity method with the priority consideration has been designed for the quick selection of related control strategies. Basically, corresponding to Urgent state, ILTC will be the main control strategy and normal UVLS strategy will be backup strategy. And for Zone 3 start state, the emergency LS control along with GR regulation will be adopted as main control strategy, the ILTC will be backup strategy. The simulation results demonstrate that the proposed special protection and control strategy (SPECS) can successfully identify the overload induced emergency states and prevent the basic blackout processes involved with unexpected relay operations.

For implementation of SPECS, a multi-agent system based control structure has been proposed. Based on the distinct merits and features of MAS, the proposed SPECS has been designed with a three-layer multi-agent system, i.e. relay and control agents in the distributed layer, agent societies in the coordination layer and Control center in the center processing layer. This MAS based SPECS has been developed based on a hybrid simulation platform which is composed by RTDS and LabVIEW. Then the cascaded blackout scenarios and the proposed SPECS have been successfully simulated and validated together in a real-time hardware in loop environment.

In order to deal with possible failures in the control execution process or when some unexpected situations occur, an advanced MAS-based SPECS has been proposed with consideration of process control and regulation. This advanced SPECS can monitor the progress of cascading events under proposed control strategies, and timely define effective regulation controls on those abnormal or failing control processes. The basic processes are confirmed and identified by state signals and sensitivity based identification methods. The simulation results based on hybrid simulation platform have demonstrated

this advanced SPECS has the ability to successfully and reliably prevent the long term voltage instability induced emergency states and unexpected relay operations.

The main contributions of this thesis:

- Voltage instability induced cascading events on Eastern Denmark power system have been simulated in RTDS. The progress of cascading events has been analyzed based on impedance loci and decomposed into different phases.
- A system wide detection method for overloading situations has been proposed based on improved distance relay system considering loadability.
- A sensitivity method based on impedance margin of distance relay has been proposed in order to fast define the variation relationships between the relay margins and other system variables. Also, for load flow transferring induced overloading situation, an impedance sensitivity method has been proposed to identify this overloading situation from faulty situations.
- Based on sensitivity analysis, a special protection and emergency control scheme has been proposed to correspondingly adjust the different overload induced emergency states.
- A multi agent system based SPECS has been proposed to effectively and reliably coordinate distributed relay agents and controller agents, which realize the final purpose of preventing the unexpected cascading trips.
- A hybrid real time simulation platform has been built based on RTDS and LabVIEW. Then the multi agent system based SPECS can be validated and demonstrated in a real-time hardware-in-loop simulation environment.

7.2 Future work

During the progress of this research work, some interesting and relevant topics are identified, which could be considered for further investigation in the future and listed as follows:

- Adaptive relay setting regulation considering voltage instability

The voltage stability margin will be changed when system network or operation condition changes. The fixed settings of encroachment element is not enough for voltage

instability detection under cascading events, especially for the relays on the transmission lines, which should be updated and adapted online with WAMS based system wide information.

- Rotor angle instability induced unexpected relay operations

There were also many rotor angle instability induced cascading events in the history. The reasons and mechanism of this kind of events are very different from voltage instability induced ones. Normally, these two instability problems would trigger each other during the cascading events. Under these situations, the sensitivity based methods are fast but with big errors. So the suitable algorithms of analysis, identification and regulation control on angle instability should be further investigated and designed.

Also, the other characteristics of relays could be considered in the local relay function improvement, such as adaptive power swing blocking settings in the distance relay.

- Local identification based on relay detected electrical variables

When communication network is not developed in some parts of power system, the accurate identification and estimation method for overloading situation based on local measurements will be relied on.

- Further consideration on special protection and emergency control

Smart islanding control strategy could be considered as a last defense backup control when load shedding strategy fails to adjust the emergency state and unexpected relay operation occurs. Also, the black start control should be designed to effectively restore the power system after a cascaded blackout.

- Communication network development for MAS based control system

In order to timely prevent the unexpected control and relay operations, the fast information communication between dispersed agents is very importance. So communication network development and the function of agent societies should be further investigated to minimize the time delay and possible information loss.

- Further investigation on reliability of SPECS

Many other reasons, which could induce failure control processes, could be considered in the design of Supervisory Control center, such as communication failures, virus attack, diverse agent failures and etc. Meanwhile, other intelligent algorithm could

be applied in MAS to improve the efficiency of whole control system, such as particle swarm optimization, fuzzy control algorithm and etc.

References

[1] P. Kundur, *Power Sytem Stability and Control*, McGraw-Hill Press, 1993.

[2] J. Bertsch, C. Carnal, D. Karlson, J. McDaniel, and V. Khoi, "Wide-Area Protection and Power System Utilization," *Proceedings of the IEEE*, vol. 93, pp. 997-1003, May, 2005.

[3] D. Karlsson, M. Hemmingsson and S. Lindahl, "Wide area system monitoring and control," *IEEE Power & Energy Magazine*, Sep/Oct 2004.

[4] P. M. Anderson, *Power System Protection*, A John Wiley & Sons, Inc., 1999.

[5] K. Morison, L. Wang and P. Kundur, "Power system security assessment," *IEEE Power and Energy Magazine*, vol. 2, pp. 30-39, 2004.

[6] G. Anderssen, P. Donalek, R. Farmer, N. Hatziargyriou, I. Kamwa, *et al.*, "Causes of the 2003 major grid blackouts in North America and Europe, and recommended means to improve system dynamic performance," *IEEE Transactions on Power Systems*, vol. 20, no. 4, pp.1922-1928, Nov 2005.

[7] P. Pourbeik, P. S. Kundur and C. W. Taylor, "The anatomy of a power grid blackout - root causes and dynamics of recent major blackouts," *IEEE Power & Energy Magazine*, pp. 22-29, 2006.

[8] U.S.-Canada Power System Outage Task Force, "Final Report on the August 14th blackout in the United States and Canada," United States Department of Energy and National Resources Canada, April 2004. [Online] available: https:// reports.energy.gov/BlackoutFinal-Web.pdf.

[9] C. Taylor, *Power System Voltage Stability*, McGraw Hill Inc., 2004.

[10] S. Larsson, and E. Ek, "The black-out in southern Sweden and eastern Denmark," *IEEE PES General meeting*, Denver Colorado, USA, pp. 309-313, 2004.

[11] T. Kimura, S. Nishimatsu, Y. Ueki, and Y. Fukuyama, "Development of an expert system for estimating fault section in control center based on protective system simulation," *IEEE Transactions on Power Delivery*, vol. 7, pp. 167-172, 1992.

[12] I. Kamwa, R. Grondin, V. K. Sood, C. Gagnon, N. Van Thich, and J. Mereb, "Recurrent neural networks for phasor detection and adaptive identification in

power system control and protection," *IEEE Transactions on Instrumentation and Measurement*, vol. 45, pp. 657-664, 1996.

[13] T. Xiaoyang, W. Xiaoru, W. Rui, H. Fei, D. Xueyuan, K. M. Hopkinson, and S. Gongyi, "The Study of a Regional Decentralized Peer-to-Peer Negotiation-Based Wide-Area Backup Protection Multi-Agent System," *IEEE Transactions on Smart Grid*, vol. 4, pp. 1197-1206, 2013.

[14] R. Giovanini, K. Hopkinson, D. V. Coury, and J. S. Thorp, "A primary and backup cooperative protection system based on wide area agents," *IEEE Transactions on Power Delivery*, vol. 21, pp. 1222-1230, 2006.

[15] B. Zhang, "Strengthen the protection relay and urgency control system to improve the capability of security in the interconnected power network", *Proceedings of the CSEE*, (in Chinese), 24(7): 1-6, 2004.

[16] T. Cutsem and C. Vournas, *Voltage Stability of Electric Power System*, Springer, 2008.

[17] P. Kundur, J. Paserba, V. Ajjarapu, G. Andersson, A. Bose, *et.al*, "Definition and classification of power system stability IEEE/CIGRE joint task force on stability terms and definitions," *IEEE Transactions on Power Systems*, vol. 19, pp. 1387-1401, 2004.

[18] H. Johannsson, *Development of Early Warning Methods for Electric Power Systems*, PhD thesis, 2011.

[19] C. Liu; L. Claus, Z. Chen, Z. Liu, "Adaptive Voltage Stability Protection Based on Load Identification Using Phasor Measurement Units", *Proceedings of the IEEE International Conference on Advanced Power System Automation and Protection, APAP 2011*, 2011.

[20] J. J. Romero, "Blackouts illuminate India's power problems", *Spectrum, IEEE*, vol. 49, pp. 11-12, Jan. 2012.

[21] S. Larsson and E. Ek, "The blackout in Southern Sweden and Eastern Denmark, September 23, 2003," *in Proc. IEEE PES General Meeting*, Denver, 2004.

[22] A. Berizzi, "The Italian 2003 blackout," *in Proc. IEEE PES General Meeting*, Denver, 2004.

[23] L. Chunyan, S. Yuanzhang and C. Xiangyi, "Analysis of the blackout in Europe on November 4, 2006," *in Power Engineering Conference*, International, pp. 939–944. 2007.

[24] N. Voropai and T. Hammons, "Blackouts: Remedial measures and restoration practices; Asian and Australian experience," *in Power and Energy Society General Meeting - Conversion and Delivery of Electrical Energy in the 21st Century*, pp. 1–4, 2008.

[25] K. U. Z. Mollah, M. Bahadornejad and N. K. Nair, "Automatic under-frequency load shedding in New Zealand power system: A systematic review," *in Universities Power Engineering Conference (AUPEC)*, Australasian, pp. 1–7, 2011.

[26] T. Ohno and S. Imai, "The 1987 Tokyo Blackout," *in Power Systems Conference and Exposition, IEEE PES*, pp. 314–318, 2006

[27] P. Gomes and F. J. M. Ordacgi, "Brazilian defense plan against extreme contingencies," *in Quality and Security of Electric Power Delivery Systems, CIGRE/PES 2003. CIGRE/IEEE PES International Symposium*, pp. 181–186, 2003.

[28] I. C. Decker, M. N. Agostini, A. S. E Silva and D. Dotta, "Monitoring of a large scale event in the Brazilian Power System by WAMS," *in Bulk Power System Dynamics and Control (iREP) - VIII (iREP)*, pp. 1–8, 2010.

[29] C. A. Ruiz, N. J. Orrego and J. F. Gutierrez, "The Colombian 2007 black out," *in Transmission and Distribution Conference and Exposition:* Latin America, IEEE/PES, pp. 1–5, 2008

[30] A. Burlando, The Impact of Electricity on Work and Health: Evidence from a Blackout in Zanzibar, Research report, University of Oregon, Dec. 2010

[31] K. Yamashita, L. Juan, Z. Pei and L. Chen-Ching, "Analysis and control of major blackout events," *in Power Systems Conference and Exposition*, PSCE '09. IEEE/PES, pp. 1–4, 2009.

[32] N. B. Bhatt, "August 14, 2003 U.S.-Canada blackout," *presented at the IEEE PES General Meeting*, Denver, 2004.

[33] Power failure in Eastern Denmark and Southern Sweden on 23 September 2003, Final report on the course of events. [Online]. Available: www.geocities.jp%2Fps_dictionary%2Fblackout%2FFinal_report_uk-web.pdf

[34] P. Pourbeik, P. S. Kundur and C. W. Taylor, "The anatomy of a power grid blackout - Root causes and dynamics of recent major blackouts," *Power and Energy Magazine, IEEE*, vol.4 no.5, pp. 22–29, Sept. 2006.

[35] N. I. Voropai and D. N. Efimov, "Analysis of blackout development mechanisms in electric power systems," in *Power and Energy Society General Meeting, 2008 IEEE*, pp. 1–7, 2008.

[36] M. Begovic, D. Novosel, D. Karlsson, C. Henville and G. Michel, "Wide-Area Protection and Emergency Control," *Proceedings of the IEEE*, vol.93 no.5, pp. 876–891, May, 2005.

[37] K. Yamashita, S. Joo, J. Li, P. Zhang and C. Liu, "Analysis, control, and economic impact assessment of major blackout events," *European Transactions on Electrical Power*, vol.18 no.8, pp. 854–871, 2008.

[38] C. Kim, J. Heo and R. Aggarwal, "An Enhanced Zone 3 Algorithm of a Distance Relay Using Transient Components and State Diagram," *IEEE Transactions on Power Delivery*, vol. 20, no. 1, pp. 39-46, 2005.

[39] C. C. Liu, K. Yamashita, J. Li, P. Zhang, M. Hofmann, *Learning to recognize vulnerable patterns of cascaded events*, EPRI Technical Report, 2007.

[40] Y. Paithankar, S. Bhide, *Fundamentals of Power System Protection*, PHI Learning Pvt. Ltd., 2004.

[41] S. H. Horowitz and A. G. Phadke, "Third zone revisited," *IEEE Transactions on Power Delivery*, vol.21 no.1, pp. 23–29, Jan, 2006.

[42] A. N. Sarwade, P. K. Katti and J. G. Ghodekar, "Advanced distance relay characteristics suitable for dynamic loading," *in IPEC, 2010 Conference Proceedings*, pp. 509–514, 2010.

[43] K. Yunus, G. Pinares, L. Tuan, L. Bertling, "A combined zone-3 relay blocking and sensitivity-based load shedding for voltage collapse prevention," *Innovative Smart Grid Technologies Conference Europe (ISGT Europe)*, 2010.

[44] V. Terzija, G. Valverde, C. Deyu, P. Regulski, V. Madani, *et.al*, "Wide-Area Monitoring, Protection, and Control of Future Electric Power Networks," *Proceedings of the IEEE*, vol.99 no.1, pp. 80–93, Jan, 2011.

[45] R. H. Khan and J. Y. Khan, "A comprehensive review of the application characteristics and traffic requirements of a smart grid communications network," *Computer Networks*, vol.57 no.3, pp. 825–845, Feb. 2013.

[46] M. Panteli, P. A. Crossley, D. S. Kirschen and D. J. Sobajic, "Assessing the Impact of Insufficient Situation Awareness on Power System Operation," *IEEE Transactions on Power Systems*, vol.28 no.3, pp. 2967–2977, Aug. 2013.

[47] R. Umakishore, K. Hong, L. Iftode, R. Jain, R. Kumar, K. Rothermel, S. Junsuk and R. Sivakumar, "Large-Scale Situation Awareness With Camera Networks and Multimodal Sensing," *Proceedings of the IEEE*, vol.100 no.4, pp. 878–892, April, 2012.

[48] C. Alcaraz, C. Fernandez-Gago and J. Lopez, "An Early Warning System Based on Reputation for Energy Control Systems," *IEEE Transactions on Smart Grid*, vol.2 no.4, pp. 827–834, Dec. 2011.

[49] S. Kai, S. Likhate, V. Vittal, V. S. Kolluri and S. Mandal, "An Online Dynamic Security Assessment Scheme Using Phasor Measurements and Decision Trees," *IEEE Transactions on Power Systems*, vol.22 no.4, pp. 1935–1943, Nov. 2007.

[50] J. L. Mathieu, S. Koch and D. S. Callaway, "State Estimation and Control of Electric Loads to Manage Real-Time Energy Imbalance," *IEEE Transactions on Power Systems*, vol.28 no.1, pp. 430–440, Feb. 2013.

[51] C. Sungyun, K. Beungjin, G. J. Cokkinides and A. P. S. Meliopoulos, "Feasibility Study: Autonomous State Estimation in Distribution Systems," *IEEE Transactions on Power Systems*, vol.26 no.4, pp. 2109–2117, Nov. 2011.

[52] E. Muneender and D. M. Vinodkumar, "Real Coded Genetic Algorithm based dynamic Congestion Management in open power markets," in *Transmission and Distribution Conference and Exposition (T&D), 2012 IEEE PES*, pp. 1–5, 2012.

[53] S. C. Muller, A. Kubis, S. Brato, U. Hager, C. Rehtanz and J. Gotze, "New applications for wide-area monitoring, protection and control," in *Innovative Smart Grid Technologies (ISGT Europe), 2012 3rd IEEE PES International Conference and Exhibition on*, pp. 1–8, 2012.

[54] I. Kamwa, S. R. Samantaray and G. Joos, "Compliance Analysis of PMU Algorithms and Devices for Wide-Area Stabilizing Control of Large Power

Systems," *IEEE Transactions on Power Systems*, vol.28 no.2, pp. 1766–1778, May, 2013.

[55] B. Tianshu, Y. Hao, W. Jingtao and W. Shuyi, "The implementation of wide-area protection and control experimental system," in *Innovative Smart Grid Technologies - Asia (ISGT Asia), 2012 IEEE*, pp. 1–5, 2012.

[56] Draft Standard PRC-019-1, "Coordination of Generator Voltage Regulator Controls with Unit Capabilities and Protection," NERC Phase III-IV Draft Standards for Field Tests, Sep. 2006

[57] S. Li, N. Yorino, M. Ding, Y. Zoda, "Sensitivity Analysis to Operation Margin of Zone 3 Impedance Relays with Bus Power and Shunt Susceptance," *IEEE Transactions on Power Delivery*, vol. 23, no. 1, January 2008.

[58] H. Song, B. Lee and V. Ajjarapu, "Control strategies against voltage collapse considering undesired relay operations," *IET Generation, Transmission & Distribution*, vol. 3, no. 2, pp. 164-172, 2009.

[59] B. Naduvathuparambil, M. Valenti, A. Feliachi. "Communication delays in wide area measurement systems," *Proceedings of the 34th southeastern symposium on system theory*, pp. 118-122, 2002.

[60] Q. Jiang, Z. Zou, Y. Cao, Z. Han, "Overview of Power System Stability Analysis and Wide area Control in Consideration of Time Delay," *Automation of Electric Power System (Chinese)*, vol. 29, no. 3, pp. 1-7, Feb. 2005.

[61] M. Yang, Y. Zhu, "Study on adaptive distance protection using multi-agent technology," *Power Engineering Conference, IPEC 2005. The 7th International*, vol. 2, pp. 618 -622, 2005.

[62] S. Sheng, D. Shi, X. Duan, "Adaptive Agent-Based Wide-Area Current Differential Protection System," *IEEE Transactions on Industry Applications*, vol. 46, no. 5, pp. 2111-2117, 2010.

[63] J. Li, K. Yamashita, C. C. Liu, P. Zhang, M. N. Hofmann, "Identification of cascaded generator over-excitation tripping events," *Proceedings of 16th Power Systems Computation Conference*, Glasgow, Scotland, 2008.

[64] C. C. Liu, K. Yamashita, Juan Li, P. Zhang, M. N. Hofmann, "Learning to recognize vulnerable patterns of cascaded events," PRI, Palo Alto, CA, Technical Report, 1016197, Feb. 2008.

[65] L. Cheng, B. Zhang, Z. Hao, J. Shu, Z. Bo, "Feasibility Study on Active Power Security Protection of Transmission Section", *Power and Energy Engineering Conference, 2009, APPEEC*, 2009.

[66] B. Zhang, "Strengthen the protection relay and urgency control system to improve the capability of security in the interconnected power network [J]," *Proceedings of the CSEE*, pp. 1-6, 2004.

[67] T. Bi, H. Xu, S. Huang, Q. Yang, "Flow transferring identification algorithm with consideration of transient period", *Power & Energy Society General Meeting*, 2009.

[68] X. Dong, L. Ding, K. Liu, S. Shi, B. Wang, L. Cui, Z. Bo, "Smart system protection based on local information", *10th IET International Conference on Developments in Power System Protection (DPSP 2010)*, pp. 1-4, 2010.

[69] Maintaining reliability in a competitive U.S. electricity industry: Final report of the North American Electric Reliability Council (NERC) Task Force on Electric System Reliability. [Online]. Available: http://www.nerc.com/~filez/reports.html

[70] C. D. Vournas and T. Van Cutsem, "Local identification of voltage emergency situations;" *IEEE Transactions on Power Systems*, vol. 23, no. 3, pp. 1239-1248, August, 2008.

[71] P. Mandoulidis, C. Lanbrou and C. Vournas, "Effect of load restoration on an integrated autonomous protection system against voltage instability," *PowerTech, 2011 IEEE Trondheim*, 2011, pp. 1-8.

[72] C. Vournas, A. Metsiou, M. Kotlida, V. Nikolaidis, M. Karystianos, "Comparison and combination of emergency control methods for voltage stability," *in Proc. IEEE Power Eng. Soc. General Meeting*, vol. 2, 2004, pp. 1799-1804.

[73] T. Van Cutsem, "Voltage instability: phenomena, countermeasures, and analysis methods," *Proceedings of the IEEE*, vol. 88, no. 2, pp. 208-227, 2000.

[74] W. Elmore, "Protective Relaying Theory and Applications," ABB Power T&D Company Inc., 2003.

[75] RTDS Technologies Inc. http://www.rtds.com

[76] IEEE committee report, "Dynamic models for steam and hydro turbines in power system studies," *IEEE Transactions on Power Apparatus and Systems*, vol. PAS-92, no. 6, pp. 1904-1915, 1973.

[77] IEEE Recommended Practice for Excitation System Models for Power System Stability Studies, in *IEEE Std 421.5-1992*, 1992.

[78] CIGRE TF 38-02-08, "Long Term Dynamics Phase II", 1995.

[79] "American National Standard Requirements for Cylindrical-Rotor Synchronous Generators," in *ANSI C50.13-1977 (Revision of C50.13-1965)*, pp. 1-16, 1977.

[80] NERC, Aug. 2005, "Relay loadability exceptions: determination and application of practical relaying loadability ratings," [Online]. Available: http://www.nerc.com/~filez/spctf.html

[81] W. Elmore, *Protective Relaying Theory and Applications*, ABB Power T&D Company Inc., 2003.

[82] Draft Standard PRC-019-1, "Coordination of Generator Voltage Regulator Controls with Unit Capabilities and Protection", NERC Phase III-IV Draft Standards for Field Tests, Sep. 2006.

[83] V. Akhmatov, *Analysis of dynamic behaviour of electric power systems with large amount of wind power*, Ph.D. dissertation, Dept. Electric Power. Eng., Technical Univ. Denmark, Kgs. Lyngby, 2003.

[84] J. Zhu, *Optimization of power system operation*, vol. 49: Wiley-IEEE Press, 2009.

[85] H. Saadat, *Power system analysis*, McGraw-Hill, 1999.

[86] J. Qiu, Z. Han, and X. Jiang, "The PIf bus in power flow analysis," Proc. Chinese Soc. Elect. Eng., vol. 15, no. 5, pp. 323-327, Sep. 1995.

[87] A. M. Abed, "WSCC voltage stability criteria, undervoltage load shedding strategy, and reactive power reserve monitoring methodology," in *Power Engineering Society Summer Meeting, 1999. IEEE*, Edmonton, Alta., 1999, pp. 191-197 vol.1.

[88] F. Bellifemine, G. Caire, D. Greenwood, *Developing Multi-Agent Systems with JADE*, John Wiley & Sons, Lt, 2007.

[89] M. Woodridge and N. Jennings, *Intelligent Agent*, Springer-Verlag, 1995.

[90] A. Hayzelden and John Bigham, Software Agents for Future Communication systems, Springer, 1999.

[91] T. Wagner and O. Rana, *Infrastructure for Agents, Multi-Agent systems, and Scalable Multi-Agent Systems*, Springer, 2001.

[92] L. Yilmaz and T. Oren, *Agent-Directed Simulation and System Engineering*, Willey-Verlag, 2009

[93] J. Shu and C. Jiang. *Design and implementation of MAS in renewable energy power generation system*. in Human System Interactions (HSI), 2010 3rd Conference on. 2010. Rzeszow.

[94] K. Koen, S. Karnouskos, D. Nestle, et al, "Smart houses for a smart grid," in *Electricity Distribution - Part 1, 2009. 20th International Conference and Exhibition on*, pp. 1–4, CIRED 2009.

[95] T. Nagata, H. Nakayama，M. Utatani, et al, "A multi-agent approach to Power system Normal state operations," *IEEE PES Summer Meeting Proceedings*, pp. 1582-1586, 2002.

[96] B. Zhao, C. X. Guo, Y. J. Cao, "A Multi agent-Based Particle Swarm Optimization Approach for Optimal Reactive Power Dispatch," *IEEE Transactions on Power Systems*, vol. 20, no. 2, pp.1070-1078, 2005.

[97] P. Taylor, and X. Tao, et al. "Integrating voltage control and power flow management in AuRA-NMS," *Smart Grids for Distribution, IET-CIRED. CIRED Seminar*, 2008.

[98] L. Jinghua, and W. Hua, et al, "The multi-agent model and method for Energy-Saving Generation Dispatching system," *Power System Technology (POWERCON), International Conference on*, 2010.

[99] P. Wei, Y. Yan, Y. Ni, J. Yen, F. F. Wu, "A Decentralized Approach for Optimal Wholesale Cross-Border Trade Planning Using Multi-Agent Technology," *IEEE Transactions on Power Systems*, vol. 16, no. 4, pp. 833-838, 2001.

[100] R. J. Bessa and M. A. Matos, et al, "Optimized Bidding of a EV Aggregation Agent in the Electricity Market," *IEEE Transactions on Smart Grid,* vol. 3, no. 1, pp. 443-452, 2002.

[101] H. Liu, and T. Ding, et al, "Research on Fault Diagnosis of Hydroelectric Sets Vibration Based on MAS and Petri Net," *Power and Energy Engineering Conference,* Asia-Pacific, Wuhan, 2009.

[102] G. Wang, and X. Feng, et al, "Research on Intellectualized Fault Diagnosis System Based on Distributed Multi-Agent Technology," *Electronic Measurement and Instruments*, 2007.

[103] C. Hong, and W. Min, et al, "The Fault Diagnosis System of Electric Locomotive Based on MAS. Intelligent Information Technology Application," *IITA 2009. Third International Symposium on, Nanchang*, 2009.

[104] P. Mao and H. Weng, et al, "Study of Fault Diagnosis for Power Network Based on MAS," *Power System Technology, PowerCon 2006. International Conference on*, Chongqing, 2006.

[105] Li, L. and K. P. Logan, et al, "Fault Detection, Diagnostics, and Prognostics: Software Agent Solutions," *IEEE Transactions on Vehicular Technology*, vol. 56, no. 4, pp. 1613-1622, 2007.

[106] Hossack, J. A. and J. Menal, et al, "A multiagent architecture for protection engineering diagnostic assistance," *IEEE Transactions on Power Systems*, vol. 18, no. 2, pp. 639-647, 2003.

[107] J. S. Heo and K. Y. Lee, "A Multi-Agent System-Based Intelligent Identification System for Power Plant Control and Fault-Diagnosis," *IEEE Congress on Evolutionary Computation*, pp. 1544-1551, 2006 .

[108] S. Su, and K. K. Li, et al, "Adaptive Agent-Based Wide-Area Current Differential Protection System," *IEEE Transactions on Industry Applications*, vol. 46, no. 5, pp. 2111-2117, 2010.

[109] R. Giovanini, and K. Hopkinson, et al, "A primary and backup cooperative protection system based on wide area agents," *IEEE Transactions on Power Delivery*, vol. 21, no. 3, pp. 1222-1230, 2006.

[110] X. Tong and X. Wang, et al, "The Study of a Regional Decentralized Peer-to-Peer Negotiation-Based Wide-Area Backup Protection Multi-Agent System," *IEEE Transactions on Smart Grid*, vol. 4, no. 2, pp. 1197-1206, 2013.

[111] D. Panasetsky, and P. Etingov, et al, "Multi-agent approach to emergency control of power system," *Electric Utility Deregulation and Restructuring and Power Technologies, DRPT 2008, Third International Conference on*, Nanjing, 2008.

[112] D. Panasetsky and N. Voropai, "A Multi-agent approach to coordination of different emergency control devices against voltage collapse," *PowerTech, 2009 IEEE Bucharest, Bucharest*, 2009.

[113] E. Ciapessoni, and E. Corsetti, "DefPlans: Agent Modeling Techniques for Power System Emergency Control," *Intelligent System Applications to Power Systems, 2009. ISAP '09. 15th International Conference on*, Curitiba, 2009.

[114] C. Liu. and J. Jung, et al, "The strategic power infrastructure defense (SPID) system. A conceptual design," *IEEE Control Systems*, vol.20, no. 4, pp. 40-52, 2000.

[115] C. Liu, "Strategic power infrastructure defense (SPID): a wide area protection and control system," *in Transmission and Distribution Conference and Exhibition 2002: Asia Pacific. IEEE/PES*. 2002.

[116] C. Liu, "Strategic power infrastructure defense (SPID)," *in Power Engineering Society General Meeting, IEEE*, 2004.

[117] N. Watson and J. Arrillaga, *Power System Electromagnetic Transients Simulation, The Institution of Engineering and Technology*, London, 2003.

[118] K. Hopkinson, W. Xiaoru, R. Giovanini, J. Thorp, et al, "EPOCHS: a platform for agent-based electric power and communication simulation built from commercial off-the-shelf components," *IEEE Transactions on Power Systems*, vol.21 no.2, pp. 548–558, 2006

[119] J. S. Thorp, X. Wang, K. M. Hopkinson, D. Coury, and R. Giovanini, "Agent technology applied to the protection of power systems," *Autonomous systems and Intelligent agents in power system control and operation*, pp. 115-154, 2004.

[120] T. Issarriyakul and E. Hossain, *Introduction to Network Simulator NS2*, Springer, 2012

[121] G. Morejon, S. Srivastava, D. Cartes, "Integration Virtual Test Bed and JADE Agent Platform Using CORBA for Reconfiguration of Shipboard Power Systems," *IEEE Power Engineering Society General Meeting*, pp: 18-22, 2006.

[122] J. Conway and S. Watts, *A Software Engineering Approach to LabVIEW*, Pearson Education, 2003.

[123] D. Varsakelis, W. Levine, *Handbook of Networked and Embedded Control Systems*, Springer, 2005.

[124] NI X Series Multifunction Data Acquisition, [Online]. Available: http://sine.ni.com/ds/app/doc/p/id/ds-151/lang/da

[125] Introduction to LabVIEW Real-Time Symmetric Multiprocessing (SMP), [Online]. Available: http://www.ni.com/white-paper/6403/en

[126] Real-Time FIFO for Deterministic Data Transfer Between Vis, [Online]. Available: http://www.ni.com/white-paper/3934/en

[127] J. D. Schwartz, W. Wang and D. E. Rivera, "Simulation-based optimization of process control policies for inventory management in supply chains," *Automatica*, vol.42, no.8, pp. 1311–1320, 2006.

[128] R. He, H. Wan and X. Gu, "Advanced process control technology implementation in ammonia plant," in *Control and Decision Conference (CCDC), 25th Chinese*, pp. 1200–1204, 2013.

[129] W. Wang, D. E. Rivera and K. G. Kempf, "Model predictive control strategies for supply chain management in semiconductor manufacturing," *International Journal of Production Economics*, vol.107, no.1, pp. 56–77, 2007.

[130] T. R. McCalla, *Digital Logic and Computer Desin*. New York: Macmillan, 1992, pp:261-275.

[131] D. Luckham, *The power of event: an introduction to complex event processing in distributed enterprise systems*. USA: Addison-Wesley, 2002.

List of publications

2013:

[1] Z. Liu, Z. Chen, H. Sun, Y. Hu, "Multi Agent System Based Wide Area Protection Scheme for Post Fault Voltage Recovery", *IET Generation, Transmission & Distribution*. Submitted.

[2] Z. Liu, Z. Chen, Y. Hu, "Wide Area Protection Scheme Preventing Cascading Events based on Improved Impedance relay", *2013 China-Korea Relay Protection Forum*, Xinjiang, Sep. 2013.

[3] Z. Liu, Z. Chen, H. Sun, Y. Hu, "Multi Agent System Based Wide Area Protection and control Scheme against Cascading Events", *IEEE Transactions on Power Delivery*. Second reviewing.

[4] Z. Liu, Z. Chen, H. Sun, Y. Hu, "Wide Area Protection Scheme Preventing Cascading Events Caused by Load Flow Transferring", *Power & Energy Society General Meeting*, Vancouver, July, 2013.

[5] Z. Liu, Z. Chen, H. Sun, Y. Hu, "Multi Agent System Based Process Control in Wide Area Protection against Cascading Events", *POWERTECH 2013*, France, Grenoble, June, 2013.

2012:

[6] Z. Liu, Z. Chen, H. Sun, C. Liu, Y. Hu, "Multi Agent System Based Wide Area Protection against Cascading events", *The 10th International Power and Energy Conference (IPEC)*, Ho Chi Minh City , Dec. 2012.

[7] Z. Liu, Z. Chen, H. Sun, C. Liu, "Emergency Load Shedding Strategy Based on Sensitivity Analysis of Relay Operation Margin against Cascading Events", *IEEE PES International Conference on Power Systems Technology (POWERCON)*, Auckland, New Zealand, Oct. 2012.

[8] Z. Liu, Z. Chen, H. Sun, C. Liu, "Control and Protection Cooperation Strategy for Voltage Instability", *47th International Universities' Power Engineering Conference (UPEC)*, London, Sep. 2012.

Appendix

A.1 Relevant data of the power system model of Eastern Denmark

The one line diagram of 19-bus test system simplified from Eastern Denmark power system is built by RSCAD/RTDS in Fig. A.1.

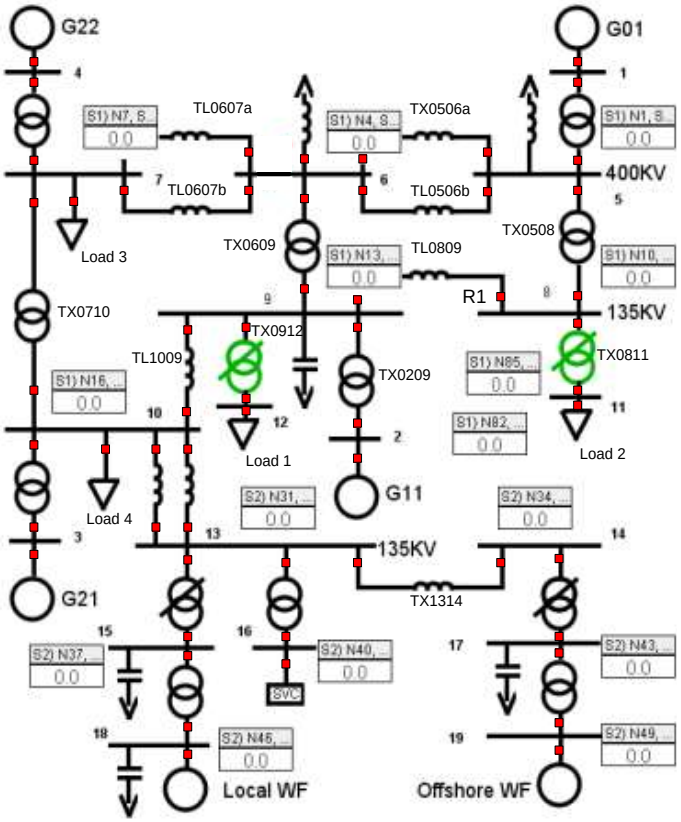

Fig. A.1 The one line diagram of 19-bus test system in RTDS

The initial load flow data of generators and loads are given in Table A.1 and Table A.2 [83]. The dynamic data about synchronous generators, excitation system, governor system, LTC data are given in Table A.3 -Table A.8 [1][75][76][77][78][79].

Table A.1 Generation data in the initial Normal state

Gen no.	*Bus. no*	*S0 (MVA)*	*P (MW)*	*Q (Mvar)*	*S (MVA)*	*Vset (p.u.)*
G01	1	2500	845	231	876	1.02
G11	2	1500	1218.6	722.3	1416.6	1.03
G21	3	1400	621.8	388	732.9	1.025
G22	4	750	634.56	111.6	644.3	1.03
LWF	18	550	300	0	300	1.01
OWF	19	181	150	0	150	1.01

Table A.2 Load consumptions information in the initiate Normal state

Load no.	*Bus no.*	*P (MW)*	*Q (Mvar)*	*S (MVA)*
Load 3	7	100	-50	111.8
Load 4	10	330	300	446
Load 2	11	650	140	665
Load 1	12	2450	1370	2807

Table A.3 Dynamic data of Generators

Gen no.	$H(s)$	$X_a(p.u.)$	X_d	X_q	X'_d	X'_q	X''_d	X''_q	T'_{do}	T'_{qo}	T''_{do}	T''_{qo}
G01	20	0.15	2	2	0.3	0.7	0.2	0.2	6.6	2.5	0.04	0.06
G11	5	0.15	2.09	2.04	0.254	0.39	0.2	0.2	6.6	1.3	0.038	0.06
G21	5	0.15	2.1	2	0.365	0.7	0.2	0.2	7.4	2.5	0.041	0.08
G22	5	0.15	2.43	2.33	0.307	0.6	0.2	0.2	7.5	2.5	0.029	0.06

Table A.4 Exciter data of BBSEX1

G01				G11			
T_f	0.04	T_4	0.02	T_f	0.04	T_4	0.02
K	40	VR_{max}	6.1	K	110	VR_{max}	5
T_1	4	VR_{min}	-6.1	T_1	8	VR_{min}	-5
T_2	1.2	EF_{max}	5.2	T_2	2	EF_{max}	5
T_3	0.1	EF_{mIN}	-4.1	T_3	0.05	EF_{mIN}	-5
G21				G22			
T_f	0.04	T_4	0.02	T_f	0.04	T_4	0.02
K	140	VR_{max}	5.25	K	40	VR_{max}	6.1
T_1	12.09	VR_{min}	-4.75	T_1	4	VR_{min}	-6.1
T_2	1.37	EF_{max}	5.25	T_2	1.2	EF_{max}	5.3
T_3	0.0565	EF_{mIN}	-4.75	T_3	0.1	EF_{mIN}	-4.1

Table A.5 FCL data

For G22					
I_{fdmax1}	2.85	I_{fdmax2}	3	$-I_{LIM}$	-3.85
K_1	0.248	K_2	12.6		
For G01, G11, G21					
I_{fdmax1}	2.68	I_{fdmax2}	3	$-I_{LIM}$	-3.85
K_1	0.248	K_2	12.6		

Table A.6 Governor System data of IEEE Type 1

K	20	U_c	-0.1	K_2	0	T_5	10.1
T_1	0.001	P_{mx}	1.0	K_3	0.24	K_4	0
T_2	0.001	P_{mn}	0	T_6	0.5	K_5	0.47
T_3	0.05	T_4	0.376	K_6	0	T_7	0
U_o	0.1	K_1	0.29	K_7	0	K_8	0

Table A.7 PSS data of IEE2ST

V_{rate}	20	T_3	3	T_8	0.05
K_1	24.4	T_4	3	T_9	0
K_2	0	T_5	0.15	T_{10}	0.001
T_1	0	T_6	0.05	UL	-0.1
T_2	0	T_7	0.15	LL	0.1

Table A.8 LTC data

LTC	Delay on first step (s)	Delay on next step (s)	Δr *(pu)*	*r (p.u.)* $[r^{min}, r^{max}]$	Controlled bus	V^{min} *(p.u.)*	*Dead band*
TX0912	30	5	0.01	[0.8, 1.2]	12	0.92	0.02
TX0811	30	5	0.01	[0.8, 1.2]	11	0.92	0.02

A.2 The hybrid simulation platform based on RTDS and LabVIEW

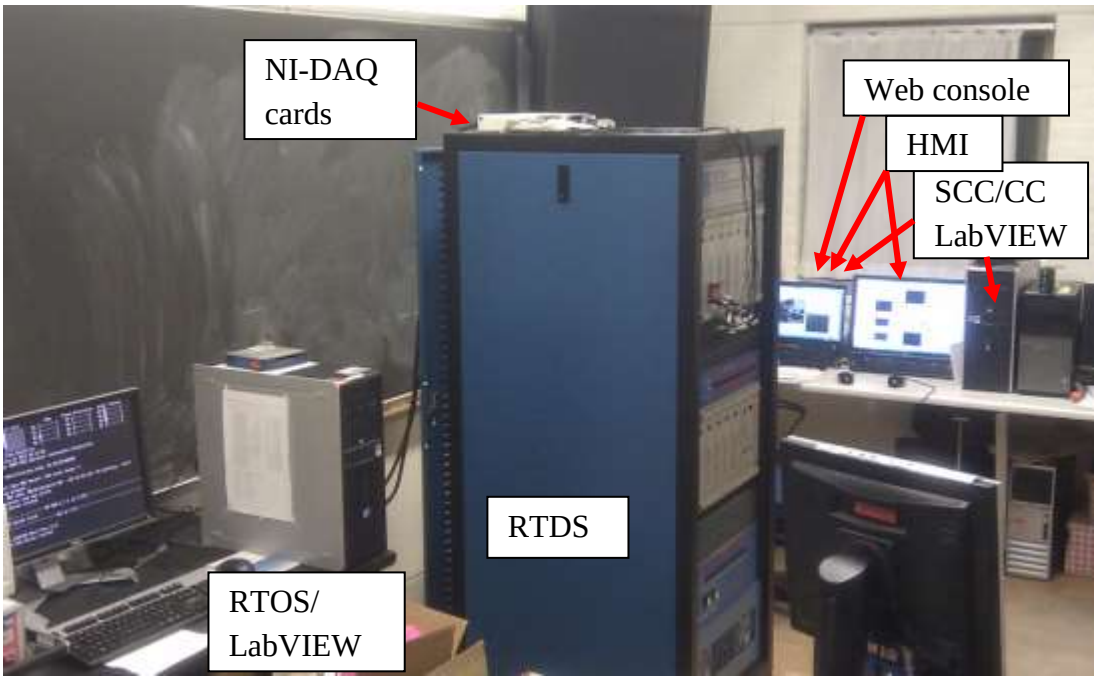

Fig. A.2 The real time hybrid simulation platform

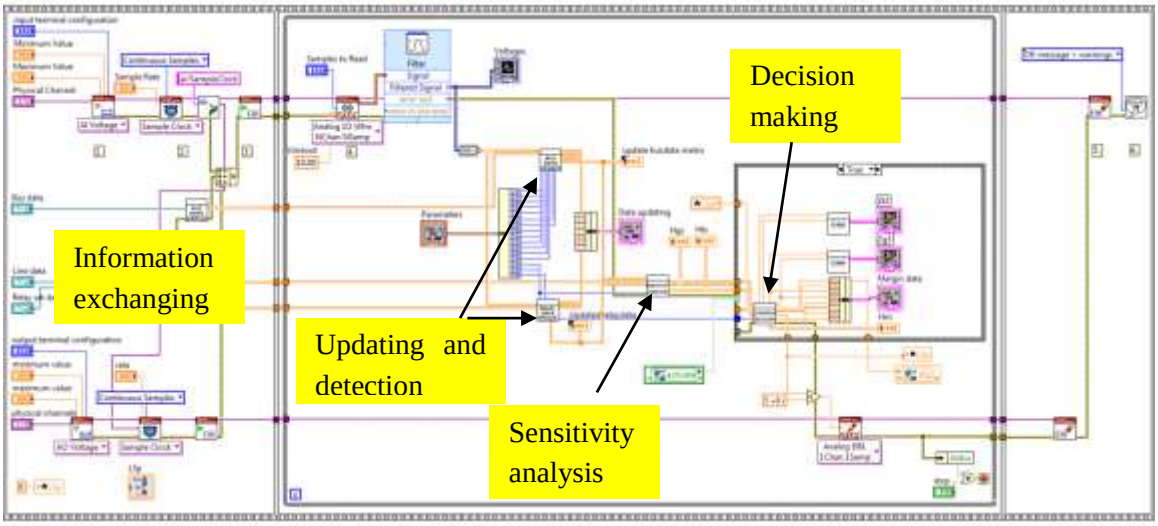

Fig. A.3 Block diagram of CC

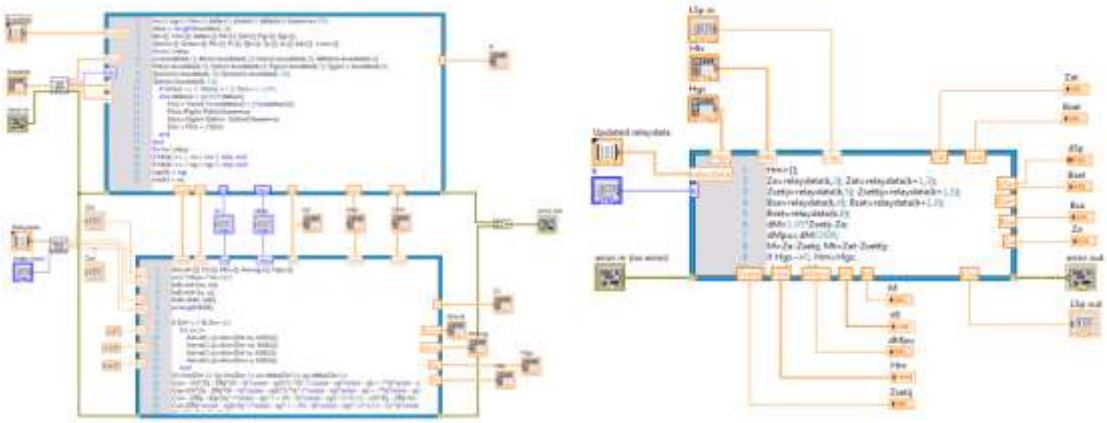

(a) Sub VI of sensitivity analysis VI (b) Sub VI of decision making VI

Fig. A.4 Block diagram of sub VIs in Control center

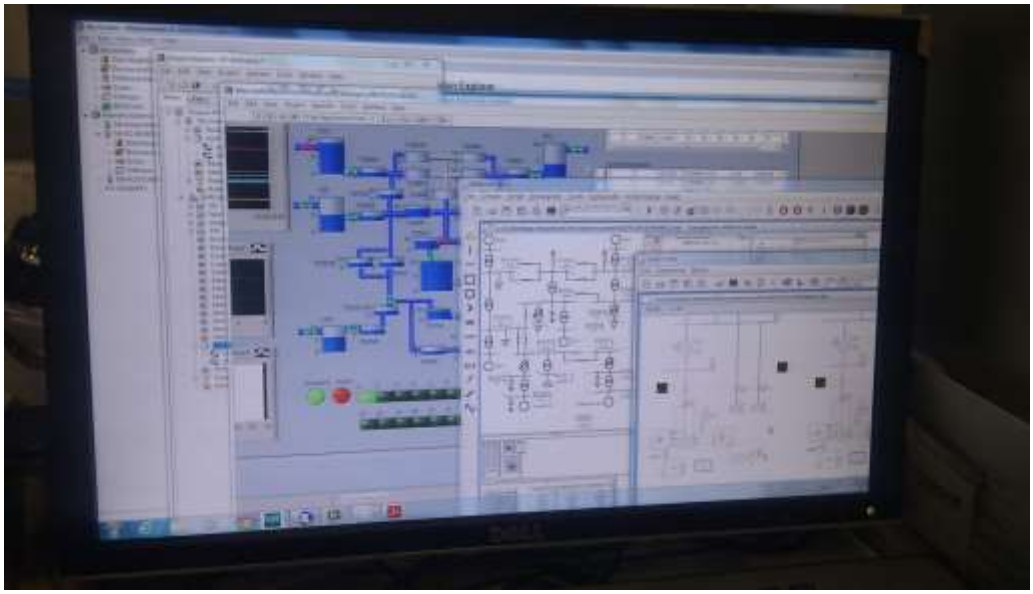

Fig. A.5 HMI in Supervisory Control Center